Evolving plasticity in brain and behaviour after targeted memory reactivation during sleep

Martyna Anna Rakowska

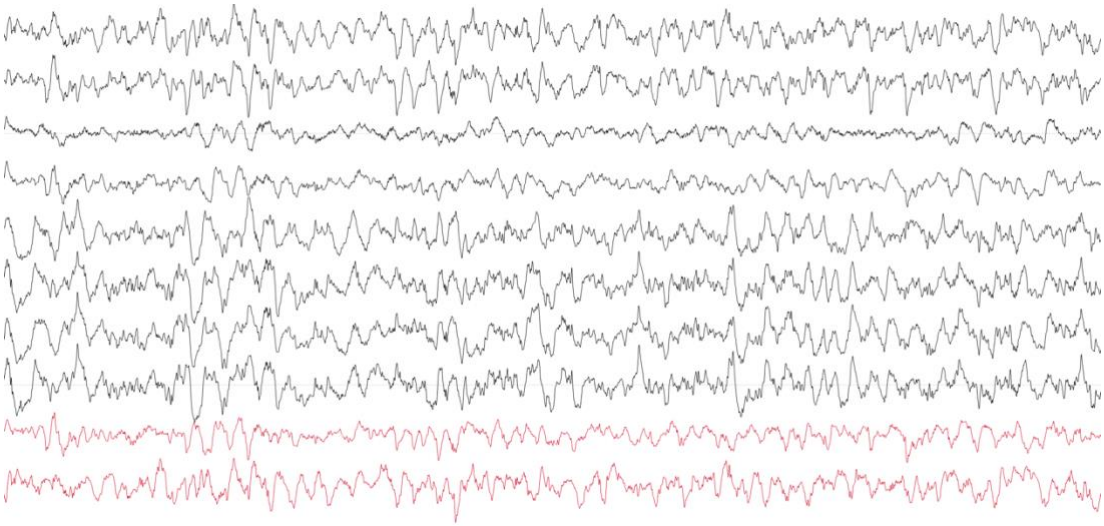

A thesis submitted for the degree of Doctor of Philosophy

Cardiff University

School of Psychology

April 2022

CARDIFF UNIVERSITY

PRIFYSGOL CAERDYDD

Thesis summary

Sleep is a remarkably complex and universal neuro-behavioural state. We spend one third of our lives asleep, but we still do not know exactly why that is. There is now overwhelming evidence that memories spontaneously reactivate during sleep, and this is thought to be essential for memory consolidation. However, the precise role of memory reactivation in long-term consolidation remains to be understood. Targeted memory reactivation (TMR) taps into the sleep-dependent consolidation process, providing a valuable tool to study memory reactivation. This thesis combines TMR during NREM sleep with examination of behaviour and multimodal neuroimaging to track the impact of cued replay on motor memories over time.

Chapter 2 demonstrates that memory-enhancing effects of TMR evolve over time, and that repeated reactivation of procedural memories over one night of sleep can affect motor performance up to 10 days post-stimulation. It also shows a surge in spindle density and slow oscillation-spindle coupling strength upon cue onset, indicative of early processing of memory traces. **Chapter 3** utilises the same paradigm to examine the functional and structural evolution of the reactivated memory representations. In this chapter, TMR led to gradual development of behavioural benefit that fully emerged at day 20, marking the longest effect of TMR reported so far. Importantly, this chapter shows that precuneus is functionally involved in early consolidation of the reactivated memories, whereas slowly evolving reorganisation of sensorimotor representations underpins long-term effects of TMR. Lastly, **Chapter 4** builds on these findings by showing microstructural plasticity across precuneus and task-related areas which continues days after the stimulation night and drives the emergence of memory benefits at the behavioural level.

Together, this thesis provides evidence for distributed and gradual structural, microstructure, and functional changes that track the development of long-term behavioural benefits from memory reactivation. In light of our results, we argue that memory reactivation is a powerful mechanism that facilitates the persistence of memories over long periods of time.

Declaration and Statements

Declaration

This thesis is the result of my own independent work, except where otherwise stated, and the views expressed are my own. Other sources are acknowledged by explicit references. The thesis has not been edited by a third party beyond what is permitted by Cardiff University's Use of Third Party Editors by Research Degree Students Procedure.

Signed: Martyna Rakowska Date: 11/04/2022

Statement 1

This thesis is being submitted in partial fulfilment of the requirements for the degree of PhD.

Signed: Martyna Rakowska Date: 11/04/2022

Statement 2

This work has not been submitted in substance for any other degree or award at this or any other university or place of learning, nor is it being submitted concurrently for any other degree or award (outside of any formal collaboration agreement between the University and a partner organisation)

Signed: Martyna Rakowska Date: 11/04/2022

Statement 3

I hereby give consent for my thesis, if accepted, to be available in the University's Open Access repository (or, where approved, to be available in the University's library and for inter-library loan), and for the title and summary to be made available to outside organisations, subject to the expiry of a University-approved bar on access if applicable.

Signed: Martyna Rakowska Date: 11/04/2022

Word count: 55,033

(Excluding summary, acknowledgements, declarations, contents pages, appendices, tables, diagrams and figures, references, bibliography, footnotes, and endnotes)

Table of Contents

Acknowledgements

The completion of this thesis would not have been possible without the support, expertise, encouragement, and love of many people, whom I would like to thank from the bottom of my heart. First and foremost, I want to thank my supervisor, ***Penny Lewis****, for her enthusiasm, guidance, and constant support throughout. Thank you for sharing your knowledge and passion for sleep, and for providing me with the freedom to pursue my research interests. I also owe a thank you to* ***Chen Song, Aline Bompas, and Heidi Johansen-Berg*** *for their critical feedback and suggestions that helped improve this work; and to the* ***European Commission (ERC)*** *for supporting my PhD.*

My gratitude and love go to all members of the ***NAPs Laboratory****, past and present, for their friendship, thought-provoking discussions, and tips on how to survive those long and weary nights. I have been truly fortunate to work with such a wonderful team of sleep researchers. Anne, Sofia, Miguel, Holly, Imogen, Lorena, Mo, Tamas, Jen, Yihe, Simon, Viviana, Duarte, Shi Wei, Nat, Ralph, Ibad, Niall, Elena, Paulina, Chelsea, Joe, Sophie, and Dominic – thank you for introducing me to sleep research and bearing with me through my early attempts at wiring up and sleep scoring. For keeping me going through the darkest days of data collection and the countless hours you have spent helping me become a doctor. To all the* ***participants*** *who so bravely participated in my studies – thank you for sharing your life stories with me and for your endless enthusiasm in letting me look inside your (sleeping) brains.*

I am forever indebted to ***Miguel Navarrete****, whose knowledge and wisdom helped me become a better scientist. Thank you for your enormous patience, unique sense of humour, for challenging my thinking and cheering on my MATLAB combats. I am also extremely grateful to have had the opportunity to learn from* ***Alberto Lazari and Mara Cercignani****. Completion of Chapters 3 and 4 would not have been possible without their expertise and untiring support. Thank you for guiding me through the wonderful world of MRI!*

I am beyond thankful to ***my partner, Max****, who has taken this journey with me despite being thousands of miles away. Thank you for your boundless support and unwavering faith in me; for keeping me in shape, bearing with me when I was too busy writing, and somehow knowing exactly when to clock me off for the day. My immeasurable gratitude also goes to* ***my best friend, Paulina****, who let me grumble endlessly about this thesis. Thank you for being there when I needed you most, for reminding me that there is life beyond PhD and for all the support, encouragement, and seemingly infinite supply of research memes that you provided.*

*I extend a special thanks to **Fine**, for showing me how to live in the moment and cherish the Now. To **Raya**, for being evermore entertaining and absolutely adorable. There were also **many seagulls and my calamondin plant** who kept me company and offered their own kind of support. I shall also thank my early art teacher, **Pani Ewa Solska**, who taught me lino printing and thereby provided the necessary resources to ensure that I stayed sane(ish) through it all.*

*My deepest and warmest thanks go to **my loving parents** who made this endeavour possible. Mamo, Tato, dziękuję Wam za Waszą bezwarunkową miłość, dumę i nieustające wsparcie w walce o marzenia. Dziękuję za to, że nauczyliście mnie wytrwałości, pokory i ambicji, i za niegasnącą wiarę w moje możliwości. Również za to, że z ogromną ciekawością i zaangażowaniem słuchaliście moich naukowo-sennych opowieści i za wszelkie próby nauczenia mnie gotowania. Obrigada za gościnę, za sobotnie spacery i za te wszystkie chwile spędzone w podróży. Dziękuję, że jesteście!*

*Above all, of course, I thank **my beloved sister, Aleks**, who makes my life so much more beautiful and worthwhile. Thank you for being by my side all these years – from the day of my interview until the very last 'I've finished!'. Thank you for your words of wisdom, for inspiring this research and proofreading so many parts of it. Thank you for the six-hour long phone calls, for the laughs we shared and the tears we cried. Thank you for the Valentine's cards. For your frequent visits and warmest welcomes, for our Welsh adventures and Cosy Club breakfasts. Thank you for celebrating all the exciting moments of this PhD with me and for always knowing how to cheer me up. I could not have wished for a better soulmate on this journey, and I am forever grateful to share this life with you.*

Contributors

Study design for **Chapter 2** was done jointly with Mahmoud Abdellahi. Together, we converted the SRTT task script, originally written by Suliman Belal, to fit our design. Anne Koopman provided a pdf version of the explicit memory task. I wrote the questionnaires' scripts. Participant recruitment was performed by Niall McGinley, Ibad Kashif, and myself. Mahmoud Abdellahi, Paulina Bagrowska, and I collected the data. Niall McGinley, Ibad Kashif, Paulina Bagrowska, and I sleep scored the data using a custom-made interface written by Miguel Navarrete. Spindle and phase amplitude coupling analysis scripts were based on a set of functions written by Miguel Navarrete. I analysed the data, created the figures, and wrote the chapter. Mahmoud Abdellahi, Paulina Bagrowska, Miguel Navarrete, and Penny Lewis reviewed the original draft.

Chapters 3 and 4 were written based on the data collected during a single research study. Slawomir Kusmia, Chen Song, Prof Derek Jones, Prof Heidi Johansen-Berg, Chantal Tax, John Evans, and Mark Drakesmith advised on the choice of MRI scans and parameters. I adapted the SRTT task script to fit the fMRI paradigm. Jennifer Roebber shared her SRTT script for online data collection on Pavlovia and helped adapt it for our design. The explicit memory task and questionnaires' scripts were the same as in Chapter 2. Participants' recruitment was shared between Paulina Bagrowska, Chelsea Bryant, Joe Davis, and me. Paulina Bagrowska, Mahmoud Abdellahi, Chelsea Bryant, Joe Davis, and I collected behavioural data and performed the overnights. Dominic Carr and Mahmoud Abdellahi helped with 0T ('mock') scanner procedures. Peter Hobden, Holly Kings, Paulina Bagrowska, Sofia Pereira, Marco Bigica, Alix Plumley, Wojciech Zajkowski, and Chelsea Bryant assisted with MRI data acquisition. Paulina Bagrowska and I sleep scored the data using a custom-made interface written by Miguel Navarrete. Spindle analysis scripts were based on a set of functions written by Miguel Navarrete. Chen Song, Eleonora Patitucci, Marco Bigica, Sofia Pereira, Sonya Foley, Alberto Lazari, and Prof Mara Carcignani contributed to various stages of MRI analysis. Chantal Tax and Greg Parker developed the Modular Pipeline for Multishell DTI processing used to pre-process DW-MRI data. I analysed the data, created the figures, and wrote the chapters. Alberto Lazari, Miguel Navarrete, Prof Heidi Johansen-Berg, Prof Mara Carcignani, Paulina Bagrowska, Mahmoud Abdellahi, and Penny Lewis reviewed the original drafts.

Publications arising from this Thesis

Chapter 2 has been published as a research article in the NeuroImage.

Rakowska, M., Abdellahi, M. E., Bagrowska, P., Navarrete, M., & Lewis, P. A. (2021). Long term effects of cueing procedural memory reactivation during NREM sleep. NeuroImage, 244, 118573.

Chapter 3 has been published as a pre-print on bioRxiv and submitted for consideration as an Article in *eLife.*

Rakowska, M., Bagrowska, P., Lazari, A., Navarrete, M., Abdellahi, M. E., Johansen-Berg, H., & Lewis, P. A. (2022). Cueing motor memory reactivation during NREM sleep engenders learning-related changes in precuneus and sensorimotor structures. *bioRxiv*.

Chapter 4 is based on a manuscript which is being prepared for submission for peer review.

Rakowska, M., Lazari, A., Cercignani, M., Bagrowska, P., Johansen-Berg, H., & Lewis, P. A. (2022). Distributed and gradual microstructure changes track the emergence of behavioural benefit from memory reactivation. *bioRxiv*.

CHAPTER 1

General Introduction

1 PREFACE

Every day the life on this planet enters a rather unusual state of mind that, for some yet unknown reason, is considered completely normal. You lie down, close your eyes, and suddenly become unaware of your surroundings. Your consciousness is lost and so is the control over your body, leaving you completely vulnerable for the next few hours. Meanwhile, your mind wanders into the most bizarre places, talks to strangers and plays out unimaginable scenarios in your head. Then, you wake up, drink some coffee to keep yourself from entering that ridiculous state again and resume life as usual – that is, until the sun goes down again... Oddly enough, other animals, including fish, frogs, and sparrows, experience similar states (Siegel, 2008). Intriguing, right? Yet, we still do not have a clear answer as to *why* that would be.

Why *do* we sleep? Sleep can be defined as a "recurring, reversible neuro-behavioural state of relative perceptual disengagement from and unresponsiveness to the environment" (Carskadon & Dement, 2005). It is homeostatically regulated, appears to be fundamental for many species and, more often than not, essential for survival (Siegel, 2008). Yet, until the discovery of Rapid Eye Movement sleep, sleep was regarded merely as an inactive state of the brain, an inevitable consequence of sensory overload during wake (Dement, 2005). The history of sleep research begins in 1920s when Berger (1929) provided scientists with a window to brain's activity, now known as the electroencephalography (EEG). He identified different patterns of electrical activity during wake and during sleep, paving the way for later discoveries in the field. Soon enough, it became widely accepted that sleep is characterised by cyclic variation of oscillatory patterns (i.e., sleep stages) which serve countless functions (Dement, 2005; Zielinski et al., 2016). The last decades has seen many attempts to understand the purpose of sleep. Thanks to them, we now appreciate that sleep is restorative for our brain, body, and mind. It plays a major role in hormonal, immune, and metabolic regulation, clears out molecular waste that accumulates during wakefulness and is essential for a range of cognitive processes (Assefa et al., 2015; Zielinski et al., 2016; Miller et al., 2014).

This thesis will focus on the function of sleep in memory and learning. Just like sleep, memory is an evolutionarily conserved process and impacts on almost every aspect of our life. Furthermore, there is now compelling evidence that sleep plays an active role in various memory processes (Diekelmann & Born, 2010b; Rasch & Born, 2013). Apart from protecting memories against interference, sleep-dependent plasticity seems critical for strengthening

the newly acquired traces, their integration into the existing networks, and even memory restructuring. All of this is thought to be achieved through repeated reactivation of memory traces during sleep (Born et al., 2006; Diekelmann & Born, 2010b). Indeed, the brain quite literally 'replays' past experiences while we sleep (Wilson & McNaughton, 1994; Skaggs & McNaughton, 1996), and this has been consistently shown to strengthen memories overnight (Dupret et al., 2010; Peigneux et al., 2004; Yotsumoto et al., 2009; Deuker et al., 2013; Schönauer et al., 2017; Zhang et al., 2018). Nowadays, we can tap into this otherwise spontaneous process with a technique called Targeted Memory Reactivation (TMR). During wake, the learning material is paired with sensory cues, usually sounds or odours. The same cues are then covertly re-presented to the subjects while they sleep, in hope to trigger reactivation of the associated memories and thus boost their consolidation (Oudiette & Paller, 2013; Schouten et al., 2017; Cellini & Capuozzo, 2018; Paller et al., 2017).

TMR has taught us a whole lot about the mechanisms underlying memory consolidation during sleep, particularly with regards to memory reactivation. However, a number of critical questions remain unanswered. *What is the evolution of the reactivated memory representation? Do they change over time? And how long do the effects of TMR last?* The aim of this thesis is to advance our understanding of the role of sleep in long-term procedural memory consolidation, with a particular use of TMR. This chapter will provide a broad overview of the current state of knowledge with regards to sleep, memory, and their intertwined history. I will first introduce the basic physiology of sleep and the oscillatory patterns that characterise each sleep stage. Then, I will focus on memory and its relationship with sleep, discussing the most prominent models of sleep-dependent memory consolidation. Next, I will delve deeper into memory reactivation and review some of the major breakthroughs in both human and rodent literature. I will also take a closer look at TMR, how it works and what are the different applications of this technique. A unique insight that TMR offers into the mechanisms underlying memory reactivation during sleep will be highlighted. Finally, attention will focus on the recent efforts to tackle the long-term effects of reactivating memories during sleep. The role of sleep in procedural memory consolidation will be discussed as well. The chapter will conclude with a summary of the key points and an outline of the main objectives of this thesis.

2 SLEEP AS A PHYSIOLOGICAL STATE

Sleep is not a uniform state. Instead, it consists of several physiological stages characterised by distinct oscillatory patterns (Fig.1). This fundamental property of sleep was brought to light through polysomnography (PSG) - a combination of electroencephalography (EEG), electrooculography (EOG) and electromyography (EMG) often used to study sleep. A closer look into the PSG recordings in humans revealed two main sleep stages: rapid eye movement (REM) sleep and non-rapid eye movement (NREM) sleep, where the latter can be further subdivided into stages 1-4 (Iber et al., 2007). During the night, our body alternates between these two states approximately every 90 minutes. NREM sleep predominates during the first few cycles but as the night progresses the contribution of REM sleep increases (Patel et al., 2020) (as seen on the hypnogram in Fig.1B).

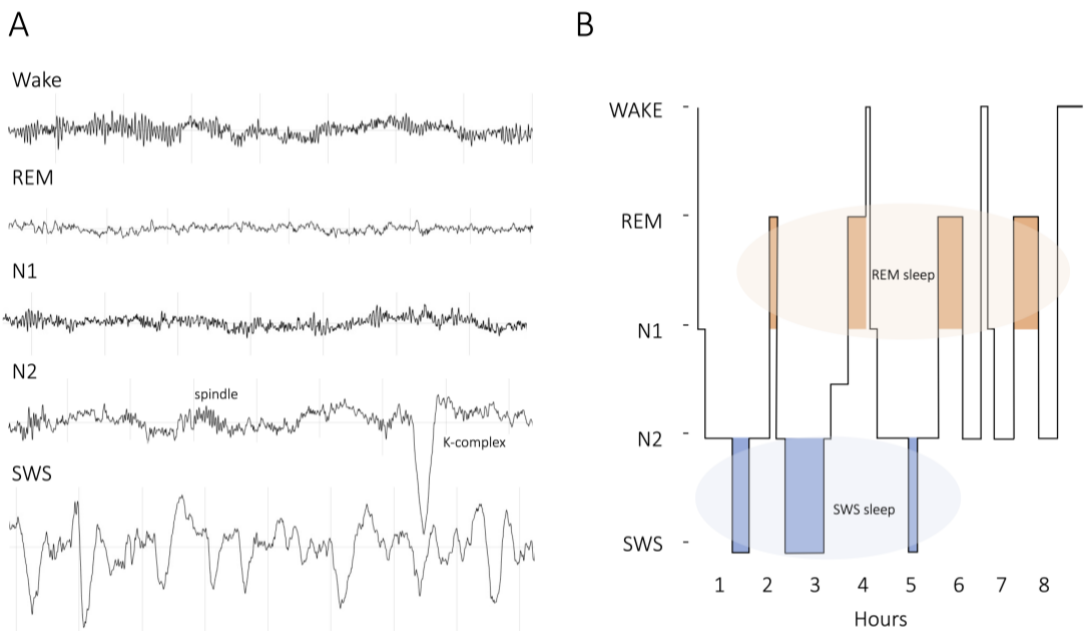

Fig. 1. Sleep physiology. (A) *Exemplary EEG traces for wake and each of the sleep stages.* ***(B)*** *Hypnogram of human sleep. REM: Rapid Eye Movement sleep; N1-N2: Stage 1-2 of Non-Rapid Eye Movement Sleep; SWS: Slow Wave Sleep (stages 3-4 of Non-Rapid Eye Movement Sleep).*

Stage 1 of NREM sleep (N1), also known as 'light sleep', is a transitional stage between wake and sleep. It is characterised by low-amplitude mixed-frequency activity (2-7 Hz) which starts to replace the wake-like alpha rhythm (8-13 Hz) (Silber et al., 2007). Slow rolling eye movements and vertex sharp waves can also be observed (Silber et al., 2007). N1 constitutes only around 5% of the total sleep time (TST) (Patel et al., 2020) and is often followed by stage 2.

Stage 2 of NREM sleep (N2) makes up the majority (50%) of the night (Patel et al., 2020). Thalamo-cortical sleep spindles and K-complexes are the two morphologically distinct waveforms that emerge and predominate during this sleep stage. Sleep spindles are rapid (≥ 0.5 s) bursts of high frequency activity that originate in thalamus. The exact frequency range is still being debated but it is generally thought to be between 11 Hz and 16 Hz (Iber et al., 2007: 11-16 Hz; Barakat et al., 2013: 11-15 Hz; Schabus et al., 2007: 11-15 Hz; Fernandez & Lüthi, 2020: 10-15 Hz; Purcell et al., 2017: 11-15 Hz; Cox et al., 2017: 9-16 Hz). A further subdivision occurs between slow (<13 Hz) and fast (>13 Hz) spindles, where the former dominate over frontal cortical regions and the latter are widespread over centro-parietal EEG sites (Mölle et al., 2011; Schabus et al., 2007; Barakat et al., 2013; Cox et al., 2017). Sleep spindles have been implicated in memory and learning (Ulrich, 2016; Fogel & Smith, 2011; Peyrache & Seibt, 2020), intellectual abilities (Fogel & Smith, 2011), maintaining sleep architecture (Purcell et al., 2017; Kim et al., 2012; Ni et al., 2016; Wimmer et al., 2012), sensory gating and processing (Dang-Vu et al., 2010; Wimmer et al., 2012; Sato et al., 2007), as well as synaptic plasticity (Rosanova & Ulrich, 2005) (see Fernandez and Lüthi (2020) for review). K-complexes, in turn, are cortically generated slow oscillations (< 1 Hz, ≥ 0.5 s), each composed of a negative sharp wave followed by a longer-lasting positive component (Amzica & Steriade, 1997). They can occur spontaneously or in response to external stimuli (Fushimi et al., 1998). In fact, the emergence of K-complexes upon sound presentation led to their discovery (Loomis et al., 1938). K-complexes are thought to be involved in both sleep maintenance (Forget et al., 2011; Cash et al., 2009) and arousals generation (Roth et al., 1956), while their function in memory has also been suggested (Forget et al., 2011; Cash et al., 2009; Johnson et al., 2010) (see Ioannides et al. (2019) for review). Due to their slow rhythmicity and waveform, K-complexes and slow waves (see below) are often believed to be identical phenomena. This, however, has been a topic of debate (Amzica & Steriade, 1997; Halász, 2016; Cash et al., 2009).

Stage 3 and 4 of NREM sleep have now been combined into a single sleep stage (N3), usually referred to as slow-wave sleep (SWS) (Iber et al., 2007). SWS is considered the deepest and most restorative stage of sleep. It constitutes around 15-20% of the TST in adults (Shrivastava et al., 2014) but its total duration is known to decrease with age (Ohayon et al., 2004). Although sleep spindles can be observed during SWS, they occur less frequently than in N2. Instead, SWS is characterised by high-amplitude, low-frequency brain waves, namely slow oscillations (SOs, < 1 Hz) and delta waves (1-4 Hz) (Steriade, 2006). This slow-wave activity

(SWA) is generated cortically and reflects the alternations between states of cortical excitation, or depolarisation (UP states), and relative neuronal silence, or hyperpolarisation (DOWN states) (Amzica & Steriade, 1998). Hippocampal sharp wave ripples (SWRs) are transient (~100 ms) bursts of high frequency oscillations (150-250 Hz) (Buzsáki, 1986; Ylinen et al., 1995) that are temporally linked to sleep spindles and SOs (Clemens et al., 2007). Although not visible on a scalp EEG, SWRs are a common feature of SWS. Importantly, they have been proposed to play an active role in memory consolidation (Wilson & McNaughton, 1994) and synaptic plasticity (Buzsáki, 1986), as discussed in more detail later (see section *3.2 Sleep and memory models*). Thus, SWS is well known to be important for memory processing (Diekelmann & Born, 2010a; Diekelmann & Born 2010b; Walker, 2009; Rasch & Born, 2013; Born, 2010). However, it has also been linked to homeostatic regulation (Tononi & Cirelli, 2003), energy restoration (Dworak et al., 2010), cleaning of metabolites (Xie et al., 2013), immune system (Lange et al., 2010) and hormonal regulation (Born & Fehm, 1998; Sassin et al., 1969) (see Léger et al. (2018) for review).

The final sleep stage is **REM sleep**, accounting for ~25% of the TST (Shrivastava et al., 2014). Initially referred to as 'paradoxical sleep', REM sleep EEG highly resembles that of wakefulness, with low-amplitude, mixed frequency activity and rapid eye movements. The distinguishing features include muscle atonia (visible as low chin EMG) and sawtooth waves (2-6 Hz) (Iber et al., 2007). REM sleep is also known for the frequent occurrence of vivid dreams (Crick & Mitchison, 1983). Of particular importance here are the phasic events recorded in pons, lateral geniculate nucleus and occipital cortex – the ponto-geniculo-occipital (PGO) waves. They are thought to trigger the rapid eye movements of REM sleep and give rise to the visual dream imagery (Amzica & Steriade, 1996; Karashima et al., 2001; Ramírez-Salado & Cruz-Aguilar, 2014). Nevertheless, the PGO waves cannot be clearly identified on a human scalp EEG and the majority of evidence for their existence comes from deep brain recordings in experimental animals (Amzica & Steriade, 1996; Karashima et al., 2001; Datta, 1997) (but see Fernández-Mendoza et al. (2009) and Lim et al. (2007) for direct observations in humans).

In fact, evidence from both human and **animal literature** is key in understanding sleep and its relationship with memory. Thus, it is important to appreciate the differences and similarities between species (reviewed by Campbell and Tobler (1984)). Mice and rats, for instance, sleep during the day and in shorter bouts than humans. Furthermore, rodent literature often lacks the distinction between the different subdivisions of NREM sleep

(Genzel et al., 2014) (but see Lacroix et al. (2018)). Nevertheless, the key EEG waveforms present during sleep, such as spindles, slow waves and SWRs, are remarkably similar between humans and rodents, making them one of the most common animal model in sleep research (Datta & Hobson, 2000; Doran et al., 2008; Tobler et al., 1992).

3 ROLE OF SLEEP IN MEMORY

Memory is the ability to save and recover information. It is therefore essential to every aspect of our life, from learning from the past to planning for the future. There is a common belief that memories are physically stored in the brain, with a fixed form and in a particular location. Thanks to the advances in neuroscience and cognition over the last century we now know that memories are not stored through the act of creation (i.e., birth of new cells), but instead through the act of strengthening what already exists – the connections between neurons. Memories can therefore be stored across different brain regions and for different lengths of time. Given the tremendous amount of research in the memory field, the following section will not attempt to cover all its aspects. Rather, it will provide a broad overview of the various types of memories and memory processes, particularly in relation to sleep.

3.1 DIFFERENT FACETS OF MEMORY

3.1.1 MEMORY TYPES

Memory can be divided into many types, with the key distinction typically made between declarative (explicit, knowing *that*) and nondeclarative (implicit, knowing *how*) memories (Cohen, & Squire, 1980; Squire, & Zola, 1996) (Fig.2). **Declarative memory** refers to information, such as facts (semantic) or events (episodic), that can be consciously recalled, or 'declared'. The division between semantic and episodic memory is based on the presence (episodic) or absence (semantic) of a spatial and temporal context within which the memory is being remembered (Tulving, 1983). On the other hand**, nondeclarative memory** refers to a heterogeneous collection of abilities, such as procedural or perceptual skills, that are learned without awareness and expressed through performance rather than conscious recollection (Squire & Zola, 1996; Squire, 2004). While formation of declarative memories is thought to be dependent on hippocampus and other structures in the medial temporal lobe (MTL), nondeclarative memories are generally considered hippocampus-independent and supported by various other brain structures (Squire & Zola, 1996; Squire & Dede, 2015).

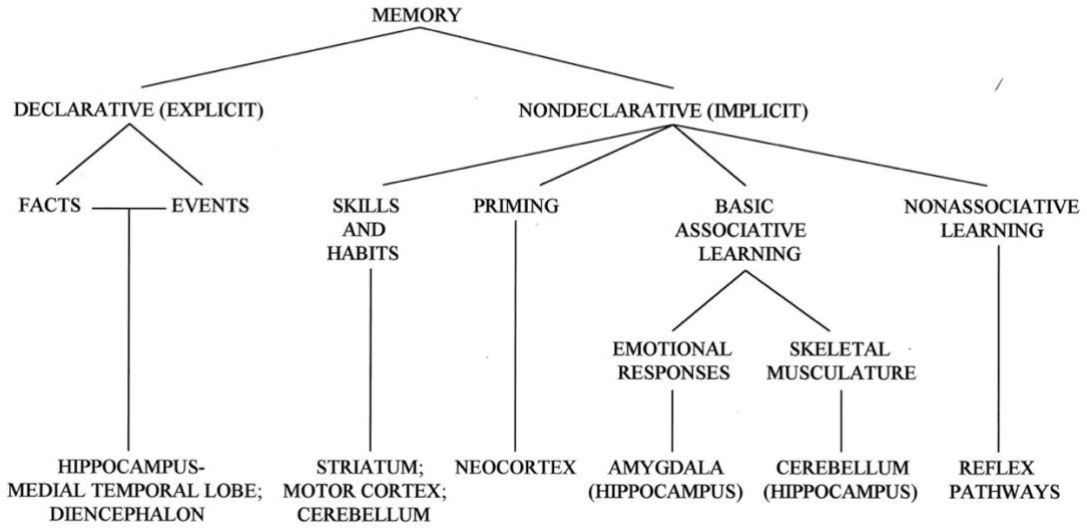

Fig. 2. The taxonomy of memory systems and the associated brain structures. *Figure source: Thompson & Kim (1996).*

The taxonomy of memory systems provides a practical way of referring to the different kinds of memories and, in an experimental context, memory tasks. However, it should be pointed out that not all forms of learning conform to this division. Language, for instance, includes both declarative and nondeclarative components (Ullman, 2004; Ullman, 2001). Likewise, some procedural tasks have a declarative aspect to them (e.g., a motor sequence) and have been shown to depend on the hippocampus (Albouy et al., 2008; Albouy et al., 2013a; Albouy et al., 2013b; Albouy et al., 2015). The necessity of consciousness for declarative memories formation has also been questioned (Henke, 2010), with several studies reporting successful encoding of both episodic (Wuethrich et al., 2018; Schneider et al., 2021) and semantic (Henke et al., 2003; Duss et al., 2014) memories without conscious awareness. Regardless of the classification system, however, sleep seems to be important for all kinds of memories (Stickgold, 2005; Rasch & Born, 2013) and at different stages of their formation and restructuring, as discussed below.

3.1.2 MEMORY PROCESSES

The process of memory formation starts with **encoding**, whereby perception of a stimulus results in the emergence of a memory trace. The newly encoded traces are initially susceptible to changes and forgetting. However, with time and through **consolidation**, memories gradually become more stable, resistant to interference, reorganised, and integrated into the existing networks of knowledge (i.e., schemas) (Rasch & Born, 2013). The

reorganisation that happens during this stage can also lead to gist abstraction (or generalisation) and eventually formation of a new schema (Stickgold & Walker, 2013; Morris, 2006). The stored memories can then be accessed or recalled during a process called memory **retrieval** (Rasch & Born, 2013). However, recalling or 'reactivating' an already consolidated memory trace makes it once again fragile, requiring another consolidation to take place. This process, termed **reconsolidation**, allows memories to be modified and updated every time they are retrieved (Alberini & LeDoux, 2013).

The memory function of sleep starts with memory encoding, wherein sleep is thought to restore encoding capacity and thereby increase brain's ability to learn new information (Mander et al., 2011; Cousins et al., 2018; Van Der Werf et al., 2009; Antonenko et al., 2013). As far-fetched as it may seem, some recent studies suggest that the formation of new memories is also possible *during* sleep (Arzi et al., 2012; De Lavilléon et al., 2015; Andrillon et al., 2017; Züst et al., 2019). However, it is the sleep's role in consolidation that has gathered the greatest attention, and justifiably so (Diekelmann & Born, 2010b; Rasch & Born, 2013; Stickgold, 2005).

3.1.3 MEMORY CONSOLIDATION

The literature distinguishes between two types of memory consolidation: cellular, or synaptic consolidation and systems consolidation (Dudai, 2004; Frankland & Bontempi, 2005). **Synaptic consolidation** takes place minutes to hours after learning, transforming memory representation at a single-cell level. It involves changes in synaptic efficiency through modulation of gene expression and reorganisation, modification, and synthesis of synaptic proteins. All these lead to synaptic remodelling and growth, thereby stabilising the memory trace (Dudai, 2004). Long-term potentiation (LTP) and long-term depression (LTD) are the best understood forms of synaptic plasticity (Clopath, 2012). Which synapses will be primed for long-lasting changes (and thereby which memory traces will last) is explained by the **synaptic tagging and capture (STC) hypothesis** (Frey, & Morris, 1997; Redondo & Morris, 2011). The STC proposes that a strong stimulation of a synaptic pathway initiates two dissociable events: synthesis of plasticity-related proteins (PRPs) and creation of a local 'tag' at the potentiated synapse. The tagged synapses will then capture the diffusible PRPs required for the maintenance of late-LTP, as well as structural plasticity. Although the exact nature of the tag is still unknown, it is believed that the STC mechanism allows the tagged synapses to persist (Frey, & Morris, 1997; Redondo & Morris, 2011). Recently it has been

proposed that sleep may play a role in this process (Seibt & Frank, 2019). According to the new model, the synaptic tagging happens during wakefulness, while the reactivation of primed neurons and synapses during NREM sleep promotes synaptic capture of PRPs. Translation of the captured proteins is thought to occur during REM sleep, leading to structural plasticity and stabilisation of memory traces (Seibt & Frank, 2019). The reactivation events during NREM sleep are also believed to play a key role in systems consolidation, as detailed below.

Systems consolidation occurs over relatively long periods of time (from days to even years), where the newly encoded memory representations are rearranged on a neural circuit level or, in other words, throughout the brain (Dudai, 2004; Frankland & Bontempi, 2005). The **standard model for systems consolidation** has its origin in the observation that MTL damage produces not only anterograde amnesia, i.e., inability to form new memories, but also temporarily graded retrograde amnesia, i.e., loss of recent but not remote memories (Penfield & Milner, 1958; Scoville & Milner, 1957; Corkin, 2002). Thus, it has been postulated that the MTL must have a time-limited role in memory storage and that the information is, at some point, transferred elsewhere for a permanent store. Indeed, at the core of a **two-stage model of memory consolidation** is the idea that the newly encoded memories are initially saved in a fast-learning store (e.g., hippocampus in case of declarative memories) but, over time, they are moved to a long-term slow-learning store (e.g., the neocortex) wherein they are stabilised, integrated with existing traces, and reorganised (Marr, 1970; Squire & Alvarez, 1995). As the memories become gradually distributed over the cortical networks, they become independent of the hippocampus (Squire & Alvarez, 1995) and thus resistant to catastrophic interference with the incoming information (McClelland et al., 1995). The model has been computationally implemented in a **Complementary Learning Systems (CLS)** framework (McClelland et al., 1995), which explains *why* the brain needs the two complementary, yet differentially specialised memory systems. Importantly, it also posits that the transfer of memories between the two systems occurs through repeated reinstatement of memory traces in the fast-learning store. This, in turn, gives rise to the reinstatement in the slow-learning store, gradually strengthening the cortico-cortical connections and allowing the traces to be fully integrated into the pre-existing neocortical networks. This hippocampal-cortical network reactivation is believed to occur both during active rehearsal and inactive periods of rest, including sleep (Marr et al., 1970; McClelland et al., 1995; Rasch & Born, 2013).

Nevertheless, the importance of sleep in memory consolidation was speculated long before the formulation of the two-stage model of memory consolidation. In fact, several models of sleep and memory have been formulated in the history of sleep research, with the most prominent ones outlined in the section below.

3.2 SLEEP AND MEMORY MODELS

In 1885, Hermann Ebbinghaus noticed reduced forgetting after an interval containing sleep (Ebbinghaus, 1885). This provided the first instance of the beneficial effects of sleep on memory, with similar observations later made by others (Heine, 1914; Jenkins & Dallenbach, 1924; Van Ormer, 1933). At the time, it was believed that **sleep plays a passive role in memory consolidation** (Wixted, 2004). While the decreased amount of encoding and interference with the consolidation process during sleep would indeed explain the reduced forgetting afterwards, this view was challenged by studies reporting differential effects of SWS and REM sleep on memory consolidation (Barrett & Ekstrand, 1972; Ekstrand, 1967; Fowler, 1973; Plihal & Born, 1997; Plihal & Born, 1999; Schoen & Badia, 1984; Yaroush et al., 1971). This led to the formulation of the **Dual Process Hypothesis** which assumes that consolidation of different types of memories is supported by different sleep stages (Smith, 2001; Gais & Born, 2004; Rauchs et al., 2005). Specifically, it posits that the first half of the night (rich in SWS) benefits declarative memories, while the second half (rich in REM sleep) supports nondeclarative and emotional memories, as evidenced by the 'night-half paradigm' studies (Yaroush et al., 1971; Fowler, 1973; Plihal & Born, 1997; Plihal & Born, 1999; Wagner et al., 2002; Smith, 1995). However, the Dual Process Hypothesis was later challenged by studies showing reverse dissociation (Huber et al., 2004; Huber et al., 2006; Aeschbach et al., 2008; Gais et al., 2000; Fogel et al., 2007; Rauchs et al., 2004). An alternative hypothesis - **the Sequential Hypothesis** - posits that the memory function of sleep arises from orderly succession of NREM sleep and REM sleep (Giuditta et al., 1995; Ambrosini & Giuditta, 2001). Thus, it focuses on the interaction and complementary roles of the different sleep stages in memory consolidation, regardless of the memory type. Specifically, the Sequential Hypothesis, also referred to as the 'Double-Step' Hypothesis, assumes that the first step of memory consolidation takes place during NREM sleep, whereby non-adaptive, irrelevant, or competing memory traces are eliminated or downscaled. The second step happens during REM sleep, which strengthens the useful memories and integrates them with pre-existing knowledge. The hypothesis has been supported by several studies in rats (Ambrosini et al., 1988a, 1988b, 1992, 1995) and humans (Ficca et al., 2000; Stickgold et al., 2000; Mednick et

al., 2003; Gais et al., 2000). It is important to stress, however, that the Dual Process Hypothesis and the Double-Step Hypothesis are not mutually exclusive - while both NREM and REM sleep are essential for memory consolidation, they could benefit different kinds of memories to different extents (Rauchs et al., 2005; Deliens et al., 2013).

Nowadays, perhaps the most prominent model in the field is **The Active System Consolidation Hypothesis (ASC)** (Fig.3). On the one hand it integrates the two previous models, on the other it goes far beyond the simple distinction between NREM and REM sleep. At the core of the ASC is the idea that sleep plays an active role in memory consolidation and that repeated reactivation of the newly encoded traces during sleep is essential for this process (Born et al., 2006; Diekelmann & Born, 2010b). The model originates from the standard two-stage model of consolidation and assumes that the repeated reinstatement of memory traces that mediates their transfer from the temporal store to the long-term store happens preferentially during SWS. REM sleep is thought to then stabilise the transferred memories through processes of synaptic consolidation. Indeed, as mentioned earlier, SWS is known to be involved in memory processing (Diekelmann & Born, 2010a; Diekelmann & Born 2010b; Walker, 2009; Rasch & Born, 2013; Born, 2010) and both slow-wave ripples (SWRs) and sleep spindles that occur during SWS have been linked to consolidation (SWRs: Wilson & McNaughton, 1994; Zhang et al., 2018; Spindles: Ulrich, 2016; Fogel & Smith, 2011; Peyrache & Seibt, 2020). In fact, hippocampal reactivation was shown to happen during sharp-wave ripples (SWRs) (Zhang et al., 2018; for review see Buzsáki, 2015), while the coordinated interplay, or coupling, between SWRs, thalamocortical sleep spindles and neocortical slow waves is thought to drive the active process of consolidation (Rasch & Born, 2013). At the scalp EEG level, the coupling between the phase of SOs and amplitude of sleep spindles (phase-amplitude coupling) was shown to correlate with performance improvements on several memory tasks (Niknazar et al., 2015; Mikutta et al., 2019; Muehlroth et al., 2019; Hahn et al., 2020; Denis et al., 2020; Schreiner et al., 2021).

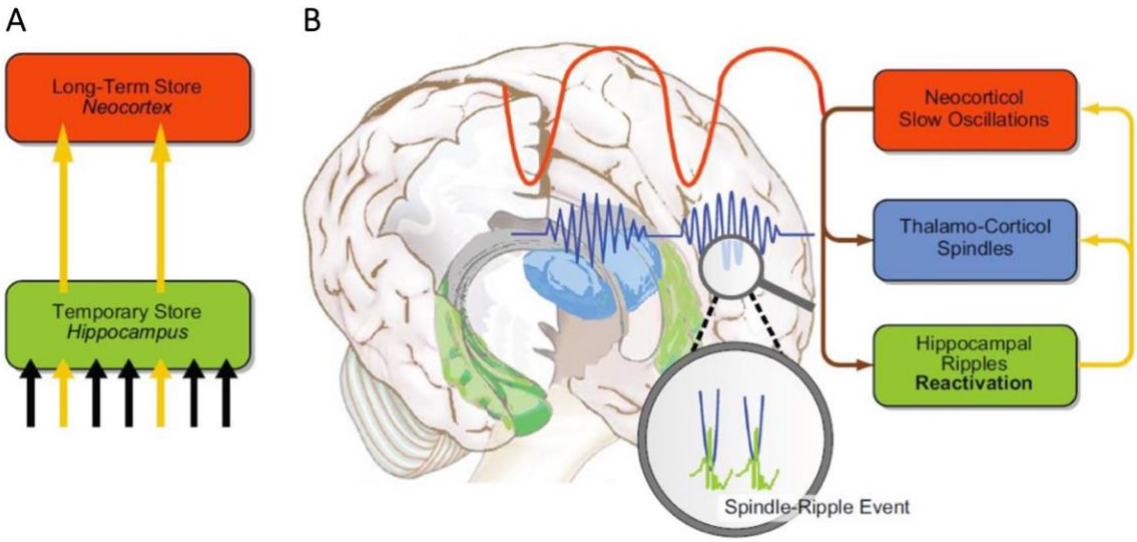

Fig. 3. Active system consolidation model. (A) *The two-stage model of consolidation forms the basis of ASC. New memories are encoded into a temporary store (e.g., hippocampus for the hippocampus-dependent memories) and transferred to the long-term store (i.e., the neocortex) via their repeated reactivation.* ***(B)*** *Systems consolidation occurs during SWS. The cortico-hippocampal dialogue is controlled by neocortical slow oscillations (red), which drive repeated reactivation within the hippocampus. Hippocampal sharp wave ripples (green), that accompany reactivation of neuronal ensembles in the hippocampal networks, synchronise with the excitable troughs of sleep spindles (blue), and together form a 'spindle-ripple event'. The 'spindle-ripple event' itself is nested within the depolarizing up-phase of the slow oscillations, actively driving the transmission of hippocampal memories to the neocortical networks (yellow arrows) and thus memory consolidation (Inostroza & Born, 2013; Latchoumane et al., 2017; Staresina et al., 2015; Klinzing et al., 2019). Figure source: Rasch & Born (2013).*

An alternative view to the now widely accepted ASC is the **Synaptic Homeostasis Hypothesis (SHY)** (Tononi & Cirelli, 2003; Tononi & Cirelli, 2006) (Fig.4). In a nutshell, SHY proposes that sleep restores synaptic homeostasis. According to the model, synaptic strengthening, or potentiation that occurs during wakeful learning increases cellular demands for energy, saturates encoding capabilities and leads to an imbalance between synaptic potentiation and depression. The fundamental function of SWS is to globally down-scale the synaptic weights, thereby restoring the brain's ability to learn and maintaining synaptic homeostasis in check. Importantly, assuming there is a threshold below which synapses become silent, proportional downscaling renders 'weak' synapses ineffective while maintaining the 'strong' ones above the threshold. This leads to enhanced signal-to-noise ratio, promoting memory consolidation and gist abstraction (Tononi & Cirelli, 2003; Tononi & Cirelli, 2014).

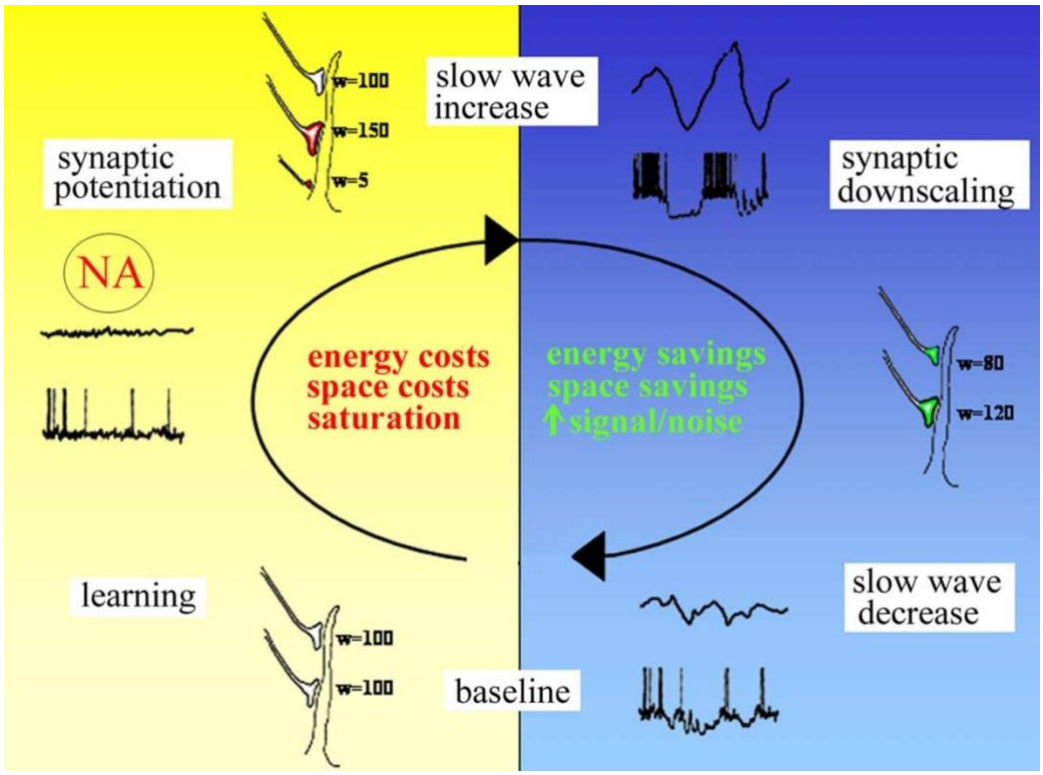

Fig. 4. Synaptic Homeostasis Hypothesis. *Wakeful learning (yellow background) is associated with synaptic potentiation, which is favoured by high levels of noradrenaline (NA) and results in increased synaptic strength of learning-relevant synapses as well as formation of new ones (red). The net increase in synaptic weight (w) increases energy and space requirements, eventually saturating learning capacity. During sleep (blue background), changes in neuromodulatory milieu, combined with high neuronal synchrony, trigger slow oscillations. Slow oscillations drive non-specific downscaling of synapses which results in decreased strength of all synapses or their disappearance all together (green). As the neurons become less synchronised with each other, slow wave activity decreases and a reduction in synaptic downscaling follows. Thus, the total synaptic weight returns to baseline levels, saving energy and space. However, the signal-to-noise ratio has now increased, preserving the newly encoded traces. Figure source: Tononi & Cirelli (2006).*

Although a plethora of studies support SHY (Riedner et al., 2007; Vyazovskiy et al., 2007; 2008; Huber et al., 2007; Faraguna et al., 2008; Bushey et al., 2011), the model has been criticised by the ASC supporters for not acknowledging the *enhanced* protein synthesis and synaptic strength observed during SWS (Nakanishi et al., 1997; Chauvette et al., 2012), and the preferential consolidation of *weak* memories over the strong ones during sleep (Drosopoulos et al., 2007; Kuriyama et al., 2004; Rasch & Born, 2013). On the other side of the debate, the original SHY posits that memory reactivation alone cannot explain the beneficial effects of sleep (Tononi & Cirelli, 2006; Tononi & Cirelli, 2014), especially given that it can also occur outside of sleep (Davidson et al., 2009; Diba & Buzsáki, 2007; Foster & Wilson, 2006; Karlsson & Frank, 2009). However, the latest refinements of the SHY incorporate memory reactivation into the model, suggesting that reactivation during NREM

sleep may protect synapses from downscaling (Tononi & Cirelli, 2014). This is somewhat consistent with the idea that synapses subjected to reactivation are 'tagged' for subsequent potentiation during REM sleep (Diekelmann & Born, 2010b; Rasch & Born, 2013).

Alternatively, reactivated synapses could first undergo selective potentiation and then global downscaling (Lewis & Durrant, 2011). This, in fact, has been proposed as a potential mechanism underpinning schema formation and integration of new information into the pre-existing knowledge networks. Specifically, replay of multiple memories during SWS is thought to strengthen neural connections that are shared between the reactivated memory representation which, when combined with global downscaling, leads to (gist) abstraction of the overlapping elements and gradual formation of a new schema (Lewis & Durrant, 2011). The mechanism is referred to as the '**information Overlap to Abstract**' (iOtA) and forms the basis of the **Broader form of iOtA** (BiOtA) **model** which also considers REM sleep (Lewis et al., 2018). The BiOtA model proposes that while NREM sleep only allows simultaneous reactivation of thematically related memories, REM sleep makes room for concurrent activity in randomly chosen schemas. This leads to the formation of novel links between seemingly unrelated concepts, thereby explaining the role of sleep in creativity and problem solving (Lewis et al., 2018).

4 MEMORY REACTIVATION

The previous section provided a brief outline of sleep and memory models. While most are somewhat competing and others complement each other, all seem to agree on one thing - the importance of memory reactivation during sleep.

4.1 SPONTANEOUS MEMORY REACTIVATION

4.1.1 RODENT LITERATURE

The first evidence for spontaneous memory reactivation during sleep comes from rodent literature surrounding hippocampal place cells. Place cells are hippocampal neurons in CA1 and CA3 which activate when the animal occupies a specific location in the environment (O'Keefe & Dostrovsky, 1971). Almost two decades after place cells' discovery, Pavlides and Winson (1989) demonstrated that place cells' activity in wake influences their firing characteristics during subsequent sleep. The authors allowed rats to enter place fields of

some cells but not others, while recording their activity both during wake and the sleep that followed. Firing rates of the cells that were exposed to their individual place fields during wake increased in subsequent sleep (SWS and REM) relative to the firing rates of the unexposed cells. In a seminal study, Wilson and McNaughton (1994) recorded activity from pairs of hippocampal place cells during both a spatial navigation task and SWS that preceded and followed the run. **Cells that fired together during the task also showed a higher tendency to fire together during the post-run sleep**, but this was not true for the pre-run sleep. Importantly, the pattern of activity during sleep followed a temporal order of cell firing during wake, giving rise to the term **'replay'** (Skaggs & McNaughton, 1996) (Fig.5) (for the correct use of terms 'replay' vs 'reactivation' as well as many others, see Genzel et al., 2020).

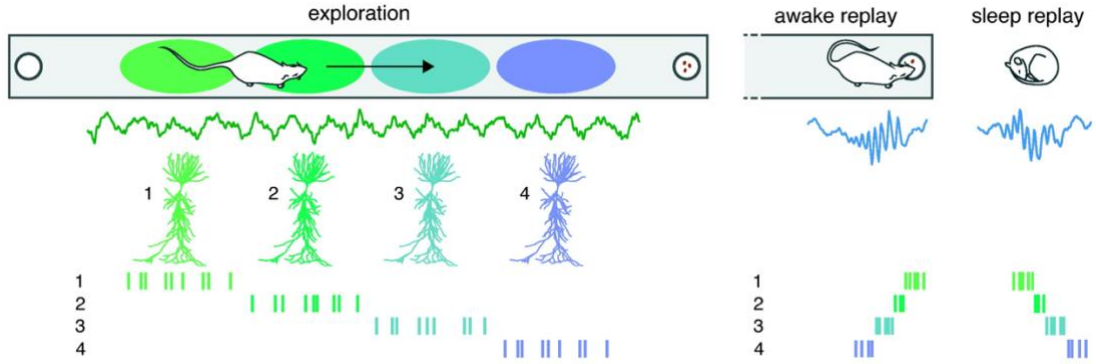

***Fig. 5. Sequential replay of neuronal activity during sleep**. During awake exploration, hippocampal place cells (here four cells shown) are successively activated as the animal enters their place fields (four ellipses coloured as their respective place cells) while running on a linear track. This yields a sequence of neuronal activity (vertical bars) which is then replayed in a reverse order during the subsequent wake period. When the animal enters slow-wave sleep, the same sequence of neuronal activity is replayed again but this time in a forward manner. Both awake and sleep replays are temporally compressed and occur predominantly during sharp-wave ripples (blue traces). Figure source: Girardeau & Zugaro (2011).*

Since then, a lot has been revealed about the nature and mechanisms of memory reactivation, or replay, during sleep (O'Neill et al., 2010; Sutherland & McNaughton, 2000). The spontaneous reinstatement of firing patters during SWS was found to be particularly **strong during SWRs** (Wilson & McNaughton, 1994; Kudrimoti, et al., 1999; Girardeau et al., 2014; Nakashiba et al., 2009). We further know that replay of sequential experiences is **compressed in time** (Skaggs et al., 1996; Nádasdy et al., 1999; Hirase et al., 2001; Lee & Wilson, 2002; Ji & Wilson, 2007) and decays after learning (Shen et al., 1998; Kudrimoti et al., 1999; Battaglia et al., 2005). Reactivation during sleep has also been observed **outside hippocampal place cells** but often preceded by hippocampal reactivation (Ji & Wilson, 2007;

Lansink et al., 2008; Lansink et al., 2009). This is in line with the ASC and the idea that recently acquired memories are transferred from the hippocampus to neocortex through repeated reinstatement of memory traces during SWS (Diekelmann & Born, 2010b; Born et al., 2006). The non-hippocampal areas that exhibit memory reactivation include parietal (Qin et al., 1997), prefrontal (Euston et al., 2007; Peyrache et al., 2009; Benchenane et al., 2010; Johnson et al., 2010), visual (Ji & Wilson, 2007) and sensorimotor (Hoffman & McNaughton, 2002) cortices, as well as ventral striatum (Lansink et al., 2008; Lansink et al., 2009; Pennartz et al., 2004). Furthermore, reactivation was shown to **correlate with K-complexes, spindles, and slow oscillations** (Johnson et al., 2010), providing additional support for the ASC.

Nevertheless, if reactivation of memory traces during sleep is really *the* mechanism underlying memory consolidation, then reactivation patterns should not only reflect the learning experience, but they should also show a **relationship with subsequent behavioural performance**. Indeed, impaired reactivation in aged rats correlated with low spatial memory scores (Gerrard et al., 2008), while suppression of hippocampal SWRs or SWR-associated activity after learning impaired subsequent memory performance (Girardeau et al., 2009; Nakashiba et al., 2009; Ego-Stengel & Wilson, 2010). Furthermore, reactivation of newly encoded spatial memory traces during offline rest periods predicted later memory recall (Dupret et al., 2010). Human literature also provides a lot of compelling evidence in this regard, as discussed in sections *4.1.2 Human studies* and *4.2 Targeted Memory Reactivation*.

While rodent evidence for memory reactivation during SWS is indisputable, the literature regarding **REM sleep reactivation** is scarce, but not inexistent (Hennevin et al., 1995; Poe et al., 2000; Louie & Wilson, 2001; Howe et al., 2019; Eckert et al., 2020). Interestingly, the speed of temporal sequence reinstatement during REM sleep was found to be similar to, or even slower than, the timescales seen in wake (Louie & Wilson, 2001). This, together with the wake-like EEG patters of REM sleep raises the possibility that reactivation during REM sleep may share some characteristics with wake activity. As a matter of fact, reactivation can also occur outside sleep, especially during awake periods of rest (Carr et al., 2011; Tambini, & Davachi, 2019). Just like reactivation during sleep, **wake reactivation** also happens during SWRs (Foster & Wilson, 2006). Strikingly though, and in contrast to neuronal replay during sleep (Lee & Wilson, 2002), wake replay can occur in reverse order (Foster & Wilson, 2006; Fig.5) as much as it does in the forward one (Diba & Buzsáki, 2007). Likewise, in addition to 'local' replay (i.e., from the current environment), wake periods also showed reinstatement of 'remote' experiences from the past (Karlsson & Frank, 2009). Thus, it has been suggested

that awake replay could play a different but perhaps complementary role to sleep replay (Carr et al., 2011). A particularly intriguing observation is that of hippocampal sequence events predicting future (but yet unknown) trajectories, suggesting that wake replay could serve as a planning mechanism during goal-directed behaviour (Pfeiffer & Foster, 2013). A related phenomenon termed 'preplay' describes a temporal pattern of activity that arises during an offline period *preceding* a novel experience, but which sequential organization reflects the order in which the same cells would eventually fire during that experience (Dragoi & Tonegawa, 2011; Ólafsdóttir et al., 2015; Dragoi & Tonegawa, 2013). The phenomenon is, however, still debated (Silva et al., 2015; Eichenbaum, 2015).

4.1.2 HUMAN STUDIES

Although the amount of evidence for memory reactivation in humans is growing, it is experimentally limited when compared to animal studies. Human sleep literature mostly relies on the use of **non-invasive imaging techniques**, such as EEG, Positron Emission Tomography (PET) or functional Magnetic Resonance Imaging (fMRI), which suffer from substantially lower spatial and temporal resolution than cellular recordings. Nevertheless, a handful of studies using these methods were able to show that brain regions active during learning reactivated during subsequent sleep (Maquet et al., 2000; Peigneux et al., 2003; Peigneux et al., 2004; Yotsumoto et al., 2009). For instance, brain areas that were active during a serial reaction time task execution (including cuneus, premotor cortex, and mesencephalon) were also active during subsequent REM sleep, but more so in the trained than the untrained subjects (Maquet et al., 2000). A few years later, the same group showed higher functional connectivity between the task-related regions during REM sleep of trained vs untrained participants (Laureys et al., 2001), and a correlation between pre-sleep performance levels and the amount of cuneus reactivation during subsequent REM sleep (Peigneux et al., 2003). Evidence for memory reactivation during SWS was obtained using a spatial navigation task, whereby hippocampal activation during route learning in a virtual town was reinstated during SWS that followed. Importantly, the amount of hippocampal reactivation showed a positive correlation with next-day memory performance (Peigneux et al., 2004). Similarly, primary visual cortex activation in post-training NREM sleep correlated with later performance on a visual perceptual learning task (Yotsumoto et al., 2009).

The studies discussed so far used univariate analysis of imaging data which, simply speaking, averages functional activity of cerebral blood flow over relatively long periods of time.

Although the approach allows to identify regions that are active during awake learning and post-learning sleep, it cannot be used to establish correspondence between patterns of brain activations, which is a crucial aspect necessary to demonstrate that memory reaction is taking place. In turn, pattern classification methods such as **Multivariate Pattern (Classification) Analysis (MVPA)**, **Representational Similarity Analysis (RSA)** and **machine learning classifiers** can help address this issue. Indeed, with the use of MVPA of fMRI data Deuker et al. (2013) identified spontaneously reoccurring, content-specific activation patterns from encoding during post-learning sleep and rest period. Furthermore, they were able to show that the frequency of these reactivation events for each stimulus in a previously learned paired-associate learning task predicted subsequent memory success on the respective items. Similar results were obtained when MVPA was performed on sleep EEG data to determine if participants had seen pictures of faces or houses the day before (Schönauer et al., 2017). Again, content-related patterns of brain activity were successfully decoded during both NREM and REM sleep, and the strength of memory reprocessing during SWS sleep correlated with memory performance during later recall (Schönauer et al., 2017). Recently, Sterpenich et al. (2021) used a more advanced pattern recognition approach to demonstrate that spontaneous reactivation in human sleep favours rewarded information, and that the activity in task-related areas during sleep predicts subsequent performance on the task. Finally, Zhang et al. (2018) combined intracranial EEG (iEEG) with RSA to study SWR-associated replay in human epilepsy patients. They found that stimulus-specific activity was spontaneously reactivating during both waking state and sleep, but only ripple-triggered replay during NREM sleep was associated with memory processes (Zhang et al., 2018).

The studies reviewed here provide compelling evidence for memory reactivation in human sleep. Combined with rodent literature, they offer a valuable insight into the possible neurophysiological mechanisms underlying memory consolidation during sleep. However, the methods described so far can only provide *correlational* link between the detected activity during sleep and post-sleep memory performance, thus inferring a relationship between memory reactivation and consolidation. Targeted Memory Reactivation (TMR) provides a means to demonstrate a *causal* link between the two.

4.2 TARGETED MEMORY REACTIVATION (TMR)

4.2.1 EARLY ATTEMPTS TO CUE MEMORIES DURING SLEEP

TMR involves associating learning items with sensory stimuli (usually sounds or odours) during wake and then covertly re-presenting these stimuli during sleep in hope to bias the naturally occurring memory reactivation process towards the cued items. The aim of this procedure is to selectively improve memory consolidation of the cued material, as assessed in subsequent memory tests. Some early attempts to manipulate memories during sleep with cues to recent learning had been made even before memory reactivation was discovered (Emmons & Simon, 1956; Tilley, 1979; Hars et al., 1985; Hars & Hennevin, 1987; Guerrien et al., 1989). Using a classical fear-conditioning task, Hard and colleagues (Hars et al., 1985; Hars & Hennevin, 1987; Hars & Hennevin, 1990) cued rats with a stimulus previously associated with an electrical shock (conditioned stimulus, CS) during different stages of post-learning sleep. Animals cued during REM sleep showed performance improvements (Hars et al., 1985), whereas cueing in SWS sleep resulted in impaired learning (Hars & Hennevin, 1987). Although unsuccessful, the first attempt to cue memories in human sleep was made as early as in 1956 by Emmons & Simon. A fraction of previously learned words was repeated to participants during sleep, but no evidence of memory improvements was found (Emmons & Simon, 1956). However, when participants were presented with pictures of objects and spoken names of half of these objects were repeated to them during NREM sleep, substantial memory benefits were observed for the cued items (Tilley, 1979). On the other hand, auditory cueing during REM sleep, whereby sounds associated with the learned material were re-presented again concurrently with eye movement during sleep, improved performance on a Morse code task (Guerrien et al., 1989) and a complex logic task (Smith & Weeden, 1990).

Despite the promising results brought by these early studies, the potential for targeting memory reactivation during sleep remained rather neglected until relatively recently. This was largely due to the criticism of ‘sleep learning’, whereby a lack of proper electrophysiological verification of sleep would pose a risk of stimuli application during brief periods of waking (Oudiette & Paller, 2013).

4.2.2 TMR REVIVED

Fuelled by the early efforts to cue memory reactivation during sleep, **Rasch et al. (2007)** revived the TMR field. In their seminal study, the team successfully cued declarative memories during SWS using an **olfactory stimulus** (Fig.6). Participants learned an object-location task while smelling a scent of a rose. This contextual olfactory stimulus was re-presented to the participants again during SWS, without disrupting their sleep and in hope to modulate hippocampus-dependent declarative memories. Indeed, next-day retention of the object-location pairs was enhanced for the TMR group as compared to any of the control groups (Fig.6B). Furthermore, the TMR procedure was shown to elicit a functional response in the hippocampus, suggesting a hippocampus-dependent reactivation of the cued memories (Rasch et al., 2007).

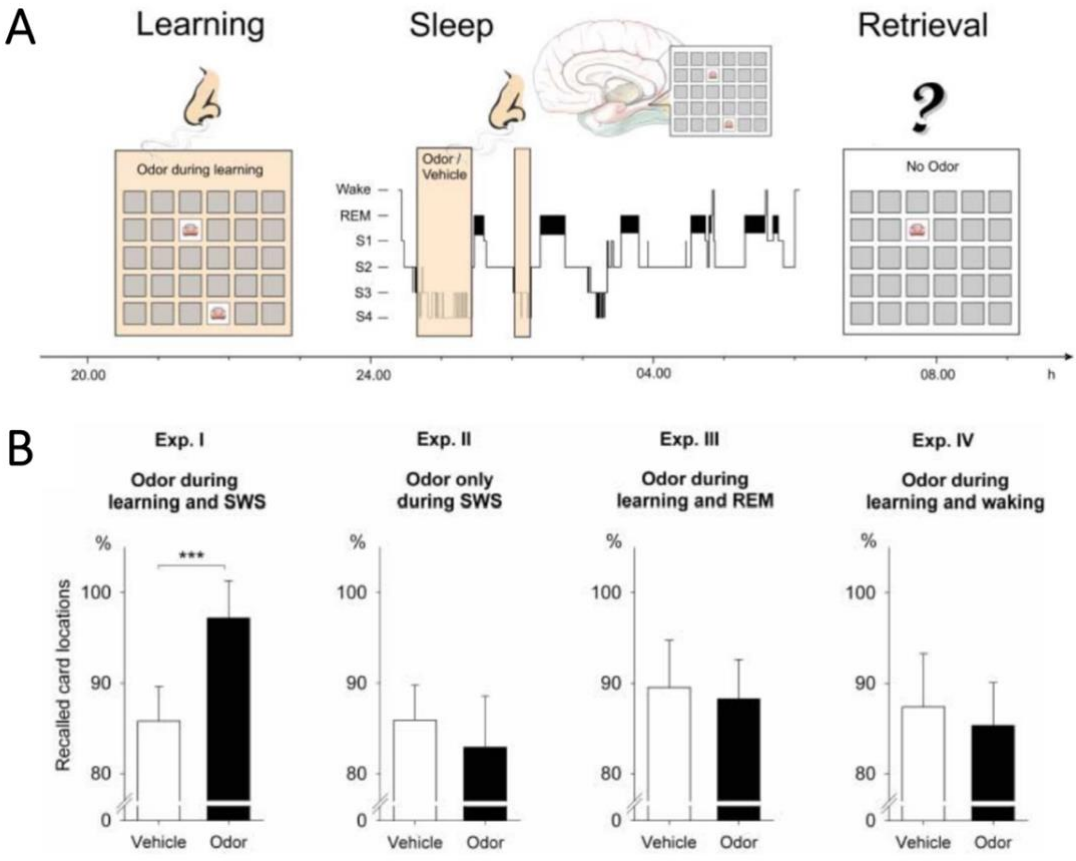

Fig. 6. A seminal study in the TMR field. (A) *Rasch and colleagues administered a rose odour while the participants were learning an object location task and re-presented the same odour (or vehicle) during subsequent bouts of SWS. Memory retrieval was tested the next day.* ***(B)*** *Retention performance on the object location task was enhanced only when a contextual odour (i.e., previously paired with learning) was re-presented during SWS (Exp. I). Odour that was not associated with the learned material and only presented during SWS did not differ from an*

odourless vehicle (Exp. II). Likewise, cueing during REM sleep (Exp. III) or wakefulness (Exp. IV) was ineffective. Figure source: Rasch et al. (2007).

Triggering memory reactivation using odour cues has its advantages, including the fact that puffs of scented air are unlikely to disrupt sleep (Carskadon & Herz, 2004). Unlike in other sensory systems, olfactory information is projected directly to the hippocampus (Zelano & Sobel, 2005), thus explaining why odours evoke memories in such a profound way when compared to other senses (Herz, 2016). However, odour TMR has a relatively low specificity, in a sense that it can only cue contextual memory of the task.

Although potentially much more disruptive than odour cueing, TMR with sound stimuli can achieve much higher specificity, allowing *individual* task items to be reactivated. Indeed, **auditory TMR** of the same object-location task was shown to strengthen individual memories (**Rudoy et al., 2009**). Each learning pair was associated with a semantically related sound and half of the sounds were covertly re-played to the participants in NREM sleep. During a post-nap recall test, locations of objects cued by their sounds during sleep were remembered more accurately than those of the uncued items. Thus, the authors argue that presenting auditory cues during sleep induces preferential processing of the corresponding memories (Rudoy et al., 2009).

Alongside the growing excitement around TMR, a fundamental question remained unanswered: does TMR *trigger* new reactivation events, or does it only tap into this naturally occurring phenomenon? The answer came from **Bendor & Wilson (2012)** who recorded place cells' activity in the hippocampus during awake learning and subsequent sleep. Rats learned to associate different sounds (sound L and sound R) with reward locations (left vs right end of the track). The task-related sounds, as well as meaningless tones, were played to the animals during post-learning sleep. The experiment revealed that TMR cues have no effect on the overall number of the reactivation events, which was the same regardless of the type of stimulus delivered. However, re-playing sound L during sleep resulted in higher firing rate of place cells with left-sided place fields than those with right-sided place fields, whereas the opposite was true for sound R. Thus, the results demonstrated that **TMR can bias the content of reactivation events** towards the memories associated with the cue.

Since then, TMR has mostly been applied during SWS, however beneficial effects of cueing memory reactivation during other sleep stages have been reported as well. Likewise, TMR

application has gone beyond strengthening simple declarative memory tasks to include real-life settings. Numerous review articles have done an excellent job at integrating the currently available data (Oudiette & Paller, 2013; Schouten et al., 2017; Cellini & Capuozzo, 2018; Paller et al., 2017). In the following subsections I will also take a closer look at this cutting-edge sleep manipulation technique and what it has taught us about sleep.

4.2.3 BEYOND SIMPLY BOOSTING MEMORIES

SWS is by far the most common choice for TMR and has been mainly shown to strengthen **declarative memories**. Beneficial effects of TMR delivered during either SWS alone or NREM sleep in general have been demonstrated not only for the object-location task (Rasch et al., 2007; Rudoy et al., 2009; Diekelmann et al., 2011; Diekelmann et al., 2012) but also associative learning (Cairney et al., 2017; Cairney et al., 2018), spatial navigation (Shimizu et al., 2018) and language acquisition (Göldi et al., 2019b; Fuentemilla et al., 2013; Schreiner & Rasch, 2015; Schreiner et al., 2015). It also appears that SWS TMR can strengthen consolidation of emotional memories in humans (Cairney et al., 2014) and enhance fear conditioning in rodents (Barnes & Wilson, 2014; Rolls et al., 2013), as some early experiments would suggest (Hars et al., 1985). Yet, other studies hint that reactivating fear memories during sleep may promote their extinction (Hauner et al., 2013; He et al., 2015), thus potentially opening a new avenue for treatment of emotional disorders. By associating TMR cues with instructions to forget specific items, the procedure was also shown to boost intentional forgetting (Simon et al., 2018; Schechtman et al., 2020). This kind of TMR could be used to weaken unpleasant memories and perhaps enhance treatments of memory-related impairments, such as post-traumatic stress disorder. Nevertheless, whether TMR could complement, or perhaps even replace conventional treatments is an active area of research, with large patient cohorts required to confirm clinical relevance of the manipulation (Klinzing et al., 2021).

Procedural consolidation also seems to benefit from TMR. This is especially true for motor sequence learning (Antony et al., 2012; Cousins et al., 2014a; Cousins et al., 2016; Schönauer et al., 2014), though improvements on real-world sensorimotor skills (e.g., arm throwing task) have been reported as well (Johnson et al., 2018; Johnson et al., 2019). TMR in N2 sleep has been particularly impactful when it comes to motor skill learning (Laventure et al., 2016; Laventure et al., 2018). This has been attributed to the active involvement of sleep spindles (Nishida & Walker, 2007; Barakat et al., 2013; Morin et al., 2008; Lutz et al., 2021; Fogel et

al., 2017a; Fogel et al., 2017b; Boutin & Doyon, 2020; Fogel & Smith, 2006), and thus spindle rich N2 in general (Walker et al., 2002), in consolidation of this type of memories. Despite the ample evidence, cueing motor skill with tactile stimuli during N2 did not alter motor skill learning (Pereira et al., 2017), neither did olfactory cueing (Diekelmann et al., 2016; Rasch et al., 2007). Such discrepancies in the literature can be attributed to the fact that several different factors are likely to determine the fate of the reactivated memories, as discussed in the next section (*4.2.4 Factors modulating the effectiveness of TMR*). Nevertheless, procedural TMR has recently proven to be effective in a clinical setting, whereby cueing a real-life motor task during a 1-hour nap enhanced motor learning in stroke patients (Johnson et al., 2021).

Some of the unusual uses of TMR include cueing counter-stereotype information during SWS, which was shown to reduce social biases even 1 week after the manipulation (Hu et al., 2015; for long-term effects of TMR see section *4.3 Long term effects of reactivating memories during sleep*). Perhaps even more strikingly, listening to spoken names of familiar snack items (e.g., 'M & M's candies') during N2, but not during wakefulness, increased one's preference for the previously cued product (Ai et al., 2018), raising some ethical concerns associated with subliminal conditioning in sleep.

TMR during REM sleep has received less attention. This is partly because REM sleep TMR has been attempted less frequently due to the challenges associated with stimulating early in the morning (when REM sleep is most prevalent), and partly because the results have not been as exciting as for cueing in NREM sleep. Although some of the early work on TMR points to its beneficial effects when applied during REM sleep (see section *4.2.1 Early attempts to cue memories during sleep*), later attempts were mostly unsuccessful (procedural memories: Laventure et al., 2016; Koopman et al., 2020b; declarative memories: Cordi et al., 2014; Rasch et al., 2007). Since REM sleep is thought to play a role in consolidation of emotional memories (Hutchison & Rathore, 2015; Walker & van Der Helm, 2009), many pinned their hopes on targeting emotional memories during REM sleep. Nevertheless, attempts to do this have generally not been successful either (Lehmann et al., 2016; Rihm & Rasch, 2015; but see Hutchison et al., 2021 for reduced arousal responses after REM sleep TMR). Interestingly though, one study found that REM sleep TMR improved both the accurate recollection of faces and their false recognition (Sterpenich et al., 2014), suggesting that REM sleep may favour generalisation of the reactivated memories. Nevertheless, similar conclusions were drawn when ambiguous pictures were cued during SWS (Groch et al., 2016). In fact, odour

TMR administered during sleep (both NREM and REM) was found to improve creative performance (Ritter et al., 2012), providing support for the BiOtA model (Lewis et al., 2018).

As sleep engineering becomes more and more popular, today's research on TMR and memory reactivation extends beyond experimental settings and now also includes **real-life applications**. Göldi & Rasch (2019) tested the effects of unsupervised TMR (i.e., without any control over sleep stages) applied during multiple nights and at participants' own homes. They found benefits for vocabulary learning in participants who reported no disturbances during sleep, but impaired memory for those who experienced auditory-induced awakening. Thus, it was concluded that proper electrophysiological verification of sleep stages is critical for successful TMR application (Göldi & Rasch, 2019), as feared by the critics of the early TMR studies (Oudiette & Paller, 2013). Conversely, odour TMR seems to be more suitable for unsupervised cueing of memory reactivation (Neumann et al., 2020). Not only did it work when applied throughout the night and without sleep monitoring, but it also led to performance benefits in a regular school setting (Neumann et al., 2020). The results of this and other studies (e.g., Gao et al., 2020) suggest that TMR can be regarded as a promising tool in an educational context. Nevertheless, it is necessary to bear in mind that the limited control over experimental settings could pose some serious limitations to studying the effects of TMR in real-life scenarios (Göldi & Rasch, 2019; Neumann et al., 2020, Gao et al., 2020). Furthermore, lack of group randomization (Neumann et al., 2020), sample size inequality (Gao et al., 2020) and insufficient number of control conditions (Gao et al., 2020), present a significant challenge in interpreting the findings.

4.2.4 FACTORS MODULATING THE EFFECTIVENESS OF TMR

In the previous section I have highlighted the most common, as much as unusual, applications of TMR, as well as outlined its use in experimental, clinical, and real-life settings. Notably though, the previous section also pointed out some discrepancies in the TMR literature, whereby not all attempts to cue memory reactivation during sleep have been successful. The aim of this section is to summarise factors that are thought to determine TMR's success, as well as those that do not seem to impact the effectiveness of the procedure.

A recent meta-analysis on TMR research (Hu et al., 2020) should perhaps be crucial in this discussion. The authors compiled 91 TMR experiments to conclude that TMR is highly effective during **SWS and N2** sleep but does not influence memory consolidation when

applied during REM or wakefulness. Notably, the beneficial effects of stimulation were found for **all types of learning** (spatial memories, associative learning, language acquisition, skill learning, memory bias), except for fear conditioning and emotional memories. However, the effects differed depending on how the outcomes were measured, with significant benefits of TMR on **recall and reaction time** but not on recognition, skin conductance response or subjective rating. Cueing modality was not associated with TMR effectiveness and similar results were reported for both auditory and olfactory stimulation. Likewise, neither sex nor age or sleep duration seems to impact on TMR effects (Hu et al., 2020).

Other studies addressed the question of whether the strength of cued memory representations, or **prior learning**, can affect TMR's success. Creery et al. (2015) found that participants with higher pre-sleep accuracy and items with medium strength before TMR benefited the most from the manipulation. The authors speculate that indeed, strongly encoded memories are likely to be reactivated spontaneously, thus yielding the additional TMR-cued reactivations redundant. On the other hand, reactivating incorrectly learned items could lead to their poor recall at a later performance re-test, whereas cueing very weak memories may not even lead to their reactivation (Creery et al., 2015). Yet, other studies do report preferential benefits of TMR on weaker memory representations (Cairney et al., 2016; Drosopoulos et al., 2007; Tambini et al., 2017; Koopman et al., 2020b), with further evidence suggesting that hippocampal replay itself prioritises memories most prone to forgetting (Schapiro et al., 2018). More studies are needed to fully understand the impact of prior learning on the effectiveness of TMR. By the same token, future research should take into consideration interindividual factors that confer susceptibility to the manipulation.

Regarding the **cueing procedure** itself, Schechtman et al. (2021) found that post-TMR memory benefits do not seem to depend on the number of items cued, suggesting that multiple reactivation events can occur simultaneously. The capacity for such events is still unknown, given a relatively small number of items used in the experiment (6 items maximum), though other sleep studies suggest that it is likely to be limited (Feld et al., 2016). The number of cues per item does not show a relationship with the behavioural effects of TMR either (Schechtman et al., 2020). On the other hand, a clear semantic link between the cue and the newly encoded material may increase the chances of TMR's success (Cairney et al., 2016), but this remains controversial (Schouten et al., 2017). Furthermore, sounds may be ineffective if they are presented continuously as that can lead to sensory habituation, whereas sounds that are too commonplace (e.g., sound of an ocean) may cue other memories that they are associated with instead of the encoded event (Donohue & Spencer,

2011). However, results of other studies contradict such claims (e.g., rose scent used by Rasch et al. (2007) or a meow of a cat used by Rudoy et al. (2009) could be even more commonplace than a sound of an ocean). Future studies should address these methodological considerations to fully characterise the factors that are involved in determining TMR's success.

4.2.5 NEURAL CORRELATES OF TMR AND WHAT IT HAS TAUGHT US ABOUT MEMORY REACTIVATION

We have now seen how different factors may come into play when determining the fate of the cued memories. As good as it may sound though, TMR is not just about successfully boosting human cognition. The real value of the technique lies in how it can be used to study the mechanisms of memory reactivation. The ground-breaking study by Bendor & Wilson (2012) has paved the way for major advances in this field, which I will focus on in this section.

To begin with, TMR research has made a fundamental contribution to the **detection of memory reactivation** in humans. Cairney et al. (2018) showed that cueing associative memories in NREM sleep evokes a surge in fast spindles from 1.7 to 2.3 seconds after cue onset. Importantly, during that surge, the type of the memory representation associated with the auditory cue (object vs scene) could be reliably decoded using RSA of the EEG data. Moreover, the level of category distinctiveness correlated with the overnight benefit of cueing (Cairney et al., 2018). Similarly, Shanahan et al. (2018) was able to decode category-level information using MVPA of fMRI data collected from ventromedial prefrontal cortex during olfactory cueing. The degree of this odour-evoked reactivation was also associated with post-sleep cueing benefit (Shanahan et al., 2018). Finally, Wang et al., (2019) showed that lateralised activity discriminating left- and right-hand movements can also be decoded during sleep, increases with post-cue spindle power, and predicts subsequent memory strength. Together, these studies demonstrate that TMR during sleep can trigger behaviourally relevant processing of the cued memories.

Although undeniably compelling, decoding learning-related information from sleep data is not enough to demonstrate that the detected reactivation is a true reinstatement of the learning-associated activity pattern. The challenge of searching for 'wake-like' patterns during sleep lies in the obvious differences in oscillatory characteristics between sleep and wake periods. Nevertheless, Schreiner et al. (2018) and Belal et al. (2018) were able to

achieve this, providing irrefutable evidence for wake-like activity patterns re-emerging upon cue presentation during sleep. Schreiner et al. (2018) used low-frequency oscillatory phase to look at phase-related similarity between different reactivation processes. The team showed that content-specific activity patterns that characterise reactivation of word-pair memories during wakefulness re-emerge during NREM sleep following TMR cue delivery. Both sleep and wake reactivation events were accompanied by theta oscillations, but only the activity patterns during sleep recurred at 1 Hz frequency suggesting slow-oscillatory modulation. Similar results were achieved by Belal et al. (2018) who opted for a machine learning classifier as a primary tool to detect human reactivation during sleep. First, the classifier was trained on wake EEG data from a motor imagery task, during which participants were asked to imagine a previously learned sequence of motor presses. The classifier was then applied to the EEG data collected during subsequent sleep. It showed that TMR cues do indeed elicit memory reactivation, both when applied during SWS and N2. Additionally, the rate of successful classification reduced with successive cue repetitions, suggesting that the responsiveness to TMR cues decreases over time. Alternatively, the neural signature of reactivation changed and was no longer recognised by the classifier, thus indicating plasticity-related changes as a result of cueing (Belal et al., 2018). Nevertheless, neither neural plasticity of the memory-related activity patterns, nor physical brain changes following TMR have been studied.

Along with providing causal evidence for memory reactivation during human sleep, TMR research has helped **characterise the electrophysiological characteristics** of such reactivation. The results of Cairney et al. (2018) and Wang et al., (2019), for instance, point to the functional significance of **spindles** in information processing during sleep. In fact, sleep spindles are thought to orchestrate reactivation of newly encoded memories during sleep (Bergmann et al., 2012) and contribute to correct classification of previously learned content (Schönauer et al., 2017). Additionally, studies looking at the electrophysiological effects of TMR revealed that spindles react locally to cueing of specific memories (Cox et al., 2014) and that successful reactivation is accompanied by a surge in spindle power between 500 ms and 1200 ms after the onset of the cues that were associated with later-remembered items (Schreiner & Rasch, 2015: 600-800 ms; Lehmann et al., 2016: 800 - 1200 ms; Schreiner et al., 2015: 500 – 1000 ms), and 100 – 1300 ms after the cues related to prior learning (Groch et al., 2017b) (note that spindle activity surge reported in Cairney et al. (2018) occurred as long as ~2 seconds after the cue). Importantly, post-cue sleep spindles were also shown to predict

TMR-induced performance gains (Rihm et al., 2014; Creery et al., 2015; Fuentemilla et al., 2013; Antony et al., 2012; Cousins et al., 2014a; Lehmann et al., 2016; Groch et al., 2017b).

Theta power during NREM sleep also increased in response to cues that were associated with later-remembered items, surging around similar time after cue presentation as the spindle activity (Lehmann et al., 2016: 300 – 900 ms; Schreiner & Rasch, 2015: 700 – 900 ms; Schreiner et al., 2015: 500 – 800 ms; Oyarzún et al., 2017: 500 – 2000 ms; Groch et al., 2017b: 500 – 800 ms post-cue). Nevertheless, a direct relationship between theta power and subsequent memory performance is rarely reported, with one study showing no such correlation (Groch et al., 2017b). Notably, neither the enhanced theta power nor the surge in sleep spindles were evident after control sounds presentation (i.e., sounds that were never associated with learning material), affirming that the post-cue increase in spindle/theta power is not merely a simple response to *a* sound (Oyarzún et al., 2017). Combined, these studies show that sleep spindles as well as theta activity during NREM sleep are likely to be involved in successful reactivation of newly encoded memories.

Interestingly, using their famous vocabulary-learning paradigm Schreiner et al. (2015) found that if the cue (Dutch word) is immediately followed by another auditory stimulation (e.g., correct, or incorrect German translation of the cue) the characteristic surge in spindles and theta activity is abolished. Strikingly, the memory benefits of cueing were not observed either. However, when the presentation of an auditory stimulation was delayed relative to the cue, both the electrophysiological and memory effects of cueing were restored. Thus, it was concluded that there must be a certain plasticity period, perhaps associated with spindle and theta oscillations, that occurs immediately after the cue and which is necessary for the beneficial effects of TMR to emerge (Schreiner et al., 2015). Similar results were reported by others (Farthouat et al., 2017).

Finally, the discussion on the electrophysiological correlates of memory reactivation would be incomplete without bringing **slow waves** to the table. Although not as common in the literature as a spindle surge, an increase in delta power upon cue delivery has been reported as well (Rihm et al., 2014; Creery et al., 2015). Nevertheless, the currently available data is insufficient to conclude whether delta power is behaviourally relevant in this context (correlational results reported: Creery, et al., 2015; Oudiette et al., 2013; no relationship reported: Rihm et al., 2014). On the other hand, recent evidence suggests that slow oscillatory up-states may represent critical time windows for memory reactivation to occur

(Göldi et al., 2019b). Indeed, when the TMR cues were delivered precisely during oscillatory up-states improved recall performance was recorded. In turn, cueing during down-states of the slow oscillations did not lead to behavioural benefits (Göldi et al., 2019b). Although the results provide support for the ASC (see section *3.2 Sleep and memory models*), the exact phase of slow-oscillation that supports TMR-induced memory processing is still debated (down-to-up transition: Shimizu et al., 2018; pre-down-state: Batterink et al., 2016).

4.3 LONG TERM EFFECTS OF REACTIVATING MEMORIES DURING SLEEP

Although memory reactivation during sleep has been repeatedly portrayed as the mechanism underlying memory consolidation, perhaps even in the long term, very little research has been conducted on how the effects of TMR or memory reactivation per se evolve over time. In a very elegant way and with the use of optogenetics, Dag et al. (2019) linked memory reactivation during sleep with long-term consolidation in a fruit fly. Using simultaneous calcium imaging and electrophysiology in mice, Grosmark et al. (2021) has very recently been able to track hippocampal place cells' activity over 2 weeks. Their results demonstrate that offline reactivation of place cells predicts long-term stability of cognitive maps. Even though the study does not distinguish between awake and sleep periods of the 'offline' epochs, the reactivation events that predicted future stability coincided with SWR and were specific to the previously explored environment. The results of both studies suggest that, as hypothesised, memory reactivation does support long-term consolidation. By the same token, one could hypothesise that TMR should also result in long-term memory benefits. If so, will the effects of TMR continue to increase over time or is there a limit to the TMR memory boost?

To date, only four studies examined how the effects of TMR develop over time (Hu et al., 2015; Groch et al., 2017a; Shanahan et al., 2018; Simon et al., 2018), half of which failed to show an enduring effect of TMR. The study conducted by **Hu et al. (2015)** was already mentioned in the context of unusual applications of the technique (see section *4.2.3 Beyond simply boosting memories*). Participants were presented with counter-stereotype information (counter-gender bias and counter-racial bias) paired with bias-specific sounds. One of the sounds was repeatedly re-presented during a subsequent nap (SWS) and the implicit bias associated with the cue was reduced straight after sleep. Importantly, the effects of stimulation endured for 1 week (Hu et al., 2015). On the other hand, **Shanahan et al. (2018)** (see section *4.2.5 Neural correlates of TMR and what it has taught us about memory*

reactivation) found that the positive effects of TMR on an object-location memory task were no longer evident at 1-week follow-up. In **Groch et al. (2017a)** participants learned associations between emotionally neutral pictures and either positive or negative words, re-presented to them during subsequent sleep. In keeping with Shanahan et al. (2018), the team found no difference between the cued and uncued items 1 week after cuing, even though retention of the cued memories, both positive and negative, was facilitated the next morning. Interestingly though, when the participants were asked to rate the subjective pleasantness of the pictures 1 week after cueing, social anxiety disorder (SAD) patients, but not healthy controls, rated the negative information as less pleasant than immediately after TMR (Groch et al., 2017a). Finally, rather than strengthening memories, **Simon et al. (2018)** used TMR to induce forgetting. Participants were trained on an object-location task, where each object was paired with a distinct sound. Before sleep, they also learned to associate an auditory 'forget' tone with the act of forgetting. During sleep, the 'forget' tone was played to the participants in close temporal proximity with some of the object tones, in hope to induce their forgetting. One week after the intervention the reactivated objects were recalled less often than the control ones, thus indicating both successful cueing and long-term effects of TMR.

Although these studies demonstrate that the TMR effect can indeed endure over time, the mechanisms driving long-term effects of the manipulation remain poorly understood. Likewise, the current state of literature is unable to explain how these effects *evolve*, nor does it provide a sufficient understanding on the neuro-plastic evolution of the underlying memory representations.

5 MOTOR SEQUENCE LEARNING DURING SLEEP

Given the richness and extensiveness of the sleep literature, in this final section I would like to centre the discussion on the role of sleep in procedural memory consolidation, and particularly motor sequence learning which will ultimately become the focus of my thesis.

As noted in section *3.1.1 Memory types*, procedural memory is a form of nondeclarative memory which, by definition, is generally considered hippocampus independent (Squire, & Zola, 1996; Squire & Dede, 2015). Neural correlates of motor learning are extremely well characterised (Seidler, 2010; Lage et al., 2015; Dayan & Cohen et al., 2011), with the specific brain regions involved in different paradigms extensively studied (Hardwick et al., 2013;

Janacsek et al., 2020). Broadly speaking, the cortico-striatal system is thought to be involved in motor sequence learning, whereas the cortico-cerebellar system supports motor adaptation (Doyon et al., 2003). The significance of sleep in consolidation of procedural memories is now also firmly established and supported by a number of behavioural studies (for review see Loganathan, 2014). In contrast to motor adaptation (Donchin et al., 2002; Debas et al., 2010), **motor sequence learning** has been widely reported to benefit from sleep. The most common motor sequence learning paradigms used to demonstrate this include a pursuit rotor task (PRT; Smith & MacNeill, 1994), oculomotor sequence learning (OSL; Albouy et al., 2006), finger tapping task (FTT; Walker et al., 2002; Fig.7A) and the serial reaction time task (SRTT; Nissen & Bullemer, 1987; Fig.7B).

In their seminal study, Walker and colleagues show that sleep, particularly N2, leads to a 20% increase in the FTT performance speed, with no benefit from an equivalent period of wake (Walker et al., 2002). In the same year, Fischer and colleagues report similar findings, with post-practice sleep relative to wake enhancing the speed of FTT performance by 33% and task accuracy by 30% (Fischer et al., 2002). In contrast to Walker et al. (2002), they show a relationship between performance improvements and the time spent in REM sleep rather than N2 (Fischer et al., 2002). Eventually, the differential, yet often overlapping, contribution of N2 and REM sleep has been linked to different stages of motor learning (Smith et al., 2004a). The cortico-cerebellar system has been proposed to mediate early task acquisition and operate during REM sleep, while N2 is thought to support long-term storage of motor memories in the cortico-striatal network (Smith et al., 2004a). The role of spindles in procedural memory consolidation is now also well recognised (see section *4.2.3 Beyond simply boosting memories*), while REM sleep has been further implicated in the reactivation of SRTT memories during sleep (see section *4.1.2 Human studies* for more details). Indeed, increased activation of cuneus (Maquet et al., 2000; Peigneux et al., 2003), striatum, midbrain, and premotor cortex (Maquet et al., 2000) was observed both during the SRTT training and the post-training REM sleep. These studies also paved the way for further research into the **neural substrates underlying sleep-dependent motor consolidation**.

For the PRT, a comparison between learning-dependent brain activity changes after post-training sleep and post-training sleep deprivation revealed greater activity in the superior temporal sulcus for the sleeping group (Maquet et al., 2003a). The interaction between superior temporal sulcus and cerebellum, and supplementary eye field and frontal eye field was also increased (Maquet et al., 2003a). Similar design was employed by Fischer et al.

(2005) who trained their participants on the FTT and found that post-training sleep results in a decreased neocortical brain activity during retrieval compared to learning, specifically in the primary motor, premotor and prefrontal areas, as well as in a greater involvement of parietal cortical regions. This was, however, not the case in the sleep-deprived condition. Walker et al. (2005), on the other hand, compared brain activity changes after FTT training followed by 12 hours of either sleep or wake. Increased activation in contralateral primary motor cortex, hippocampus, cerebellum, and striatum after the retention period containing sleep relative to wake supported faster and more precise consolidation. In turn, decreased signal intensity was observed in parietal, insular and temporal cortices. Thus, the study provided evidence for overnight systems-level changes in motor memory representations after sleep (Walker et al., 2005). Finally, the importance of striatum in motor sequence learning (Debas et al., 2010; Walker et al., 2005) and its interaction with hippocampus (Albouy et al., 2008; Albouy et al., 2013c) have also been highlighted. Not only does the early recruitment of both structures predict subsequent overnight gain in sequence-specific performance, but the linear relationship between hippocampal and striatal responses to OSL becomes significantly tighter overnight (Albouy et al., 2008). In line with the ASC model (see section *3.2 Sleep and memory models*), these results suggest the emergence of a cooperative interaction between hippocampus and striatum during sleep.

An important distinction needs to be discussed between the **implicit and explicit components of motor learning**. Although procedural learning is often portrayed as implicit, it is possible to become aware of the skill at hand. In fact, the FTT is generally used to assess explicit motor skill learning as the sequence of finger movements is often short (e.g., 5 items in Fischer et al., 2002) and disclosed at the beginning of the experiment (Fig.7A). Conversely, the sequence used in the SRTT is relatively long (e.g., 12 items in Cousins et al., 2014a) and the participants are generally blind to its order (Fig.7B). Thus, any knowledge acquired about the SRTT sequence during training is largely implicit. However, if the participants are told the order of the sequence (or practise the task long enough to become aware of such), they can still gain explicit knowledge about it (Robertson, 2007). Thus, the SRTT provides a unique but challenging approach to study sleep-dependent memory consolidation. The task engages distinct brain structures and rely on different underlying neurocognitive mechanisms depending on the declarative vs nondeclarative contribution to its learning (Hardwick et al., 2013; Janacsek et al., 2020). Furthermore, the implicit aspect of the SRTT leaves more room for learning, allowing continuous behavioural improvements over several days of training

(e.g., 10 days, Verstynen et al., 2012). This contrasts with the FTT, where the ceiling level is reached relatively quickly (e.g., after 11 – 36 trials, Bönstrup et al., 2020).

Sleep has been initially thought to only benefit explicitly learned SRTT (Robertson et al., 2004; Fischer et al., 2006). However, sleep-dependent consolidation was also observed when the implicit sequence contained contextual associations that are known to engage the hippocampus (Spencer et al., 2006). Matching the design of the latter study, Cousins and colleagues (2014a) showed that TMR can promote the emergence of explicit knowledge of the cued sequence representation, and the result was later replicated by another study (Diekelmann et al., 2016). Importantly, the technique was also shown to reliably improve the SRTT skill performance by three independent groups (Antony et al., 2012; Schönauer et al., 2014; Cousins et al., 2016). Nevertheless, the TMR literature does not distinguish between the implicit and explicit aspect of the skill learning and the difference between the cued sequence and the uncued sequence is often reported when looking at the accuracy (Antony et al., 2012; Schönauer et al., 2014) or reaction time (Cousins et al., 2016). However, and again as opposed to the FTT, the SRTT allows distinguishing between sensorimotor-mapping and sequence-specific learning (Janacsek et al., 2020). By subtracting the performance on the sequence blocks from the blocks with random stimuli order (i.e., 'random blocks'), the visual and motor demands, as well as fatigue, are controlled for, thus allowing to probe sequence learning only (e.g., Robertson et al., 2004; Cousins et al., 2014a; Cousins et al., 2016).

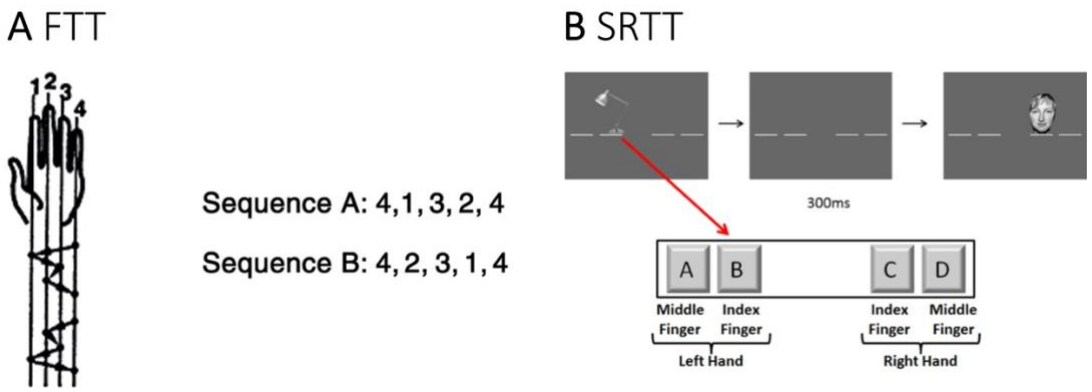

Fig. 7. Two most common motor sequence learning paradigms. (A) *A schematic representation of the Finger Tapping Task (FTT), also referred to as a finger-to-thumb opposition task. Participants are asked to repeatedly tap a sequence of button presses as quickly and as accurately as possible for a certain amount of time and using the fingers of their non-dominant hand. The sequences (here A and B shown) are often short (e.g., 5-elements long) and known to the participants prior to the task. Figure adapted from: Fischer et al. (2002).* ***(B)*** *A schematic representation of the Serial Reaction Time Task (SRTT). Participants are asked to respond to the visual cues appearing on the screen by pressing a key corresponding to the cue location as quickly and as accurately as*

possible (e.g., key 'B' is pressed in response to a lamp cue appearing in position 2). Each key needs to be pressed with an appropriate finger (e.g., key 'A' – middle finger of the left hand, key 'B' – index finger of the left hand etc.). The stimulus remains on the screen until a correct button is pressed, followed by a blank screen and the next cue in the sequence. The SRTT sequences are often long (e.g., 12 items) and their order is rarely revealed to the participants prior to the task. The sequences come in blocks and the sequence blocks are accompanied by random blocks during which the cues appear in random order (not shown). Figure adapted from Cousins et al. (2014b).

6 SUMMARY

Sleep is not a uniform state but instead consists of different stages, each characterised by unique oscillatory patterns and supporting distinct, though sometimes overlapping, physiological functions. The memory function of sleep has been receiving increasing attention in recent years and because of its undeniable importance, became the central focus of this thesis. Sleep has been strongly implicated in various types of memories and memory processes. Most notably, it has been proposed to play an active role in memory consolidation, and reactivation of memories during sleep is thought to be key in this process. Indeed, a plethora of both rodent and human experiments have now confirmed that learning-dependent patterns of brain activity spontaneously re-emerge during offline periods of rest, particularly during SWS, and that the phenomenon is tightly linked to the subsequent memory performance. Remarkably, the content of reactivation events can now be biased with a technique known as Targeted Memory Reactivation (TMR). TMR involves pairing learning items with sounds or odours during learning and then covertly re-presenting the same stimuli during post-learning sleep. The procedure has shown a lot of success in boosting consolidation of the targeted memories in laboratory, clinical and real-life settings, especially when applied during NREM sleep. Importantly though, TMR has taught us a lot about sleep and made a fundamental contribution to the detection and characterisation of memory reactivation in humans. Yet, the long-term effects of TMR are largely understudied and it remains to be established how the effects of this manipulation evolve over time. Likewise, the literature still lacks sufficient understanding of the plasticity induced by TMR, nor does it fully comprehend the interindividual factors that make one more susceptible to the stimulation.

7 THESIS OBJECTIVES

The overarching aim of this thesis is to investigate the evolution of TMR effects over time, with a particular focus on the neuroplasticity underlying reactivation of procedural memories during sleep. In **Chapter 2,** I aimed to determine whether the memory-enhancing effects of TMR persist over time, which would provide an insight into the temporal dynamics of the processes initiated by the stimulation. To this end, I applied TMR of a SRTT in NREM sleep and tested the difference between the cued and uncued sequence performance at different points in time. I was further interested in the electrophysiological correlates of the behavioural benefits of TMR, particularly in relation to sleep spindles given their functional importance in motor learning. In **Chapter 3**, I used the same TMR protocol and behavioural task as in Chapter 2 but combined it with structural and functional MRI to track the evolution of a motor engram over time. Specifically, I aimed to probe whether repeated reactivation of a motor memory trace during sleep engenders learning-related plasticity in the brain. This would advance our understanding of the neural processes underlying sleep-dependent memory consolidation and indicate if memory reactivation during sleep can support engram development. Finally, **Chapter 4** examines the microstructural plasticity associated with the behavioural effects of TMR. I look at the longitudinal changes in different MRI modalities to determine the impact of TMR on brain microstructure. Furthermore, I was curious about whether baseline brain characteristics correlate with TMR's success – something that has never been probed before.

CHAPTER 2

Long term effects of cueing procedural memory reactivation during NREM sleep

This chapter has been accepted for publication in NeuroImage.

Rakowska, M., Abdellahi, M. E., Bagrowska, P., Navarrete, M., & Lewis, P. A. (2021). Long term effects of cueing procedural memory reactivation during NREM sleep. NeuroImage, 244, 118573.

Abstract

Targeted memory reactivation (TMR) has recently emerged as a promising tool to manipulate and study the sleeping brain. Although the technique is developing rapidly, only a few studies have examined how the effects of TMR develop over time. Here, we use a bimanual serial reaction time task (SRTT) to investigate whether the difference between the cued and uncued sequence of button presses persists long-term. We further explore the relationship between the TMR benefit and sleep spindles, as well as their coupling with slow oscillations. Our behavioural analysis shows better performance for the dominant hand. Importantly, there was a strong effect of TMR, with improved performance on the cued sequence after sleep. Closer examination revealed a significant benefit of TMR at 10 days post-encoding, but not 24 h or 6 weeks post-encoding. Time spent in stage 2, but not stage 3, of NREM sleep predicted cueing benefit. We also found a significant increase in spindle density and SO-spindle coupling during the cue period, when compared to the no-cue period. Together, our results demonstrate that TMR effects evolve over several weeks post-cueing, as well as emphasising the importance of stage 2, spindles and the SO-spindle coupling in procedural memory consolidation.

1 INTRODUCTION

The essential role of sleep in memory processing is supported by a multitude of studies (for reviews see Diekelmann & Born (2010b), Rasch & Born (2013) and Dudai (2012)). Both declarative (summarised in Gais & Born, 2004) and procedural (summarised in Loganathan, 2014) memory consolidation benefit from sleep. Memory reactivation, wherein a pattern of brain activity elicited during learning re-emerges during subsequent sleep, is thought to be the mechanism underpinning this process (Born et al., 2006). Although first discovered in rodents (Wilson & McNaughton, 1994), the phenomenon was also evidenced to occur in humans, where its magnitude predicts the next-day memory improvements (Peigneux et al., 2003). Recently, a procedure known as targeted memory reactivation (TMR) emerged as a promising tool to manipulate and study the mechanisms of memory reactivation. In a typical TMR experiment, a tone or an odour previously associated with a newly encoded memory is covertly re-presented during sleep (e.g., Rasch et al., 2007; Rudoy et al., 2009). This elicits reactivation of the associated memory representation, or rather intentionally biases this otherwise spontaneous process towards the memories targeted by the procedure (e.g., Bendor & Wilson, 2012). In humans, the manipulation has been found to be effective for both declarative (Rasch et al., 2007; Rudoy et al., 2009; Fuentemilla et al., 2013) and procedural

(Antony et al., 2012; Schönauer et al., 2014; Cousins et al., 2014a; Cousins et al., 2016) memories, enhancing performance gains on the cued compared to the uncued task items.

Although TMR research has developed rapidly, becoming one of the most used sleep manipulation techniques, only a few studies have examined how the effects of TMR develop over time (Hu et al., 2015; Shanahan et al., 2018; Groch et al., 2017a; Simon et al., 2018). One of the most recent attempts was made by Cairney et al. (2018), where participants encoded pairwise associations, followed by three retrieval sessions: before and after a 90 min nap of cueing, and following a full night of sleep with no stimulation. While memory performance did not differ between cued and uncued pairs immediately after the nap, the memory-enhancing effect of TMR was evident the next morning. Cairney et al. (2018) argues that, during the TMR-induced windows of spindle-mediated memory processing, the synapses relevant for the task may be 'tagged' for plastic changes during subsequent sleep, hence uncovering TMR benefits the next day. Such a 'tag' could potentially also allow the cued memories to persist for longer than the uncued ones. While long-term effects of TMR were first reported for implicit biases (Hu et al., 2015), neither object-location (Shanahan et al., 2018) nor emotional (Groch et al., 2017a) memory seems to benefit a week after the manipulation. Procedural memory, on the other hand, has to our knowledge, never been investigated in this context.

Here, we set out to determine whether the memory-enhancing effects of TMR on motor memory consolidation (Antony et al., 2012; Schönauer et al., 2014; Cousins et al, 2014a; Cousins et al., 2016) persist over time, by using a bimanual serial reaction time task (SRTT) and investigating the difference between the cued and uncued sequence of button presses at different points in time. Participants learned two sequences of 12-item button presses, each associated with a different set of auditory tones. Tones associated with one of the sequences were replayed to the participants during subsequent sleep and the performance was re-tested 24 h, 10 days and ~6 weeks post-learning.

We delivered TMR in both stages 3 (N3) and 2 (N2) of NREM sleep due to procedural memory improvements reported following TMR delivery during N3 (Antony et al., 2012; Cousins et al., 2014a; Cousins et al., 2016) and N2 (Laventure et al., 2016, 2018). N3, also known as slow-wave sleep (SWS), has a well-established role in memory processing (Walker, 2009). It is the most common choice for declarative-memories TMR (Rasch et al., 2007; Rudoy et al., 2009; Diekelmann et al., 2012; Fuentemilla et al., 2013) as well as TMR in general (Hu et al., 2020).

On the other hand, N2 has been consistently implied in motor sequence memory consolidation (Laventure et al., 2016; Nishida & Walker, 2007; Walker et al., 2002). Likewise, sleep spindles were shown to play an important role in procedural learning (Laventure et al., 2018; Barakat et al., 2011; Antony et al., 2012; Cousins et al., 2016; Nishida & Walker, 2007; Morin et al., 2008). Moreover, the interplay between the electrophysiological hallmarks of these two stages, i.e., the precise coupling between the amplitude of sleep spindles that characterise N2 and the phase of slow oscillations (SOs) that characterise N3, was shown to predict performance improvements for several memory tasks (Niknazar et al., 2015; Mikutta et al., 2019; Muehlroth et al., 2019; Hahn et al., 2020; Denis et al., 2020; Schreiner et al., 2021). Hence, here we aimed to describe the electrophysiology for the two sleep stages with a particular focus on sleep spindles and their coupling with SOs, as well as to explore their relationship with TMR benefits for both hands and each hand separately, and at different points in time.

2 MATERIALS AND METHODS

2.1 PARTICIPANTS

Twenty-six healthy volunteers signed a written informed consent form to take part in the study, which was approved by the Ethics Committee of the School of Psychology at Cardiff University. All participants reported being right-handed, sleeping 6-9 h per night, having normal or corrected to normal vision and no hearing impairment. Subjects who had travelled across more than two time-zones or engaged in any regular night work one month prior to the experiment were not recruited for the study. Likewise, regular nappers and smokers did not take part. Further criteria for exclusion included recent stressful life event(s), prior history of drug/alcohol abuse, neurological, psychological, or sleep disorders. None of the participants reported taking any medication or substance directly or indirectly affecting sleep quality. Additionally, they were asked to abstain from napping, extreme physical exercise, caffeine, alcohol, and other psychologically active food from 24 h prior to each experimental session. We also excluded participants with more than three years of musical training in the past five years due to a probable link between musical abilities and procedural learning (Romano Bergstrom et al., 2012; Anaya et al., 2017). The experimental procedure was explained, and participants received instructions about the tasks, but no information was provided about the objectives of the study nor the variables of interest. All participants received monetary compensation for their time.

According to our inclusion criteria, participants must: (1) have no prior knowledge of the SRTT upon the start of the study; (2) undergo an uninterrupted TMR procedure; (3) show the SRTT error rate within 2 standard deviations (SD) from the group mean during all sessions; (4) not classify as outliers using the outlier detection method from Cousins et al. (2014a), applied to the both-hands dataset. Seven participants were excluded from analysis due to these criteria as follows: (1) sudden realisation that they had participated in a previous experiment that involved SRTT (n = 1); (2) an interrupted TMR procedure caused by a high number of arousals throughout the night (n = 1), or reference electrode failure before or during the stimulation (n = 2); (3) a consistently high SRTT error rate throughout the study (>2 SD away from the group mean) (n = 1); and (4) being classified as an outlier according to the SRTT outliers detection method from Cousins et al. (2014a) which identified one participant (n = 1) whose reaction time performance before sleep was >2 SD from group mean and one participant (n = 1) for whom the disparity between the reaction time for the two sequences before sleep was >2 SD away from the group mean. One additional participant had to be removed from the dataset due to voluntary withdrawal (n = 1).

Hence, the final dataset included 18 participants (10 females, age range: 18 - 22 years, mean ±SD: 19.7 ±1.2; 8 males, age range: 18 - 24 years, mean ±SD: 21.1 ±1.7). One of the participants (n = 1) included in the dataset could not attend the last session and therefore the sample size for the analyses concerning the data collected during that session was 17. The final dataset also included two participants for whom part of the EEG data were missing due to EEG battery failure (n = 2). However, the issue occurred after the TMR procedure had been completed. Thus, the two participants were included in all the analyses except for the sleep staging analysis, as it would be impossible to state the time these participants spent in each sleep stage with a few hours of the recording missing.

2.2 STUDY DESIGN

The study consisted of four sessions (Fig.1A), all scheduled for the same time in the evening (~8 pm). Session 1 (S1) lasted 3 h and was followed by a stimulation night in the sleep lab, during which participants slept with the electroencephalography (EEG) cap on. Upon arrival, participants first completed a series of questionnaires: short version of the Edinburgh Handedness Inventory (EHI) (Veale, 2014) to assess their handedness, Stanford Sleepiness Scale Questionnaire (SQ) (Hoddes et al., 1973) to determine their current level of alertness

and Pittsburgh Sleep Quality Index (PSQI) (Buysse et al., 1989) to evaluate their sleep quality and quantity in the past month. Then, participants were asked to prepare themselves for bed before the wire up took place. With the EEG cap on, participants performed the SRTT and the imagery task. Noise-cancelling headphones (Sony MDR-ZX110NA, Sony Europe B.V., Surrey, UK) were used to deliver the tones during both tasks. Participants were ready for bed at ~11.30 pm. During sleep (N2 and N3), the same tones were replayed to the participants through speakers (Harman/Kardon HK206, Harman/Kardon, Woodbury, NY, USA) to trigger reactivation of the associated SRTT memories. Participants were woken up at a time convenient for them (on average after 8.46 ±0.45 h in bed) and had the EEG cap removed. Before leaving the lab, they were asked whether they had heard any sounds during the night.

The remaining three follow up sessions lasted 40-60 min each and included behavioural testing only. Participants were asked to come back to the lab 23-25 h (session 2, S2), 6-11 days (session 3, S3) and 6-8 weeks (session 4, S4) after S1. During S2, S3 and S4 participants completed the SQ and the SRTT again. S4 also included an explicit memory task. Since the post-learning sleep was shown to enhance consolidation of memories expected to be retrieved (Wilhelm et al., 2011), participants were told to expect SRTT re-test upon completion of each experimental session.

All tasks/questionnaires were presented on a computer screen with resolution 1920 x 1080 pixels, except for the explicit memory task, completed with pen and paper. Computer-based tasks were executed using MATLAB (The MathWorks Inc., Natick, MA, USA) and Cogent 2000 (developed by the Cogent 2000 team at the Functional Imaging Laboratory and the Institute for Cognitive Neuroscience, University College, London, UK; http://www.vislab.ucl.ac.uk/cogent.php). Questionnaires were executed using MATLAB and Psychophysics Toolbox Version 3 (Brainard, 1997).

2.3 EXPERIMENTAL TASKS

2.3.1 MOTOR SEQUENCE LEARNING – THE SERIAL REACTION TIME TASK (SRTT)

The SRTT (Fig.1B) was used to induce and measure motor sequence learning. It was adapted from Cousins et al. (2014a) and consisted of two 12-item sequences of auditorily and visually cued key presses, learned by the participants in blocks. The sequences – A (1-2-1-4-2-3-4-1-3-2-4-3) and B (2-4-3-2-3-1-4-2-3-1-4-1) – were matched for learning difficulty, did not share

strings of more than four items and contained items that were equally represented (three repetitions of each). Each sequence was paired with a set of 200 ms-long tones, either high (5^{th} octave, A/B/C#/D) or low (4^{th} octave, C/D/E/F) pitched, that were counterbalanced across sequences and participants. For each item/trial, the tone was played with simultaneous presentation of a visual cue in one of the four corners of the screen. Visual cues consisted of neutral faces and objects, appearing in the same location regardless of the sequences (1 – top left corner = male face, 2 – bottom left corner = lamp, 3 – top right corner = female face, 4 – bottom right corner = water tap). Participants were told that the nature of the stimuli (faces/objects) was not relevant for the study. Their task was to press the key on the keyboard that corresponded to the position of the picture as quickly and accurately as possible: 1 = left shift; 2 = left Ctrl; 3 = up arrow; 4 = down arrow. Participants were instructed to use both hands and always keep the same fingers on the appropriate response keys (1 = left middle finger, 2 = left index finger, 3 = right middle finger, 4 = right index finger). The visual cue disappeared from the screen only after the correct key was pressed, followed by a 300 ms interval before the next trial.

There were 24 blocks of each sequence (a total of 48 sequence blocks per session), where block type was indicated with 'A' or 'B' displayed in the centre of the screen. Each block contained three sequence repetitions (36 items) and was followed by a 15 s pause, with reaction time and error rate feedback. Blocks were interleaved pseudo-randomly with no more than two blocks of the same sequence in a row. Participants were aware that there were two sequences but were not asked to learn them explicitly. Block order and sequence replayed were counterbalanced across participants.

Following the 48 blocks of sequence A and B, participants performed 4 random blocks, indicated with 'R' appearing centrally on the screen. Those final blocks contained pseudo-randomised sequences, the same visual stimuli, and tones matching sequence A for half of them (Rand_A) and sequence B for the other half (Rand_B). Blocks Rand_A and Rand_B were interleaved, and the random sequences contained within them followed three constraints: (1) each cue was represented equally within a string of 12 items, (2) two consecutive trials could not contain the same cue, (3) random sequence did not share a string of more than four items with either sequence A or B.

2.3.2 IMAGERY TASK

Following the SRTT training, participants were instructed to do the same task again but without pressing any keys. Instead, they were told to imagine doing so, with their fingers resting immobile on the appropriate keys. The stimuli remained the same, except that the visual cues were presented for 880 ms and the inter-trial delay lasted 270 ms. The imagery task comprised 15 blocks of each sequence, with 5 s breaks in between but no performance feedback. The order of the sequence blocks was the same as during the SRTT but without the random blocks at the end. The EEG data collected during the imagery task was used to train a classifier which, when applied to the subsequent sleep data, aimed to detect memory reactivation. This, however, is beyond the scope of this thesis and will be discussed elsewhere.

2.3.3 EXPLICIT MEMORY TASK

To measure participants' explicit memory of the SRTT, a free recall test was administered during the last experimental session. Participants were instructed to mark the sequence order on printed screenshots of the SRTT, arranged vertically in two columns and with the visual cues removed.

2.4 EEG DATA ACQUISITION

EEG was recorded using 64 actiCap slim active electrodes (Brain Products GmbH, Gilching, Germany), with 62 electrodes embedded within an elastic cap (Easycap GmbH, Herrsching, Germany). This included the reference positioned at CPz and ground at AFz. The remaining electrodes were the left and right electrooculography (EOG) electrodes (placed below and above each eye, respectively), and left and right electromyography (EMG) electrodes (placed on the chin). Fig.S1 shows the EEG electrodes layout. Elefix EEG-electrode paste (Nihon Kohden, Tokyo, Japan) was used for stable electrode attachment and Super-Visc high viscosity electrolyte gel (Easycap GmbH) was inserted into each electrode to reduce impedance below 25 kOhm. To amplify the signal, we used either two BrainAmp MR plus EEG amplifiers or LiveAmp wireless amplifiers (all from Brain Products GmbH). Signals were recorded using BrainVision Recorder software (Brain Products GmbH).

2.5 TMR DURING NREM SLEEP

Tones associated with one of the learned sequences (A or B, counterbalanced across participants) were replayed to the participants during N2 and N3 (Fig.1C), as assessed with standard AASM criteria (Berry et al., 2015). The TMR protocol was executed using MATLAB and Cogent 2000. Volume was adjusted for each participant to make sure that the sounds did not wake them up. One repetition of a sequence (i.e., 12 sounds) was followed by a 20 s break during which no sounds were played. The inter-trial interval within repetitions (i.e., between the sounds in a sequence) was jittered between 2500 and 3500 ms. Upon arousal or leaving the relevant sleep stage, replay was paused immediately and resumed only when stable N2/N3 was apparent. TMR was performed for as long as the minimum threshold of ~1000 trials in N3 was reached. On average, 1612.59 (± SD 162.20) sounds were delivered. The exact number of sounds played during each sleep stage was determined offline, with the results summarised in Table S1. Once the sleep scoring procedure was complete (see section *2.6.2.1 Sleep Scoring*), the EEG data were cut into trials (defined as the time interval between cue onset and the end of the inter-trial interval) and if more than 50% of a trial fell within a given epoch, arousal, or movement, that trial was deemed as being played during the respective period.

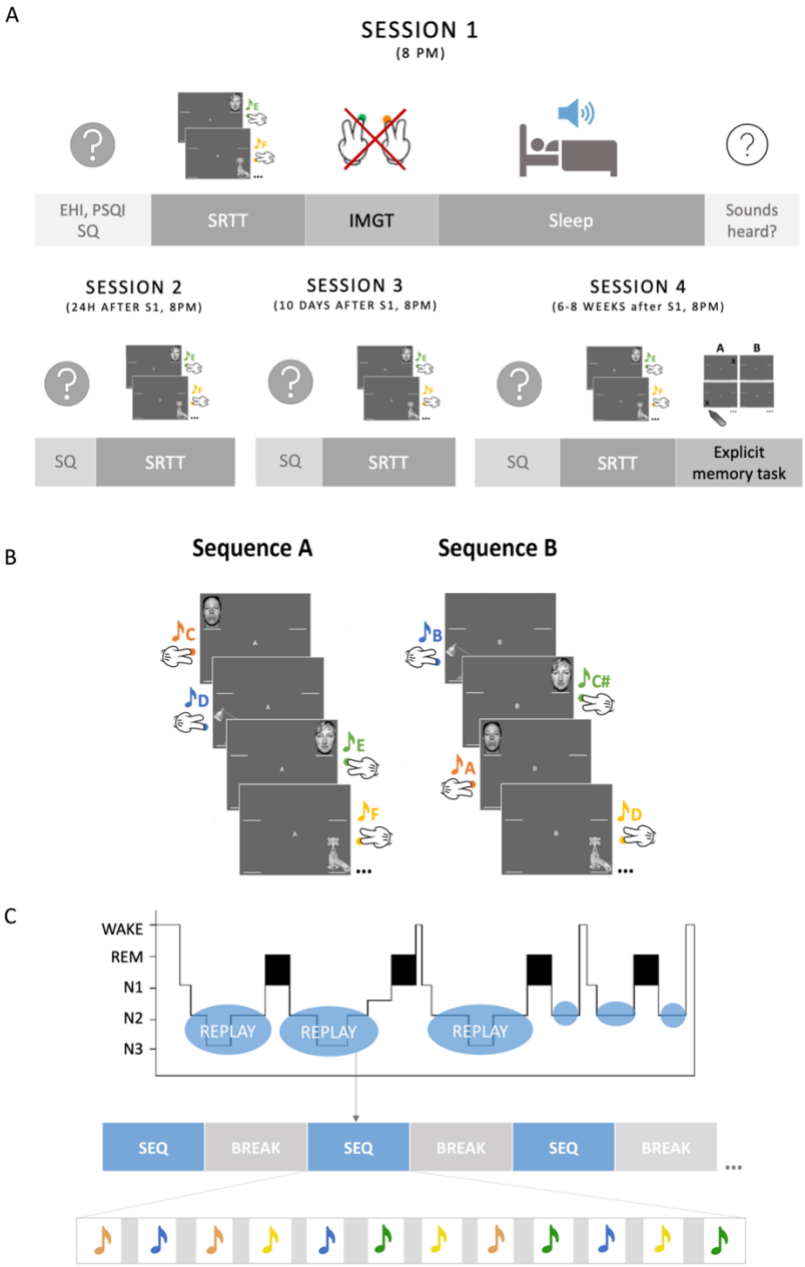

Fig. 1. Experimental methods. (A) *Study design. The study consisted of four sessions, each requiring participants to complete one or more questionnaires and the SRTT. Session 1 also involved EEG recording during the main task, the imagery task (IMGT) and the overnight stay in the lab. During sleep, the TMR protocol was delivered. After waking up the next morning we asked participants whether they had heard any sounds during the night. In addition to the SQ and the SRTT, Session 4 also required participants to perform the explicit memory task.* ***(B)*** *A schematic representation of the two sequences of the SRTT. Auditory and visual cues appeared simultaneously. The tones had a fixed duration of 200 ms and were either high or low pitched depending on the counterbalancing condition. The visual cue remained on the screen until the correct key was pressed. The next trial appeared after a 300 ms inter-trial interval.* ***(C)*** *TMR protocol. Tones associated with one of the SRTT sequences were re-played to the participants in N3 and N2 (blue bubbles on the hypnogram). A single sequence (blue rectangles) was played, followed by a 20 s break (grey rectangles). Each sequence comprised 12 tones (here shown as coloured notes) with the inter-trial interval jittered between 2500 and 3500 ms (grey vertical bars). SRTT: Serial Reaction Time Task;*

IMGT: Imagery Task; EHI: Edinburgh Handedness Inventory; PSQI: Pittsburgh Sleep Quality Index; SQ: Stanford Sleepiness Scale Questionnaire.

2.6 DATA ANALYSIS

2.6.1 BEHAVIOURAL DATA

2.6.1.1 SRTT: REACTION TIME

Performance on the SRTT was measured using mean reaction time per block of each sequence (cued and uncued). Trials with reaction time >1000 ms were excluded from the analysis; trials with incorrect button presses prior to the correct ones remained. Both hands (BH) dataset included all SRTT trials, left hand (LH) dataset included trials performed using left, non-dominant hand only, right hand (RH) dataset included trials performed using right, dominant hand only. Mean performance on 4 chosen blocks (see Fig.2A, brown and grey vertical rectangles) was then subtracted from the mean performance on 2 random blocks to separate learning of the sequence from sensorimotor mapping, thus providing a measure of 'sequence-specific skill' (SSS). SSS was calculated for each sequence and session separately, using either the first 4 blocks (early SSS) or the last 4 blocks (late SSS) since both early SSS (Koopman et al., 2020b; Cousins et al., 2016) and late SSS (Cousins et al., 2014a) have been shown to benefit from TMR. This is illustrated below, with higher outcome values indicating better performance:

1. Early sequence-specific skill (early SSS) = mean (random blocks) – mean (first 4 blocks)
2. Late sequence-specific skill (late SSS) = mean (random blocks) – mean (last 4 blocks)

It is important to note, however, that the impact of TMR on the remaining blocks has not been tested and thus remains unknown.

Finally, we calculated the difference between the SSS of the cued and uncued sequence, thus obtaining a measure of 'cueing benefit', i.e., the effect of TMR on the SRTT performance, for each participant and at each timepoint.

2.6.1.2 QUESTIONNAIRES

To identify outliers in the ordinal, PSQI and SQ datasets, a robust Modified Z-Score outlier detection method was used (Iglewicz & Hoaglin, 1993), calculated using the following formula: $M_i = (0.6745\ (x_i - \tilde{x}))/MAD$, where $MAD = \text{median}\{|x_i - \tilde{x}|\}$ and denotes Median

Absolute Deviation. Any score above 3.5 would be considered an outlier and removed from the dataset. However, that was not the case for any of the questionnaires' measures. PSQI global scores were calculated according to the original scoring system described in Buysse et al. (1989). Handedness, i.e., laterality quotient based on the short version of the EHI, was scored as in Veale (2014).

2.6.1.3 EXPLICIT MEMORY

To assess the explicit memory of each sequence, individual items were scored as correct only if they were both (1) in the correct sequence position and (2) followed or preceded by at least one other correct item, hence minimising the effect of guessing as in Cousins et al. (2014a). Chance level was determined by taking an average score of 10 randomly generated sequences per participant. The mean of those scores across all participants was considered the average number of items guessed by chance, which was then compared with the number of correct items for each sequence to determine if the explicit memory was formed.

2.6.2 EEG DATA ANALYSIS

All EEG data were analysed in MATLAB using FieldTrip Toolbox (Oostenveld et al., 2011).

2.6.2.1 SLEEP SCORING

EEG signal from eight scalp electrodes (F3, F4, C3, C4, P3, P4, O1, O2), two EOG and two EMG channels recorded throughout the night was pre-processed, re-referenced to the mastoids (TP9, TP10), and scored according to the standard AASM criteria (Berry et al., 2015). Scoring was performed by two trained and independent sleep scorers blind to the cue presentation periods using a custom-made interface (https://github.com/mnavarretem/psgScore).

2.6.2.2 SPINDLES AND SLOW WAVES DETECTION

The relationship between spindles and behavioural outcomes was determined by focusing the analysis on 8 electrodes located over motor regions: 4 left (FC3, C5, C3, C1, CP3) and 4 right (FC4, C6, C4, C2, CP4). However, for visualisation purpose, the rest of the electrodes in the International 10-20 EEG system were also pre-processed and analysed as outlined below, and included in the final figure (Fig.5A). Briefly, the raw data were first down-sampled to 250 Hz (for them to be comparable between the two EEG data acquisition systems) and filtered

using a Chebyshev Type II infinite impulse response (IIR) filter (passband: f = [0.3 – 35] Hz; stopband: f < 0.1 Hz & f > 45 Hz). Then, for each participant, the channels were visually inspected and, if deemed noisy for the majority of the night, interpolated based on their triangulation-based neighbours. The final pre-processing step involved re-referencing the data to the mastoids (TP9, TP10). Algorithms for spindles and SOs counting (Navarrete et al., 2020) were subsequently employed to detect slow oscillations (0.3 – 2 Hz) and sleep spindles (11 – 16 Hz) at each electrode and in each sleep stage separately (N2, N3) or combined (N2 and N3). Briefly, for spindles detection, the data were filtered in a sigma band using an IIR filter again (passband: f = [11 – 16] Hz; stopband: f < 9 Hz & f > 18 Hz). Then, we used a 300 ms time window to compute the root mean squared (RMS) of the signal. Any event that had surpassed the 86.64 percentile (1.5 SD, Gaussian distribution) of the RMS signal was regarded as a candidate spindle. To fit the final spindle detection criteria (based on Iber et al., 2007), an event was deemed a sleep spindle if it occurred in the target sleep stage, lasted between 0.5 and 2.0 s and had at least 5 oscillations during that period (Navarrete et al., 2020). For SOs detection, the EEG data were filtered in the 0.3 – 2 Hz band using the IIR filter (passband: f = [0.3 – 2] Hz; stopband: f < 0.1 Hz & f > 4 Hz). Waves with negative deflection between -35 and -300 mV and with zero crossing between 0.13 and 1.66 s were considered SOs. The identified spindles and SOs were then separated into those that fell within the cue and no-cue periods. The cue period was defined as the time interval between 0 and 3.5 s after a tone onset (the longest inter-trial interval allowed), thus essentially encompassing the period from the onset of the first tone in a sequence until 3.5 s after the onset of the last one. The no-cue period was defined as the time interval between the sequences - from 3.5 to 20.0 s after the onset of the last tone in the sequence.

Spindle density was calculated by dividing the total number of spindles at each electrode by the length (in minutes) of the target period (cue period during target sleep stage, no-cue period during target sleep stage). Spindle density, together with the number of spindle and SO events during the cue and no-cue period of each of the target sleep stages, are presented in Table S2. Spindle laterality was obtained by subtracting spindle density over the right motor channels from the spindle density over the left motor channels.

2.6.2.3 PHASE AMPLITUDE COUPLING

Trial-based phase-amplitude coupling was calculated for each channel using mean resultant length (MRL), as described in Canolty et. al. (2006). Similarly to the spindle analysis, the

statistical analyses concerning the phase-amplitude coupling measures were performed on the 8 motor electrodes (FC3, C5, C3, C1, CP3, FC4, C6, C4, C2, CP4), with the rest of the electrodes in the International 10-20 EEG system analysed only for visualisation purpose (Fig.6A). In short, the phase and amplitude evolving times-series was filtered using a zero-shift IIR filter in delta (passband: f = [0.3 – 2] Hz; stopband: f < 0.1 Hz & f > 4 Hz) and sigma (passband: f = [11 – 16] Hz; stopband: f < 9 Hz & f > 18 Hz) bands, respectively. Hilbert transform was then applied to obtain the instantaneous frequency of the delta- and sigma-filtered signal. Phase-amplitude coupling was computed for concurrent SO and spindles detected using the methods described above (*2.6.2.2 Spindles and slow waves detection*). The number of SO-spindle events detected during the cue and no-cue period of each of the target sleep stages is presented in Table S2. MRL was then estimated to assess how well spindles align to the same phase of the SO. MRL equal to 0 reflects no coupling (i.e., random distribution of spindles in a slow wave cycle), whereas MRL equal to 1 reflects maximal coupling (i.e., all spindles occurring at precisely the same time of every slow wave cycle). For clarity, the measure is later referred to as the coupling strength. The coupling strength was compared to a set of surrogate data (200 permutations), created by shifting the amplitude evolving time-series by a randomised time lag from the phase evolving time-series. This allowed us to assess the significance of coupling and define a normalised, or z-scored, coupling strength (CS) as below:

$CS_n = (CS_{raw} - \mu)/ \sigma$, where μ and σ denote the mean and standard deviation of surrogate's coupling strength, respectively. The normalised coupling strength is used throughout this report. To obtain the coupling phase, i.e., the phase of the SO which the spindles best align to, the phase of the SO cycle was cut into 100 equally spaced bins between $-\pi$ to π radians. The average amplitude of each phase bin was then calculated for the amplitude evolving time-series, and the circular mean was computed from the circular distribution to obtain the final value for the coupling phase. The coupling phase plots (Fig.S3) were created using the CircStat toolbox in MATLAB (Berens, 2009).

Finally, both the mean of the coupling strength and the circular mean of the coupling phase (in degrees) were calculated for all motor channel, left motor channels and right motor channels to obtain the coupling strength and phase over both hemispheres, left and right hemisphere, used in the further analyses.

2.6.3 STATISTICAL ANALYSIS

Statistical analysis was performed in MATLAB, the R environment (R Core Team, 2012) or SPSS Statistics 25 (IBM Corp., Armonk, NY, USA). Each dataset (LH, RH, BH), stimulation period (cue vs no-cue) and sleep stage (N2, N3, N2 and N3 combined) was analysed separately. Normality assumption was checked using Shapiro-Wilk test and all tests conducted were two-tailed, with the significance threshold set at 0.05. Results are presented as mean ±standard error of the mean (SEM), unless otherwise stated.

To compare two related samples, we used paired-samples t-tests (Gaussian distribution), Wilcoxon signed-rank test (non-Gaussian distribution) or Watson-Williams test (circular data). Correlations between EEG data and behavioural measures were tested with either Pearson's correlation (Gaussian distribution) or Spearman's Rho (non-Gaussian distribution) using the cor.test function in the R environment, or using the circ_corrcl function in the circStat toolbox (Berens, 2009) if correlations between circular and linear variables were evaluated. If a given data point within a linear variable was more than 1.5 interquartile ranges (IQRs) below the first quartile or above the third quartile, and if it was deemed an outlier through visual inspection, that datapoint was removed from the dataset before the correlational analysis. Multiple correlations were corrected using false discovery rate (FDR) correction ($q < 0.05$) (Benjamini & Hochberg, 1995), thus controlling for the expected proportion of falsely rejected hypotheses. The corrections were based on a total of 3 correlations, given the 3 sessions of interest (S2, S3, S4).

To test the relationship between SSS, TMR and Session we used linear mixed effects analysis to account for the non-independence of multiple responses collected from the participants over time, as well as to avoid listwise deletion due to missing data in S4. The analysis was performed on S2-S4 using lme4 package in R (Bates et al., 2015). For both late and early SSS, TMR and Session were entered into the model as fixed effects (without interaction) and random intercept was specified for each subject. The final models for BH, LH and RH dataset were as follows:

> model = lmer(SSS ~ Session + TMR + (1|Participant), data=dataset)

To assess the effect of hand, LH and RH datasets were combined and the model fitted to the data also included hand as one of the fixed effects:

> model = lmer(SSS ~ Session + TMR + Hand + (1|Participant), data=dataset)

Finally, to explore how the TMR effect evolves over time (i.e., between S2 and S4) we fitted the following model to each dataset, with cueing benefit as the dependent variable. This analysis was performed on the 'late' cueing benefit only (i.e., calculated using the late SSS data), as no TMR effect was found for the early SSS.

> model = lmer(CueingBenefit ~ Session + (1|Participant), data=dataset)

The model fitted to the LH and RH datasets combined, again, also included hand as one of the fixed effects:

> model = lmer(CueingBenefit ~ Session + Hand + (1|Participant), data=dataset)

Likelihood ratio tests of the full model against the model without the effect being tested were used to obtain the p-values. When a significant difference was found, post-hoc pairwise comparisons of least-squares means with Holm adjustment were conducted using the emmeans package in R (Lenth et al. 2019). The emmeans package was also used to calculate the effect sizes.

2.7 RESULTS PRESENTATION

Plots displaying behavioural results, pairwise comparisons and relationships between two variables were generated using *ggplot2* (version 3.3.0) (Wickham, 2009) in R. Fig.5A and Fig.6A were generated using *ft_topoplotER* function in FieldTrip Toolbox (Oostenveld et al., 2011). Fig.1 and Fig.S1 were created in Microsoft PowerPoint v16.53. Fig.S4 was generated using CircHist MATLAB package (Zittrell, 2019).

2.8 DATA AND CODE AVAILABILITY

All the data used in the study as well as the software and scripts used to present the experimental tasks to the participants and to perform the analysis have been made publicly available via the Open Science Framework and can be accessed at: https://osf.io/ksxpw/?view_only=25ca3eca34004df496302c9dc1cc7580.

3 RESULTS

3.1 QUESTIONNAIRES

The EHI confirmed that all participants were right-handed, as the laterality quotient score (ranging between -100 and +100, where the negative values indicate left-handers and positive right-handers) was +100% for all but one subject who scored +75%. PSQI global scores (on a 21-points scale) ranged between 2 and 6 points across participants, with a mean of 4.33 (±0.32), indicating, on average, a 'good quality' of sleep (Buysse et al., 1989). The median answer on the SQ (with 1 and 9 indicating the highest and lowest level of alertness, respectively) was 2 for all sessions (±IQR for S1: 1, S2: 2, S3: 1, S4: 1), indicating similar levels of alertness throughout the study.

Participants did report hearing experimental sounds during the night. On a 3-points scale, the median answer was 3 (IQR: 2), with 28% of the participants not hearing any sounds (answer 1), 11% of the participants being unsure (answer 2), and 61% of the participants hearing them clearly (answer 3). However, when asked about the number of sounds they had heard, the median answer was 3 (IQR: 3.5) sounds and only 17% of the subjects reported hearing more than 6 sounds.

3.2 SRTT

3.2.1 REACTION TIME AND SEQUENCE SPECIFIC SKILL

Before sleep, no difference was found between the average reaction time of the cued and uncued sequence for either BH (t_{17} = -0.35, p = 0.729), LH (t_{17} = -1.02, p = 0.321) or RH (t_{17} = 0.38, p = 0.710) dataset (paired-samples t-tests for all comparisons). Similar results were obtained where comparing random sequences before sleep for all datasets (BH: Z = -0.63, p = 0.528; LH: Z = -0.72, p = 0.472; RH: Z = -0.68, p = 0.500; Wilcoxon signed-rank test). Thus, any post-sleep difference between the sequences can be regarded as the effect of TMR. Furthermore, average reaction times before sleep were significantly shorter for the last 4 sequence blocks than the random blocks, confirming that the participants learned both sequences during S1 (BH cued: Z = -3.72; BH uncued: Z = -3.72; LH cued: Z = -3.59; LH uncued: Z = -3.72; RH cued and uncued: Z = -3.68; p < 0.001 for all comparisons, Wilcoxon signed-rank test). Summary statistic for each sequence and dataset during S1 are presented in Table 1.

Mean reaction time (± SEM) for the BH trials of each block during the full course of the study is shown in Fig.2A.

Table 1. SRTT summary statistics.

Mean reaction time (± SEM) (in ms) *for the BH, LH and RH trials of the cued and uncued sequence blocks (24 per sequence) as well as random blocks (2 with tones matching the cued and 2 with tones matching the uncued sequence) during Session 1. Average reaction time* (± SEM) for the last 4 blocks of each sequence is shown as well. *BH: both hands; LH: left hand; RH: right hand. n = 18.*

Dataset	Cued sequence	Uncued sequence	Cued random	Uncued random	Cued sequence (last 4 blocks)	Uncued sequence (last 4 blocks)
BH	346.64 ±6.80	347.93 ±6.86	375.27 ±7.19	378.55 ±4.97	320.13 ±7.13	312.32 ±11.41
LH	358.02 ±8.22	362.97 ±7.34	384.50 ±9.00	387.33 ±6.82	328.85 ±7.84	328.78 ±11.23
RH	335.28 ±6.08	332.90 ±7.40	366.04 ±6.79	369.83 ±5.00	311.35 ±7.74	295.86 ±12.33

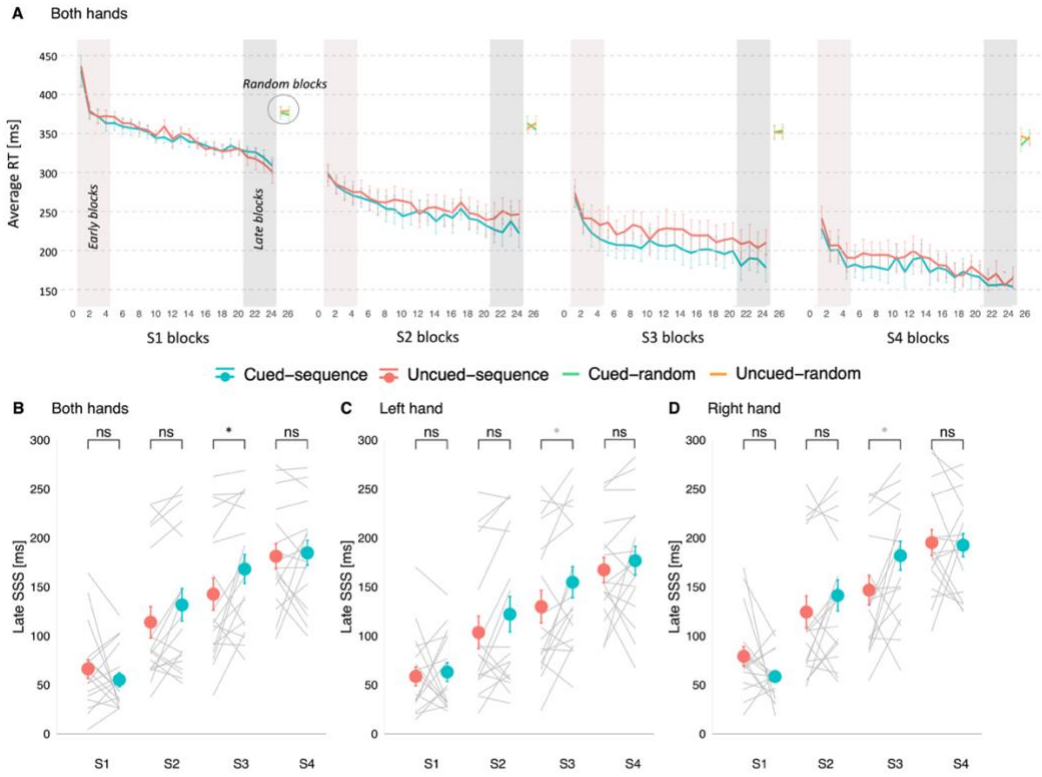

Fig. 2. (A) *Mean reaction time [ms] for the BH trials of the cued (blue) and uncued (red) sequence blocks as well as random blocks (green and orange) during all experimental sessions (S1-S4). Error bars represent SEM. Vertical rectangles highlight the first (brown) and last (grey) four blocks of each sequence used to calculate the early and late SSS, respectively.* ***(B-D)*** *TMR affects late SRTT performance on Session 3 (S3), regardless of the hand analysed. Mean late SSS for BH* ***(B)****, LH* ***(C)*** *and RH* ***(D)*** *dataset plotted against time (S1-S4). Red dots represent mean ±SEM for the uncued sequence. Blue dots represent mean ±SEM for the cued sequence. Grey lines represent performance of each subject. Although not marked with p-values, the participants showed significant improvements with time*

*on both the cued and the uncued sequence. ns: non-significant; *p < 0.05, uncorrected; when adjusted for multiple comparisons using Holm's correction the effect of TMR on S3 remained significant only for (B) (black *) but not for (C) or (D) (grey *). n = 18 for S1-S3, n = 17 for S4. S1-4: Session 1-4; SSS: Sequence Specific Skill. BH: both hands; LH: left hand; RH: right hand.*

Post-sleep SRTT re-test sessions took place 23.89 h (SD: 0.47) (S2), 9.89 days (SD: 1.02) (S3), and 43.94 days (SD: 4.43) (S4) after S1. To examine the effect of TMR on SSS (either early or late) over time (S2-S4) we performed a linear mixed effects analysis on each dataset (BH, LH, RH) separately. Results of all the likelihood ratio tests of the full model (with TMR and session as fixed effects and participant as a random effect) against the model without the fixed effect of interest are presented in Table S3A-C. No effect of TMR was revealed for the early SSS (Table S3Ai-Ci) and therefore we will focus only on the late SSS (Table S3Aii-Cii) for the rest of this report. Likewise, even though we found a main effect of hand on the SRTT performance ($p < 0.001$; Table S3D, better performance for the dominant hand), the analysis revealed similar results for all datasets (BH: Table S3-5A, LH: Table S3-5B, RH: Table S3-5C), with no interaction between either hand and session or hand and TMR ($p > 0.05$; Table S3D). Thus, we will report findings for the BH dataset only.

The analysis revealed that the inclusion of session as a fixed effect significantly improves model fit ($X^2(2) = 47.66$, $p < 0.001$), pointing to the main effect of session on the late SSS (Table S3Aii). Post-hoc tests showed a difference ($p_{adj} < 0.001$) between both S2 and S3, and S3 and S4, suggesting that the participants were getting significantly faster with each session (Table S4Aii).

When the full model was tested against the model without TMR, the likelihood ratio test revealed that the inclusion of TMR as a fixed effect significantly improves model fit for late SSS ($X^2(1) = 6.87$, $p = 0.009$) across all sessions (S2-S4) (Table S3Aii). The interaction between TMR and session was, however, not significant ($X^2(2) = 2.39$, $p = 0.303$) (Table S3Aii). The linear mixed effects analysis therefore suggested a main effect of TMR on late SSS. Given our previous findings on this task (Cousins et al., 2014a; Cousins et al., 2016; Koopman et al., 2020b), we expected higher performance for the cued than uncued sequence on S2 but sought to determine if that is also true for the remaining sessions. Hence, we carried out post-hoc pairwise comparisons to reveal the session(s) during which TMR significantly affected the SRTT performance. To our surprise, we found a significant effect of TMR on S3 ($p_{adj} = 0.045$) but no difference between the cued and uncued sequence performance on S2 ($p_{adj} = 0.179$) or S4 ($p_{adj} = 0.743$) (Table S5A, Fig.2B-D). The absence of a TMR effect at S2

could be explained by the fact that our second session occurred in the evening (24h post-stimulation), while both Cousins et al. (2014a, 2016) and Koopman et al. (2020b) who report significant findings on the same task retested their participants in the morning (12h post-stimulation). Nevertheless, the TMR effect seems to (re-)emerge following subsequent nights of sleep (i.e., at day 10 post-stimulation) but does not last until 6 weeks later.

3.2.2 CUEING BENEFIT ACROSS TIME

To explore how the TMR effect evolves over time, we compared the difference between the late SSS of the cued and uncued sequence (i.e., the cueing benefit) across sessions (S2-S4) using the linear mixed effects analysis. Inclusion of session as the fixed effect revealed a trend for improved model fit for the BH dataset ($\chi^2(2) = 5.89$, $p = 0.053$; Table S6A), a significantly better model fit for the RH dataset ($\chi^2(2) = 6.77$, $p = 0.034$; Table S6C) but no model improvement for the LH dataset ($\chi^2(2) = 2.31$, $p = 0.314$; Table S6B). We carried out post-hoc pairwise comparisons to reveal the sessions between which the cueing benefit differed. While the cueing benefit was similar between S2 and S3 (BH: $p_{adj} = 0.347$, RH: $p_{adj} = 0.334$), we found a difference between S3 and S4 for both datasets (BH: $p_{adj} = 0.040$, RH: $p_{adj} = 0.026$) (Table S7, Fig.3A, C). These results suggest a benefit of TMR 10 days post-manipulation which then decreases with time. Interestingly, there was neither a main effect of hand nor an interaction between hand and session ($p > 0.05$; Table S6D).

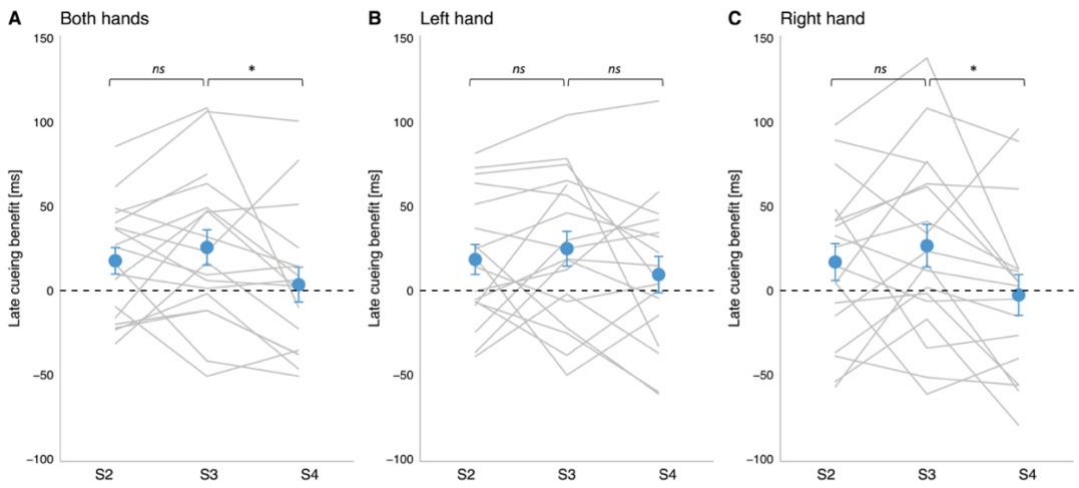

Fig. 3. *Cueing benefit over time. Mean late SSS on the uncued sequence subtracted from the cued sequence for both hands* ***(A)****, left hand* ***(B)*** *and right hand* ***(C)****, plotted against time (S2-S4). The effect of time was trending towards significance for (A) and reached significance for (C), with the post-hoc comparisons revealing a difference between S3 and S4 in both cases. Blue dots represent mean ±SEM. Grey lines represent the TMR effect for each subject. n = 18 for S2-S3; n = 17 for S4. S2-4: Session 2-4; ns: non-significant, *p < 0.05.*

3.3 EXPLICIT MEMORY TASK

Given that TMR was shown to promote the emergence of explicit knowledge the next morning (Cousins et al., 2014a), we also set out to test whether this is true after a longer period. However, we found no difference between the free recall of the cued and uncued sequence ($Z = -1.29$, $p = 0.196$, Wilcoxon signed-rank test), suggesting no TMR effect on the explicit knowledge of the sequence ~6 weeks post-encoding (Fig.S2). Nevertheless, performance on both sequences differed from chance (cued: $Z = -3.39$, $p < 0.001$; uncued: $Z = -3.43$, $p < 0.001$; Wilcoxon signed-rank test), indicating that the participants learned both sequences explicitly over the course of the experiment.

3.4 CORRELATIONS WITH SLEEP STAGES

All sleep parameters obtained through sleep scoring are summarised in Table 2. To test whether there was any relationship between sleep characteristics and the TMR effect we correlated the time spent in N2 and N3 (the two target stages for our stimulation) with the cueing benefit at S2, S3 and S4, and for each dataset (BH, LH, RH) separately. All correlational results are presented in Table S8. The percentage of time spent in N2 showed a positive correlation with the cueing benefit at S4 for BH ($R = 0.65$, $p_{adj} = 0.045$, Fig.4A) and LH ($R = 0.68$, $p_{adj} = 0.027$, Fig.4B) and with the cueing benefit at S2 for RH ($R = 0.66$, $p_{adj} = 0.018$, Fig.4C). In other words, the time spent in N2 (but not N3) predicts TMR benefit for the dominant hand earlier (24h post-TMR) than for the non-dominant hand or both hands combined (6 weeks post-TMR).

Table 2. Sleep parameters.

Total recording duration, total sleep time, time spent in each sleep stage and time scored as movement presented as average (minutes ± SEM) and as percentage of the total recording duration. Total sleep time was calculated by subtracting the time spent in wake from the total recording duration. N1-N3: stage 1 - stage 3 of NREM sleep. n = 16.

	Percentage of total recording duration [%]	Mean duration ± SEM [min]
Total recording duration	100 %	525.13 ±10.56
Total sleep time	89.74 %	469.66 ±9.27
Wake	10.26 %	55.47 ±9.50
N1	5.76 %	30.34 ±5.35
N2	41.65 %	219.56 ±12.28
N3	21.89 %	113.13 ±7.38
REM	18.78 %	97.72 ±6.22
Movement	1.54 %	8.22 ±1.56

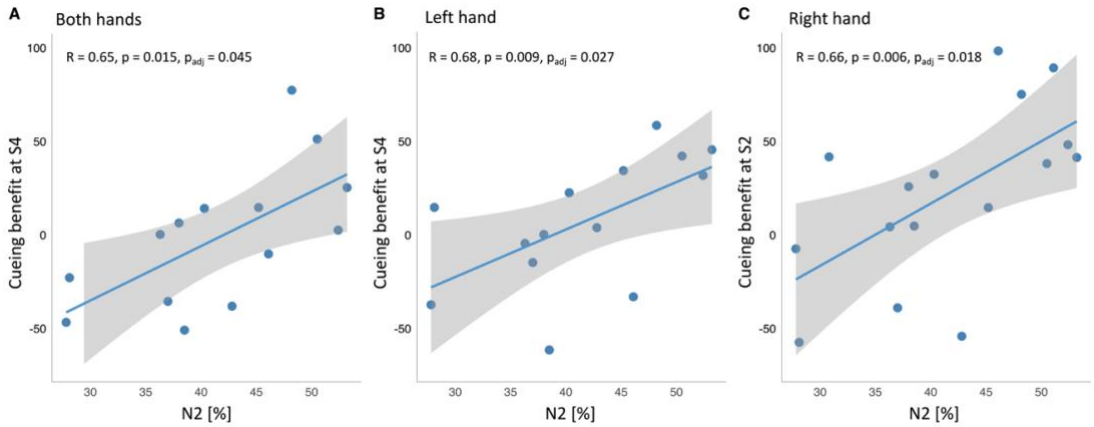

Fig. 4. *Positive correlation between the percentage of time spent in N2 and the cueing benefit (late SSS for the uncued sequence subtracted from the cued sequence) at S4 for both hands* ***(A)*** *and left hand* ***(B)****, and at S2 for right hand* ***(C)****. Grey bands around the regression line represent confidence intervals. Both the uncorrected p-values and the p-values adjusted for multiple comparisons are shown. S4: Session 4, S2: Session 2, N2: stage 2 of NREM sleep; SSS: Sequence Specific Skill. n = 14 for (A-B) and n = 16 for (C).*

3.5 SLEEP SPINDLES

Sleep spindles, i.e., short bursts of activity in sigma (11-16 Hz) frequency band, are the EEG signatures characteristic of N2 (Purcell et al., 2017). Thus unsurprisingly, the average spindle density over the task related regions in N2 was significantly higher than in N3, but only during the cue (N2: 4.39 ±0.46 vs N3: 3.75 ±0.39; z = -2.765, p = 0.006) and not the no-cue period (N2: 3.62 ±0.43 vs N3: 3.47 ±0.47; z = -0.370, p = 0.711; Wilcoxon signed-rank test). Furthermore, for N2, the average spindle density during the cue period (4.39 ±0.46) was significantly higher than during the no-cue period (3.62 ±0.43) (z = -2.81, p = 0.005; Wilcoxon signed-rank test, Fig.5). This, however, was not the case for N3 (cue: 3.75 ±0.40 vs no-cue: 3.47 ±0.47; z = -1.42, p = 0.157; Wilcoxon signed-rank test). When the two stages (N2 and N3) were combined, the spindle density averaged over the left motor areas was significantly higher than over the right motor areas, both during the cue (left: 3.84 ±0.42 vs right: 3.44 ±0.38; t(17) = 3.84, p = 0.001) and no-cue period (left: 3.36 ±0.44 vs right: 2.95 ±0.40; t(17) = 3.77, p = 0.002; paired-samples t-test). This result could relate to the fact that participants performed better on the task using their right hand, contralateral to the site of the local spindle density increase, as shown before (Nishida & Walker, 2007; Cousins et al., 2014a). Overall, these results suggest that cueing may elicit sleep spindles in N2, but not in N3. The immediate surge in spindle density upon stimulation in N2 could then be followed by a subsequent reduction after the cue period. This would explain the similar levels of spindle density in N2 and N3 observed during the no-cue period.

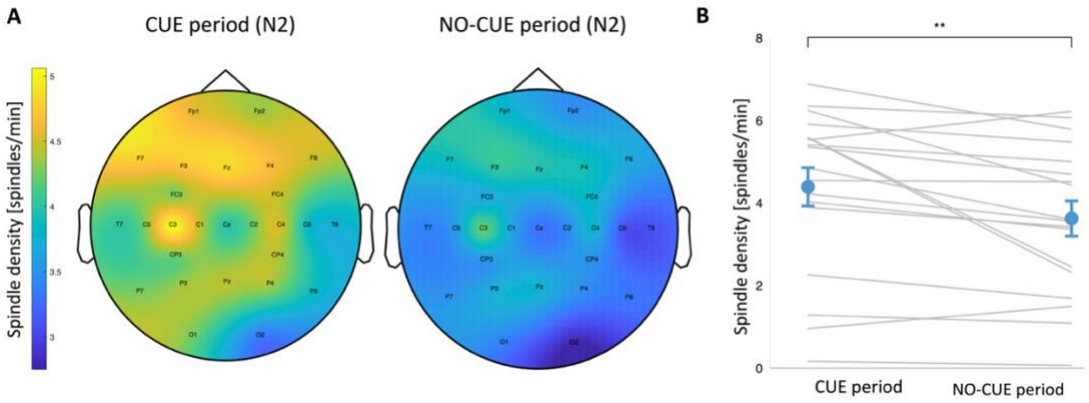

Fig. 5. (A) *Topographic distribution of spindle density (spindles per min) in N2 and N3 of the cue (left) and no-cue (right) period.* ***(B)*** *Spindle density averaged over motor channels (4 left: FC3, C5, C3, C1, CP3 and 4 right: FC4, C6, C4, C2, CP4) during N2 was significantly higher during the cue period than during the no-cue period. **p = 0.005. N2-N3: stage 2 - stage 3 of NREM sleep. n = 18.*

The literature reports spindle-related changes over brain areas involved in learning (Cox et al., 2014) which often predict behavioural improvements (Bergmann et al., 2012; Lutz et al., 2021; Fogel et al., 2017a; Barakat et al., 2013). Thus, to test whether sleep spindles relate to the cued sequence advantage in our study, we correlated cueing benefit for S2-S4 with spindle density, averaged over motor electrodes. Since we found no main effect of hand on the cueing benefit, only the BH dataset was analysed. Given the differential role of sleep spindles during different stages of NREM sleep (Cox et al., 2012; Dehnavi et al., 2019), spindles in N2 and N3 were analysed both together and separately. Nevertheless, there was no correlation surviving FDR correction ($p_{adj} > 0.05$; Table S9).

Previous studies using similar procedural learning tasks report a relationship between spindle laterality and behavioural outcomes (Cousins et al., 2014a; Nishida & Walker, 2007). Even though the task used in this study was bilateral, rather than unilateral as in Nishida & Walker (2007) and Cousins et al. (2014a), we found higher spindle density over the left vs right motor areas. Thus, we were interested to test whether lateralized spindle density (calculated by subtracting spindle density over the right motor channels from spindle density over the left motor channels) correlate with the cueing benefit of either hand (especially the right hand, contralateral to the left hemisphere). N2 and N3 were analysed both separately and combined, as before, with all the results reported in Table S10. We found that during the cue period (N2 and N3 combined), spindle laterality trended strongly towards a positive correlation with the cueing benefit in the BH dataset at S4 ($R = 0.56$, $p = 0.017$, $p_{adj} = 0.051$, Fig.S3). No other correlation between spindle laterality and cueing benefit was revealed (p_{adj}

> 0.05). This could suggest that lateralized spindles that occur over the task-related regions and during the cue period may be able to predict long-term cueing benefit for both hands, however this should be treated with caution given that it did not survive FDR correction.

3.6 PHASE AMPLITUDE COUPLING

According to the active systems consolidation theory, memory reactivation (and thus consolidation) involves a coordinated interplay, or coupling, of hippocampal sharp-wave ripples, neocortical slow waves and thalamocortical sleep spindles (Rasch & Born, 2013). At the scalp EEG level, coupling between the phase of SOs and amplitude of sleep spindles (phase-amplitude coupling) was linked to performance improvements on several memory tasks (Niknazar et al., 2015; Mikutta et al., 2019; Muehlroth et al., 2019; Hahn et al., 2020; Denis et al., 2020; Schreiner et al., 2021), but not (yet) with the SRTT. Thus, we sought to investigate phase-amplitude coupling during N2 and N3, and its relationship with our behavioural outcomes from the SRTT.

Coupling strength was higher in N3 than in N2 both for the cue (N2: 1.09 $\pm$0.21 vs N3: 2.07 $\pm$0.34; z = -2.59, p = 0.010) and the no-cue period (N2: 0.38 $\pm$0.14 vs N3: 1.39 $\pm$0.18; z = -3.64, p < 0.001) (Wilcoxon signed-rank test). For N2 and N3 combined, we found no difference in coupling strength between the two hemispheres (cue period: z = -1.02, p = 0.306; no-cue period: z = -0.72, p = 0.472; Wilcoxon signed-rank test). However, coupling strength was significantly higher during the cue period than during the no-cue period (cue: 2.29 $\pm$0.32 vs no-cue: 1.30 $\pm$0.23; z = -2.61, p = 0.009; Wilcoxon signed-rank test; Fig.6). This suggests that cueing may increase the strength of SO-spindle coupling during both N2 and N3.

Regarding the coupling phase, i.e., the phase of the SO which the spindles best align to, no significant differences were revealed. Specifically, we found no difference between the coupling phase in N2 and N3 (cue: $F_{1,35}$ = 0.843, p = 0.365; no-cue: $F_{1,35}$ = 2.05, p = 0.162), no difference between the coupling phase over the left and right motor regions (cue period: $F_{1,35}$ = 0.08, p = 0.774; no-cue period: $F_{1,35}$ = 1.16, p = 0.288), and no difference between the cue and no-cue period (N2: $F_{1,35}$ = 0.05, p = 0.820; N3: $F_{1,35}$ = 0.29, p = 0.591; N2 and N3: $F_{1,35}$ = 1.11, p = 0.300, Fig.S4) (Watson-Williams test for all comparisons).

We then correlated coupling strength with cueing benefit for S2-S4, both during the cue and no-cue period. Given that coupling strength did not differ between left and right

hemispheres, it was averaged over all motor channels (both hemispheres) and correlated with the BH dataset (Table S11). Unexpectedly, the analysis did not reveal any correlation between cueing benefit at S3 and coupling strength during the cue period (p_{adj} > 0.05). Instead, we found a negative correlation between cueing benefit at S2 and coupling strength during the no-cue period, only in N2 (R = -0.59, p_{adj} = 0.036, Fig.S5). Although the correlation could be of interest to future studies, it is hard to justify given both the existing literature and our findings so far. Furthermore, we found no correlation between cueing benefit and coupling phase (p_{adj} > 0.05, Table S12), leaving the relationship between SO-spindle coupling and behavioural performance open to debate.

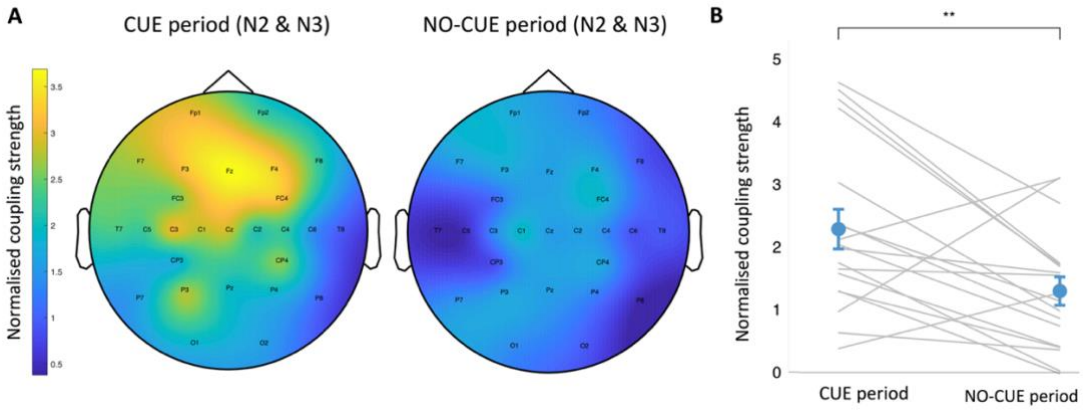

Fig. 6. (A) *Topographic distribution of the normalised (z-scored) strength of the SOs-spindle coupling during N2 and N3 of the cue (left) and no-cue (right) period.* ***(B)*** *Coupling strength over motor channels (4 left: FC3, C5, C3, C1, CP3 and 4 right: FC4, C6, C4, C2, CP4) for N2 and N3 was significantly higher during the cue period than during the no-cue period. **p = 0.009. N2-N3: stage 2 – stage 3 of NREM sleep. n = 18.*

4 DISCUSSION

In this study we primarily aimed to investigate how the memory-enhancing effects of TMR on procedural skill learning develop over time, with a particular focus on the SRTT. Participants continued to improve on the SRTT over the total course of the study (6 weeks), with significantly higher performance from one session to the next, regardless of the hand used. Overall, participants were also significantly better on the task with their dominant (right) than the non-dominant (left) hand. When all post-stimulation sessions were combined, a main effect of TMR was apparent. This was true regardless of whether the hands were analysed together or separately, but only for late SSS, with no difference for early SSS. Closer examination revealed that late SSS was comparable between sequences 24h post-manipulation but was greater for the cued than the uncued sequence 10 days later. Six weeks

after stimulation the TMR effect had disappeared from all datasets. Furthermore, we found a main effect of session on the cueing benefit: while the TMR advantage was comparable between the first two time points post-stimulation, it decreased from 10 days to 6 weeks post-TMR. Thus, our results show a benefit of TMR 10 days post-manipulation which then decreases with time.

We sought to describe the electrophysiology of N2 and N3 (the two target sleep stages for our stimulation) as well as determine whether sleep spindles and their coupling with SOs could predict the behavioural benefits of TMR. These analyses revealed that (1) the time spent in N2, but not N3, predicts cueing benefit; (2) there is a significant increase in both the average spindle density and coupling strength immediately after cue presentation, as compared to a later time period.

4.1 TMR EFFECT EVOLVES OVER TIME

We showed a main effect of TMR on the late SRTT performance across all post-sleep sessions. However, the difference between the cued and uncued sequence was the strongest at 10 days post-encoding, thus driving the main effect. The absence of a clear TMR effect the day after stimulation was unexpected, given that it was apparent on the day after stimulation in prior studies (Cousins et al., 2014a, 2016; Koopman et al., 2020b). This difference could have occurred because our second session was scheduled in the evening rather than in the morning, immediately after a full night of sleep (as in previous studies), thus also preventing direct comparison with literature. Alternatively, the reason for the delayed effects could be the jittering of the TMR cues during sleep. Jittering was introduced instead of a fixed inter-trial duration to allow better characterisation of temporal features of memory reactivation. However, this also disrupted the temporal dynamics of the cueing since the brain could no longer predict when the next cue was due to arrive. Prior work has confirmed that cueing specifically acts to consolidate the sequence (Cousins et al., 2014a; Cousins et al., 2016), and such temporally unpredictable cueing may have made it harder to consolidate the transitions which make up the sequence. Indeed, internalising the regularity of events optimises stimulus processing and allows faster learning (Nobre et al., 2007). Therefore, randomising the timing of cues, as opposed to previous studies that used constant intervals between cues (Cousins et al., 2014a; Cousins et al., 2016; Koopman et al., 2020b), could have delayed the behavioural effects of stimulation.

The significant TMR effect at 10 days post-manipulation suggests that TMR starts a process which unfolds over several days after stimulation. This is consistent with Cairney et al. (2018) who argue that synapses relevant for the task are 'tagged' for plastic changes during sleep following cue presentation, allowing the cueing benefits to persist. Alternatively, synapses relevant for both the cued and uncued sequence may be 'tagged' at encoding, priming them for further plastic changes that occur during sleep over the course of several subsequent nights (Seibt & Frank, 2019; Pereira & Lewis, 2020). This process could be facilitated by cue presentation for one of the sequences, allowing its memory trace to persist for longer. In other words, cue presentation could have preferentially strengthened the cued memory trace which thereby allowed it to be remembered for longer and gave rise to the observed effect. Thus, what we here termed as the 'cueing benefit' could be simply regarded as the difference between the strengths of two traces and their differential decay time.

The disappearance of the TMR effect at our last experimental session suggests that the TMR-related plasticity does not last until, or beyond, 6 weeks. Furthermore, the absence of any TMR benefit to explicit knowledge at 6 weeks is in keeping with the idea that all the TMR benefits fade by this time. This is not surprising given that neither object-location (Shanahan et al., 2018) nor emotional (Groch et al., 2017a) memory seems to benefit from the manipulation even a week later. Alternatively, the loss of TMR effect at S4 could have been caused by a ceiling effect which prevented further improvement on the task, and thus allowed the slower consolidating uncued sequence to catch up with the faster consolidating cued sequence. Indeed, by the end of the study the average reaction time on the sequence blocks was below 200 ms, which is lower than reported by other SRTT studies with less training sessions (Koopman et al., 2020b; Cousins et al., 2014a; Romano et al., 2010). On the other hand, Verstynen et al. (2012), who used a far more intensive study design than we did, showed that lower reaction times are possible on the same task. The study reports continuous behavioural improvements across 10 days of SRTT training (5 weekdays for 2 weeks) with reaction time reaching less than 100 ms by the tenth session (Verstynen et al., 2012). Nevertheless, the reaction times reported in the literature are not exactly comparable due to several differences in the task design (e.g., different number of trials, blocks or hands used) and, to our knowledge, the ceiling values have not yet been estimated. Assuming that the ceiling has not been reached and given the difference in cueing benefit between 10 days and 6 weeks post-stimulation, our data suggest that the TMR benefit is present at 10 days post-stimulation, and then decreases across the days that follow until it disappears altogether. Unfortunately, regardless of the reason for the loss of cueing effect at 6 weeks,

the maximum duration of the TMR impact remains unknown. Future research should thus attempt to understand this process more fully, and to determine the extent of time for which TMR can impact memories, both the explicit and implicit ones. It will also be interesting to see how these parameters vary across declarative and procedural tasks.

4.2 TMR BENEFITS BOTH HANDS

Even though the overall performance on the task was significantly better for the dominant than the non-dominant hand, data from both hands yielded similar results with respect to TMR. There was also no interaction between hand and TMR across time, or significant effect of hand on the cueing benefit. These findings were counter to our expectation, since weaker memory representations with a lot of room for improvement have been shown to be more responsive to TMR than the strongly remembered ones (Cairney et al., 2016; Drosopoulos et al., 2007; Schapiro et al., 2018; Tambini et al., 2017). Hence, we expected the non-dominant (i.e., 'weaker') hand to benefit more from the stimulation than the dominant one. Given our findings from this and a previous study in which we found selective TMR benefits for the non-dominant hand the next morning (Koopman et al., 2020b), one possibility could be that TMR is indeed more beneficial for the non-dominant hand, but only at first. The effect of TMR on the dominant hand could then catch up within 24 h post-learning, thus making it impossible for us to observe any difference between the hands at our first re-test session which occurred 24 h after the initial training. Another, more probable explanation is that the handedness effect is so subtle that the results are strongly dependent on individual variations. With two experimental sessions, 14 participants in the RH and 13 in the LH dataset, Koopman et al. (2020b) found a significant TMR x time interaction for left but not right hand, although a qualitative trend was apparent for the latter. Here, with more power (four experimental sessions, 18 participants in the RH and LH dataset), we report a significant main effect of TMR for both datasets. Nevertheless, further investigation into the effect of handedness is warranted, with a particular focus on the first 24 h post-manipulation. Studies analogous to this one but using left-handed individuals could determine whether our findings can be generalised from the right-handed sample to the entire population.

Despite the fact that both hands benefitted from TMR, cueing benefit for the dominant hand was predicted by N2 earlier (24 h post-TMR) than cueing benefit for the non-dominant hand (6 weeks post-TMR). This could suggest distinct consolidation processes for the two hands. Interestingly, time spent in N3 did not predict cueing benefit. This difference highlights the

importance of N2 in procedural memory consolidation, in line with prior work (Smith & MacNeill, 1994; Smith et al., 2004a; Korman et al., 2007; Fogel & Smith 2006; Fogel et al., 2007). It also suggests that N2 may be a better choice than N3 for this TMR.

4.3 RELATIONSHIP BETWEEN EEG FEATURES AND TMR BENEFITS

We found a significant increase in the average spindle density (N2) and coupling strength (both N2 and N3) during the cue period (0-3.5s after cue onset) as compared to the no-cue period (3.5-20s after the onset of the last cue in the sequence). This suggests that auditory stimulation can perhaps boost sleep oscillations and thereby induce an immediate processing of memory traces. Our results are consistent with other TMR studies, namely Antony et al. (2018) which reports spindle density increase early (0-2s) relative to later (2-4s) after TMR cues, and Cairney et al. (2018) which likewise observes a surge in spindle activity (modulated by the SO up-state) 1.7 to 2.3 s after cue onset. Both Antony et al. (2018) and Cairney et al. (2018) linked the cue-induced spindle activity increase to memory reactivation during sleep, as well as behavioural performance at retest.

5 CONCLUSIONS

We provide the first report on the long-term impact of TMR on procedural skill learning. While previous studies showed cueing effects lasting for up to a week (Hu et al., 2015; Simon et al., 2018), our findings are the first to suggest that TMR over one night of sleep can affect procedural memories as far as 10 days post-stimulation, with effects lost by six weeks post-stimulation. Furthermore, we show that time in N2 but not N3 predicts TMR benefit. Finally, both spindle density and SO-spindle coupling strength increase upon cue onset, thus drawing attention to the rapid memory processing which may be happening at that time. Future investigation of the mechanisms underlying long-term impact of TMR, including the plastic changes induced by such manipulation, will help us to build an understanding of the complex processes linked to memory reactivation in sleep.

6 SUPPLEMENTARY MATERIAL

SUPPLEMENTARY TABLES:

Table S1. TMR cues.

Average number and percentage of TMR cues delivered during each sleep stage, arousal, or movement. In blue: target sleep stages. N1-3: stage 1-3 of NREM sleep.

	Cues delivered ±SEM	Cues delivered [%]
Sleep stage		
Wake	24.2 ± 5.2	1.5 %
N1	21.2 ± 5.0	1.3 %
N2	515.8 ± 59.1	31.8 %
N3	974.4 ± 67.5	60.6 %
REM	46.9 ±17.3	2.9 %
Movement	11.4 ± 2.7	0.7 %
Arousal	18.5 ± 2.3	1.2 %

Table S2. Sleep spindles and slow waves.

Average number and density (number/min) of spindles and slow waves (± SEM), together with the number of concurrent spindles and slow waves. Results are presented for N2 and N3 of the cue and no-cue period. N2-3: stage 2-3 of NREM sleep.

	Cue period		No-cue period	
	N2	**N3**	**N2**	**N3**
Spindles				
number	132.89 ± 15.99	189.66 ± 100.96	49.93 ± 6.25	84.61 ± 10.52
density	4.66 ± 0.40	3.95 ± 0.34	3.83 ± 0.36	3.68 ± 0.40
Slow waves				
number	116.78 ± 14.37	790.35 ± 109.32	39.72 ± 5.07	334.35 ± 47.12
density	5.00 ± 0.91	17.62 ± 2.43	3.74 ± 0.76	14.98 ± 2.12
Spindle-slow wave events				
number	31.72 ± 4.91	112.17 ± 19.09	9.79 ± 1.55	49.02 ± 8.97

Table S3. Effect of and interaction between TMR, hand and session.

*Results of the likelihood ratio tests between the full, linear mixed effects model and reduced models, i.e., models without the fixed effect of interest, or with an interaction. The full model was used to test the effect of TMR, hand and session on the early and late SSS. df: degrees of freedom; χ2: chi-squared; AIC: Akaike Information Criterion; SSS: Sequence Specific Skill. *p < 0.05.*

	df	χ2	p-value	AIC of a reduced model	AIC of a full model
A. Both hands					
i) Early SSS					
TMR	1	1.6444	0.1997	1063.7	1064.0
Session	2	59.122	**<0.0001***	1119.1	1064.0
TMR x Session	2	0.9857	0.6109	1064.0	1067.0
ii) Late SSS					
TMR	1	6.8745	**0.0087***	1095.1	1090.2
Session	2	47.658	**<0.0001***	1133.8	1090.2

TMR x Session	2	2.3855	0.3034	1090.2	1091.8
B. Left hand					
i) Early SSS					
TMR	1	2.2429	0.1342	1078.3	1078.0
Session	2	47.796	**<0.0001***	1121.8	1078.0
TMR x Session	2	0.2217	0.8951	1078.0	1081.8
ii) Late SSS					
TMR	1	7.9449	**0.0048***	1105.4	1099.5
Session	2	42.655	**<0.0001***	1138.1	1099.5
TMR x Session	2	1.0439	0.5934	1099.5	1102.4
C. Right hand					
i) Early SSS					
TMR	1	0.5754	0.4481	1102.6	1104.0
Session	2	46.001	**<0.0001***	1146.0	1104.0
TMR x Session	2	1.5515	0.4604	1104.0	1106.4
ii) Late SSS					
TMR	1	4.0784	**0.0434***	1115.6	1113.5
Session	2	40.065	**<0.0001***	1149.6	1113.5
TMR x Session	2	3.1900	0.2029	1113.5	1114.3
D. Left and right hand combined					
i) Early SSS					
Hand	1	13.486	**0.0002**	2144.0	2132.5
Hand x Session	2	0.6384	0.7267	2132.5	2135.8
TMR x Hand	1	0.1552	0.6936	2132.5	2134.3
ii) Late SSS					
Hand	1	23.772	**<0.0001***	2181.5	2159.7
Hand x Session	2	0.3491	0.8398	2159.7	2163.4
TMR x Hand	1	0.1785	0.6727	2159.7	2161.6

Table S4. Effect of session on SSS.

*Post-hoc pairwise comparisons between sessions for the early and late SSS, conducted on each dataset separately. P-values reported are Holm adjusted. SSS: Sequence Specific Skill; S2-4: Session 2-4; df: degrees of freedom. *p < 0.05.*

	Mean S2 (±SEM) [ms]	**Mean S3 (±SEM) [ms]**	**Mean S4 (±SEM) [ms]**	**Estimate (±SEM)**	**df**	**t ratio**	**p-value** (Holm adj)	**Effect size**
A. Both hands								
i) Early SSS								
S2-S3	76.3 (13.5)	110 (13.5)	-	-33.8 (6.37)	93.3	-5.302	**<0.0001**	-1.09
S3-S4	-	110 (13.5)	134 (13.6)	-24.0 (6.51)	93.5	-3.691	**0.0004**	-0.84
ii) Late SSS								
S2-S3	123 (13.9)	155 (13.9)	-	-32.6 (7.30)	93.3	-4.473	**<0.0001**	-1.29
S3-S4	-	155 (13.9)	181 (14.0)	-25.3 (7.45)	93.5	-3.392	**0.0010**	-0.92
B. Left hand								
i) Early SSS								
S2 – S3	70.6 (14.4)	102.2 (14.4)	-	-31.7 (6.84)	93.3	-4.630	**<0.0001**	-1.124
S3 – S4	-	102.2 (14.4)	124.1 (14.5)	-21.9 (6.98)	93.3	-3.138	**0.0023**	-0.778
Ii) Late SSS								
S2 – S3	113 (14.8)	142 (14.8)	-	-29.5 (7.65)	93.3	-3.856	**0.0004**	-0.936
S3 – S4	-	142 (14.8)	169 (14.9)	-26.8 (7.82)	93.3	-3.433	**0.0009**	-0.851
C. Right hand								
i) Early SSS								
S2 – S3	82.8 (13.3)	118.1 (13.3)	-	-35.9 (8.04)	93.3	-4.466	**<0.0001**	-1.084
S3 – S4	-	118.1 (13.4)	144.2 (13.4)	-26.1 (8.21)	93.3	-3.174	**0.0020**	-0.787
ii) Late SSS								
S2 – S3	133 (13.5)	169 (13.5)	-	-35.8 (8.37)	93.3	-4.277	**0.0001**	-1.038
S3 – S4	-	169 (13.5)	192 (13.7)	-23.7 (8.55)	93.3	-2.768	**0.0068**	-0.686

Table S5. Effect of TMR on late SSS during each session.

*Post-hoc pairwise comparisons of late SSS between the cued and uncued sequence on each session (S2-S4), conducted on each dataset separately. Both the uncorrected and Holm adjusted p-values are reported. S2-4: Session 2-4; SSS: Sequence Specific Skill; df: degrees of freedom. *p < 0.05.*

Cued vs Uncued	Mean cued (± SEM) [ms]	Mean uncued (± SEM) [ms]	Estimate (± SEM)	df	t ratio	p value	p value (Holm adj)	Effect size
A. Both hands								
S2	132 (14.9)	114 (14.9)	-17.70 (10.3)	93.3	-1.716	0.090	0.179	-0.589
S3	168 (14.9)	143 (14.9)	-25.61 (10.3)	93.3	-2.482	**0.015***	**0.045***	-0.852
S4	182 (15.0)	179 (15.0)	-3.39 (10.6)	93.3	-0.329	0.743	0.743	-0.116
B. Left hand								
S2	122 (15.8)	104 (15.8)	-18.47 (10.8)	93.3	-1.707	0.091	0.182	-0.586
S3	155 (15.8)	130 (15.8)	-24.88 (10.8)	93.3	-2.300	**0.024***	0.071	-0.789
S4	174 (15.9)	164 (15.9)	-9.48 (11.1)	93.3	-0.852	0.397	0.397	-0.301
C. Right hand								
S2	141 (14.8)	124 (14.8)	-16.93 (11.8)	93.3	-1.430	0.156	0.312	-0.491
S3	182 (14.8)	155 (14.8)	-26.63 (11.8)	93.3	-2.248	**0.027***	0.081	-0.772
S4	194 (15.0)	191 (15.0)	2.65 (12.2)	93.3	0.207	0.829	0.829	0.077

Table S6. Effect of hand and session on the cueing benefit.

*Results of the likelihood ratio tests between the full, linear mixed effects model and reduced models, i.e., models without the fixed effect of interest, or with an interaction. The full model was used to test the effect of hand and session on the cueing benefit (calculated as the cued minus uncued late SSS). χ2: chi-squared; AIC: Akaike Information Criterion. df: degrees of freedom. *p < 0.05. ^p < 0.07.*

	df	χ2	p-value	AIC of a reduced model	AIC of a full model
A. Both hands					
Session	2	5.8926	0.0525^	531.64	529.75
B. Left hand					
Session	2	2.3147	0.3143	539.94	541.63
C. Right hand					
Session	2	6.7724	**0.0338***	553.35	550.58
D. Left and right hand combined					
Hand	1	0.3647	0.5459	1082.80	1084.40
Hand x Session	2	0.8668	0.6483	1084.40	1087.50

Table S7. Effect of session on the cueing benefit.

*Post-hoc pairwise comparisons between post-stimulation sessions for the cueing benefit (calculated as the cued minus uncued late SSS), conducted on both hands and right hand datasets. Both the uncorrected and Holm adjusted p-values are reported. S2-4: Session 2-4; df: degrees of freedom. *p < 0.05.*

	Mean S2 (±SEM) [ms]	Mean S3 (±SEM) [ms]	Mean S4 (±SEM) [ms]	Estimate (±SE)	df	t ratio	p-value (Holm adj)	Effect size
A. Both hands								
S2-S3	17.70 (9.52)	25.61 (9.52)	-	-7.9 (8.30)	37.1	-0.952	0.347	-0.330
S3-S4	-	25.61 (9.52)	4.98 (9.67)	-20.6 (8.48)	37.4	2.434	**0.040***	-0.850
B. Right hand								
S2 – S3	16.93 (11.9)	26.63 (11.9)	-	-9.69 (9.91)	37.1	-0.979	0.334	-0.327
S3 – S4	-	26.63 (11.9)	0.18 (12.1)	-26.45 (10.11)	37.3	2.616	**0.026***	0.853

Table S8. Cueing benefit and the duration of N2 and N3.

*Results of Spearman's correlations between the cueing benefit (SSS for the uncued sequence subtracted from the cued sequence) and the percentage of time spent in N2 and N3. Both the uncorrected and FDR corrected p-values are reported. df: degrees of freedom; S2-4: Session 2-4; SSS: Sequence Specific Skill; N2-3: Stage 2-3 of NREM sleep. *p < 0.05. ^p < 0.07.*

	Time spent in N2 [%]				Time spent in N3 [%]			
	df	Spearman's correlation	p-value	p-value (FDR corr)	df	Spearman's correlation	p-value	p-value (FDR corr)
A. Both hands								
S2	14	0.509	**0.046***	0.069^	14	0.509	0.891	0.891
S3	14	0.306	0.249	0.249	14	0.238	0.373	0.559
S4	12	0.648	**0.015***	**0.045***	12	0.437	0.120	0.360
B. Right hand								
S2	14	0.665	**0.006***	**0.018***	14	-0.153	0.571	0.571
S3	14	0.085	0.755	0.755	14	0.253	0.343	0.552
S4	13	0.357	0.192	0.288	13	0.250	0.368	0.552
C. Left hand								
S2	14	0.209	0.436	0.436	14	0.094	0.730	0.730
S3	14	0.409	0.117	0.176	14	0.109	0.689	0.730
S4	12	0.684	**0.009***	**0.027***	12	0.442	0.116	0.348

Table S9. Cueing benefit and spindle density.

*Results of Spearman's correlations (both FDR corrected and not) between the cueing benefit for BH dataset during each of the post-stimulation sessions (S2, S3, S4) and spindle density averaged over all motor channels during the cue (A) and no-cue (B) period. N2 (green) and N3 (blue) were analysed separately and together (N23, purple). df: degrees of freedom; S2-4: Session 2-4; N2-3: stage 2-3 of NREM sleep; BH: Both Hands. *p < 0.05.*

Dataset	Session	Sleep stage	Correlation coefficient	p-value	df	p-value (FDR corr)
A. Cue period						
BH	S2	N2	-0.329	0.232	13	0.456
BH	S3	N2	0.179	0.524	13	0.524
BH	S4	N2	0.292	0.310	12	0.465
BH	S2	N3	-0.335	0.174	16	0.522
BH	S3	N3	-0.086	0.736	16	0.736
BH	S4	N3	0.185	0.491	14	0.736
BH	S2	N23	-0.344	0.162	16	0.486
BH	S3	N23	-0.049	0.848	16	0.848
BH	S4	N23	0.212	0.431	14	0.646
B. No-cue period						
BH	S2	N2	-0.492	**0.040***	16	0.120
BH	S3	N2	-0.199	0.427	16	0.640
BH	S4	N2	0.044	0.874	14	0.874
BH	S2	N3	-0.183	0.467	16	0.701
BH	S3	N3	0.018	0.948	16	0.948
BH	S4	N3	0.218	0.417	14	0.701
BH	S2	N23	-0.334	0.176	16	0.528
BH	S3	N23	-0.138	0.584	16	0.625
BH	S4	N23	0.132	0.625	14	0.625

Table S10. Cueing benefit and spindle laterality.

*Results of Pearson's correlations performed between cueing benefit for each dataset (BH, LH, RH) during each of the post-stimulation sessions (S2, S3, S4) and spindle laterality (left hemispheric density – right hemispheric density) during cue (A) and no-cue (B) period. N2 (green), N3 (blue) and N2 and N3 combined (purple) were analysed separately. df: degrees of freedom; S2-S4: Session 2-4; N2-3: stage 2-3 of NREM sleep; BH: Both Hands; LH: Left Hand; RH: Right Hand. *p < 0.05. ^p < 0.07.*

Dataset	Session	Sleep stage	Correlation coefficient	p-value	df	p-value (FDR corr)
A. Cue period						
BH	S2	N2	-0.002	0.995		0.995
BH	S3	N2	-0.102	0.697		0.995
BH	S4	N2	0.169	0.546		0.995
RH	S2	N2	0.264	0.306		0.866
RH	S3	N2	-0.067	0.800		0.866
RH	S4	N2	-0.050	0.866		0.866
LH	S2	N2	-0.315	0.218		0.654
LH	S3	N2	-0.122	0.641		0.736
LH	S4	N2	0.095	0.736		0.736
BH	S2	N3	-0.210	0.419		0.668
BH	S3	N3	-0.112	0.668		0.668
BH	S4	N3	0.153	0.571		0.668
RH	S2	N3	-0.231	0.372		0.929
RH	S3	N3	-0.024	0.929		0.929
RH	S4	N3	-0.133	0.637		0.929
LH	S2	N3	-0.105	0.688		0.688
LH	S3	N3	-0.193	0.457		0.686
LH	S4	N3	0.235	0.381		0.686
BH	S2	N23	0.035	0.894		0.894
BH	S3	N23	0.179	0.492		0.738
BH	S4	N23	0.588	**0.017***		0.051^
RH	S2	N23	0.245	0.343		0.483
RH	S3	N23	0.183	0.483		0.483
RH	S4	N23	0.226	0.418		0.483
LH	S2	N23	-0.223	0.389		0.584
LH	S3	N23	0.142	0.586		0.586
LH	S4	N23	0.475	0.063^		0.189
B. No-cue period						
BH	S2	N2	-0.142	0.587		0.595
BH	S3	N2	-0.139	0.595		0.595
BH	S4	N2	0.250	0.351		0.595
RH	S2	N2	0.046	0.861		0.956
RH	S3	N2	-0.042	0.874		0.956
RH	S4	N2	-0.016	0.956		0.956
LH	S2	N2	-0.306	0.232		0.373
LH	S3	N2	-0.231	0.373		0.373
LH	S4	N2	0.285	0.284		0.373
BH	S2	N3	-0.279	0.278		0.438

BH	S3	N3	-0.271	0.292	0.438
BH	S4	N3	-0.068	0.804	0.804
RH	S2	N3	-0.310	0.226	0.571
RH	S3	N3	-0.148	0.571	0.571
RH	S4	N3	-0.227	0.415	0.571
LH	S2	N3	-0.136	0.602	0.602
LH	S3	N3	-0.372	0.142	0.426
LH	S4	N3	0.155	0.568	0.602
BH	S2	N23	-0.155	0.552	0.828
BH	S3	N23	0.030	0.910	0.910
BH	S4	N23	0.460	0.073	0.219
RH	S2	N23	0.049	0.853	0.853
RH	S3	N23	0.141	0.589	0.853
RH	S4	N23	0.089	0.754	0.853
LH	S2	N23	-0.331	0.194	0.291
LH	S3	N23	-0.116	0.656	0.656
LH	S4	N23	0.428	0.098	0.291

Table S11. Cueing benefit and coupling strength averaged over motor regions.

*Results of Spearman's correlations (both FDR corrected and not) between the cueing benefit for BH dataset during each of the post-stimulation sessions (S2, S3, S4) and coupling strength over all motor electrodes during the cue (A) and no-cue (B) period. N2 (green) and N3 (blue) were analysed separately and together (N23, purple). df: degrees of freedom; S2-4: Session 2-4; N2-3: stage 2-3 of NREM sleep; BH: Both Hands. *p < 0.05.*

Dataset	Session	Sleep stage	Correlation coefficient	p-value	df	p-value (FDR corr)
A. Cue period						
BH	S2	N2	-0.287	0.264	15	0.598
BH	S3	N2	0.185	0.477	15	0.598
BH	S4	N2	0.148	0.598	13	0.598
BH	S2	N3	-0.068	0.788	16	0.788
BH	S3	N3	0.295	0.234	16	0.483
BH	S4	N3	0.265	0.321	14	0.483
BH	S2	N23	-0.098	0.699	16	0.699
BH	S3	N23	0.191	0.448	16	0.672
BH	S4	N23	0.329	0.213	14	0.637
B. No-cue period						
BH	S2	N2	-0.585	**0.012***	16	**0.036***
BH	S3	N2	-0.434	0.073	16	0.109
BH	S4	N2	-0.209	0.436	14	0.436
BH	S2	N3	-0.286	0.249	16	0.747
BH	S3	N3	0.040	0.876	16	0.876
BH	S4	N3	0.100	0.713	14	0.876
BH	S2	N23	-0.389	0.111	16	0.333
BH	S3	N23	0.022	0.932	16	0.932
BH	S4	N23	0.256	0.339	14	0.509

Table S12. Cueing benefit and coupling phase averaged over motor regions.

*Correlation coefficient between the cueing benefit for BH dataset during each of the post-stimulation sessions (S2, S3, S4) (i.e., linear variable) and the coupling phase over all motor electrodes during the cue (A) and no-cue (B) period (i.e., circular variable). P-values (both FDR corrected and not) are presented as well. N2 (green) and N3 (blue) were analysed separately and together (N23, purple). df: degrees of freedom; coupling phase; S2-4: Session 2-4; N2-3: stage 2-3 of NREM sleep; BH: Both Hands. *p < 0.05.*

Dataset	Session	Sleep stage	Correlation coefficient	p-value	df	p-value (FDR corr)
A. Cue period						
BH	S2	N2	0.403	0.232	18	0.232
BH	S3	N2	0.630	**0.029***	18	0.077
BH	S4	N2	0.592	0.051	17	0.077
BH	S2	N3	0.467	0.140	18	0.186
BH	S3	N3	0.432	0.186	18	0.186
BH	S4	N3	0.464	0.161	17	0.186
BH	S2	N23	0.429	0.192	18	0.192
BH	S3	N23	0.447	0.166	18	0.192
BH	S4	N23	0.625	**0.029***	17	0.087
B. No-cue period						
BH	S2	N2	0.315	0.410	18	0.410
BH	S3	N2	0.383	0.267	18	0.401
BH	S4	N2	0.575	0.061	17	0.183
BH	S2	N3	0.537	0.075	18	0.225
BH	S3	N3	0.433	0.185	18	0.278
BH	S4	N3	0.189	0.739	17	0.739
BH	S2	N23	0.432	0.186	18	0.279
BH	S3	N23	0.153	0.820	18	0.820
BH	S4	N23	0.518	0.102	17	0.279

SUPPLEMENTARY FIGURES:

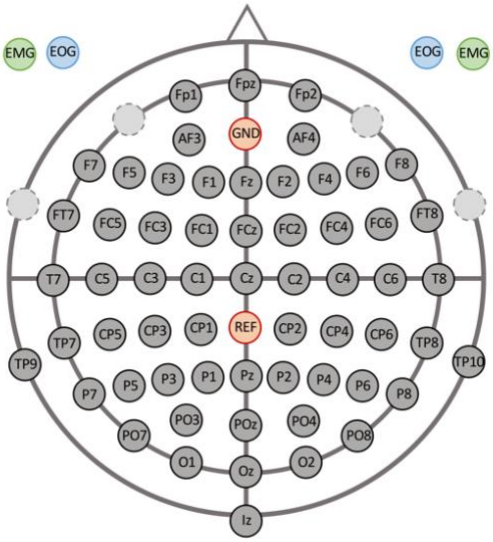

Fig. S1. EEG electrodes layout. *Orange: ground (GND) and reference (REF) electrodes; light grey (dashed circles): original position of the electrodes used to record EMG and EOG; green: EMG electrodes; blue: EOG electrodes.*

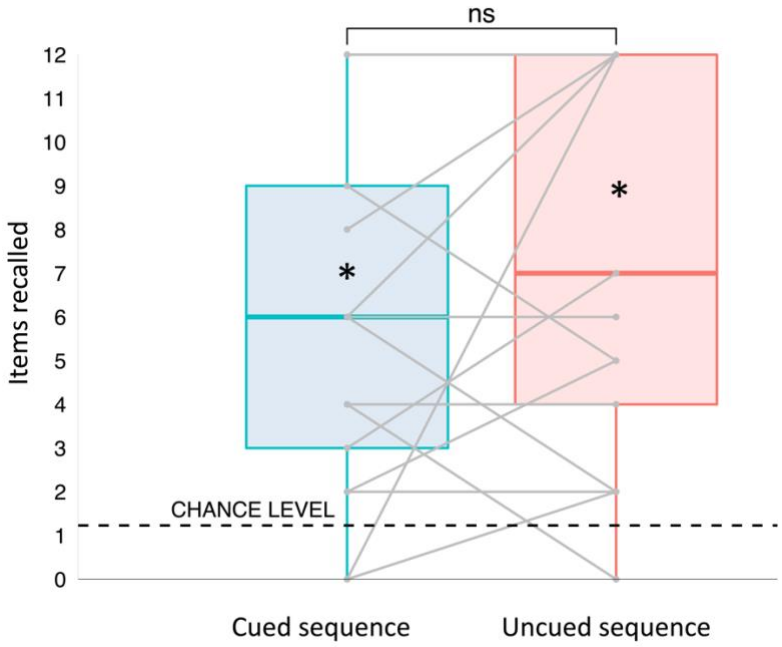

Fig. S2. Results of the explicit memory task. *Explicit knowledge of both sequences was significantly above chance (significance denoted with *) ~6 weeks post-encoding, although no effect of TMR was evident. Geoms represent median ± IQR for the cued (blue) and uncued (red) sequence, whiskers represent largest and lowest values within 1.5 IQR above and below the 75th and the 25th percentile, respectively. Grey dots represent performance of each subject. ns: non-significant. n = 17.*

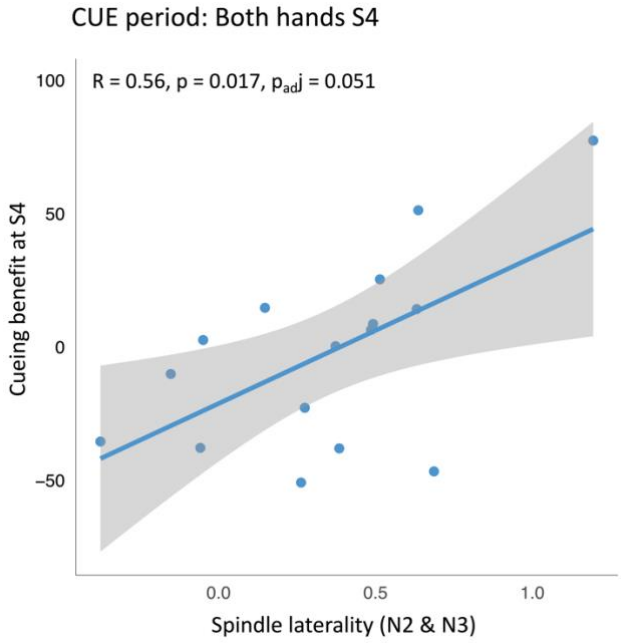

Fig. S3. Positive relationship between spindle laterality and cueing benefit at S4. *Pearson's correlation between the cueing benefit (cued – uncued) for the BH dataset during S4 and spindles laterality (left – right) during the cue period (N2 and N3 combined). Grey bands around the regression lines represent confidence intervals. Both an uncorrected p-value and a p-value adjusted for multiple comparisons are shown. S4: Session 4; N2-3: stage 2 - stage 3 of NREM sleep. n = 16.*

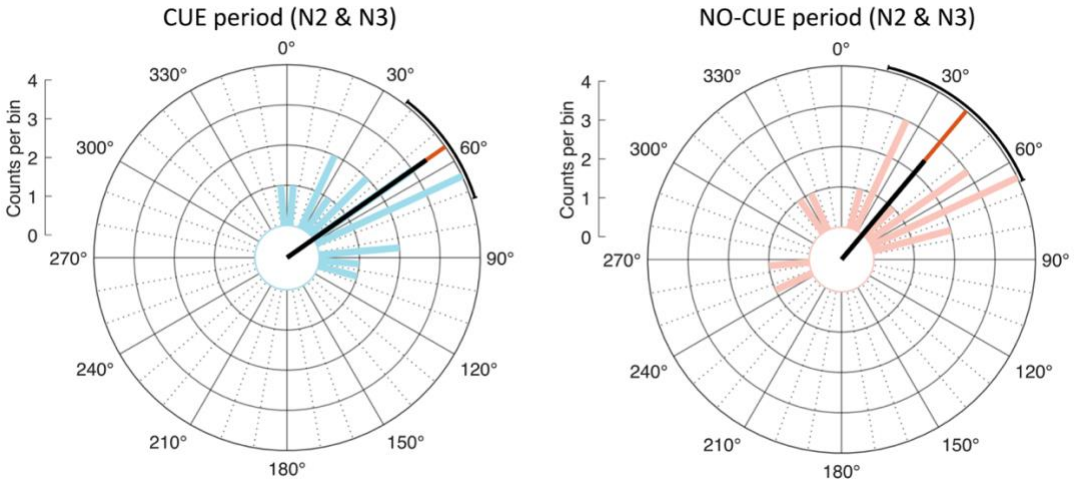

Fig. S4. Coupling phase for the cue and no-cue period. *Circular histogram of the coupling angle (in degrees) during N2 and N3 of the cue (left) and no-cue (right) period with the peak of the SO set at 0° and 10° bin size. Motor channels were analysed only. Coloured lines represent the phase of the SO which the spindles best align to for individual subjects (blue, cue period; red, no-cue period). Red line indicates the average angle; black line indicates the resultant vector length, with the line's length equal to the resultant vector's value expressed as the percent of the average angle line length. At the group level, the coupling phase did not differ between the cue and no-cue period (p > 0.05). n = 18.*

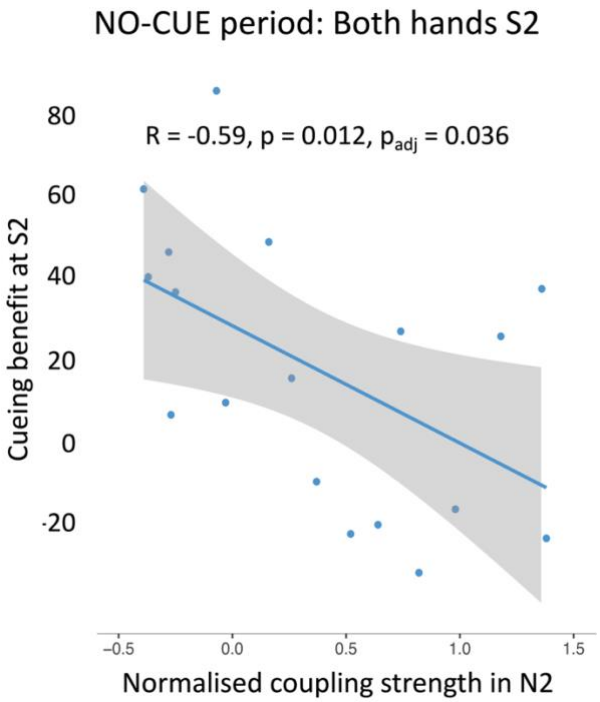

Fig. S5. Negative relationship between coupling strength and cueing benefit at S2. *A negative, Spearman's correlation between coupling strength (averaged over all motor channels) during the no-cue period in N2 and cueing benefit for the BH dataset in S2. Grey bands around the regression line represent confidence intervals. Both an uncorrected p-value and a p-value adjusted for multiple comparisons are shown. N2: Stage 2 of NREM sleep. S2: Session 2. n = 17.*

CHAPTER 3

Cueing motor memory reactivation during NREM sleep engenders learning-related changes in precuneus and sensorimotor structures

This chapter has been published as a pre-print on bioRxiv and submitted for consideration as an Article in *eLife.*

Rakowska, M., Bagrowska, P., Lazari, A., Navarrete, M., Abdellahi, M. E., Johansen-Berg, H., & Lewis, P. A. (2022). Cueing motor memory reactivation during NREM sleep engenders learning-related changes in precuneus and sensorimotor structures. *bioRxiv*.

Abstract

Memory reactivation during Non-Rapid Eye Movement (NREM) sleep is important for memory consolidation but it remains unclear exactly how such activity promotes the development of a stable memory representation. We used Targeted Memory Reactivation (TMR) in combination with longitudinal structural and functional MRI to track the evolution of a motor memory trace over 20 days. We show that repeated reactivation of motor memory during sleep leads to increased precuneus activation 24 h post-TMR. Interestingly, a decrease in precuneus activity over the next 10 days predicts longer-term cueing benefit. We also find both functional and structural changes in sensorimotor cortex in association with effects of TMR 20 days post-encoding. These findings demonstrate that TMR can engage precuneus in the short-term while also impacting on task-related structure and function over longer timescales.

1 INTRODUCTION

Memory consolidation is a process through which newly encoded memories become more stable and long-lasting. Consolidation is thought to involve repeated reinstatement, or reactivation of memory traces which allows their re-coding from short-term to long-term store (McClelland et al., 1995). Indeed, reactivation of learning-related brain activity patterns during sleep has been shown to predict subsequent memory performance (Deuker et al., 2013; Peigneux et al., 2004) and thus to play a critical role in memory consolidation (Born & Wilhelm, 2012; Diekelmann & Born, 2010b). However, it is unclear exactly how such offline rehearsal promotes the development of a stable memory representation. Here, we set out to investigate the neural plasticity underlying memory reactivation during sleep using Targeted Memory Reactivation (TMR) and magnetic resonance imaging (MRI).

TMR has recently emerged as a tool to study the mechanisms of memory reactivation. The technique involves re-presenting learning-associated cues during sleep (Rasch et al., 2007), thereby triggering reactivation of the associated memory representation and biasing their consolidation (Bendor & Wilson, 2012). In humans, this manipulation shows strong behavioural effects (e.g., procedural memories TMR: Chapter 2; Antony et al., 2012; Cousins et al., 2016; Schönauer et al., 2014), resulting in better recall of memories that were cued through TMR compared to those that were not cued. Functional activity associated with cueing has been investigated during and immediately after sleep (Cousins et al., 2016; Rasch

et al., 2007; Shanahan et al., 2018; van Dongen et al., 2012). However, little is known about precisely how the memory representations targeted by TMR evolve over longer time periods. We have previously reported behavioural effects of procedural memory cueing during sleep twenty days post-manipulation (Chapter 2). Yet, the functional plasticity underlying such benefits is unknown. It also remains to be established whether TMR can impact on brain structure and which regions support sleep-dependent memory consolidation in the long term.

In this study, we used TMR to determine if repeated reactivation of a motor memory trace during sleep engenders learning-related changes in the brain. We tracked such impacts over several weeks using functional and structural brain imaging (Fig.1A) and hypothesised that memory cueing during sleep would lead to rapid plasticity within the precuneus, a structure which houses newly formed memory representations or 'engrams' (Brodt et al., 2018). This region was of special interest since it has been shown to respond to repeated learning-retrieval epochs which help to strengthen a memory (Brodt et al., 2018) and can be thought of as a proxy for memory reactivation in sleep (Himmer et al., 2019). Although Brodt and colleagues (2018) used a declarative memory task to test precuneus function, the SRTT is thought to have a substantial declarative component (Albouy et al., 2008; Albouy et al., 2013a; Albouy et al., 2013b; Albouy et al., 2015), increasing our confidence in the hypothesis tested. Nevertheless, we expected the long-term storage of the memory engram to prevail in the task-related areas. We chose to focus specifically on a procedural memory task because the importance of sleep in procedural memory consolidation is well established (Loganathan, 2014; Walker, 2005). Furthermore procedural memory task improvements (Walker et al., 2003) and the associated structural changes (Kodama et al., 2018) have been shown to persist over time, with the same being true for the TMR effects (Chapter 2). Our participants were trained on two motor sequences in a Serial Reaction Time Task (SRTT). Each of these was associated with a different set of auditory tones (Fig.1B) but only one was reactivated during subsequent NREM sleep (Fig.1C). During learning and two post-sleep re-test sessions (24 h and 10 days post-TMR), participants were scanned with structural MRI (T1-weighted, T1w) and functional MRI (fMRI), the latter being acquired during SRTT performance. We were thus able to compare brain activity during the cued and uncued sequence performance, as well brain structure, both after one night and after 10 days. Twenty days post-TMR participants were again re-tested on the SRTT, now outside the scanner, allowing examination of the long-term impacts of TMR on behaviour. The resultant

dataset enabled us to investigate how the impact of cueing evolves across time, as well as study the relationships between structural, functional, and behavioural plasticity post-TMR.

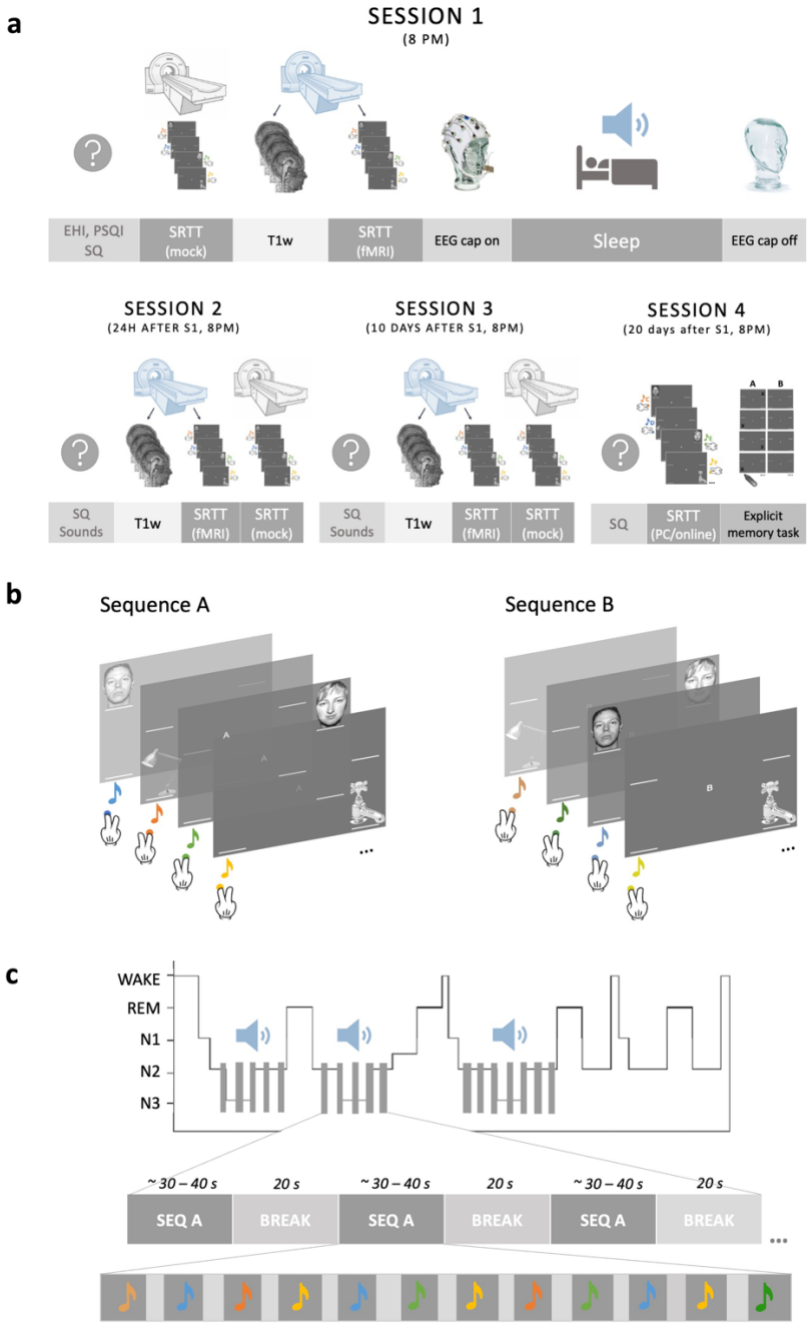

Fig. 1. Study design and methods. (a) *A schematic representation of the experimental sessions. SRTT and one or more questionnaires were delivered in each session. During S1-S3, SRTT was split in half, with the first half completed in the 0T 'mock' scanner (grey) and the second half in the 3T MRI scanner during fMRI acquisition (blue) (S1), or vice versa (S2-S3). T1w data was always acquired before fMRI. S1 also involved a stimulation night in the lab which the participants spent asleep and with the electroencephalography (EEG) cap on. During S4 SRTT data were acquired outside the MRI scanner and an explicit memory task was delivered at the very end of the study.* ***(b)*** *Two sequences of the SRTT. Only the first few trials are shown. Visual cues appeared at the same time as the auditory cues and the participants were instructed to push the key/button corresponding to the image location as*

quickly and accurately as possible. ***(c)*** *TMR protocol. Tones associated with one sequence were played during stable N3 and N2 (grey bars on the hypnogram). One repetition of the cued sequence (dark grey rectangles) was followed by a 20 s break during which no sounds were played (light grey rectangles). Each sequence repetition comprised 12 tones (depicted as coloured notes) with inter-trial interval jittered between 2500 and 3500 ms (light grey vertical bars). S1-S4: Session 1 – Session 4; EHI: Edinburgh Handedness Inventory; PSQI: Pittsburgh Sleep Quality Index; SQ: Stanford Sleepiness Scale Questionnaire; SRTT: Serial Reaction Time Task; fMRI: functional Magnetic Resonance Imaging; T1w: T1-weighted scan.*

2 MATERIALS AND METHODS

2.1 PARTICIPANTS

A pre-study questionnaire was used to exclude subjects with a history of drug/alcohol abuse, psychological, neurological or sleep disorders, hearing impairments, recent stressful life event(s) or regular use of any medication or substance affecting sleep. Participants were required to be right-handed, non-smokers, have regular sleep pattern, normal or corrected-to-normal vision, no prior knowledge of the tasks used in the study, and no more than three years of musical training in the past five years as musical training has previously been shown to affect procedural learning (Anaya et al., 2017; Romano Bergstrom et al., 2012). None of the participants reported napping regularly, working night shifts or travelling across more than two time-zones one month prior to the experiment. 33 volunteers fulfilled all inclusion criteria and provided an informed consent to participate in the study, which was approved by the Ethics Committee of the School of Psychology at Cardiff University and performed in accordance with the Declaration of Helsinki. All participants agreed to abstain from extreme physical exercise, napping, alcohol, caffeine, and other psychologically active food from 24 h prior to each experimental session. Finally, before their first session, participants were screened by a qualified radiographer from Cardiff University to assess their suitability for MRI and signed an MRI screening form prior to each scan.

Three participants had to be excluded from all analyses due to: technical issues (n = 1), voluntary withdrawal (n = 1), and low score on the handedness questionnaire (indicating mixed use of both hands), combined with a positive slope of learning curve during the first session (indicating lack of sequence learning before sleep) (n = 1). Hence, the final dataset included 30 participants (16 females, age range: 18 – 23 years, mean ±SD: 20.38 ± 1.41; 14 males, age range: 19 – 23 years, mean ±SD: 20.43 ± 1.16). However, due to the COVID-19 outbreak, six participants were unable to complete the study, missing all data from either

one (n = 1) or two (n = 5) sessions. Hence, n = 25 for all data collected during S3 and n = 24 for S4. The final dataset included one participant who could not physically attend S3. They performed the SRTT online, but their MRI data (fMRI and T1w) could not be collected and therefore the sample size for the MRI analyses of S3 had to be further decreased by one. Two additional participants were excluded from the fMRI analysis of S2 due to MRI gradient coil damage during fMRI acquisition (n = 1) and failure to save the fMRI data (n = 1). Hence, the final sample size for fMRI was n = 30 for S1, n = 28 for S2 and n = 24 for S3, whereas the final sample size for analysis of T1w data was n = 30 for S1, n = 30 for S2 and n = 24 for S3. Finally, one participant had to be excluded from all the analyses concerning EEG due to substantial loss of data caused by failure of the wireless amplifier during the night. However, the TMR procedure itself was unaffected and therefore this participant was included in the behavioural and MRI analyses. A flowchart of participants included and excluded from the different analyses is presented in Fig.S3.

2.2 STUDY DESIGN

The experiment consisted of four sessions (Fig.1A), all scheduled for ~8 pm. Upon arrival for the first session, participants completed Pittsburgh Sleep Quality Index (PSQI) (Buysse et al., 1989) to examine their sleep quality over the past month and Stanford Sleepiness Questionnaire (SQ) (Hoddes et al., 1973) to assess their current level of alertness. A short version of the Edinburgh Handedness Inventory (EHI) (Veale, 2014) was also administered to confirm that all subjects were right-handed before the learning session took place. Due to time constraints at the MRI scanner the learning session had to be split into two parts. The first half of the SRTT blocks (24 sequence blocks) were performed in a 0T Siemens 'mock' scanner (i.e., an environment that looked exactly like an MRI scanner, but with no magnetic field) which also helped to acclimate subjects to the scanner environment. The second half of the SRTT blocks (24 sequence blocks + 4 random blocks) was performed in a 3T Siemens MRI scanner during fMRI acquisition and used for functional data analysis. fMRI acquisition was preceded by a structural scan (T1w) and followed by a B0 fieldmap (see section *2.6 MRI data acquisition*). Once outside the MRI scanner, participants were asked to prepare themselves for bed. They were fitted with an EEG cap, performed the imagery task (see Chapter 2 for more details) and were ready for bed at ~11 pm. During N2 and N3 sleep stages, tones associated with one of the SRTT sequences were replayed to the participants via speakers (Harman/Kardon HK206, Harman/Kardon, Woodbury, NY, USA) to trigger

reactivation of the SRTT memories associated with them. Participants were woken up after, on average, 8.81 ±0.82 h in bed and had the EEG cap removed before leaving the lab.

We asked participants to come back for the follow-up sessions 23-26 h (session 2, S2), 10-14 days (session 3, S3) and 16-21 days (session 4, S4) after S1. During S2, participants were asked to indicate if they remember hearing any sounds during the night in the lab. S2 and S3 lasted ~2 h each and both involved the SQ and an MRI scan, during which a structural scan was acquired. This was followed by the SRTT re-test, with the first half of the SRTT blocks (24 sequence blocks + 4 random blocks) performed during the fMRI acquisition and the second half (24 sequence blocks + 4 random blocks) in the mock scanner. Note that the order of scanners (3T vs 0T) was flipped from S1 to S2 and S3 for the functional and structural assessment to occur as close to the TMR session as possible. S4 took place either in the lab or online, depending on the severity of COVID-19 restrictions at the time. During S4, SQ was delivered as before, together with the SRTT (one run, 48 sequence blocks + 4 random blocks) and an explicit memory task. Upon completion of each session, participants were informed about the upcoming SRTT re-tests as this has been shown to enhance post-learning sleep benefits (Wilhelm et al., 2011).

For offline data collection, the SRTT (S1-S3) was back projected onto a projection screen situated at the end of the MRI/mock scanner and reflected into the participant's eyes via a mirror mounted on the head coil; the questionnaires and the SRTT (S4) were presented on a computer screen with resolution 1920 x 1080 pixels, and the explicit memory task was completed with pen and paper. SRTT was presented using MATLAB 2016b (The MathWorks Inc., Natick, MA, USA) and Cogent 2000 (developed by the Cogent 2000 team at the Functional Imaging Laboratory and the Institute for Cognitive Neuroscience, University College, London, UK; http://www.vislab.ucl.ac.uk/cogent.php); questionnaires were presented using MATLAB 2016b and Psychophysics Toolbox Version 3 (Brainard, 1997).

For online data collection, SRTT (S4) was coded in Python using PsychoPy 3.2.2. (Peirce et al., 2019) and administered through the Pavlovia online platform (https://pavlovia.org/); questionnaires were distributed via Qualtrics software (Qualtrics, 2005), and the explicit memory task was sent to the participants as a .pdf document which they were asked to edit according to the instructions provided.

2.3 EXPERIMENTAL TASKS

2.3.1 MOTOR SEQUENCE LEARNING – THE SERIAL REACTION TIME TASK (SRTT)

The SRTT (Fig.1B) was used to induce and measure motor sequence learning. It was adapted from (Cousins et al., 2014a), as described in the previous chapter (Chapter 2). SRTT consists of two 12-item sequences of auditorily and visually cued key presses, learned by the participants in blocks. The task was to respond to the stimuli as quickly and accurately as possible, using index and middle fingers of both hands. The two sequences – A (1–2–1–4–2–3–4–1–3–2–4–3) and B (2–4–3–2–3–1–4–2–3–1–4–1) – were matched for learning difficulty, they did not share strings of more than four items and contained items that were equally represented (three repetitions of each). Each sequence was paired with a set of 200 ms-long tones, either high (5^{th} octave, A/B/C#/D) or low (4^{th} octave, C/D/E/F) pitched, that were counterbalanced across sequences and participants. For each item/trial, the tone was played with simultaneous presentation of a visual cue in one of the four corners of the screen. Visual cues consisted of neutral faces and objects appearing in the same location regardless of the sequences (1 – top left corner = male face, 2 – bottom left corner = lamp, 3 – top right corner = female face, 4 – bottom right corner = water tap). Participants were told that the nature of the stimuli (faces/objects) was not relevant for the study. Their task was to press the key on the keyboard (while in the sleep lab or at home) or on an MRI-compatible button pad (2-Hand system, NatA technologies, Coquitlam, Canada) (while in the MRI/mock scanner) that corresponded to the position of the picture as quickly and accurately as possible: 1 = left shift/left middle finger button; 2 = left Ctrl/left index finger button; 3 = up arrow/right middle finger button; 4 = down arrow/right index finger button. Participants were instructed to use both hands and always keep the same fingers on the appropriate response keys. The visual cue disappeared from the screen only after the correct key was pressed, followed by a 300 ms interval before the next trial.

There were 24 blocks of each sequence (a total of 48 sequence blocks per session). The block type was indicated with 'A' or 'B' displayed in the centre of the screen. Each block contained three sequence repetitions (36 items) and was followed by a 15 s pause/break, with reaction time and error rate feedback. Blocks were interleaved pseudo-randomly with no more than two blocks of the same sequence in a row. Participants were aware that there were two sequences but were not asked to learn them explicitly. Block order and sequence replayed were counterbalanced across participants.

During each run of the SRTT, sequence blocks A and B were followed by 4 random blocks except for the first half of S1 (to avoid interrupted learning). Random blocks were indicated with 'R' appearing in the centre of the screen and contained pseudo-randomised sequences. For these, visual stimuli were the same and tones matched sequence A tones for half of them (Rand_A) and sequence B tones for the other half (Rand_B). Blocks Rand_A and Rand_B were alternated, and each contained random sequences constrained by the following criteria: (1) cues within a string of 12 items were equally represented, (2) the same cue did not occur in consecutive trials, (3) the sequence did not share more than four cues in a row with either sequence A or B.

2.3.2 EXPLICIT MEMORY TASK

Explicit memory of the SRTT was assessed by a free recall test administered at the end of the study (S4). Participants were provided with printed screenshots of sequence A and sequence B trials, but the visual cues were removed. They were instructed to mark the order of each sequence by drawing an 'X' to indicate cue location.

2.4 EEG DATA ACQUISITION

EEG data was acquired with actiCap slim active electrodes (Brain Products GmbH, Gilching, Germany). 62 scalp electrodes were embedded within an elastic cap (Easycap GmbH, Herrsching, Germany), with the reference electrode positioned at CPz and ground at AFz. Electromyogram (EMG) signals were recorded from two electrodes placed on the chin, whereas the electrooculogram (EOG) was collected from two electrodes placed below the left eye and above the right eye. EEG electrodes layout is presented in Fig.S4. Elefix EEG-electrode paste (Nihon Kohden, Tokyo, Japan) was applied on each electrode for stable attachment and Super-Visc high viscosity electrolyte gel (Easycap GmbH) was used to keep impedance below 25 kOhm. Signals were amplified with either two BrainAmp MR plus EEG amplifiers or LiveAmp wireless amplifiers and recorded using BrainVision Recorder software (all from Brain Products GmbH).

2.5 TMR DURING NREM SLEEP

The TMR protocol was administered as in Chapter 2, using MATLAB 2016b and Cogent 2000. Briefly, tones associated with either sequence A or B (counterbalanced across participants) were replayed to the participants during stable N2 and N3 (Fig.1C). Replay blocks contained one repetition of a sequence (i.e., 12 sounds) and were followed by 20 s of silence. The inter-trial interval between individual sounds was jittered between 2500 and 3500 ms. Volume was adjusted for each participant to prevent arousal. However, upon leaving the relevant sleep stage, replay was paused and resumed only when stable N2 or N3 was observed. TMR was performed until ~1000 trials were delivered in N3. On average, 1385.20 ± 305.53 sounds were played.

2.6 MRI DATA ACQUISITION

Magnetic resonance imaging (MRI) was performed at Cardiff University Brain Imaging Centre (CUBRIC) with a 3T Siemens Connectom scanner (maximum gradient strength 300 mT/m). All scans were acquired with a 32-channel head-coil and lasted ~1 h in total each, with whole-brain coverage including cerebellum. Apart from the T1w and fMRI scans, the MRI protocol also included multi-shell Diffusion-Weighted Imaging and mcDESPOT acquisitions, but these are not discussed here.

2.6.1 T1-WEIGHTED IMAGING

A high resolution T1w anatomical scan was acquired with a 3D magnetization-prepared rapid gradient echoes (MPRAGE) sequence (repetition time [TR] = 2300 ms; echo time [TE] = 2 ms; inversion time [TI] = 857 ms; flip angle [FA] = 9°; bandwidth 230 Hz/Pixel; 256 mm field-of-view [FOV]; 256 x 256 voxel matrix size; 1 mm isotropic voxel size; 1 mm slice thickness; 192 sagittal slices; parallel acquisition technique [PAT] with in-plane acceleration factor 2 (GRAPPA); anterior-to-posterior phase-encoding direction; 5 min total acquisition time [AT]) at the beginning of each scanning session.

2.6.2 FUNCTIONAL MRI

Functional data were acquired with a T2*-weighted multi-band echo-planar imaging (EPI) sequence (TR = 2000 ms; TE = 35 ms; FA = 75°; bandwidth 1976 Hz/Pixel; 220 mm FOV; 220 x 220 voxel matrix size; 2 mm isotropic voxel size; 2 mm slice thickness; 87 slices with a ~25°

axial-to-coronal tilt from the anterior – posterior commissure (AC-PC) line and interleaved slice acquisition; PAT 2 (GRAPPA); multi-band acceleration factor [MB] 3; anterior-to-posterior phase-encoding direction; maximum 24 min AT and 720 scans; because the task was self-paced the exact AT and the number of scans differed between participants). Each fMRI acquisition was preceded by dummy scans to allow for saturation of the MR signal before the start of the task. Due to the nature of the task, the fMRI paradigm followed a block design consisting of sequence and random blocks (self-paced), alternating with rest blocks (15 s) (see section *2.3.1 Motor sequence learning – the serial reaction time task (SRTT)*). Presentation of the first stimulus in a block was synchronised with the scanner's trigger signal sent upon acquisition of every fMRI volume. Thus, the beginning of the task (i.e., the first stimulus of the first block) was triggered by the first fMRI volume acquisition and for that reason the initial volumes did not have to be discarded. No online motion correction was applied.

2.6.3 B0 FIELDMAP

B0-fieldmap was acquired to correct for distortions in the fMRI data caused by magnetic field (i.e., B0) inhomogeneities (TR = 465 ms; TE = 4.92 ms; FA = 60°; bandwidth 290 Hz/Pixel; 192 mm FOV; 192 x 192 voxel matrix size; 3 mm isotropic voxel size; 3 mm slice thickness; 44 slices with a ~25° axial-to-coronal tilt from the AC-PC line and interleaved slice acquisition; 1 average; anterior-to-posterior phase-encoding direction; 1 min AT).

2.7 DATA ANALYSIS

2.7.1 BEHAVIOURAL DATA

2.7.1.1 SRTT: REACTION TIME

SRTT performance was measured using mean reaction time per block of each sequence (cued and uncued). Both hands (BH) dataset contained all SRTT trials within each block, except for those with reaction time exceeding 1000 ms. Trials with incorrect button presses prior to the correct ones were included in the analysis. BH dataset was divided into the right hand (RH) dataset and left hand (LH) dataset, where each contained only the trials performed with the dominant or non-dominant hand, respectively. For each sequence within a given dataset, the mean performance on the 4 target blocks (brown and grey vertical bars in Fig.2A) was

subtracted from the mean performance on the 2 random blocks. This allowed us to separate sequence learning from sensorimotor mapping and thus obtain a measure of 'sequence-specific skill' (SSS). The target blocks were the first 4 sequence blocks, used to calculate early SSS, and the last 4 sequence blocks, used to calculate late SSS, as illustrated below:

1. Early SSS = mean (random blocks) – mean (first 4 sequence blocks)
2. Late SSS = mean (random blocks) – mean (last 4 sequence blocks)

Finally, to obtain a single measure reflecting the effect of TMR on the SRTT performance we calculated the difference between the SSS of the cued and uncued sequence and refer to it as the 'cueing benefit'.

2.7.1.2 QUESTIONNAIRES

PSQI global scores were determined in accordance with the original scoring system (Buysse et al., 1989). Answers to the short version of the EHI were scored as in (Veale, 2014) and used to obtain laterality quotient for handedness. For results, see *Supplementary Notes: Questionnaires*.

2.7.1.3 EXPLICIT MEMORY

Responses on the explicit memory task were considered correct only if they were in the correct position within the sequence and next to at least one other correct item, hence reducing the probability of guessing (Cousins et al., 2014a). The number of items guessed by chance was determined for each participant by taking an average score of 10 randomly generated sequences. To test if the explicit memory was formed, the average chance level across all participants was compared with the average number of correct items for each sequence. For results, see *Supplementary Notes: Explicit memory task* and Fig.S5.

2.7.2 EEG DATA ANALYSIS

All EEG data were analysed in MATLAB 2018b using FieldTrip Toolbox (Oostenveld et al., 2011).

2.7.2.1 SLEEP SCORING

EEG signal recorded throughout the night at eight scalp electrodes (F3, F4, C3, C4, P3, P4, O1, O2), two EOG and two EMG channels was pre-processed and re-referenced from CPz to the mastoids (TP9, TP10). For two participants, the right mastoid channel (TP10) was deemed noisy through visual inspection and had to be interpolated based on its triangulation-based neighbours (TP8, T8, P8), before it could be used as a new reference. The data was scored according to the AASM criteria (Berry et al., 2015) by two independent sleep scorers who were blind to the cue presentation periods. Sleep scoring was performed using a custom-made interface (https://github.com/mnavarretem/psgScore).

2.7.2.2 SPINDLES ANALYSIS

The relationship between sleep spindles and behavioural measures was assessed using 8 electrodes located over motor areas: FC3, C5, C3, C1, CP3, FC4, C6, C4, C2, CP4. However, for visualisation purposes (Fig.4A), the remaining electrodes in the International 10-20 EEG system were also analysed as described below. First, raw data from these channels were down-sampled to 250 Hz (for them to be comparable between the two EEG data acquisition systems) and filtered by Chebyshev Type II infinite impulse response (IIR) filter (passband: f = [0.3 – 35] Hz; stopband: f < 0.1 Hz & f > 45 Hz). All channels were visually inspected, and the noisy ones were interpolated via triangulation of their nearest neighbours. As a final pre-processing step, we re-referenced the data from CPz to the mastoids (TP9, TP10). A spindle-detection algorithm (Navarrete et al., 2020) was then employed to automatically identify sleep spindles (11 – 16 Hz). Briefly, the data were filtered in a sigma band by the IIR filter (passband: f = [11 – 16] Hz; stopband: f < 9 Hz & f > 18 Hz) and the root mean squared (RMS) of the signal was computed using a 300 ms time window. Any event that surpassed the 86.64 percentile (1.5 SD, Gaussian distribution) of the RMS signal was considered a candidate spindle. To fit the spindle detection criteria (Iber et al., 2007), only the events with unimodal maximum in the 11 – 16 Hz frequency range in the power spectrum, duration between 0.5 and 2.0 s and at least 5 oscillations were regarded as sleep spindles (Navarrete et al., 2020).

Any identified spindles that fell (partly or wholly) within a period that had been previously marked as an arousal during sleep scoring were removed. The remaining spindles were separated into those that fell within the cue and no-cue periods. We define the cue period as the 3.5 s time interval after the onset of each tone. Since 3.5 s was the longest inter-trial interval allowed, the cue period essentially covered the time interval from the onset of the

first tone in a sequence to 3.5 s after the onset of the last one. In turn, the no-cue period covered the time interval between sequences, i.e., from 3.5 to 20.0 s after the onset of the last tone in a sequence. If a spindle fell between the cue and no-cue period, that spindle was removed from further analysis. Thus, only spindles that fell wholly within the cue or no-cue period were included in the analysis.

Spindle density was calculated by dividing the number of spindles at each electrode and in each period of interest (cue period during target sleep stage, no-cue period during target sleep stage) by the duration (in minutes) of that period.

2.7.3 MRI DATA ANALYSIS

MRI data were pre-processed using Statistical Parametric Mapping 12 (SPM12; Wellcome Trust Centre for Neuroimaging, London, UK), running under MATLAB 2018b.

2.7.3.1 FMRI

PRE-PROCESSING

Functional data pre-processing consisted of (1) B0-fieldmap correction using SPM's fieldmap toolbox (Jezzard & Balaban, 1995); (2) realignment to the mean of the images using a least-squares approach and 6 parameter rigid body spatial transformation to correct for movement artifact (Friston et al., 1995); (3) co-registration with the participants' individual structural image using rigid body model (Collignon et al., 1995); (4) spatial normalisation to Montreal Neurological Institute brain (MNI space) via the segmentation routine and resampling to 2 mm voxels with a 4^{th} degree B-spline interpolation (Ashburner & Friston, 2005); (5) smoothing with 8 mm full-width half maximum (FWHM) Gaussian kernel in line with the literature (Cousins et al., 2016). All steps were performed as implemented in SPM12. B0-fieldmap correction step was omitted for one participant (n = 1) due to technical issues during B0-fieldmap acquisition. No scans had to be excluded due to excessive movement (average translations < 3.3 mm, average rotations < 0.03°).

SINGLE SUBJECT LEVEL ANALYSIS

Subject-level analysis of the fMRI data was performed using a general linear model (GLM) (Friston et al., 1994), constructed separately for each participant and session. Each block type (cued sequence, uncued sequence, cued random, uncued random) as well as the breaks

between the blocks were modelled as five separate, boxcar regressors; button presses were modelled as single events with zero duration. All of these were temporally convolved with a canonical hemodynamic response function (HRF) model embedded in SPM, with no derivatives. To control for movement artifacts, the design matrix also included six head motion parameters, generated during realignment, as non-convolved nuisance regressors. A high-pass filter with a cut-off period of 128 s was implemented in the matrix design to remove low-frequency signal drifts. Finally, serial correlations in the fMRI signal were corrected for using a first-order autoregressive model during restricted maximum likelihood (REML) parameter estimation. Contrast images were obtained for each block type of interest ([cued sequence] and [uncued sequence]), as well as for the difference between the two ([cued > uncued]). The resulting parameter images, generated per participant and per session using a fixed-effects model, were then used as inputs for the group-level (i.e., random effects) analysis. Contrast images for the difference between sequence and random blocks were not generated due to the unequal number of each block type performed in the scanner (2 random blocks vs 24 sequence blocks, per session). This, however, was in accordance with the literature (Cousins et al., 2016).

2.7.3.2 VBM

PRE-PROCESSING

Pre-processing of T1w images was performed in keeping with (Ashburner, 2010) recommendations. Images were first segmented into three tissue probability maps (grey matter, GM; white matter, WM; cerebrospinal fluid, CSF), with two Gaussians used to model each tissue class, very light bias regularisation (0.0001), 60 mm bias FWHM cut-off and default warping parameters (Ashburner & Friston, 2005). Spatial normalisation was performed with DARTEL (Ashburner, 2007), where the GM and WM segments were used to create customised tissue-class templates and to calculate flow fields. These were subsequently applied to the native GM and WM images of each subject to generate spatially normalised and Jacobian scaled (i.e., modulated) images in the MNI space, resampled at 1.5 mm isotropic voxels. The modulated images were smoothed with an 8 mm FWHM Gaussian kernel, in line with the fMRI analysis. To account for any confounding effects of brain size we estimated the total intracranial volume (ICV) for each participant at each time point by summing up the volumes of the GM, WM, and CSF probability maps, obtained through segmentation of the original images. The GM and WM images were then proportionally

scaled to the ICV values by means of dividing intensities in each image by the image's global (i.e., ICV) value before statistical comparisons.

2.7.4 STATISTICAL ANALYSIS

All tests conducted were two-tailed, with the significance threshold set at 0.05. For behavioural and EEG data analyses, normality assumption was checked using Shapiro-Wilk test. To compare two related samples, we used paired-samples t-test or Wilcoxon signed-rank test, depending on the Shapiro-Wilk test result. Results are presented as mean ± standard error of the mean (SEM), unless otherwise stated.

2.7.4.1 BEHAVIOURAL DATA

Statistical analysis of the behavioural data was performed in R (R Core Team, 2012) or SPSS Statistics 25 (IBM Corp., Armonk, NY, USA) as before (Chapter 2). Each dataset (LH, RH, BH) was analysed separately.

To assess the relationship between TMR, SSS and Session we used linear mixed effects analysis performed on S2-S4, using lme4 package (Bates et al., 2015) in R. We chose linear mixed effects analysis to avoid listwise deletion due to missing data at S3 and S4 and to account for the non-independence of multiple responses collected over time. TMR and Session were entered into the model as categorical (factor) fixed effects without interaction and random intercept was specified for each subject. The final models fitted to the BH, LH and RH datasets were as follows:

> model = lmer(early SSS ~ Session + TMR + (1|Participant), data=dataset)

> model = lmer(late SSS ~ Session + TMR + (1|Participant), data=dataset)

To test for the effect of hand, LH and RH datasets were combined and 'hand' (factor) was added as an additional fixed effect:

> model = lmer(early SSS ~ Session + TMR + Hand + (1|Participant), data=dataset)
> model = lmer(late SSS ~ Session + TMR + Hand + (1|Participant), data=dataset)

Finally, to explore how the TMR effect evolves from S2 to S4, we entered cueing benefit (calculated using the late SSS data given no TMR effect on the early SSS) as the dependent variable and the number of days post-TMR ('time', integer) as a fixed effect in the following model:

> model = lmer(CueingBenefit ~ Time + (1|Participant), data=dataset)

To test for the effect of hand, LH and RH datasets were combined as before:
> model = lmer(CueingBenefit ~ Time + Hand + (1|Participant), data=dataset)

Likelihood ratio tests comparing the full model against the model without the effect of interest were performed using the ANOVA function in R to obtain p-values. Post-hoc pairwise comparisons were conducted using the *emmeans* package (Lenth et al., 2019) in R and corrected for multiple comparisons with Holm's method. Effect sizes were calculated with the *emmeans* package as well.

2.7.4.2 EEG DATA

Statistical analysis of the EEG data was performed in R (R Core Team, 2012) or SPSS Statistics 25 (IBM Corp., Armonk, NY, USA). Each stimulation period (cue vs no-cue) and sleep stage (N2, N3, N2 and N3 combined) was analysed separately.

Correlations between our behavioural measures and EEG results were assessed with Pearson's correlation or Spearman's Rho (depending on the Shapiro-Wilk test result), using *cor.test* function in the R environment. Any datapoint that was both (1) more than 1.5 IQRs below the first quartile or 1.5 IQRs above the third quartile, and (2) deemed an outlier through visual inspection, was removed from the dataset prior to correlational analysis. False discovery rate (FDR) correction was used to correct for multiple correlations ($q < 0.05$) (Benjamini & Hochberg, 1995). FDR corrections were based on 3 correlations, given the 3 experimental sessions of interest (S2, S3, S4).

2.7.4.3 MRI DATA

Group level analysis of the MRI data was performed either in a Multivariate and Repeated Measures (MRM) toolbox (https://github.com/martynmcfarquhar/MRM) or in SPM12, both running under MATLAB 2018b. All tests conducted were two-tailed, testing for both positive and negative effects. Results were voxel-level corrected for multiple comparisons by family wise error (FWE) correction for the whole brain and for the pre-defined anatomical regions of interest (ROI), with the significance threshold set at $p_{FWE} < 0.05$. For the analysis performed in MRM, p-values were derived from 1,000 permutations, with Wilk's lambda specified as the test statistic. Pre-defined ROI included (1) bilateral precuneus, (2) bilateral hippocampus and parahippocampus, (3) bilateral dorsal striatum (putamen and caudate), (4) bilateral

cerebellum, (5) bilateral sensorimotor cortex (precentral and postcentral gyri). All ROI were selected based on their known involvement in sleep-dependent procedural memory consolidation (Albouy et al., 2013b; Debas et al., 2010; Fischer, 2005; Walker et al., 2005) and memory reactivation (Brodt et al., 2018; Cousins et al., 2016; Maquet et al., 2000; Rasch et al., 2007; van Dongen et al., 2012). A mask for each ROI was created using an Automated Anatomical Labeling (AAL) atlas in the Wake Forest University (WFU) PickAtlas toolbox (Maldjian et al., 2003). Anatomical localisation of the significant clusters was determined with the automatic labelling of MRIcroGL (https://www.nitrc.org/projects/mricrogl/) based on the AAL atlas. All significant clusters are reported in tables, but only those with an extent equal to or above 5 voxels are discussed in text and presented in figures.

FMRI DATA

To test the effect of TMR on the post-stimulation sessions (S2-S3), one-dimensional contrast images for the [cued] and [uncued] blocks of each session were entered into a repeated-measures TMR-by-Session ANOVA performed in the MRM toolbox.

To compare functional brain activity during the cued and uncued sequence we carried out one-way t-tests on the [cued > uncued] contrast for S2 (n = 28) and S3 (n = 24) in SPM12. To determine the relationship between the TMR-related functional activity and other factors, we included the behavioural cueing benefit for the BH dataset at different time points (S2, S3, S4) as covariates in separate comparisons. Finally, to investigate fMRI changes over time, images from consecutive sessions were subtracted from one another, resulting in three subtraction images per subject (S1-S2, n = 28; S2-S3, n = 22; S1-S3, n = 24). We then performed the one-way t-tests as before (either with or without a covariate of interest).

VBM DATA

Group-level analysis of the structural images was performed separately for GM and WM. First, the pre-processed and proportionally scaled images from consecutive sessions were subtracted from one another as for fMRI (S1-S2, n = 30; S2-S3, n = 24; S1-S3, n = 24). To determine the relationship between the longitudinal brain changes and other factors, one-sample t-tests were computed in SPM12, with covariates of interest added one at a time. The covariates of interest were the behavioural cueing benefit for the BH dataset at a chosen time point (S2, S3, S4). Sex was always specified as a covariate of no interest (nuisance covariate) to control for differences between males and females. Finally, the SPM12 tissue

probability maps of GM and WM were thresholded at 50% probability and the resulting binary masks were used in the analyses of the relevant tissue (Ceccarelli et al., 2012).

2.7.4.4 MEDIATION ANALYSIS

To determine the relationship between VBM, fMRI and behavioural measures, we conducted mediation effect parametric mapping based on a standard 3-variable path model (Baron & Kenny, 1986) with a bootstrap test (5,000 bootstrapped samples) for the statistical significance of the indirect effect (Tibshirani & Efron, 1993). The mediation analysis was performed using *PROCESS* macro for SPSS (Hayes, 2014). Cueing benefit at S4 was entered as the dependent variable, the average GM volume within the significant cluster from the [[Δ GM volume from S1 to S3 * cueing benefit at S4] contrast (i.e., precentral gyrus, $p_{FWE} < 0.05$, ROI corrected) was entered as the independent variable and the functional activity within the significant cluster from the [(cued > uncued) * cueing benefit at S4] contrast (i.e., postcentral gyrus, $p_{FWE} < 0.05$, ROI corrected) was entered as the mediator. All variables were standardised prior to entering in the mediation analysis. The percentage mediation denotes the ratio between the indirect effect and the total effect. Finally, a Sobel test (Sobel, 1982) was conducted to further demonstrate the significance using an interactive calculator tool for a mediation test (Preacher & Leonardelli, 2001; Preacher & Kelley, 2011).

2.8 RESULTS PRESENTATION

Plots displaying behavioural results, pairwise comparisons and relationships between two variables were generated using *ggplot2* (version 3.3.0) (Wickham, 2009) in R. Fig.4A was generated using *ft_topoplotER* function in FieldTrip Toolbox (Oostenveld et al., 2011). Fig.1, Fig.7, Fig.S3 and Fig.S4 were created in Microsoft PowerPoint v16.53. MRI results are presented using MRIcroGL, displayed on the MNI152 standard brain (University of South Carolina, Columbia, SC), except Fig.S1 and Fig.S2 which were generated by SPM12 (Wellcome Trust Centre for Neuroimaging, London, UK).

2.9 DATA AND CODE AVAILABILITY

All data collected during the study, scripts that delivered experimental tasks and codes used to conduct the analyses are publicly available at: https://osf.io/y43sb/?view_only=8b18dd7984e94c629274bbf427fb90be.

3 RESULTS

3.1 SRTT

3.1.1 REACTION TIME AND SEQUENCE SPECIFIC SKILL

Analysis of baseline SRTT performance indicated that participants learned both sequences before sleep and confirmed that any post-sleep differences between the sequences can be regarded as the effect of TMR (see *Supplementary Notes: Baseline SRTT performance* and Table S1). Fig.2A shows the mean reaction time (± SEM) for both hands (BH) trials of each SRTT block over the whole length of the study.

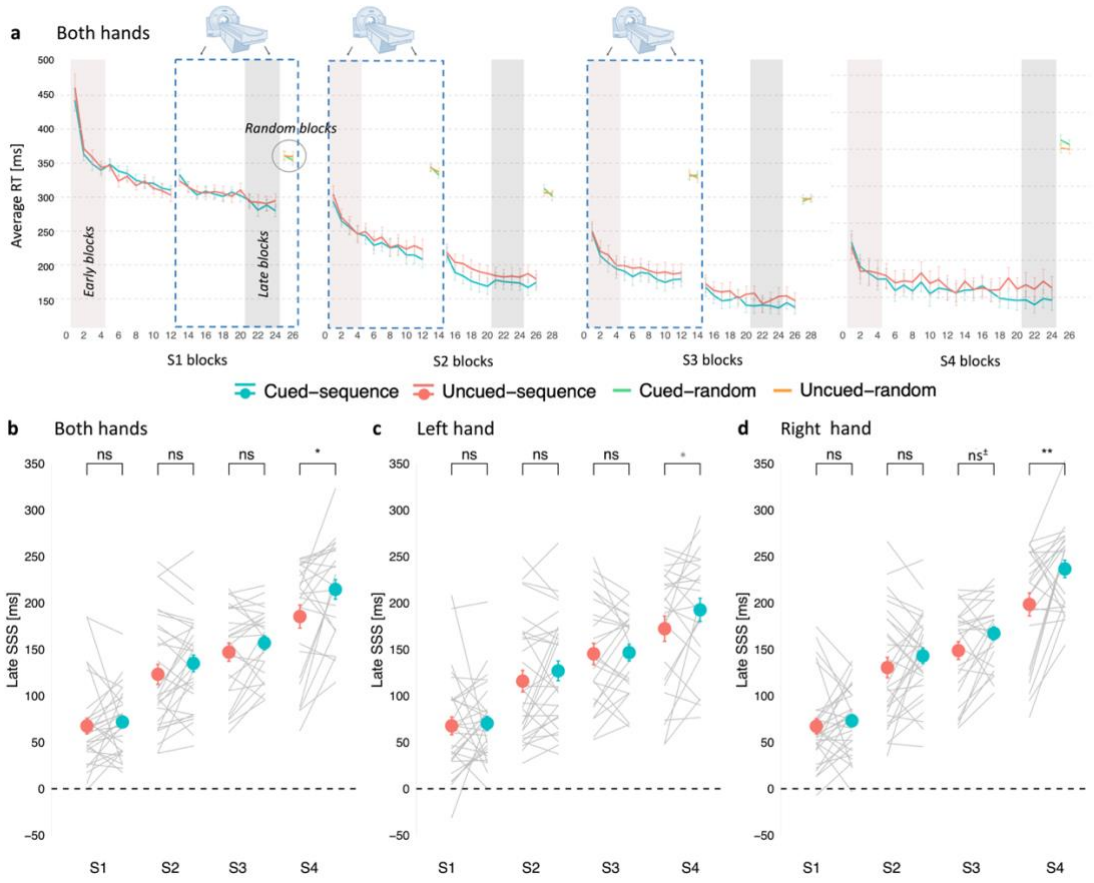

Fig. 2. A single night of TMR benefits procedural memories up to 20 days later. (a) *Mean reaction time for both hands trials of the cued sequence (blue), uncued sequence (red) and random blocks (green and orange) of the SRTT performed before sleep (S1), 24 h post-TMR (S2), 10 days post-TMR (S3) and 20 days post-TMR (S4). Error bars depict SEM. Vertical bars mark the first (brown) and last (grey) four sequence blocks used to determine early and late sequence specific skill (SSS), respectively. Blue dashed rectangle frames mark the SRTT blocks performed during fMRI acquisition.* ***(b-d)*** *Mean late SSS for the cued (blue dots) and uncued (red dots) sequence plotted against experimental sessions (S1-S4). Both hand trials* ***(b)****, left-hand trials* ***(c)*** *and right-hand trials* ***(d)*** *are shown*

*separately. Error bars depict SEM. Grey lines represent individual participants. For (a-d): n = 30 for S1-S2, n = 25 for S3, n = 24 for S4. S1-4: Session 1-4; RT: reaction time; SSS: Sequence Specific Skill. **p < 0.001; *p < 0.05; ns±: non-significant trend (p = 0.060); ns: non-significant; p-values uncorrected; when adjusted for multiple comparisons using Holm's correction the effect of TMR at S4 remained significant only for (B) and (D) (black *) but not for (C) (grey *).*

Post-sleep SRTT re-test sessions occurred 24.67 h (SD: 0.70) (S2), 10.48 days (SD: 0.92) (S3), and 20.08 days (SD: 0.97) (S4) after session 1 (S1). SRTT performance was measured by subtracting the mean reaction time on the last or first four blocks of each sequence from that of the random blocks, thereby providing a measure of both late and early sequence specific skill (SSS). To test the effect of cueing on the SSS (either early or late) over time we fitted a linear mixed effects model to each dataset (both hands, BH; left hand, LH; right hand, RH) separately, with TMR and session entered as fixed effects, and participant entered as a random effect. Results of all the likelihood ratio tests comparing the full model against the model without the fixed effect of interest are shown in Table S2A-C.

The linear mixed effect analysis revealed a main effect of session on both early ($X^2(2) = 175.77$, $p < 0.001$; Table S2Ai) and late SSS ($X^2(2) = 93.04$, $p < 0.001$; Table S2Aii) for the BH dataset, with similar results for the LH (Table S2B) and RH datasets (Table S3C). Post-hoc comparisons showed a difference between subsequent sessions (S2 vs S3, S3 vs S4) ($p_{adj} < 0.002$; Table S3), suggesting continuous learning over time. All p_{adj} values are Holm-corrected.

Inclusion of TMR as a fixed effect in the BH dataset improved model fit across all sessions (S2-S4) for late SSS ($X^2(1) = 11.01$, $p = 0.001$; Table S2Aii), but not early SSS ($X^2(1) = 1.55$, $p = 0.214$; Table S2Ai). Similar results were revealed for LH (Table S2B) and RH datasets (Table S3C). Thus, the linear mixed effects analysis points to a main effect of TMR on the late SSS across all post-stimulation sessions. Given our previous findings on this task (Chapter 2), we expected better performance on the cued sequence at S3 (10 days post-stimulation) but wanted to determine if this TMR benefit (i.e., the difference between the SSS of the two sequences) persists until S4 (20 days post-stimulation). Likewise, we also aimed to probe if the TMR benefit emerges at S2 (24 h post-stimulation) as other studies would suggest (Cousins et al., 2016), or whether it is non-significant at that time point (as in Chapter 2). Hence, we performed post-hoc comparisons to reveal the session(s) during which late SSS differed between the two sequences. Contrary to our expectations, we found a significant difference between the cued and uncued sequence performance at S4 ($p_{adj} = 0.004$) but not at S2 ($p_{adj} = 0.282$) or S3 ($p_{adj} = 0.282$) for the BH dataset (Table S4A, Fig.2B). Similar results

were found for the RH dataset (S2: p_{adj} = 0.163; S3: p_{adj} = 0.119; S4: p_{adj} = 0.001; Table S4C, Fig.2D). However, for the LH dataset, the TMR benefit at S4 (p_{uncorr} = 0.040) did not survive Holm correction (S4: p_{adj} = 0.121; S2: p_{adj} = 0.421; S3: p_{adj} = 0.890) (Table S4B, Fig.2C). Together, these findings point to a main effect of TMR across all post-stimulation sessions, with the difference between the cued and uncued sequence being the strongest 20 days post-TMR, particularly for the dominant hand. Nevertheless, it is worth noting that although we do report a main effect of hand on the SSS (better performance for the dominant hand; $p < 0.001$), there was no interaction between hand and TMR ($p > 0.05$).

3.1.2 CUEING BENEFIT ACROSS TIME

To explore how the TMR effect evolves over time, we calculated the difference between late SSS of the cued and uncued sequence for each session, which we refer to as the (late) cueing benefit. Next, we used a linear mixed effects analysis to determine if the cueing benefit changes with post-stimulation time. Inclusion of the number of days post-TMR as the fixed effect improved model fit on the extent of cueing benefit for BH ($\chi2(2) = 3.97$, $p = 0.046$; Fig.3A) and RH dataset ($\chi2(2) = 6.58$, $p = 0.010$; Fig.3C), but not for LH dataset ($\chi2(2) = 0.74$, $p = 0.391$; Fig.3B) (Table S5). Interestingly, there was neither a main effect of hand nor an interaction between hand and session ($p > 0.05$; Table S5D). These results suggest that the effects of TMR develop in a gradual time-dependent manner.

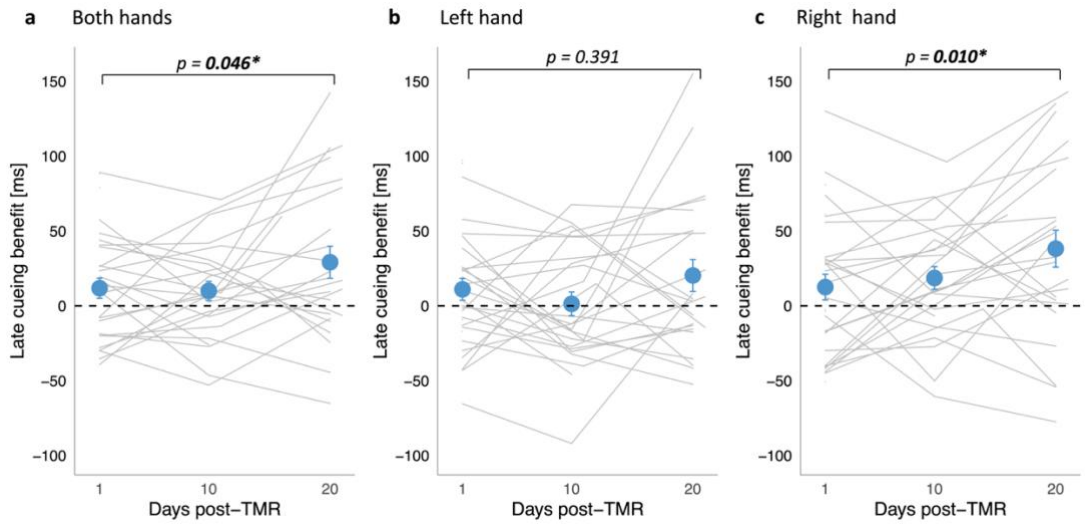

Fig. 3. Cueing benefit over time. *Mean late SSS of the uncued sequence subtracted from the cued sequence for both hands* ***(a)****, left hand* ***(b)*** *and right hand* ***(c)****, plotted over time (number of days post-TMR). The effect of time was significant for both-hands dataset and right-hand dataset. Blue dots represent mean ± SEM calculated for S2, S3 and S4. Grey lines represent cueing benefit for each subject. N = 30 for S2, n = 25 for S3; n = 24 for S4. S2-S4: Session 2-4.*

3.2 CORRELATIONS WITH SLEEP STAGES

To determine the relationship between sleep parameters derived from sleep stage scoring (Table S6) and the behavioural effect of our manipulation, we correlated the percentage of time spent in stage 2 (N2) and stage 3 (N3) of NREM sleep (the two target stages for our stimulation) with the cueing benefit at each session (S2, S3, S4) and for each dataset (BH, LH, RH) separately. Results are presented in Table S7, with no correlation surviving FDR correction ($p_{adj} > 0.05$).

3.3 SLEEP SPINDLES

Given the well-known involvement of sleep spindles in motor sequence memory consolidation (Boutin & Doyon, 2020), we set out to describe electrophysiological changes within the spindle frequency in relation to the cueing procedure. The average spindle density over the task related regions was higher in N2 than in N3 during both the cue period (0-3.5 s after cue onset; $t(28) = 4.48$, $p < 0.001$) and the no-cue period (3.5-20 s after the onset of the last cue in the sequence; $t(28) = 4.23$, $p < 0.0001$) (paired-samples t-test). Next, we compared spindle density over left and right motor areas during N2 and N3 combined. The analysis revealed higher spindle density over the left versus right motor areas for the cue period ($t(28) = 2.59$, $p = 0.015$) but not for the no-cue period ($t(28) = 1.98$, $p = 0.057$) (paired-samples t-test). As in the previous chapter (Chapter 2), we also found that the average spindle density during the cue period was higher than during the no-cue period ($t(28) = 4.37$, $p < 0.001$; paired-samples t-test, Fig.4A-B), suggesting that cueing may elicit sleep spindles. Spindle density and the number of spindle events during each period and sleep stage are summarised in Table S8.

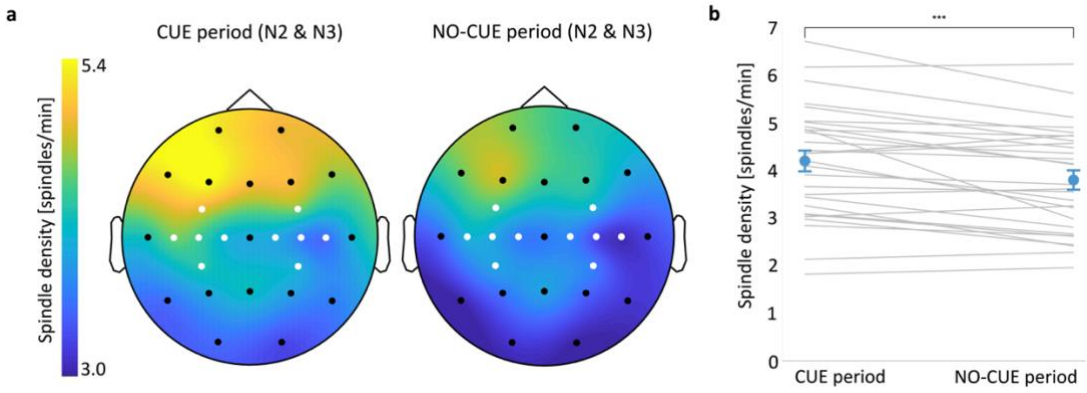

Fig. 4. Spindle density increases immediately upon cue onset. (a) *Topographic distribution of spindle density (spindles per min) in the cue (left) and no-cue (right) period of NREM sleep (N2 and N3 combined). Motor channels*

in white. ***(b)*** *Spindle density averaged over motor channels during the cue period was higher than during the no-cue period. Blue dots represent mean ± SEM. Grey lines represent individual subjects. *** p = 0.001. N2-N3: stage 2 – stage 3 of NREM sleep. n = 29.*

Spindle-related changes over brain regions involved in learning (Cox et al., 2014) often predict behavioural performance (Barakat et al., 2013). However, we found no correlation between spindle density averaged over bilateral motor regions and cueing benefit for the BH dataset ($p_{adj} > 0.05$, Table S9).

3.4 TMR-RELATED CHANGES IN FMRI RESPONSE

We next examined BOLD responses to the cued and uncued sequence over time. To test our hypothesis that procedural memory cueing during sleep would engender learning-related changes within precuneus, we performed a TMR-by-Session ANOVA of the fMRI data acquired during sequence performance at S2 and S3. In line with our hypothesis, the analysis revealed increased activity in the precuneus (right precuneus, 8, -72, 58) for the main effect TMR (cued vs uncued sequence across S2 and S3) (peak F = 22.67, p = 0.032; Table S10A). We have previously shown cueing-related functional activity the morning after TMR (Cousins et al., 2016). Similarly, microstructural plasticity and functional engagement of posterior parietal cortex (PPC) has been detected relatively quickly after learning (Brodt et al., 2018). Thus, we expected functional activity changes at S2. Indeed, one-way t-tests on the [cued > uncued] contrast revealed increased activity in the dorsal-anterior subregion of left precuneus (-9, -62, 66) 24 h post-TMR (peak T = 4.79, p = 0.020; Fig.5A-B, Table S10B, Fig.S1A). Given our behavioural findings at S4, we also sought to determine if a TMR effect could be detected in fMRI data at S3, but no difference between cued and uncued activity was found at this time point (p > 0.05). These results show that TMR alters functional activity in precuneus, with the TMR-related increase in functional response apparent relatively quickly (i.e., 24 h) post-stimulation.

Next, we looked for a relationship between post-sleep performance improvements and brain activity changes, as shown previously (Albouy et al., 2013b; Debas et al., 2010; Shanahan et al., 2018). Thus, we analysed the same [cued > uncued] contrast again, both for each session and for changes between sessions (S1 < S2, S2 < S3, S1 < S3). This time we included three regressors in separate models: behavioural cueing benefit at S2, S3 and S4 for the BH dataset. All clusters significant at $p_{FWE} < 0.05$ are reported in Table S10 D-F. As expected, when

examining the cueing benefit at S2 as a regressor [(cued > uncued) * cueing benefit at S2] we found a TMR-related functional increase at S2 in left dorsal-posterior precuneus (-4, -78, 46; peak T = 5.18, p = 0.009; Fig.5C-D, Table S10Di, Fig.S1B). Interestingly, a ventral subregion of left precuneus (-2, -54, 10) showed a decreased response to TMR from S2 to S3 when considering behavioural cueing benefit at S4 as a regressor in the [Δ(cued > uncued) from S2 to S3] contrast (peak T = 6.66, p = 0.002; Fig.5E-F, Table S10Ei, Fig.S1C). Taken together, these results suggest that activity in dorsal precuneus 24 h post-encoding predicts behavioural effects of cueing in the short-term. However, longer-term benefits of cueing appear to be associated with an eventual decrease in response of the ventral precuneus.

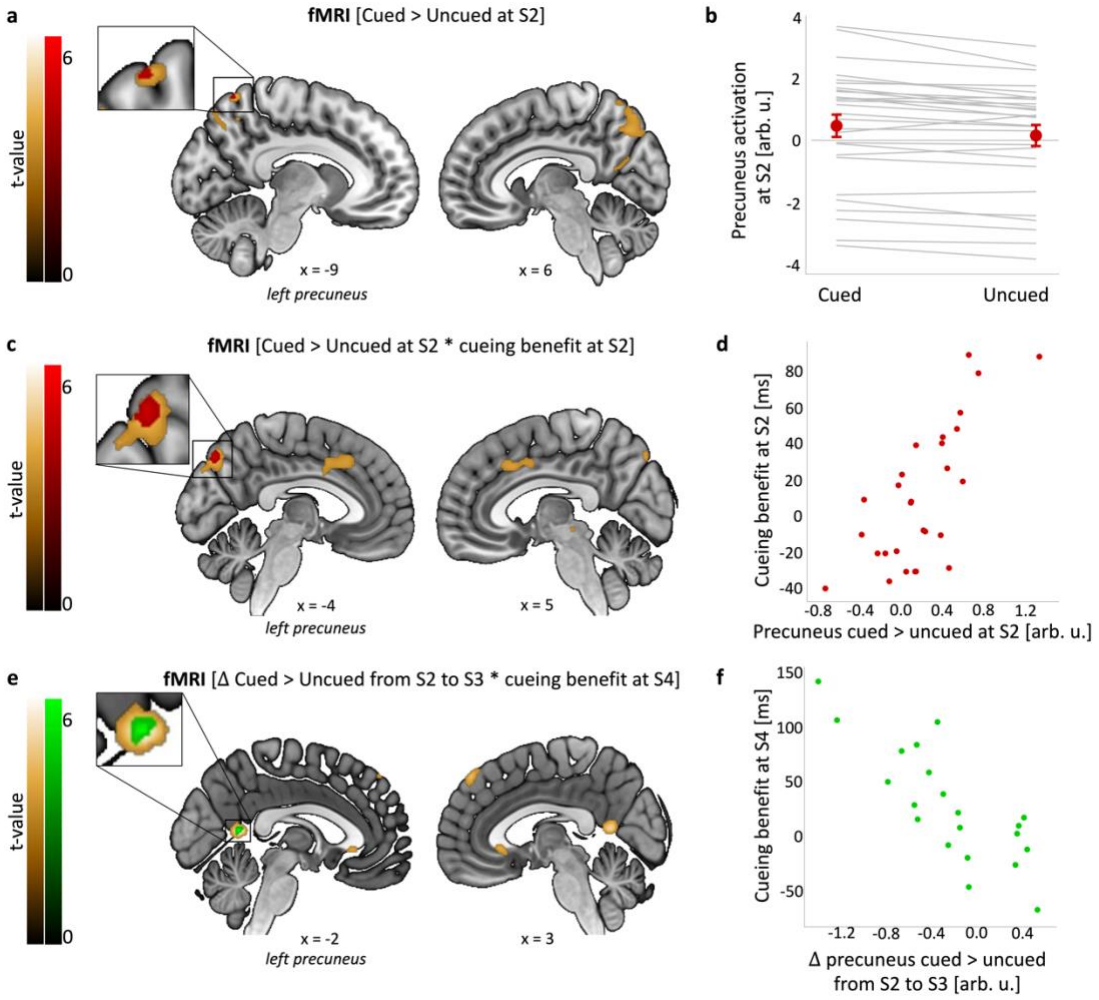

Fig. 5. TMR-related functional activity in precuneus. (a-b) *TMR-dependent increase in left precuneus activity 24 h post-stimulation.* ***(c-d)*** *Activity for the [cued > uncued] contrast in the left precuneus at S2 is positively associated with behavioural cueing benefit at the same time point.* ***(e-f)*** *Change in activity from S2 to S3 for the [cued > uncued] contrast in the left precuneus is negatively associated with behavioural cueing benefit at S4. (**a, c, e**) Group level analysis. In red/green, colour-coded t-values for each contrast thresholded at a significance level of $p_{FWE} < 0.05$, corrected for multiple voxel-wise comparisons within a pre-defined ROI for bilateral precuneus. Increased activity shown in red; decreased activity shown in green. In gold, colour-coded t-values for each contrast*

thresholded at a significance level of p < 0.001, uncorrected and without masking. Results are overlaid on a Montreal Neurological Institute (MNI) brain. Note that although the significant clusters in (a), (c) and (e) all fall within the Automated Anatomical Labeling (AAL) definition of precuneus, the peak coordinates are different (see Table S10, Bi, Di, Ei). ***(b, d, f)*** *Mean functional activity extracted from clusters significant at $p_{FWE} < 0.05$ shown in (a, c, e). The scatterplots are presented for visualisation purposes only and should not be used for statistical inference. (b) Red dots represent group mean ± SEM. Grey lines represent individual subjects. (d, f) Each data point represents a single participant. arb. u.: arbitrary units; S2-4: Session 2-4; n = 28 for (a-d), n = 21 for (e-f).*

In addition to precuneus, the cueing benefit at S4 regressor showed a positive relationship with TMR-related functional activity [(cued > uncued) * cueing benefit at S4] in the right postcentral gyrus at S3 (58, -18, 38; peak T = 5.50, p = 0.022; Fig.6A-B, Table S10Fi, Fig.S1D). This suggests that the way TMR impacts on activation of primary somatosensory cortex 10 days post-encoding may underpin the long-term behavioural effects of this cueing.

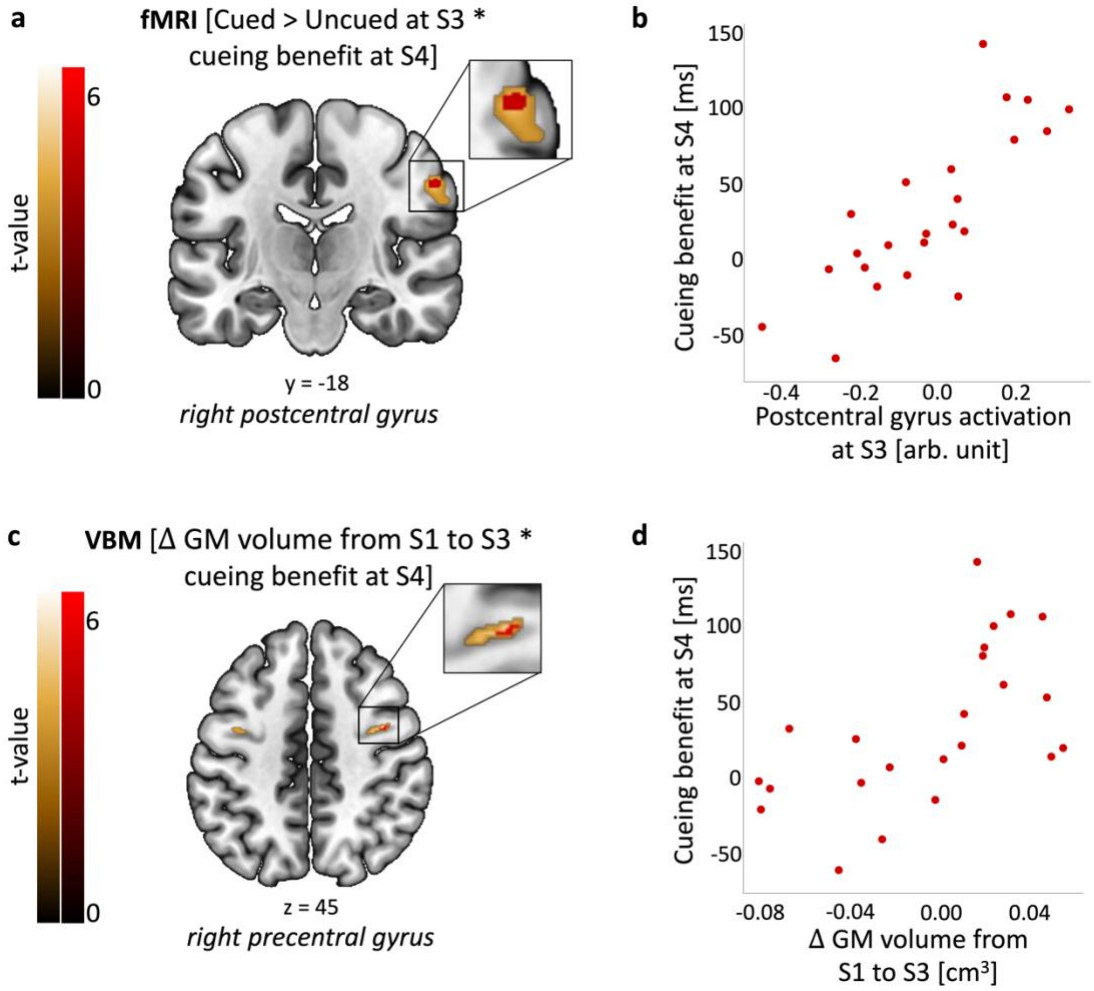

Fig. 6. Functional activity and structural brain changes are associated with long-term cueing benefit. (a-b) *Activity for the [cued > uncued] contrast in the right postcentral gyrus at S3 is positively associated with behavioural cueing benefit at S4.* ***(c-d)*** *Grey matter volume in the right precentral gyrus at S3 relative to S1 is positively associated with behavioural cueing benefit at S4. (**a, c**) Group level analysis. In red, colour-coded t-values for increased fMRI activity (a) and grey matter volume (c), both thresholded at a significance level of $p_{FWE} < 0.05$,*

corrected for multiple voxel-wise comparisons within a pre-defined ROI for bilateral sensorimotor cortex. In gold, colour-coded t-values for increased fMRI activity (a) and grey matter volume (c), both thresholded at a significance level of p < 0.001, uncorrected and without masking. Results are overlaid on a Montreal Neurological Institute (MNI) brain. Colour bars indicate t-values. ***(b, d)*** *Mean functional activity (b) and grey matter volume (d) extracted from clusters significant at $p_{FWE} < 0.05$ shown in (a, c). The scatterplots are presented for visualisation purposes only and should not be used for statistical inference. Each data point represents a single participant. arb. u.: arbitrary units; GM: grey matter; S1-4: Session 1-4; n = 23.*

3.5 TMR-RELATED STRUCTURAL PLASTICITY

To determine whether the behavioural effects of TMR were associated with volumetric changes, we performed voxel-based morphometry (VBM) analysis of the T1w scans. We thus carried out one-way t-tests on the subtraction images obtained for different time periods (S1 < S2, S2 < S3, S1 < S3), with behavioural regressors added as before. All clusters significant at $p_{FWE} < 0.05$ are reported in Table S11. When considering cueing benefit at S4 as a regressor we found a positive correlation with grey matter (GM) volume change from S1 to S3 [Δ GM volume from S1 to S3 * cueing benefit at S4] in the right precentral gyrus (42, -2, 45; peak T = 6.21, p = 0.020; Fig.6C-D, Table S11A, Fig.S2A). No correlations with volumetric changes were revealed in white matter. This is consistent with our fMRI finding (Fig.6A-B) and suggests that the time-dependent change in GM volume within a sensorimotor structure predicts long-term behavioural effects of cueing.

3.6 MEDIATION ANALYSIS

Having found that cueing benefit at S4 is associated with both TMR-related fMRI increase in right postcentral gyrus at S3 (Fig.6A-B) and GM volume increase from S1 to S3 in right precentral gyrus (Fig.6C-D), we set out to test for a mediation effect of the fMRI result on the relationship between the VBM result and behavioural cueing benefit. We reasoned that the early structural changes we observed may be shaping later functional changes in task-relevant areas, which in turn may be a direct driver of long-term cueing benefit. In line with our hypothesis, we found evidence for a significant mediation effect (Fig.7, 1-step mediation, β = 0.336, 95% CI = [0.146 – 0.604], indirect effect explaining 56% of total effect; Sobel test, Z = 2.32, p = 0.020). Furthermore, given that the direct effect was not significant (β = 0.597, p = 0.088; 95% CI: [-0.043 – 0.564]), we argue that the mediation is indirect-only (Zhao et al., 2010). Thus, our results suggest that GM change within the primary motor cortex drives the functional activity within the primary somatosensory cortex and thereby leads to the behavioural effects.

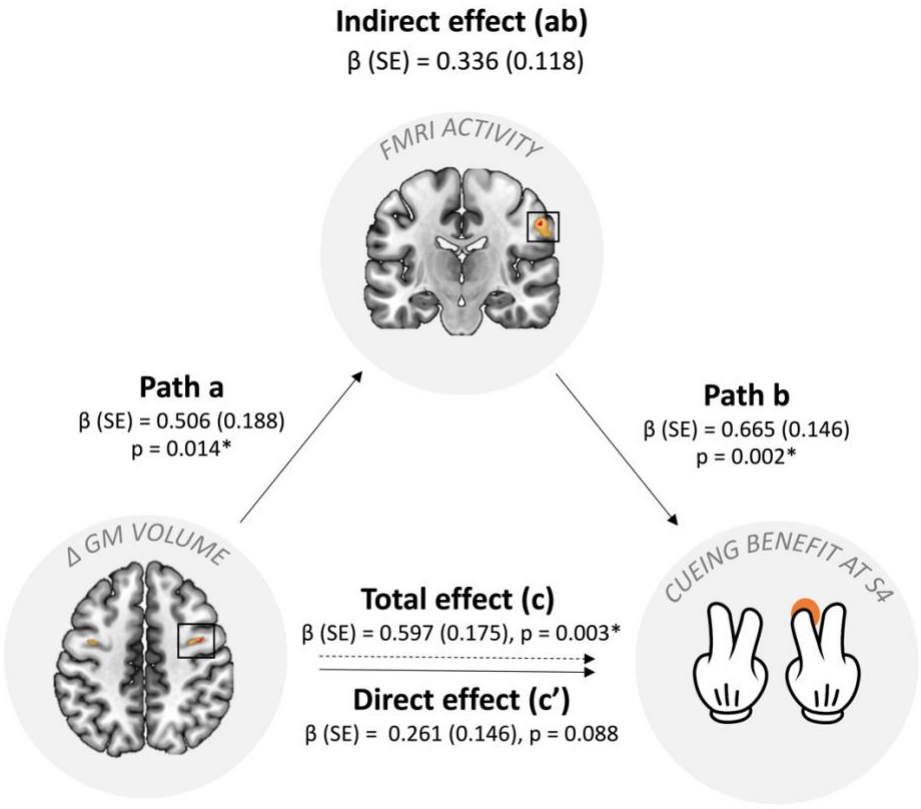

Fig. 7. Results of mediation analysis. *The diagram depicts standardised regression coefficients (β) for the relationship between the VBM result ([Δ GM volume from S1 to S3 * cueing benefit at S4] contrast) and cueing benefit at S4, mediated by the fMRI finding ([cued > uncued * cueing benefit at S4]). The associated standard error estimates (SE) are in parenthesis. Parameter estimates for the indirect effect were computed for 5000 bootstrapped samples. Total effect explained 36% of the variance in behavioural cueing benefit and was significant (p = 0.003; 95% CI: [0.233- 0.961]). Mediated model explained 68% of the variance. GM: grey matter; S4: Session 4. *p < 0.05. n = 23.*

4 DISCUSSION

In this study we aimed to determine if repeated reactivation of a motor memory trace during sleep engenders learning-related changes within the PPC and sensorimotor areas. To this end, we tested the temporal dynamics of the TMR-related changes across structural, functional, electrophysiological, and behavioural measures. Firstly, we showed a main effect of TMR on the SRTT performance across all post-stimulation sessions, with the biggest difference between the cued and uncued sequence emerging 20 days post-stimulation. In line with our hypothesis, dorsal precuneus showed a functional response that was both related to the manipulation and predicted its behavioural effects the next day. However, over time, both functional disengagement in the ventral subregion of precuneus and an increase in functional activity and volumetric grey matter in somatosensory and motor regions predicted the long-term behavioural benefit of our manipulation.

4.1 TMR BENEFITS PROCEDURAL MEMORIES UP TO 20 DAYS POST-MANIPULATION

The strongest behavioural difference between the cued and uncued sequence occurred 20 days post-manipulation, suggesting that the benefits of cueing may last longer than previously believed. This is especially true given that neither object-location (Shanahan et al., 2018) nor emotional (Groch et al., 2017a) memory seems to benefit from the manipulation even a week later. One-week-later effects of TMR have been reported for implicit biases (Hu et al., 2015), but this failed to replicate (Humiston & Wamsley, 2019). Our prior work showed behavioural effects of TMR 10 days post-manipulation but not 6 weeks later (Chapter 2). Hence, the long-term effect of procedural memory cueing that we observe here appears to be the longest reported in the literature so far. Our findings also suggest that TMR starts a process which then unfolds over several weeks, gradually leading to the emergence of behavioural benefits over time.

4.2 CUEING ENGAGES PRECUNEUS FUNCTIONALLY

Precuneus showed a TMR-dependent (cued > uncued) BOLD increase 24 h post-stimulation. Interestingly, this functional response predicted the behavioural cueing benefit at the same time point. These results combine to suggest that repeated reactivation of memory traces during sleep engages parts of the PPC in a behaviourally relevant manner. PPC has been identified as a hippocampus-independent memory store, whereby both hippocampal activity and hippocampal connectivity with PPC decreases after encoding, but (conversely) PPC activity increases over 24 h, as an independent memory representation builds up (Brodt et al., 2016). We believe that sleep plays a crucial role in this process and that the reactivation-mediated reorganisation of memories between the hippocampal-dependent short-term store and neocortex-dependent long-term store (Born et al., 2006; Diekelmann & Born, 2010b) fosters engram development in the precuneus. We speculate that memory reactivation could be taking place in precuneus (Himmer et al., 2021), such that procedural memories are stored and processed in the same location. Indeed, PPC has repeatedly been implicated in memory formation, retrieval, and storage (Gilmore et al., 2015; Myskiw & Izquierdo, 2012; Wagner et al., 2005) and is traditionally associated with the motor system (Cohen & Andersen, 2002; Shadmehr & Holcomb, 1997). Our results suggest that precuneus may be particularly involved in early consolidation of memories that are reactivated during sleep.

Although we showed that TMR-related functional activity in precuneus is associated with behavioural cueing benefit 24 h post-manipulation, it is important to note that we find no group level evidence for behavioural cueing benefit at that time point. This could be due to the jittering of our TMR cues during sleep *(*see Chapter 2, section *4.1. TMR effect evolves over time*). By randomising the inter-trial-interval between the TMR sounds we disrupted the temporal dynamics of sequence replay, decreasing the predictability of sequence elements. This may have delayed the impact of this manipulation on behaviour, such that behavioural impacts of TMR were not significant until 20 days post-manipulation. Even so, the absence of a TMR-related behavioural plasticity 10 days after cueing was unexpected given that cueing benefit was apparent at this time point in the previous chapter which used the same jittered TMR (Chapter 2). One possibility is that doing the task while lying down in the MRI scanner, and with somewhat clunky MR-safe button boxes, impacted on the behavioural effects of TMR which would otherwise have been apparent. Indeed, the only session during which we observed a significant cueing benefit was the one which was performed online and in participants' own homes using a computer keyboard. However, comparison between the SRTT reaction times at S3 and S4 revealed that the participants were, in fact, faster in the MRI environment (S3) than while performing the task on a PC (S4), with equal variance in the two sessions (Fig.S6). The MRI environment could have still influenced our behavioural results, but there is no reason to expect that it would impact differentially on the two sequences and thus the difference between them (i.e., cueing benefit).

Despite comparable performance on cued and uncued sequences 24 h post-TMR, participants exhibited distinct fMRI activation patterns for these two sequences at this time point. Indeed, we demonstrate that the dorsal subregion of precuneus is more functionally involved during production of the cued sequence 24 h post-TMR. Given that dorsal precuneus is specialised for somato-motor and visual-spatial processing (Zhang & Li, 2012), this finding raises the possibility that visuomotor integration of the reactivated memories may underpin short-term cueing benefits, even if it is not enough to drive the behavioural plasticity. In turn, we show that the functional disengagement of ventral precuneus over time facilitates cueing benefits 20 days post-TMR. In contrast to the dorsal precuneus, its ventral subregion has been mostly implicated in episodic memory retrieval (Zhang & Li, 2012). Hence, as ventral precuneus disengages, it perhaps allows other regions to take over, thus indirectly supporting long-term consolidation and behavioural performance.

4.3 PLASTICITY IN MOTOR REGIONS PREDICTS LONG-TERM CUEING BENEFITS

Our results suggest that a slowly evolving reorganisation of sensorimotor representations may underpin motor learning over a 20-day timescale. Specifically, we show that TMR-related functional activity in the right postcentral gyrus 10 days post-stimulation predicts behavioural benefits 20 days post-stimulation. Similarly, an increase in grey matter volume in the right precentral gyrus over the first 10 days post-stimulation predicts the behavioural benefits observed 20 days post-stimulation. In other words, both the functional activation and the volumetric grey matter increase in the sensorimotor cortex at 10 days post-TMR predict long-term cueing benefits.

Our mediation results further suggest that the functional activation of primary somatosensory cortex may be mediating a relationship between volumetric grey matter change in primary motor cortex and behavioural benefit from TMR. Indeed, these structures are known to be strongly linked (White & DeAmicis, 1977). In line with our findings, recent studies also demonstrate information flow from primary motor to primary sensory cortex, and vice versa (see Borich et al., 2015 for review). Importantly, slowly evolving reorganisation of primary motor cortex after learning has been linked to long-term retention of motor skills (Kami et al., 1995; Kleim, 2004; Matsuzaka et al., 2007) and even referred to as the long-term motor engram (Ganguly & Carmena, 2009; Gao et al., 2018). Our findings suggest that memory reactivation during sleep may be crucial in the formation of this type of representation, reinforcing the long-suggested involvement of motor regions in sleep-dependent procedural memory consolidation (Fischer, 2005; Walker et al., 2005). Furthermore, we expand the existing literature by showing that task-related structural and functional plasticity can emerge weeks after a single night of cueing during sleep. Our data show that just one night of TMR can impact on brain plasticity in the long run, perhaps facilitating the development of a stable memory trace over subsequent nights of un-manipulated sleep.

Interestingly, both SRTT training and post-training REM sleep are linked to increased premotor activity, suggesting that REM sleep may be involved in the reactivation of motor memories (Maquet et al., 2000). Furthermore, an association has been observed between increased sensorimotor responses to the cued SRTT sequence and REM sleep (Cousins et al., 2016). Although the increased involvement of sensorimotor regions reported here was not related to the amount of time spent in REM sleep during the stimulation night, it was

observed 10 days after encoding. In line with the suggestion that the delayed benefits of sleep may be due to processing in REM (Pereira & Lewis, 2020) we propose that REM reactivation during post-TMR nights, rather than immediately after cueing, may contribute to the long-term effects of TMR. However, it is unknown whether sensorimotor reactivation is taking place in post-TMR REM sleep and whether it contributes to the behavioural and neural benefits of the manipulation in the long run.

4.4 THE ROLE OF N2 AND SLEEP SPINDLES

Finally, we recognise a fundamental similarity between the reactivation of memory traces via TMR and repeated encoding-retrieval episodes during wake, which have also been shown to engender rapid memory engram formation within precuneus (Brodt et al., 2018). Indeed, repeated retrieval is a powerful way to consolidate memories and shares a lot of parallels with offline reactivation (Antony et al., 2017). However, in line with other studies (Himmer et al., 2019), we argue that the role of sleep goes beyond simply allowing opportunity for more rehearsal. Both N2 (Laventure et al., 2016; Nishida & Walker, 2007) and sleep spindles (Boutin & Doyon, 2020) have been consistently implicated in motor sequence memory consolidation. Although we found no relationship between behavioural cueing benefit and either the time spent in N2 or spindle density, we did find a surge in spindle density during the cue period relative to the no-cue period. This is in line with our prior report (Chapter 2) and indicates that auditory cueing may elicit sleep spindles and thereby engender an immediate processing of memory traces (Antony et al., 2018; Cairney et al., 2018). Thus, our current results further support the relationship between spindles and procedural memory cueing.

4.5 THE SEARCH FOR AN ENGRAM

A neuronal ensemble that holds a representation of a stable memory is known as an engram (Tonegawa et al., 2018). The term ‘engram’ also refers to the physical brain changes that are induced by learning and that enable memory recall (Josselyn et al., 2015). Due to their widely distributed and dynamic nature, engrams have long remained elusive. However, recent technological advances allow us to study memory engrams in humans (Brodt & Gais, 2021; Josselyn et al., 2015). PPC, for instance, has received increasing attention in memory research (Gilmore et al., 2015). Precuneus is a subregion of PPC and has been shown to undergo learning-dependent plasticity, fulfilling all criteria for a memory engram (Brodt et al., 2018). These defining criteria require an engram to (1) emerge as a result of encoding and reflect

the content of the encoded information, (2) engender a persistent, physical change in the underlying substrate that (3) enables memory retrieval, and (4) exists in a dormant or inactive state, i.e., between encoding and retrieval processes (Josselyn et al., 2015). Evidence for a relationship between engram formation and memory reactivation during sleep has so far been lacking. While previous literature suggests that changes in the precuneus alone fulfil all proposed criteria for an engram (Brodt et al., 2018), our data show no TMR-related structural changes in this region, and thus fail to fulfil criterion 2. This could be due to our use of different MRI modalities (i.e., structural rather than microstructural MRI as in Brodt et al., (2018)). Nevertheless, if our results are considered collectively across regions, we can argue that they do fulfil the criteria for an engram. Specifically, we find that memory representations stored in precuneus and postcentral gyrus reflect the encoded information (criterion 1), and enable memory recall (criterion 3), whereas the precentral gyrus undergoes structural changes (criterion 2) over a relatively long period of time (criterion 4). Thus, our results suggest that memory reactivation during sleep could support the development and evolution of an engram that encompasses several cortical areas.

5 CONCLUSION

We show that the behavioural benefits of procedural memory cueing in NREM sleep develop over time and emerge 20 days post-encoding. Increased TMR-related engagement of dorsal precuneus underpins the short-term effects of stimulation (over 24 hours), whereas sensorimotor regions support the long-term effects (over 20 days). These results advance our understanding of the neural changes underpinning long-term offline skill consolidation. They also shed new light on the TMR-induced processes that unfold over several nights after auditory cueing.

6 SUPPLEMENTARY MATERIAL

SUPPLEMENTARY NOTES: BASELINE SRTT PERFORMANCE

Before sleep, no difference was found between the average reaction time of the cued and uncued sequence for either both hands (BH, $t_{29} = -0.25$, $p = 0.801$), left hand (LH, $t_{29} = 0.27$, $p = 0.786$) or right hand (RH, $t_{29} = -0.50$, $p = 0.621$) (paired-samples t-tests) dataset. Similar results were obtained where comparing random sequences before sleep for all datasets (BH: $z = -0.57$, $p = 0.572$; LH: $z = -0.63$, $p = 0.530$; Wilcoxon signed-rank tests; RH: $t_{29} = -0.16$, $p = 0.872$; paired-samples t-test). Thus, any post-sleep difference between the sequences can be regarded as the effect of TMR. Furthermore, average reaction times before sleep were significantly shorter for the last 4 sequence blocks than for the random blocks, confirming that the participants learned both sequences during S1 (BH cued: $z = -4.74$, BH uncued: $z = -4.49$; LH cued: $z = -4.78$, LH uncued: $z = -4.33$; $p < 0.001$ for all comparisons, Wilcoxon signed-rank test; RH cued: $t_{29} = 7.21$, RH uncued: 6.49; $p < 0.001$ for all comparisons, paired-samples t-test). Summary statistics for each sequence and dataset during S1 are presented in Table S1.

SUPPLEMENTARY NOTES: EXPLICIT MEMORY TASK

Given that TMR was shown to promote the emergence of explicit knowledge the next morning (Cousins et al., 2014), we also set out to test whether this is true after a longer period. However, we found no difference between the free recall of the cued and uncued sequence ($z = -0.568$, $p = 0.570$, Wilcoxon signed-rank test), suggesting no TMR effect on the explicit knowledge of the sequence 20 days post-encoding (Fig.S1). Nevertheless, performance on both sequences differed from chance (cued: $z = -4.14$, $p < 0.001$; uncued: $z = -4.29$, $p < 0.001$; Wilcoxon signed-rank test), indicating that the participants learned both sequences explicitly over the course of the experiment.

SUPPLEMENTARY NOTES: QUESTIONNAIRES

The EHI confirmed that all participants were right-handed, as the laterality quotient score (ranging between -100 and +100, where the negative values indicate left-handers and positive right-handers) was +100% for all but one subject who scored +75%. PSQI global scores (on a 21-points scale) ranged between 1 and 7 points, with a mean of 3.67 ($\pm$0.28), indicating, on average, a 'good quality' of sleep (Buysse et al., 1989). The median answer to the SQ (with 1 and 9 indicating the highest and lowest level of alertness, respectively) was 2 (IQR: 1) for all sessions, suggesting similar levels of alertness throughout the study.

Participants did report hearing experimental sounds during the night: On a 3-points scale, the median answer was 2 (IQR: 2), with 33% of the participants not hearing any sounds (answer 1), 20% of the

participants being unsure (answer 2), and 47% of the participants hearing them clearly (answer 3). However, when asked about the number of sounds they had heard, the maximum number selected was 4 (reported by 13% of the participants), with the median answer of 2 (IQR: 2) sounds.

SUPPLEMENTARY TABLES:

Table S1. SRTT summary statistics.

Mean reaction times (± SEM) (in ms) *for the BH, LH and RH trials of the cued and uncued sequence blocks (24 blocks per sequence) as well as random blocks (2 blocks with tones matching the cued sequence and 2 blocks with tones matching the uncued sequence) during Session 1. Average reaction times* (± SEM) for the last 4 blocks of each sequence are shown as well. *BH: both hands; LH: left hand; RH: right hand. n = 30.*

Dataset	Cued sequence	Uncued sequence	Cued random	Uncued random	Cued sequence (last 4 blocks)	Uncued sequence (last 4 blocks)
BH	321.82 ± 6.46	322.89 ± 7.83	357.81 ± 6.63	360.10 ± 6.69	286.05 ± 8.09	292.64 ± 9.99
LH	335.98 ± 7.18	334.90 ± 7.82	376.86 ± 7.45	371.60 ± 6.60	297.44 ± 9.19	303.92 ± 10.55
RH	307.67 ± 6.28	310.92 ± 8.44	347.77 ± 6.95	348.60 ± 7.76	274.62 ± 7.81	281.40 ± 10.20

Table S2. Effect of and interaction between TMR, hand and session.

*Results of the likelihood ratio tests between the full, linear mixed effects model and reduced models, i.e., models without the fixed effect of interest, or with an interaction. The full model was used to test the effect of TMR, hand and session on the early and late SSS. df: degrees of freedom; χ2: chi-squared; AIC: Akaike Information Criterion; SSS: Sequence Specific Skill. *p < 0.05.*

	df	χ2	p-value	AIC of a reduced model	AIC of a full model
A. Both hands					
i) Early SSS					
TMR	1	1.5450	0.2138	1632.4	1632.9
Session	2	175.77	**<0.0001***	1804.6	1632.9
TMR x Session	2	0.0740	0.9637	1636.3	1632.9
ii) Late SSS					
TMR	1	11.009	**0.0009***	1621.3	1612.3
Session	2	93.041	**<0.0001***	1701.3	1612.3
TMR x Session	2	3.0133	0.2216	1613.3	1612.3
B. Left hand					
i) Early SSS					
TMR	1	0.1878	0.6648	1666.5	1668.3
Session	2	132.02	**<0.0001***	1796.3	1668.3
TMR x Session	2	0.1044	0.9492	1672.2	1668.3
ii) Late SSS					
TMR	1	4.015	**0.0451***	1646.3	1644.2
Session	2	64.529	**<0.0001***	1704.8	1644.2
TMR x Session	2	1.9750	0.3725	1646.3	1644.2
C. Right hand					
i) Early SSS					
TMR	1	3.2309	0.0723	1651.0	1659.8

Session	2	181.60	**<0.0001***	1827.4	1649.8
TMR x Session	2	0.3741	0.8294	1653.4	1649.8
ii) Late SSS					
TMR	1	15.458	**<0.0001***	1636.8	1650.3
Session	2	96.024	**<0.0001***	1728.9	1636.2
TMR x Session	2	3.9605	0.1380	1636.9	1636.8
D. Left and right hand combined					
i) Early SSS					
Hand	1	22.423	**<0.0001***	3286.3	3265.9
Hand x Session	2	9.1678	**0.0102***	3260.7	3265.9
TMR x Hand	1	0.8955	0.3440	3267.0	3265.9
ii) Late SSS					
Hand	1	25.927	**<0.0001***	3261.5	3237.5
Hand x Session	2	6.4262	**0.0402***	3237.5	3235.9
TMR x Hand	1	2.1656	0.1411	3237.4	3237.5

Table S3. Effect of session on SSS.

*Post-hoc pairwise comparisons between sessions for the early and late SSS, conducted on each dataset separately. P-values reported are Holm adjusted. SSS: Sequence Specific Skill; S2-4: Session 2-4; df: degrees of freedom. *p < 0.05.*

	Mean S2 (±SE) [ms]	**Mean S3 (±SE) [ms]**	**Mean S4 (±SE) [ms]**	**Estimate (±SE)**	**df**	**t ratio**	**p-value** (Holm adj)	**Effect size**
A. Both hands								
i) Early SSS								
S2-S3	39.2 (9.88)	81.7 (10.20)	-	-42.5 (6.49)	135	-6.553	**<0.0001***	-1.320
S3-S4	-	81.7 (10.20)	163.1 (10.27)	-81.3 (6.63)	131	-12.270	**<0.0001***	-2.520
ii) Late SSS								
S2-S3	129.0 (8.92)	154.0 (9.24)	-	-24.7 (6.14)	135	-4.018	**0.0001***	-0.807
S3-S4	-	154.0 (9.24)	200 (9.30)	-46.2 (6.27)	131	-7.367	**<0.0001***	-1.513
B. Left hand								
i) Early SSS								
S2 – S3	35.3 (11.10)	73.3 (11.40)	-	-37.9 (7.34)	135	-5.227	**<0.0001***	-1.050
S3 – S4	-	73.3 (11.40)	144.1 (11.5)	-70.8 (7.50)	131	-9.553	**<0.0001***	-1.960
ii) Late SSS								
S2 – S3	121.0 (10.20)	149.0 (10.50)	-	-27.4 (6.74)	135	-4.064	**0.0001***	-0.817
S3 – S4	-	149.0 (10.50)	183 (10.6)	-34.4 (6.89)	131	-4.996	**<0.0001***	-1.026
C. Right hand								
i) Early SSS								
S2 – S3	43.0 (9.13)	90.0 (9.53)	-	-46.9 (7.13)	136	-6.627	**<0.0001***	-1.330
S3 – S4	-	90.0 (9.53)	182 (9.61)	-91.9 (7.30)	132	-12.670	**<0.0001***	-2.600
ii) Late SSS								
S2 – S3	137.0 (8.27)	159.0 (8.69)	-	-21.9 (6.90)	137	-3.167	**0.0019***	-0.634
S3 – S4	-	159.0 (8.69)	217 (8.77)	-58.1 (7.08)	132	-8.207	**<0.0001***	-1.685

Table S4. Effect of TMR on late SSS during each session.

*Post-hoc pairwise comparisons of late SSS between the cued and uncued sequence on each session (S2-S4), conducted on each dataset separately. Both the uncorrected and Holm adjusted p-values are reported. S2-4: Session 2-4; SSS: Sequence Specific Skill; df: degrees of freedom. *p < 0.05. ^p < 0.07.*

Cued vs Uncued	**Mean cued (± SE) [ms]**	**Mean uncued (± SE) [ms]**	**Estimate (± SE)**	**df**	**t ratio**	**p value**	**p value** (Holm adj)	**Effect size**
A. Both hands								

S2	135 (9.94)	123 (9.94)	-11.78 (7.95)	133	-1.482	0.1408	0.2815	-0.390
S3	157 (8.70)	147 (8.70)	-9.98 (8.71	133	-1.146	0.2537	0.2815	-0.331
S4	215 (11.60)	185 (11.60)	-29.13 (8.89)	133	-3.277	**0.0013***	**0.0040***	-0.965
B. Left hand								
S2	127 (11.20)	116 (11.20)	-11.02 (8.76)	133	-1.258	0.2106	0.4212	-0.3212
S3	146 (10.30)	145 (10.30)	-1.33 (9.60)	133	-0.139	0.8897	0.8897	-0.0401
S4	193 (13.10)	172 (13.10)	-20.29 (9.79)	133	-2.072	**0.0401***	0.1206	-0.6101
C. Right hand								
S2	143 (9.73)	130 (9.73)	-12.50 (8.94)	133	-1.401	0.1634	0.1634	-0.369
S3	167 (8.37)	149 (8.37)	-18.60 (9.79)	133	-1.899	0.0597^	0.1193	-0.548
S4	237 (11.00)	198 (11.00)	-38.20 (9.99)	133	-3.822	**0.0002***	**0.0006***	-1.125

Table S5. Effect of time and hand on the cueing benefit.

*Results of the likelihood ratio tests between the full, linear mixed effects model and reduced models, i.e., models without the fixed effect of interest, or with an interaction. The full model was used to test the effect of hand and number of days post-TMR ('Time') on the cueing benefit (SSS for the uncued sequence subtracted from the cued sequence). χ2: chi-squared; AIC: Akaike Information Criterion. df: degrees of freedom. *p < 0.05. ^p < 0.07.*

	df	χ2	p-value	AIC of a reduced model	AIC of a full model
A. Both hands					
Time	2	3.965	**0.046***	809.14	807.18
B. Left hand					
Time	2	0.736	0.391	825.46	826.73
C. Right hand					
Time	2	6.581	**0.010***	834.01	829.43
D. Left and right hand combined					
Hand	1	3.760	0.052^	1641.70	1639.90
Hand x Time	2	1.424	0.233	1639.9	1640.8

Table S6. Sleep parameters.

Total recording duration, total sleep time, time spent in each sleep stage and time scored as movement presented as average (minutes ± SEM) and as percentage of the total recording duration. Total sleep time was calculated by subtracting the time spent awake from the total recording duration. N1-N3: stage 1 – stage 3 of NREM sleep. REM: Rapid Eye Movement sleep. n = 29.

	Percentage of total recording duration [%]	Mean duration ± SEM [min]
Total recording duration	100%	524.19 ± 10.29
Total sleep time	88.38%	463.29 ± 12.89
Wake	11.50%	60.90 ± 10.37
N1	4.52%	23.33 ± 1.73
N2	46.35%	242.45 ± 8.41
N3	19.91%	104.22 ± 4.05
REM	15.86%	83.43 ± 4.30
Movement	1.61%	8.43 ± 1.32

Table S7. Cueing benefit and the duration of N2 and N3.

*Results of Pearson's correlations between cueing benefit and the percentage of time spent in N2 and N3. Both the uncorrected and FDR corrected p-values are reported. df: degrees of freedom; S2-4: Session 2-4; SSS: Sequence Specific Skill; N2-3: Stage 2-3 of NREM sleep. *p < 0.05.*

	Time spent in N2 [%]				Time spent in N3 [%]			
	df	Pearson's correlation	p-value	p-value (FDR corr)	df	Pearson's correlation	p-value	p-value (FDR corr)
A. Both hands								
S2	25	0.197	0.324	0.324	27	-0.015	0.939	0.939
S3	20	0.378	0.082	0.144	21	-0.031	0.887	0.939
S4	19	0.372	0.096	0.144	21	0.089	0.697	0.939
B. Left hand								
S2	23	0.101	0.632	0.632	25	0.036	0.857	0.974
S3	19	0.432	**0.045***	0.135	21	0.070	0.746	0.974
S4	19	0.324	0.152	0.228	21	0.007	0.974	0.974
C. Right hand								
S2	24	-0.030	0.884	0.884	26	-0.053	0.788	0.788
S3	19	0.177	0.431	0.657	21	-0.125	0.562	0.788
S4	19	0.377	0.092	0.276	21	0.144	0.511	0.788

Table S8. Summary statistics for sleep spindles.

Average number and density (number/min) of spindles (± SEM). Results are presented for N2 and N3 of the cue (A) and no-cue (B) period. N2-3: stage 2-3 of NREM sleep.

	Density			Number		
	Average	Left	Right	Average	Left	Right
A. Cue						
N2	5.28 ±0.27	5.43 ±0.29	5.13 ±0.19	124.02 ±11.31	127.68 ±11.70	120.35 ±11.23
N3	4.24 ±0.16	4.31 ±0.16	4.17 ±0.16	191.58 ±13.14	195.39 ±13.88	187.77 ±12.74
N2 & N3	4.20 ±0.22	4.43 ±0.25	3.96 ±0.24	286.91 ±18.50	301.06 ±19.81	272.76 ±18.70
B. No-Cue						
N2	4.85 ±0.27	5.02 ±0.29	4.68 ±0.28	51.71 ±5.07	53.17 ±5.22	50.24 ±5.08
N3	3.86 ±0.16	3.94 ±0.17	3.78 ±0.17	79.48 ±5.68	81.30 ±5.79	77.66 ±5.69
N2 & N3	3.80 ±0.20	4.01 ±0.23	3.59 ±0.21	117.74 ±7.69	123.59 ±8.12	111.89 ±7.79

Table S9. Cueing benefit and spindle density.

Results of Pearson's (A) and Spearman's (B) correlations (both FDR corrected and not) between the cueing benefit for BH dataset during each of the post-stimulation sessions (S2, S3, S4) and spindle density averaged over all motor channels during the cue (A) and no-cue (B) period. N2 (green) and N3 (blue) were analysed separately and together (N23, purple). df: degrees of freedom; S2-4: Session 2-4; N2-N3: stage 2 - stage 3 of NREM sleep; BH: Both Hands.

Dataset	Session	Sleep stage	Correlation coefficient	p-value	df	p-value (FDR corr)
A. Cue period						
BH	S2	N2	0.237	0.224	26	0.288
BH	S3	N2	-0.254	0.231	22	0.288
BH	S4	N2	-0.231	0.288	21	0.288
BH	S2	N3	-0.04	0.840	25	0.840
BH	S3	N3	-0.337	0.126	20	0.192

BH	S4	N3	-0.343	0.128	19	0.192
BH	S2	N23	0.196	0.309	27	0.322
BH	S3	N23	-0.277	0.191	22	0.322
BH	S4	N23	-0.216	0.322	21	0.322
B. No-cue period						
BH	S2	N2	0.135	0.485	27	0.485
BH	S3	N2	-0.317	0.132	22	0.396
BH	S4	N2	-0.227	0.296	21	0.444
BH	S2	N3	0.227	0.235	27	0.546
BH	S3	N3	-0.171	0.422	22	0.546
BH	S4	N3	-0.132	0.546	21	0.546
BH	S2	N23	0.189	0.326	27	0.639
BH	S3	N23	-0.172	0.419	22	0.629
BH	S4	N23	-0.042	0.851	21	0.851

Table S10. Functional TMR-related activity.

Clusters showing increased (inc) and decreased (dec) activity for the cued relative to uncued sequence alone (A - S2 and S3, B - S2) or when considering covariates of cueing benefit during S2 (C) and cueing benefit during S4 (E). (D) Decrease in activity from S2 to S3 for the [cued > uncued] contrast when considering behavioural cueing benefit at S4 as a covariate. No significant clusters were found when considering cueing benefit during S3 as a covariate.

Region	MNI x, y, z (mm)	Number of voxels	F/T peak	P_{FWE} peak
A. Main effect of TMR for S2 and S3				
i. Right Precuneus (inc)	8, -72, 58	9	22.67	0.032
B. [Cued > Uncued at S2]				
i. Left Precuneus (inc)	-9 -62, 66	9	4.79	0.020
C. [Cued > Uncued at S2 * cueing benefit at S2]				
i. Left Precuneus (inc)	-4, -78, 46	40	5.18	0.009
ii. Left Precuneus (inc)	-18, -68, 36	1	4.44	0.046
iii. Right Cerebellum (inc)	28, -58, -30	1	4.94	0.044
iv. Left Putamen (inc)	-24, 4, 6	3	4.41	0.034
D. [Δ Cued > Uncued from S2 to S3 * cueing benefit at S4]				
i. Left Precuneus (dec)	-2, -54, 10	18	6.66	0.002
E. [Cued > Uncued at S3 * cueing benefit at S4]				
i. Right Postcentral gyrus (inc)	58, -18, 38	7	5.50	0.022
ii. Left Parahippocampus (dec)	-22, -26, -16	1	4.52	0.047

Regions listed were significant at peak voxel threshold of $p_{FWE} < 0.05$, after correction for multiple voxel-wise comparisons within pre-defined bilateral ROI for precuneus (A.i, B.i, C.i, C.ii, D.i), hippocampus and parahippocampus (E.ii), cerebellum (C.iii), dorsal striatum (C.iv), sensorimotor cortex (E.i). Peak voxel MNI coordinates and peak F (A) and T (B-E) values are given. n = 22 for (A), n = 28 for (B) and (C), n = 23 for (E), n = 21 for (D).

Table S11. Structural brain changes over time.

Clusters showing increased (inc) and decreased (dec) changes in grey matter volume over time and when considering covariates of cueing benefit during S3 and S4. No significant clusters were found when considering cueing benefit during S2 as a covariate. No significant clusters were found in white matter either.

Region	MNI x, y, z (mm)	Number of voxels	T peak	P_{FWE} peak
A. [Δ GM volume from S1 to S3 * cueing benefit at S4]				
Right Precentral gyrus $_{(inc)}$	42, -2, 45	5	6.21	0.018
B. [Δ GM volume from S1 to S3 * cueing benefit at S3]				
Left Fusiform $_{(dec)}$	-28, - 26, -24	5	5.51	0.025

Regions listed were significant at peak voxel threshold of $p_{FWE} < 0.05$, after correction for multiple voxel-wise comparisons within pre-defined bilateral ROI for sensorimotor cortex (A) and hippocampus and parahippocampus (B). Since fusiform gyrus was not our ROI, the result in (B) has likely arisen due to the imperfection of the method and is thus not discussed any further. Peak voxel MNI coordinates and peak T values are given. n = 24 for (A), n = 29 for (B).

SUPPLEMENTARY FIGURES:

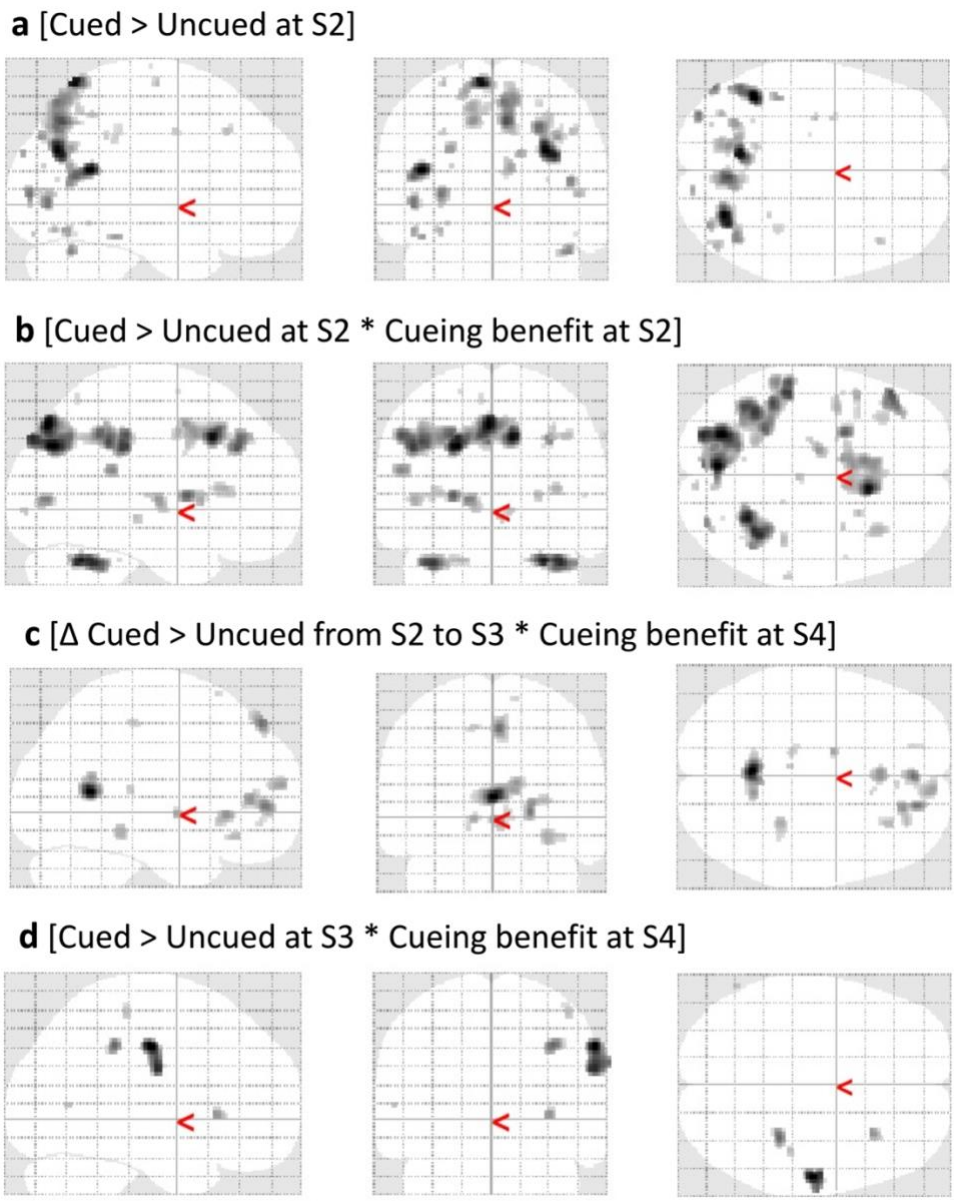

Fig. S1. Glass brain fMRI results. *SPM fMRI results in glass brain projection displayed at p < 0.001, uncorrected, for the same contrasts as in Fig.5 and Fig.6A-B.* ***(a)*** *TMR-dependent increase in brain activity 24 h post-stimulation.* ***(b)*** *Brain activity for the [cued > uncued] contrast at S2 was positively associated with behavioural cueing benefit at the same time point.* ***(c)*** *A change in brain activity from S2 to S3 for the [cued > uncued] contrast was negatively associated with behavioural cueing benefit at S4.* ***(d)*** *Brain activity for the [cued > uncued] contrast at S3 was positively associated with behavioural cueing benefit at S4. S2-4: Session 2-4; n = 28 for (a-b), n = 21 for (c), n = 23 for (d).*

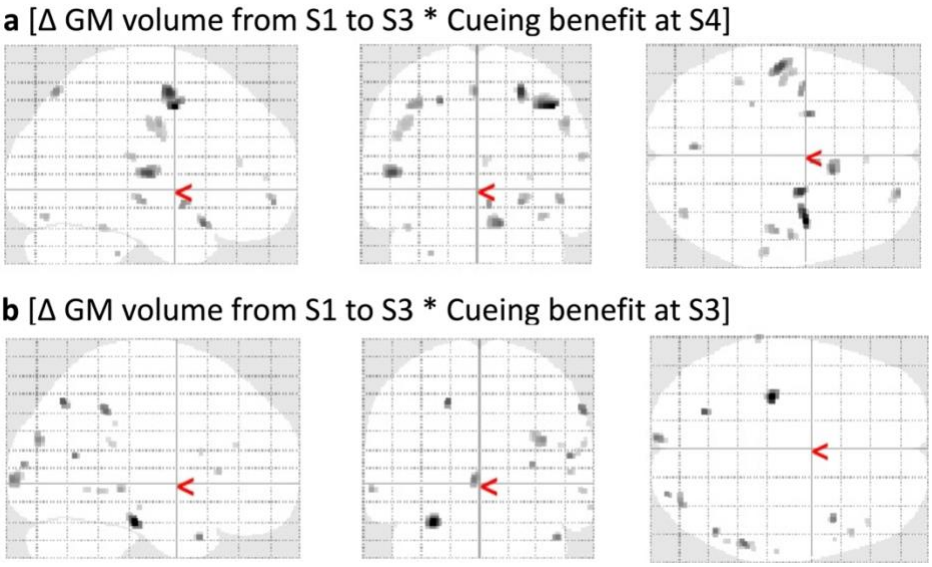

Fig. S2. Glass brain VBM results. *SPM VBM results in glass brain projection displayed at p < 0.001, uncorrected, for the same contrasts as in Fig.6C-D (a) and Table S11 (a, b).* ***(a)*** *An increase in grey matter volume at S3 relative to S1 was associated with an increase in behavioural cueing benefit at S4.* ***(b)*** *Reduction in grey matter volume at S3 relative to S1 associated with cueing benefit at S3. S1-4: Session 1-4. n = 24 for (a), n = 29 for (b).*

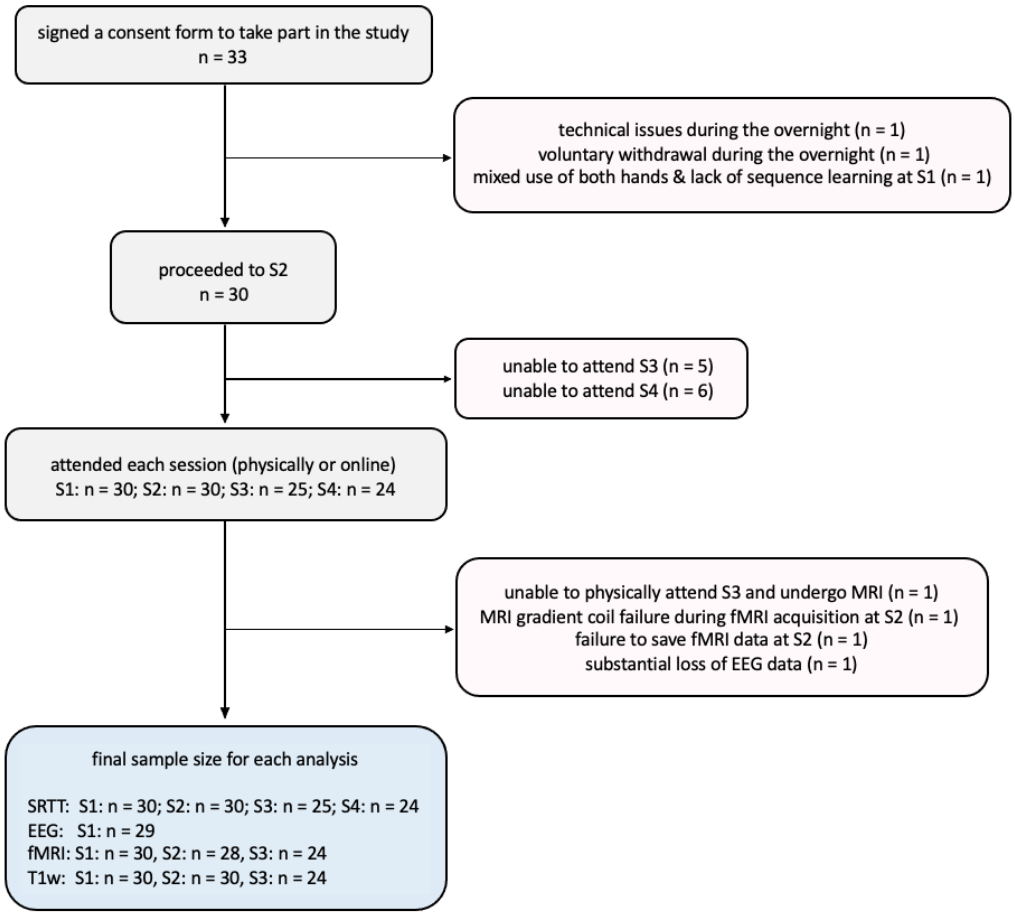

Fig. S3. A flowchart illustrating participants included in and excluded from the analysis. *On the left, the number of participants included in the study at different time points, with the final sample size shown at the bottom. On the right, the number of participants excluded (in red) together with a reason for the exclusion.*

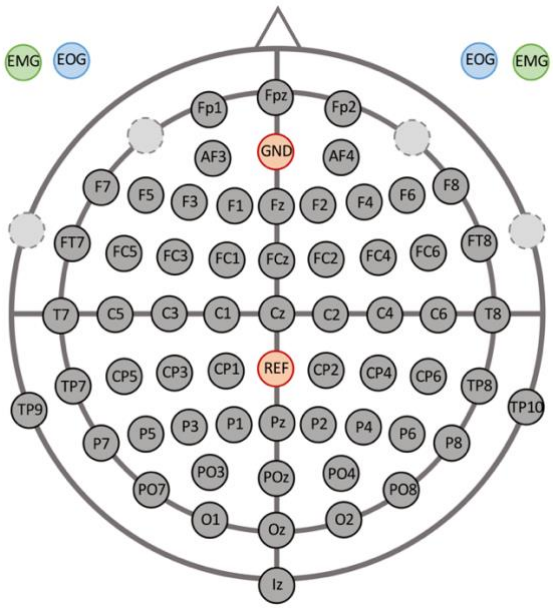

Fig. S4. EEG electrodes layout. *Orange: ground (GND) and reference (REF) electrodes; light grey (dashed circles): original position of the electrodes used to record EMG and EOG; green: EMG electrodes; blue: EOG electrodes.*

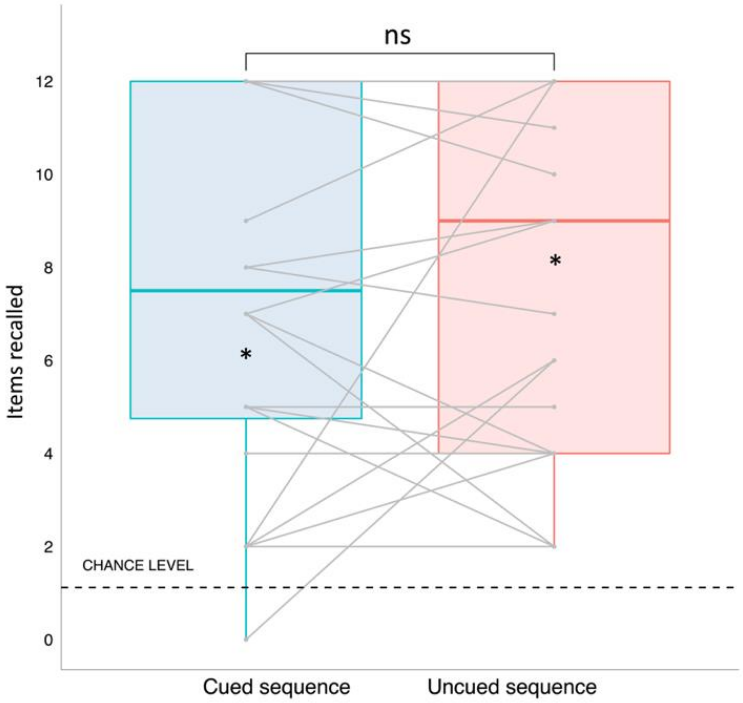

Fig. S5. Cueing memory reactivation during sleep does not affect explicit memory of the sequence. *Explicit knowledge of both sequences was significantly above chance (significance denoted with *) 20 days post-encoding, although no effect of TMR was evident. Geoms represent median ± IQR for the cued (blue) and uncued (red) sequence, whiskers represent largest and lowest values within 1.5 IQR above and below the 75th and the 25th percentile, respectively. Grey dots represent performance of each subject. ns: non-significant. n = 24.*

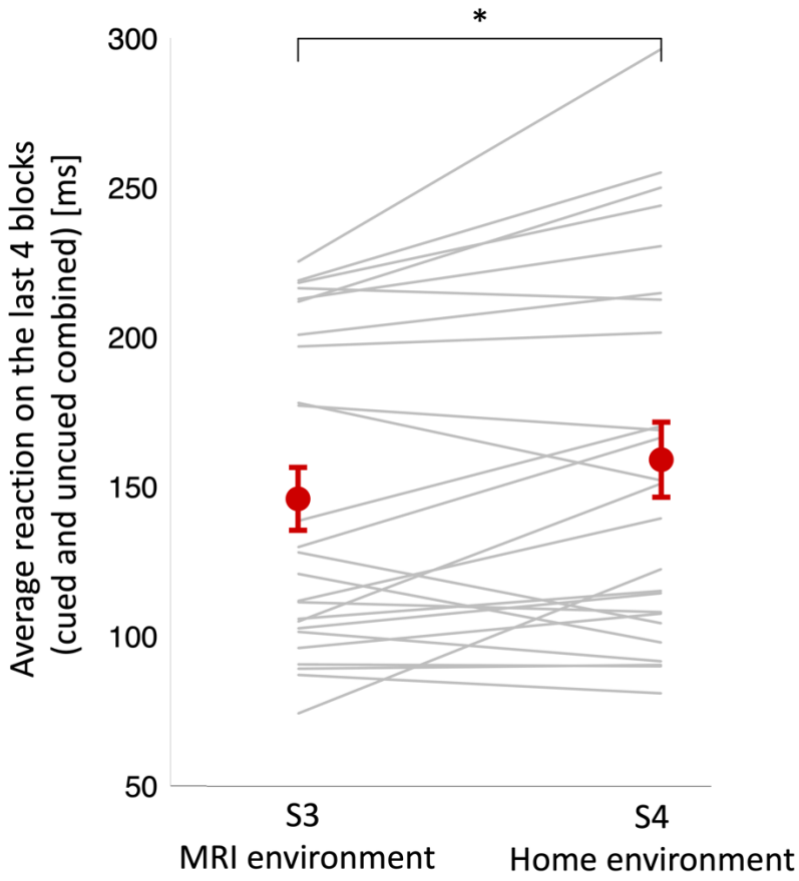

Fig. S6. MRI environment does not limit performance on the SRTT. *Difference between the average reaction time on the last 4 blocks of S3 (performed in the MRI environment) compared to S4 (performed in home environment). Participants were significantly faster by the end of S3 than S4 (paired t-test: $t_{48} = -2.10$, $p = 0.041$), suggesting that the MRI environment does not limit performance on the SRTT. No difference in variance between the two sessions was found (F test: $F_{24} = 1.42$, $p = 0.200$). * $p < 0.05$, $n = 25$.*

CHAPTER 4

Distributed and gradual microstructure changes track the emergence of behavioural benefit from memory reactivation

This chapter is based on a manuscript which is being prepared for submission for peer review.

Abstract

Memory traces are thought to develop gradually and link to neural plasticity. Memory reactivation during sleep is crucial for consolidation, but its impact on plasticity and contribution to long-term memory storage remains unclear. We used multimodal diffusion weighted imaging to track the location and timescale of microstructural changes following Targeted Memory Reactivation (TMR) of a motor task, previously shown to benefit memories 20 days post-manipulation. We found changes suggestive of continuous plasticity in the microstructure of precuneus across 10 days post-TMR. These changes parallel the gradual development of behavioural benefit. Both early (0 – 24 h post-TMR) and late (24 h – 10 days post-TMR) microstructural changes in striatum and sensorimotor cortex were associated with the emergence of TMR behavioural effect at day 20. Our analysis also revealed a relationship between baseline microstructural architecture of sensorimotor cortex and TMR susceptibility, independent of participants' demographics, sleep patterns, and baseline performance on the task. These findings demonstrate that repeated reactivation of memory traces during sleep engenders microstructural plasticity across memory and task-related areas which continues days after the stimulation night and is associated with the emergence of memory benefits at the behavioural level.

1 INTRODUCTION

The ability to change and adapt in response to internal or external stimuli by reorganising neural connections, structure, and function is a fundamental property of the brain (Mateos-Aparicio & Rodríguez-Moreno, 2019). The remarkably plastic nature of the nervous system forms the basis of learning and memory (Zatorre et al., 2012; Voss et al., 2017; Barco et al., 2006). Learning-associated neural processes occurring during sleep have been receiving increasing attention in recent times. The active systems consolidation model suggests that newly encoded memories are reactivated during non-rapid eye movement (NREM) sleep, and that this enables their re-coding from a temporary store to a more permanent location (Born & Wilhelm, 2012; Born et al., 2006; Rasch & Born, 2013). However, while the process of memory consolidation is gradual and occurs over long timescales (Frankland & Bontempi, 2005), it is unclear whether reactivation of memories during sleep leads to plasticity in the neural substrate over time. Moreover, there is increasing evidence for distributed long-term cortical storage of memories (Josselyn & Tonegawa, 2020; Dudai, 2004; Josselyn et al., 2015), but it is unclear whether replay-driven consolidation of memories is associated with plasticity

at different cortical sites. Likewise, how such plasticity could lead to long-term memory storage in humans has not been studied sufficiently (Stee & Peigneux, 2021).

Here we set out to track the location and timescale of microstructural changes underlying long-term effects of memory reactivation during sleep using Targeted Memory Reactivation (TMR). TMR involves associating learning items with sensory cues during wake and then covertly re-presenting them during sleep (e.g., Rasch et al., 2007; Rudoy et al., 2009). This is thought to trigger reactivation of the cue-associated memory representation which leads to a better recall of the cued items compared to those that were not cued during the night (i.e., uncued) (Chapter 2; Antony et al., 2012; Schönauer et al., 2014; Cousins et al., 2014a; Cousins et al., 2016). In recent years, TMR has become a valuable tool to study the mechanisms of sleep-dependent memory processes. It has allowed us to establish a causal link between memory reactivation and consolidation (Schreiner et al., 2018; Belal et al., 2018), and to identify brain regions that are functionally involved in such relationship (Chapter 3; Rasch et al., 2007; van Dongen et al., 2012; Shanahan et al., 2018; Cousins et al., 2016). Previous chapters of this thesis further demonstrated that the behavioural effects of TMR develop over time and can last up to three weeks (Chapter 2 and Chapter 3). However, the physical brain changes driving the long-term functional and behavioural benefits of TMR remain poorly understood. In Chapter 3 we have shown that TMR can impact on grey matter volume within the task-related regions, thus shaping their functional response and the behavioural benefit of cueing in the long run. Yet, it is still unclear whether repeated reactivation of a memory trace can also modify tissue microstructure and what the time scale of such changes might be.

We used diffusion-weighted MRI (DW-MRI) to examine short- and long-term microstructural plasticity after TMR of a procedural memory task. DW-MRI is sensitive to the random motion of water molecules within tissue, thus providing indirect information about microstructure (Mori & Zhang, 2006). It is a task-independent measure which, in contrast to functional MRI, allows probing of the microstructural substrate without being affected by task specific-activity. Importantly, the technique is also known to be sensitive to experience-driven plasticity within memory-related areas (Sagi et al., 2012; Hofstetter et al., 2013, Tavor et al., 2020, Tavor et al., 2013) and has been used to track the development of a neocortical engram, with the microstructural changes driving gains in behavioural performance (Brodt et al., 2018). This makes DW-MRI an excellent technique for studying the gradual structural plasticity which is associated with memory formation over long timescales. The simplest

approach to measure diffusion is diffusion tensor (DT) MRI, which assumes a Gaussian behaviour of water molecules within a single water compartment and allows the quantification of parameters such as mean diffusivity (MD) and fractional anisotropy (FA) (Afzali et al., 2021). More complex models have been developed to account for the different behaviour of intra- and extra-cellular water, such as the Composite Hindered And Restricted Model of Diffusion (CHARMED, Assaf et al., 2004). The relative sizes of the restricted (Fr, intracellular) and hindered compartments can then be estimated.

Our participants learned two motor sequences of a Serial Reaction Time Task (SRTT), each associated with a different set of auditory tones. Tones associated with one of the sequences were replayed to the participants during subsequent NREM sleep, successfully improving cued vs uncued sequence performance post-TMR (see Chapter 3 for behavioural effects). During both learning and the two re-test sessions (24 h and 10 days post-TMR), participants were placed in the scanner to acquire structural (T1-weighted, T1w) and DW-MRI data, with the final re-test session taking place online, 20 days after TMR. MD has recently been shown to decrease in precuneus in response to a series of repeated learning-retrieval epochs during wake (Brodt et al., 2018), which could be regarded of as a proxy of memory reactivation during sleep (Himmer et al., 2019). We thus hypothesised that TMR during sleep would also lead to rapid MD-driven plasticity within precuneus, thereby supporting the functional activation of this structure in association with TMR that we observed in the previous chapter (Chapter 3). However, we expected the motor-related regions to undergo long-term microstructural changes, thereby reflecting their slowly evolving reorganisation (Kami et al., 1995; Kleim et al., 2004; Matsuzaka et al., 2007; Gao et al., 2018; Ganguly & Carmena, 2009), as well as long-term functional engagement and volumetric increase in response to TMR (Chapter 3). In the current study, we also used Restricted Water Fraction (Fr), as modelled by the CHARMED framework (Assaf et al., 2004). Fr is thought to be more sensitive to microstructural changes than MD, especially in long-term assessment (Tavor et al., 2013). We thus combined MD with Fr in a multimodal analysis protocol to uncover common microstructural patterns across the two MRI markers and their relationship with TMR benefits across time. Finally, despite the importance of tissue microstructure for memory formation (Brodt et al., 2018), it is unclear whether baseline tissue (micro)structure is predictive of memory encoding capacity. To clarify this, we tested whether baseline brain characteristics (both in terms of brain microstructure and volume) can determine TMR susceptibility, thus adding to our current understanding of the factors that influence the effectiveness of TMR (Hu et al., 2020).

2 MATERIALS AND METHODS

2.1 PARTICIPANTS

The same sample of 33 healthy volunteers that was reported in Chapter 3 signed a written informed consent to take part in the study, which had been approved by the Ethics Committee of the School of Psychology at Cardiff University. All participants reported being right-handed, sleeping approximately 8 h per night, having normal or corrected to normal vision, no hearing impairment, and no prior knowledge of the experimental tasks before commencing the study. Regular nappers, smokers, subjects who had travelled across more than two time-zones or engaged in any regular night work during one month prior to the experiment were not recruited. Further criteria for exclusion included recent stressful life event(s), regular use of any medication or substance affecting sleep, prior history of drug/alcohol abuse, and neurological, psychological, or sleep disorders. Additionally, participants were asked to abstain from napping, extreme physical exercise, caffeine, alcohol, and other psychologically active food from 24 h prior to each experimental session. We also excluded participants with more than three years of musical training in the past five years due to a probable link between musical abilities and procedural learning (Romano Bergstrom et al., 2012; Anaya et al., 2017). Participants were screened by a qualified radiographer from Cardiff University to assess their suitability for MRI and signed an MRI screening form prior to each scan.

Four participants had to be excluded from all analyses due to: technical issues (n = 1), voluntary withdrawal (n = 1), interrupted EEG recording during the night (n = 1), and low score on the handedness questionnaire (indicating mixed use of both hands), combined with positive slope of learning curve during the first session (indicating lack of sequence learning before sleep) (n = 1). Due to COVID-19 outbreak, four participants were unable to complete the study, missing either one (n = 1) or two (n = 5) sessions. One additional participant could not physically attend S3; they performed the SRTT online, but their MRI data could not be collected and therefore the sample size for the MRI analyses of S3 had to be decreased by one. Hence, 29 participants remained in the MRI dataset (15 females, age range: 18 - 23 years, mean ±SD: 20.33 ± 1.45; 14 males, age range: 19 - 23 years, mean ±SD: 20.43 ± 1.16), but data from only 23 of them was acquired during S3. This final dataset was used for T1w data analysis, but six additional participants had to be removed from the DW-MRI analyses due to posterior (n = 2) or anterior (n = 4) part of the radiofrequency coil failure. Finally, Fr

maps collected from three additional participants failed a visual quality check after pre-processing and were thus excluded from the Fr analysis (n = 3). Hence, the final sample size for MD analysis was n = 23 for S1, n = 23 for S2 and n = 19 for S3, and the sample size for Fr analysis was n = 20 for S1, n = 20 for S2 and n = 16 for S3. A flowchart of participants included and excluded from the different analyses is presented in Fig.S1.

2.2 STUDY DESIGN

The study consisted of four sessions (Fig.1a), all scheduled for the same time in the evening (~8 pm). Upon arrival for the first session (S1), participants completed Pittsburgh Sleep Quality Index (PSQI) (Buysse et al., 1989) to examine their sleep quality over the past month. S1 consisted of a motor sequence learning task (the SRTT), MRI data acquisition and overnight stay in the lab. The SRTT learning session was split in half, such that the first half of the SRTT blocks (24 sequence blocks) was performed in a 0T Siemens 'mock' scanner (i.e., an environment that looked exactly like an MRI scanner, but with no magnetic field) and the other half (24 sequence blocks + 4 random blocks) in a 3T Siemens MRI scanner, immediately after T1w structural data acquisition. This was followed by DW-MRI (see section 2.*6 MRI data acquisition*). Participants were then asked to prepare themselves for bed and were fitted with an electroencephalography (EEG) cap. While in stable stage 2 (N2) or 3 (N3) of NREM sleep, the TMR protocol was initiated (see section *2.5 TMR during NREM sleep*). Briefly, to trigger reactivation of the associated SRTT memories, tones associated with one of the SRTT sequences were replayed to the participants through speakers (Harman/Kardon HK206, Harman/Kardon, Woodbury, NY, USA). After, on average, 8.81 $\pm$ 0.82 hours in bed participants were woken up and had the EEG cap removed before leaving the lab.

Session 2 (S2), session 3 (S3) and session 4 (S4) took place 23-26 h, 10-14 days, and 16-21 days after S1, respectively. During S2 and S3 T1w and DW-MRI data were acquired as before, followed by an SRTT re-test. Here, the first half of the SRTT blocks (24 sequence blocks + 4 random blocks) was performed in the 3T scanner and the second half (24 sequence blocks + 4 random blocks) in the 0T scanner. Note that the order of scans (3T vs 0T) was flipped from S1 to S2 and S3 for the microstructural assessment to occur as close to TMR as possible. S4 was performed either in the lab or online, depending on the severity of COVID-19 restrictions at the time. During S4, SRTT was delivered in one run (48 sequence blocks + 4 random blocks).

For offline data collection, the SRTT (S1-S3) was back projected onto a projection screen situated at the end of the MRI/mock scanner and reflected into the participant's eyes via a mirror mounted on the head coil; during S4 SRTT was presented on a computer screen with resolution 1920 x 1080 pixels and executed using MATLAB 2016b (The MathWorks Inc., Natick, MA, USA) and Cogent 2000 (developed by the Cogent 2000 team at the Functional Imaging Laboratory and the Institute for Cognitive Neuroscience, University College, London, UK; http://www.vislab.ucl.ac.uk/cogent.php). For online data collection (S4), SRTT was programmed in Python using PsychoPy 3.2.2. (Peirce et al., 2019) and administered through Pavlovia online platform (https://pavlovia.org/).

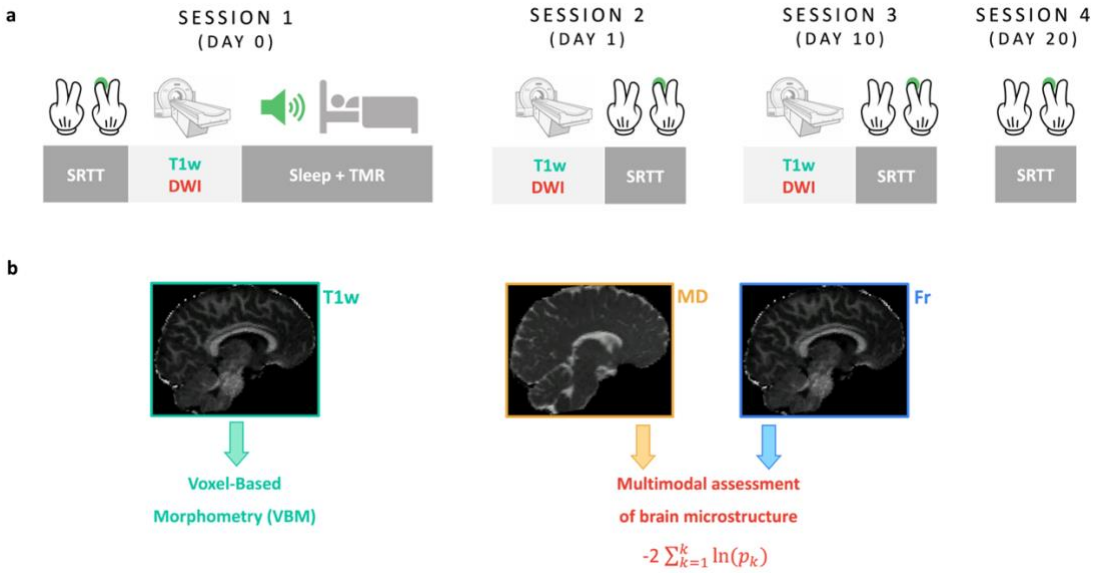

Fig. 1. Experimental methods. (a) *Study design. The study consisted of four sessions, each requiring participants to complete the SRTT. During S1, SRTT was followed by DW-MRI acquisition. During S2 (24 h post-TMR) and S3 (10 days post-TMR), the order was flipped, with the SRTT following MRI data collection. Structural T1w data was acquired at the beginning of each scan (S1-S3). S1 also involved EEG recording during the stimulation night. While asleep, tones associated with one of the sequences were replayed to the participants during stable N2 and N3. During S4 (20 days post-TMR) SRTT was delivered outside the scanner. (**b**) MRI data analysis. Voxel-based morphometry (VBM) analysis was performed on the T1w scans to study volumetric grey matter structure. MD and Fr maps were extracted from the DW-MRI data and combined in a multimodal approach to uncover common trends related to microstructural plasticity of grey matter. Multimodal analysis was followed by unimodal post-hoc tests to determine the contribution of each modality to the multimodal results (not shown). SRTT: Serial Reaction Time Task; T1w, T1-weighted data; DW-MRI: Diffusion Weighted MRI; MD: Mean Diffusivity; Fr: Restricted Water Fraction.*

2.3 EXPERIMENTAL TASKS – THE SERIAL REACTION TIME TASK (SRTT)

The SRTT was used to induce and measure motor sequence learning. It was adapted from Cousins et al. (2014a) and implemented exactly as described in Chapter 3. Briefly, participants learned two 12-item sequences of auditorily and visually cued key presses. The task was to respond to the stimuli as quickly and accurately as possible, using index and middle fingers of both hands. The two sequences – A (1-2-1-4-2-3-4-1-3-2-4-3) and B (2-4-3-2-3-1-4-2-3-1-4-1) – were matched for learning difficulty, did not share strings of more than four items and contained items that were equally represented (three repetitions of each). Each sequence was paired with a set of 200 ms-long tones, either high (5^{th} octave, A/B/C#/D) or low (4^{th} octave, C/D/E/F) pitched, that were counterbalanced across sequences and participants. For each item/trial, the tone was played with simultaneous presentation of a visual cue in one of the four corners of the screen. Visual cues consisted of neutral faces and objects, appearing in the same location regardless of the sequences (1 – top left corner = male face, 2 – bottom left corner = lamp, 3 – top right corner = female face, 4 – bottom right corner = water tap). Participants were told that the nature of the stimuli (faces/objects) was not relevant for the study. Their task was to press the key on the keyboard (while in the sleep lab or at home) or on an MRI-compatible button pad (2-Hand system, NAtA technologies, Coquitlam, Canada) (while in the MRI/mock scanner) that corresponded to the position of the picture as quickly and accurately as possible: 1 = left shift/left middle finger button; 2 = left Ctrl/left index finger button; 3 = up arrow/right middle finger button; 4 = down arrow/right index finger button. Participants were instructed to use both hands and always keep the same fingers on the appropriate response keys. The visual cue disappeared from the screen only after the correct key was pressed, followed by a 300 ms interval before the next trial.

There were 24 blocks of each sequence (a total of 48 sequence blocks per session), where block type was indicated with ‘A’ or ‘B’ displayed in the centre of the screen. Each block contained three sequence repetitions (36 items) and was followed by a 15 s pause/break, with reaction time (RT) and error rate feedback. Blocks were interleaved pseudo-randomly with no more than two blocks of the same sequence in a row. Participants were aware that there were two sequences but were not asked to learn them explicitly. Block order and sequence replayed were counterbalanced across participants.

During each run of the SRTT, sequence blocks A and B were followed by 4 random blocks, except for the first half of S1 (to avoid interrupted learning). Random blocks were indicated with 'R' appearing centrally on the screen and contained pseudo-randomised sequences, the same visual stimuli, and tones matching sequence A for half of them (Rand_A) and sequence B for the other half (Rand_B). Blocks Rand_A and Rand_B were interleaved, and the random sequences contained within them followed three constraints: (1) each cue was represented equally within a string of 12 items, (2) two consecutive trials could not contain the same cue, (3) random sequence did not share a string of more than four items with either sequence A or B.

2.4 EEG DATA ACQUISITION

EEG was recorded using 64 actiCap slim active electrodes (Brain Products GmbH, Gilching, Germany), with 62 electrodes embedded within an elastic cap (Easycap GmbH, Herrsching, Germany). This included the reference positioned at CPz and ground at AFz. The remaining electrodes were the left and right electrooculography (EOG) electrodes (placed below and above each eye, respectively), and left and right electromyography (EMG) electrodes (placed on the chin). Fig.S2 shows the EEG electrodes layout. Elefix EEG-electrode paste (Nihon Kohden, Tokyo, Japan) was used for stable electrode attachment and Super-Visc high viscosity electrolyte gel (Easycap GmbH) was inserted into each electrode to reduce impedance below 25 kOhm. To amplify the signal, we used either two BrainAmp MR plus EEG amplifiers or a LiveAmp wireless amplifier (all from Brain Products GmbH). Signals were recorded using BrainVision Recorder software (Brain Products GmbH).

2.5 TMR DURING NREM SLEEP

Tones associated with one of the learned sequences (A or B, counterbalanced across participants) were replayed to the participants during N2 and N3, as assessed with standard AASM criteria (Berry et al., 2015). Volume was adjusted for each participant to make sure that the sounds did not wake them up. One repetition of a sequence was followed by a 20 s break, with the inter-trial interval jittered between 2500 and 3500 ms. Upon arousal or leaving the relevant sleep stage, replay was paused immediately and resumed only when stable N2/N3 was apparent. The TMR protocol was delivered using MATLAB 2016b and Cogent 2000 and performed for as long as a minimum threshold of ~1000 trials in N3 was reached. On average, 1552.91 ± 215.00 sounds were delivered.

2.6 MRI DATA ACQUISITION

Magnetic resonance imaging (MRI) was performed at Cardiff University Brain Imaging Centre (CUBRIC) with a 3T Siemens Connectom scanner (maximum gradient strength 300 mT/m). All scans were acquired with a 32-channel head-coil and lasted ~1 h in total each, with whole-brain coverage including cerebellum. This chapter is concerned with the analysis of the multi-shell DW-MRI and T1w scans, but the MRI protocol also included functional MRI (fMRI) and mcDESPOT acquisitions (for fMRI analysis see Chapter 3).

2.6.1 T1-WEIGHTED IMAGING

A high resolution T1-weighted anatomical scan was acquired with a 3D magnetization-prepared rapid gradient echoes (MPRAGE) sequence (repetition time [TR] = 2300 ms; echo time [TE] = 2 ms; inversion time [TI] = 857 ms; flip angle [FA] = 9°; bandwidth 230 Hz/Pixel; 256 mm field-of-view [FOV], 256 x 256 voxel matrix size, 1 mm isotropic voxel size; 1 mm slice thickness; 192 sagittal slices; parallel acquisition technique [PAT] with in-plane acceleration factor 2 (GRAPPA); anterior-to-posterior phase-encoding direction; 5 min total acquisition time [AT]) at the beginning of each scanning session.

2.6.2 MULTI-SHELL DIFFUSION-WEIGHTED IMAGING

Diffusion-Weighted MRI data was acquired with a monopolar sequence (TR = 3000 ms; TE = 59 ms; FA = 90°; 266 gradient directions distributed over 6 shells (b = 200, 500, 1200, 2400, 4000, 6000 s/mm^2); 13 interspersed b = 0 images; bandwidth 2272 Hz/Pixel; 220 mm FOV; 220 x 200 voxel matrix size; 2 mm isotropic voxel size; 2 mm slice thickness; 66 axial-to-coronal slices obtained parallel to the AC–PC line with interleaved slice acquisition; PAT 2 (GRAPPA); multi-band acceleration factor = 2; AT = 14 min) in an anterior-to-posterior phase-encoding direction, with one additional b = 0 posterior-to-anterior volume.

2.7 DATA ANALYSIS

2.7.1 BEHAVIOURAL DATA

PSQI global scores were determined in accordance with the original scoring system (Buysse et al., 1989) and the SRTT analysis was performed as in Chapter 3. Briefly, the SRTT performance was measured using mean reaction time per block of each sequence (cued and

uncued). All trials within each block were considered (i.e., trials performed by both hands), except for those with reaction time exceeding 1000 ms. For each sequence during each session, the mean performance on the last 4 blocks was subtracted from the mean performance on the 2 random blocks, thus yielding a measure of late 'sequence-specific skill' (SSS). We chose to focus on late SSS rather than early SSS given our prior results showing a main effect of TMR on the former only (see Chapter 2 and Chapter 3).

To obtain a single measure reflecting the effect of TMR on SRTT performance at each session we calculated the difference between the late SSS of the cued and uncued sequence and refer to it as the 'cueing benefit'. Cueing benefit at S2, S3, and S4 were entered as the main regressors in the analysis testing the relationship between microstructural plasticity and cueing benefit at different sessions (see section *2.7.4.2 DW-MRI: multimodal analysis of TMR-related plasticity).*

Finally, to obtain a single measure reflecting an overall susceptibility to the manipulation, we performed Principal Component Analysis (PCA) on the cueing benefit at S2, S3 and S4 (i.e., the three post-TMR sessions). This yielded a PCA-transformed cueing benefit, derived from the first PCA component and referred to as the 'TMR susceptibility'. TMR susceptibility was entered as the main regressor in the analysis testing the relationship between inter-individual variability in brain (micro)structure and susceptibility to the manipulation (see section *2.7.4.4 DW-MRI and VBM: Individual differences in baseline (micro)structure).*

2.7.2 SLEEP SCORING

EEG data collected during the night were pre-processed and sleep scored as described in Chapter 3. In short, the pre-processing and re-referencing steps were carried out in MATLAB 2018b, using FieldTrip Toolbox (Oostenveld et al., 2011). Sleep scoring was conducted on eight scalp electrodes (F3, F4, C3, C4, P3, P4, O1, O2), two EOG and two EMG channels. Each recording was scored based on the AASM criteria (Berry et al., 2015) and using a custom-made interface (https://github.com/mnavarretem/psgScore). The amount of time spent in each sleep stage were used as the main regressors in the analyses testing the relationship between overnight brain plasticity and different sleep stages (see section *2.7.4.3 DW-MRI and VBM: Sleep-related changes).*

2.7.3 MRI DATA

2.7.3.1 DW-MRI DATA PRE-PROCESSING

DW-MRI data pre-processing was performed as described in previous publications (Tax et al., 2021; Genc et al., 2020). The pre-processing steps included (1) Slicewise OutLIer Detection (SOLID) (Sairanen et al., 2018); (2) full Fourier Gibbs ringing correction (Kellner et al., 2016) using Mrtrix mrdegibbs software (Tournier et al., 2012); and (3) a combined topup, eddy and DISCO step (Rudrapatna et al., 2018) to (i) estimate susceptibility-induced off-resonance field and correct for the resulting distortions using images with reversed phase-encoding directions, (ii) correct for eddy current distortions and (iii) correct for gradient nonlinearity. To generate Mean Diffusivity (MD) maps, the diffusion tensor model was fitted to the data using the DTIFIT command in FSL for shells with $b < 1500$ s/mm^2. To estimate Restricted Water Fraction (Fr) metric, the composite hindered and restricted model of diffusion (CHARMED) was fitted to the data using an in-house non-linear least square fitting algorithm (De Santis et al., 2014) coded in MATLAB 2015a. The two indices (MD, Fr) were chosen based on the existing human literature on the microstructural changes following learning (MD: Brodt et al., 2018; Hofstetter et al., 2013; Sagi et al., 2012; Tavor et al., 2019; Fr: Tavor et al., 2013). MD describes the average mobility of water molecules and has shown sensitivity to changes in grey matter (Brodt et al., 2018; Sagi et al., 2012; Tavor et al., 2019). It is thought to reflect the underlying, learning-dependent remodelling of neurons and glia, i.e., synaptogenesis, astrocytes activation and brain-derived neurotrophic factor (BDNF) expression, as confirmed by histological findings (Sagi et al., 2012), which were of particular interest in this study. As opposed to DTI, the CHARMED model separates the contribution of water diffusion from the extra-axonal (hindered) and intra-axonal (restricted) space (Assaf et al., 2004), thereby providing a more sensitive method to look at the microstructural changes than DTI (Tavor et al., 2013). Fr is one of the outputs from the CHARMED framework. In grey matter, Fr changes are thought to reflect remodelling of dendrites and glia, and were observed both short-term (2 h) and long-term (1 week) following a spatial navigation task (Tavor et al., 2013).

Co-registration, spatial normalisation and smoothing of the MD and Fr maps were performed in SPM12, running under MATLAB 2015a. First, we co-registered the pre-processed diffusion images with participants' structural images using a rigid body model. The co-registration output was then spatially normalised to MNI space. This step involved resampling to 2 mm

voxel with B-spline interpolation and utilised T1 deformation fields generated during fMRI analysis of the same participants (Chapter 3). That way, the resulting diffusion images were in the same space as the fMRI and T1w data. Finally, the normalised data was smoothed with an 8 mm FWHM Gaussian kernel.

2.7.3.2 T1W DATA PRE-PROCESSING

Pre-processing of T1w images was performed as in Chapter 3, using Statistical Parametric Mapping 12 (SPM12; Wellcome Trust Centre for Neuroimaging, London, UK), running under MATLAB 2018b. All pre-processing steps were carried out in keeping with previous recommendations (Ashburner, 2010). Briefly, the images were segmented into three tissue probability maps (grey matter, GM; white matter, WM; cerebrospinal fluid, CSF). We used two Gaussians to model each tissue class, 60 mm bias full-width half maximum (FWHM) cut-off, very light bias regularisation (0.0001), and default warping parameters (Ashburner & Friston, 2005). Spatial normalisation of GM tissue was performed using DARTEL (Ashburner, 2007) to generate spatially normalised and Jacobian scaled images in the Montreal Neurological Institute (MNI) space, resampled at 1.5 mm isotropic voxels. An 8 mm FWHM Gaussian kernel was used to smooth the resultant images, in line with the DW-MRI data. Finally, to account for any confounding effects of brain size, each image was proportionally scaled to the total intracranial volume (ICV) value, calculated by summing up the volumes of the three tissue probability maps obtained earlier (GM, WM, CSF).

2.7.4 STATISTICAL ANALYSIS

All behavioural tests conducted were two-tailed, and both positive and negative contrasts were performed for the MRI analyses. MRI results were voxel-level corrected for multiple comparisons by family wise error (FWE) correction for the whole-brain GM and for the pre-defined anatomical regions of interest (ROI, see section *2.7.4.6 Regions of Interest*), with the significance threshold set at $p_{FWE} < 0.05$. To obtain a whole-brain GM mask, the SPM12 tissue probability map of GM was thresholded at 50% probability (Ceccarelli et al., 2012).

2.7.4.1 BEHAVIOURAL DATA

Statistical analyses of behavioural data were conducted in the previous chapter (Chapter 3). We used lme4 package (Bates et al., 2015) in R to fit two linear mixed effects models to our data. The first model (model 1) was used to test the effect of TMR (cued vs uncued) and

Session (S2, S3, S4) on the late SSS. The second model (model 2) was used to test the effect of Time (i.e., number of days post-TMR) on cueing benefit. To account for the repeated measures design, participant code was always entered as a random intercept.

> model 1 = lmer(late SSS ~ Session + TMR + (1|Participant), data=dataset)

> model 2 = lmer(CueingBenefit ~ Time + (1|Participant), data=dataset)

An ANOVA function in R was used to run likelihood ratio tests between the full model and the model without the effect of interest. This allowed us to obtain a p-value for each effect tested. Emmeans package (Lenth et al., 2019) was used to conduct Holm-adjusted post-hoc pairwise comparisons. The results of both the likelihood ratio tests and post-hoc comparisons are cited in this chapter and discussed in relation to the underlying tissue (micro)structure.

2.7.4.2 DW-MRI: MULTIMODAL ANALYSIS OF TMR-RELATED PLASTICITY

Group level analyses of DW-MRI data was performed in FSL (FMRIB's Software Library, http://www.fmrib.ox.ac.uk/fsl) (Smith et al., 2004b). To examine the relationship between brain characteristics and our variables of interest we performed non-parametric combination (NPC) for joint interference analysis (Fig.1b), as described before (Lazari et al., 2021; Sampaio-Baptista et al., 2020). Specifically, NPC was performed over MD and Fr maps to uncover common trends related to non-myelin GM microstructure (Tavor et al., 2013; Sagi et al., 2012).

The analysis was performed through Permutation Analysis of Linear Models (PALM) in FSL (Winkler et al., 2016), using voxel-wise Fisher test with the following equation:

$$-2 \sum_{k=1}^{k} \ln(p_k)$$

where k denotes the total number of modalities being combined, and p_k denotes the p-value for a given modality (Winkler et al., 2016).

NPC Fisher's combining function tests for effects with concordant directions across modalities of choice. Thus, to test for positive effects across our modalities, imaging data with mismatching directions (here MD) were multiplied by (-1). The significance of the resulting, single joint statistic was assessed through 5000 permutations of each of the separate tests and a cluster-forming threshold of $t > 1.75$ (equivalent to $p < 0.05$, based on

the degrees of freedom for the smallest sample) at 5% FWE rate. Correction for multiple comparisons was carried out both for the whole brain GM and for the pre-defined ROIs.

Having previously established that TMR can impact on GM volume (Chapter 3), here we investigated the relationship between early (S1 vs S2) and late (S2 vs S3) microstructural plasticity and cueing benefit at different time points. To this end, the images used to assess the longitudinal effects of time were generated by subtracting the pre-processed MD and Fr parameter maps from consecutive sessions. The resultant images were entered into a one-sample t-test with cueing benefit at S2, S3, and S4 added as regressors. We run separate contrasts for each session, whereby the session of interest was specified as the main regressor whereas the remaining sessions were treated as the covariates of no interest (nuisance covariates). This ensured that the results were specific to the session analysed. Additionally, the nuisance covariates also included sex and age to control for the differences between males and females, as well as the effect of age. Baseline reaction time (i.e., average reaction time on the random blocks performed during S1) and baseline learning capabilities (i.e., difference between the average of the last 4 blocks and the first 4 blocks performed during S1) were also specified as the variables of no interest to ensure that the results were independent of baseline SRTT performance.

2.7.4.3 DW-MRI AND VBM: SLEEP-RELATED CHANGES

Next, we tested the relationship between overnight (S1 vs S2) (micro)structural plasticity and sleep. To this end, we performed both the multimodal analysis of the DW-MRI data (see previous section *2.7.4.2*) and voxel-based morphometry (VBM) of the T1w data (performed in SPM12 as in Chapter 3). The MD, Fr and GM maps from S1 and S2 were subtracted from each other, and the resultant images were entered into one-sample t-tests with the percentage of time spent in N2, N3, and REM sleep added as regressors. We ran separate contrasts for each sleep stage, whereby the sleep stage of interest was specified as the main regressor whereas the remaining sessions were treated as nuisance covariates to ensure that the results were specific only to the sleep stage tested. Nuisance covariates also included sex and age.

2.7.4.4 DW-MRI AND VBM: INDIVIDUAL DIFFERENCES IN BASELINE (MICRO)STRUCTURE

To determine whether individual differences in baseline brain characteristics can predict susceptibility to the manipulation we tested the relationship between baseline (S1) GM (micro)structure and the variance shared between cueing benefit at the post-TMR sessions. Thus, the PCA-transformed cueing benefit, here referred to as the 'TMR susceptibility' was entered as a covariate of interest in a one-sample t-test, either in the multimodal (MD and Fr maps) or VBM (T1w images) framework. The nuisance covariates for this analysis included: sex, age, PSQI, baseline reaction time, baseline learning capabilities, and percentage of time spent in N2 (given the results described in section *3.2 Sleep-related changes*). This approach ensured that the results were independent of demographics, general sleep patterns and baseline SRTT performance, all of which could be related to baseline characteristics of the brain.

2.7.4.5 DW-MRI: UNIMODAL ANALYSIS

To determine individual contribution of each microstructural modality to the multimodal results, we performed unimodal analyses of individual modalities, in FSL and through non-parametric, permutation-based voxel-wise comparisons using *randomise* function (Winkler et al., 2014). Results were derived from 5000 permutations. Correction for multiple comparisons was carried out by FWE correction both for the whole brain GM and for the pre-defined ROIs, as for the multimodal analysis. Multiple modalities correction was performed based on the number of modalities entered in the multimodal analysis (here two: MD and Fr).

2.7.4.6 REGIONS OF INTEREST

All MRI results were voxel-level corrected for multiple comparisons within the whole-brain GM and the pre-defined anatomical ROIs. We used the same pre-defined ROIs as in Chapter 3. These included (1) bilateral precuneus, (2) bilateral hippocampus and parahippocampus, (3) bilateral dorsal striatum (putamen and caudate), (4) bilateral cerebellum, (5) bilateral sensorimotor cortex (precentral and postcentral gyri). All ROIs were selected based on their known involvement in sleep-dependent procedural memory consolidation (Fischer et al., 2005; Walker et al., 2005; Albouy et al., 2008; Debas et al., 2010) and memory reactivation (Maquet et al., 2000; Maquet et al., 2003b; Rasch et al., 2007; van Dongen et al., 2012; Brodt et al., 2018; Cousins et al., 2016). A mask for each ROI was created using an Automated

Anatomical Labeling (AAL) atlas in the Wake Forest University (WFU) PickAtlas toolbox (Maldjian et al., 2003).

2.8 RESULTS PRESENTATION

Anatomical localisation of the significant clusters from both unimodal and multimodal analyses was determined with the automatic labelling of MRIcroGL (https://www.nitrc.org/projects/mricrogl/) based on the AAL atlas. Results in Fig.3-6 and Fig.S3-S4 are presented using MRIcroGL, displayed on the MNI152 standard brain (University of South Carolina, Columbia, SC). All significant clusters are reported in supplementary tables, but only those with an extent equal to or above 5 voxels are discussed in text and presented in figures. Fig.1, Fig.S1 and Fig.S2 were created in Microsoft PowerPoint v16.53, Fig.2a was generated using *ggplot2* (version 3.3.0) (Wickham, 2009) in R, Fig.2b was generated using Prism 9 (GraphPad Software, San Diego, CA, USA), and Fig.2c was generated using *corrplot* command in MATLAB.

3 RESULTS

Post-sleep SRTT re-test sessions took place 24.67 hours (SD: 0.70) (S2), 10.48 days (SD: 0.92) (S3), and 20.08 days (SD: 0.97) (S4) after S1. As we have reported previously (Chapter 3), analysis of behavioural data showed a main effect of TMR on the late sequence specific skill of the SRTT ($p = 0.001$), with the difference between the cued and uncued sequence strongest at S4, i.e., 20 days post-TMR ($p_{adj} = 0.004$, Fig.2a). Furthermore, there was a main effect of the amount of time post-TMR on cueing benefit ($p = 0.046$, Fig.2a), suggesting that the effects of our manipulation develop over time before they emerge at S4 (Chapter 3).

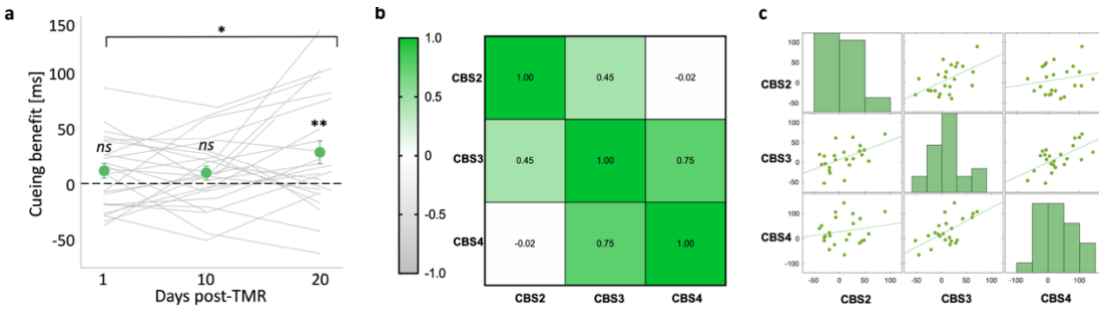

Fig. 2. Behavioural effects of TMR. (a) *Difference between the late sequence specific skill of the cued and uncued sequence (i.e., the cueing benefit) plotted against the number of days post-TMR. Green dots represent mean ± SEM calculated for S2 (1 day post-TMR), S3 (10–14 days post-TMR) and S4 (16–21 days post-TMR). Grey lines represent cueing benefit for each subject. A linear mixed effects analysis showed a main effect of time on cueing benefit,*

*which itself was significant at S4. * $p < 0.05$; ** $p_{adj} = 0.004$.* ***(b)*** *Heatmap of Pearson's correlation coefficient matrix showing the relationships between cueing benefit (CB) at different sessions.* ***(c)*** *Scatterplots showing the same correlations as in (b). CBS2, CBS3, CBS4: cueing benefit at S2, S3, S4; S1-4: Session 1-4; For (a): n = 30 for S2, n = 25 for S3; n = 24 for S4. For (b-c): n = 23.*

3.1 TMR-RELATED PLASTICITY

We sought to examine whether repeated reactivation of a motor memory trace could engender microstructural plasticity in the brain. We tested whether cueing benefit at different sessions is associated with changes in brain microstructure within predefined ROIs over different periods of time. Thus, individual modality maps collected at different sessions were subtracted from each other, yielding measures of early (S1-S2) and late (S2-S3) microstructural plasticity. The resultant difference maps were used as inputs in the multimodal analysis, set out to uncover common trends in MD and Fr change measures. Cueing benefit at S2, S3 and S4 were entered as regressors and separate contrasts were run for cueing benefit at each session. Given the correlations between cueing benefits at different sessions (Fig.2b-c), sessions of no interest in any given contrast were covaried out to test if the effects are specific to the cueing benefit tested. We hypothesised that TMR during sleep would lead to rapid plasticity within precuneus. Consistent with this, the analysis revealed a positive relationship between early plasticity in left precuneus (-6, -60, 18) and cueing benefit at S3 when controlling for the behavioural effects at S2 and S4 ($p = 0.041$; Fig.3a-c, Table S1A, Fig.S3a), such that greater cueing benefit was associated with greater reductions in MD and greater increases in Fr. In addition, late plasticity in bilateral precuneus (4, -58, 16) was associated with cueing benefit at S4 when controlling for the behavioural effects at S2 and S3 ($p = 0.027$; Fig.3d-f, Table S1B, Fig.S3b), again reflecting greater cueing benefit being associated with greater reductions in MD and greater increases in Fr. These results demonstrate that TMR can impact on precuneus microstructure both early and late in the consolidation process, thus supporting the development of behavioural effects of TMR over time.

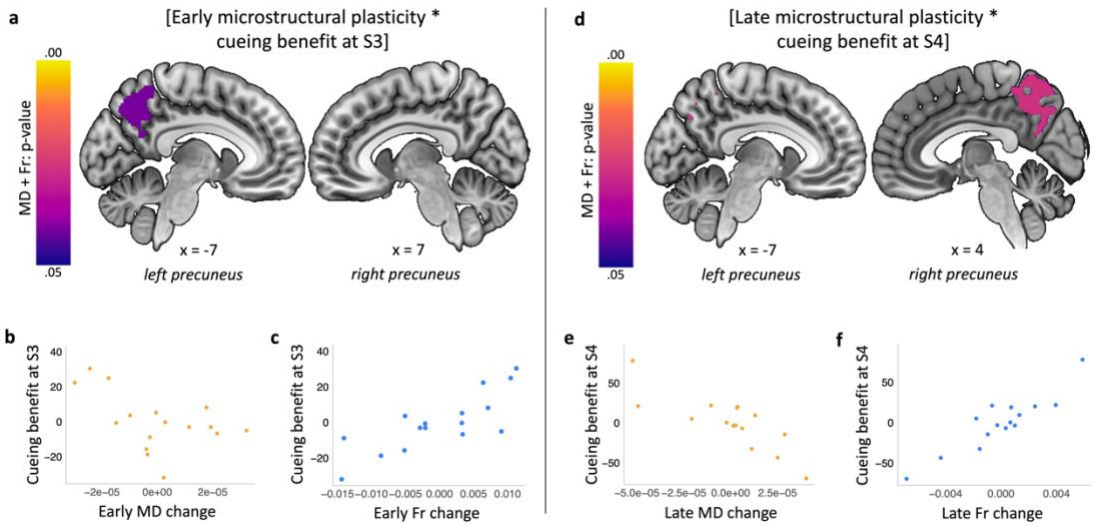

Fig. 3. Multimodal plasticity in precuneus is associated with long-term cueing benefits. (a) *Early (from S1 to S2) microstructural plasticity in left precuneus is associated with cueing benefit at S3.* ***(d)*** *Late (from S2 to S3) microstructural plasticity in bilateral precuneus is associated with cueing benefit at S4. Purple-yellow colour bars indicate p-values for the results thresholded at a significance level of $p_{FWE} < 0.05$, corrected for multiple voxel-wise comparisons within pre-defined ROI for bilateral precuneus. Results are overlaid on a Montreal Neurological Institute (MNI) brain. (**b, c, e, f**) Mean MD (b, e) and Fr (c, f) change values extracted from multimodal clusters significant at $p_{FWE} < 0.05$ shown in (a) and (d). Scatterplots are presented for visualisation purposes only and should not be used for statistical inference. Each data point represents a single participant, axes represent residual values after correcting for age, sex, PSQI score, baseline reaction time, baseline learning capabilities on the SRTT, cueing benefit at S2 and either cueing benefit at S4 (b-c) or at S3 (e-f). MD: Mean Diffusivity; Fr: Restricted Water Fraction; S1-4: Session 1-4; n = 16 for (a-c), n = 15 for (d-f).*

We further hypothesised that task-related sensorimotor regions would undergo longer-term microstructural changes. Our multimodal voxel-wise ROI analyses revealed that both early plasticity in right putamen (34, -6, -8) and late plasticity in left sensorimotor cortex (-60, -18, 14) were associated with cueing benefit at S4 when controlling for the behavioural effects at S2 and S3 (putamen: p = 0.016; Fig.4a-c, Table S1C, Fig.S3c; sensorimotor cortex: p = 0.018; Fig.4d-f, Table S1D, Fig.S3d). To confirm that the results were specific to S4, we also tested the relationship between microstructural plasticity and cueing benefit at S2 and S3. In line with our expectations, we find no relationship between motor network plasticity and cueing benefit at S2 or S3 (p > 0.05).

Together, we provide evidence for gradual plasticity in the microstructure of precuneus, striatum and sensorimotor cortex that underpins long-term behavioural effects of TMR. Interestingly, both the early and late plasticity results for motor ROIs seem to be specifically related to S4, the time point at which the behavioural impact of TMR emerged.

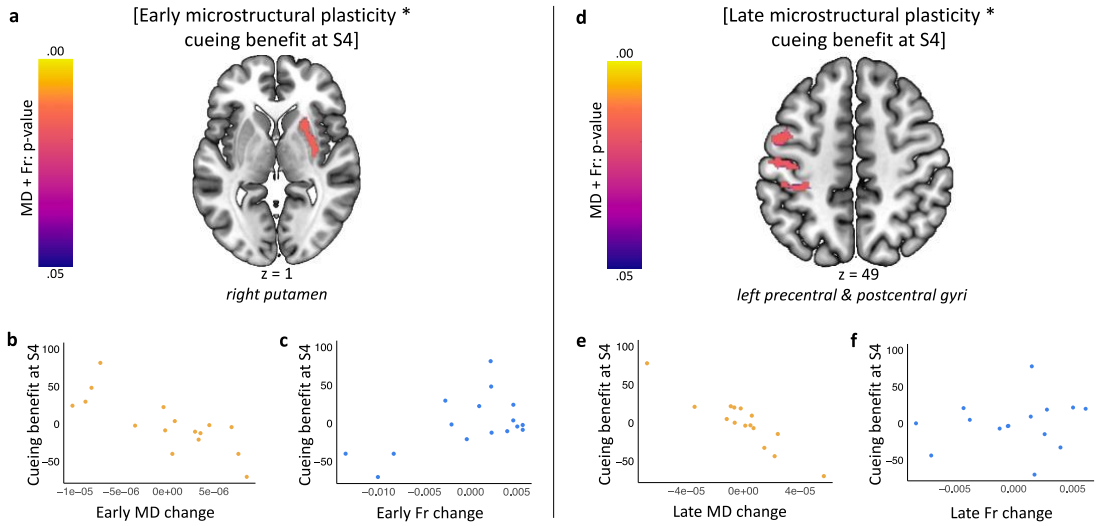

Fig. 4. Multimodal plasticity within task-related structures is associated with long-term cueing benefits. ***(a)*** *Early (from S1 to S2) microstructural plasticity in right putamen correlates with cueing benefit at S4.* ***(d)*** *Late (from S2 to S3) microstructural plasticity in left sensorimotor cortex correlates with cueing benefit at S4. Purple-yellow colour bars indicate p-values for the results thresholded at a significance level of $p_{FWE} < 0.05$, corrected for multiple voxel-wise comparisons within pre-defined bilateral ROI for putamen (a) and sensorimotor cortex (d). Results are overlaid on a Montreal Neurological Institute (MNI) brain. (**b, c, e, f**) Mean MD (b, e) and Fr (c, f) change extracted from multimodal clusters significant at $p_{FWE} < 0.05$ shown in (a) and (d). Scatterplots are presented for visualisation purposes only and should not be used for statistical inference. Each data point represents a single participant, axes represent residual values after correcting for age, sex, PSQI score, baseline reaction time, baseline learning capabilities on the SRTT, and cueing benefit at S2 and S3. MD: Mean Diffusivity; Fr: Restricted Water Fraction; S1-4: Session 1-4; n = 16 for (a-c), n = 15 for (d-f).*

3.2 SLEEP-RELATED CHANGES

Prior work has shown that the time spent in different sleep stages is associated with distinct TMR-related changes in task-related functional activity (Cousins et al., 2016). Here we were interested in determining whether the time spent in N2, N3 or REM could also be associated with overnight changes in GM (micro)structure. First, we performed voxel-based morphometry (VBM) of the T1w scans, as described in Chapter 3. Then, we carried out one-way t-tests on the subtraction images between pre-sleep (S1) and post-sleep (S2) data, with the percentage of time spent in N2, N3, and REM added as regressors in separate comparisons. Our analysis showed that the time spent in N2 correlates negatively with an overnight change in left parahippocampal (-16, -33, -14) GM volume ([Δ GM volume from S1 to S2 * N2]; peak T = 5.70, p = 0.018; Fig.5a-b, Table S2A). This finding is specific to N2, and we report no significant clusters associated with any of the other sleep regressors (p > 0.05).

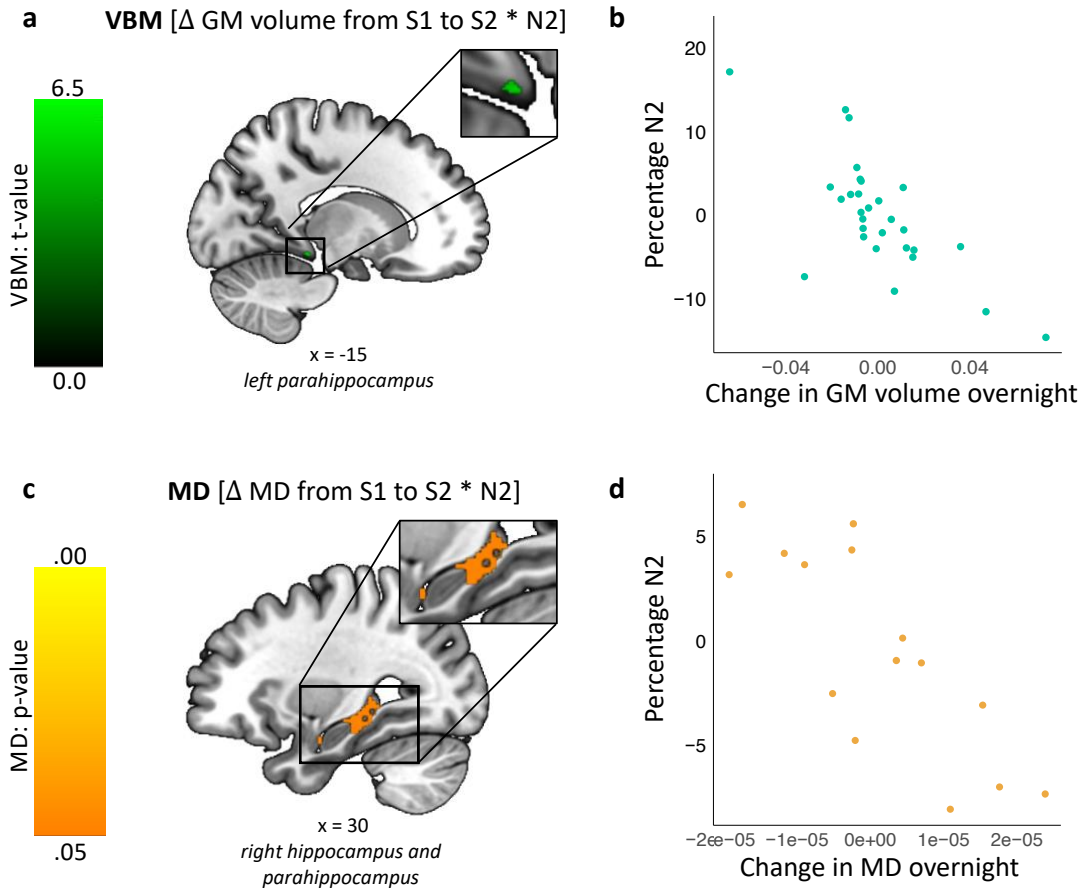

Fig. 5. Relative amount of N2 is negatively associated with an overnight change in (para)hippocampal grey matter volume and mean diffusivity. ***(a)*** *Results of VBM. Green colour bar indicates t-values for the results thresholded at a significance level of* $p_{FWE} < 0.05$*, ROI corrected for bilateral hippocampus and parahippocampus.* ***(c)*** *Results of a unimodal, group level analysis conducted on the DW-MRI data. Orange-yellow colour bar indicates p-values for the results thresholded at a significance level of* $p_{FWE} < 0.05$*, ROI corrected for bilateral hippocampus and parahippocampus. Results shown in (a) and (c) are overlaid on a Montreal Neurological Institute (MNI) brain.* ***(b, d)*** *Mean GM volume (b) and MD (d) change extracted from the clusters significant at* $p_{FWE} < 0.05$ *shown in (a) and (c). Scatterplots are presented for visualisation purposes only and should not be used for statistical inference. Each data point represents a single participant, axes represent residual values after correcting for age, sex, percentage N3, and percentage REM. GM: grey matter; MD: Mean Diffusivity; VBM: voxel-based morphometry; S1-2: Session 1-2; N2: percentage of time spent in stage 2 of NREM sleep. n = 29 for (a-b), n = 16 for (c-d).*

Next, we looked at the relationship between sleep parameters and overnight change in brain microstructure. MD and Fr maps estimated at S1 and S2 were subtracted from each other, and the resultant maps were used as inputs in separate multimodal analyses as before (section *3.1 TMR-related plasticity*), but with sleep parameters entered as main regressors. The analysis revealed no significant findings (Table S2Ci, $p > 0.05$), suggesting that the amount of time spent in any of these three sleep stages is not associated with microstructural plasticity, as measured by our combined measure of MD and Fr. Changes in both MD and Fr are thought to reflect learning-dependent remodelling of synaptic and glial processes (Tavor

et al., 2013; Sagi et al., 2012) which were of particular interest in this study. However, MD describes the average mobility of water molecules within a given voxel (Maffei et al., 2015), whereas Fr reflects the volume fraction occupied by intra-axonal (restricted) water only (Assaf et al., 2004). Hence, we aimed to probe whether the relationship between sleep and microstructure could be uniquely associated with only one of the markers, rather than their combination. Thus, we performed unimodal analyses testing the same contrasts and covariates as before, but for MD and Fr separately. This showed a negative relationship between the percentage of time spent in N2 and an overnight change in right hippocampal and parahippocampal (36, -8, -26) microstructure measured by MD (peak T = 5.28, p = 0.045; Fig.5c-d, Table S2Cii) when controlling for the effect of other sleep stages. There were no significant clusters associated with Fr (Table S2Ciii), nor do we find any microstructural changes associated with the time spent in N3 or REM ($p > 0.05$).

Together, our results suggest that both an overnight change in GM volume and an overnight change in MD of (para)hippocampus are associated with the percentage of time spent in N2. Given these findings, we sought to determine if N2 could have contributed to our TMR-related results. Thus, we re-run the multimodal analyses as in section *3.1* but with the percentage of time spent in N2 covaried out. The analyses revealed similar findings as before (Table S3). Specifically, we report a relationship between early microstructural plasticity in left precuneus (-8, -58, 18) and cueing benefit at S3 (p = 0.030; Table S3A). Cueing benefit at S4 was associated with late plasticity in bilateral precuneus (6, -54, 14; p = 0.034; Table S3B), right putamen (34, -8, -6; p = 0.021; Table S3C), and left sensorimotor cortex (-62, -16, 14; p = 0.026; Table S3D). These results suggest that the TMR-related plasticity that we report in section *3.1* is independent of the relative amount of time spent in N2.

3.3 INDIVIDUAL DIFFERENCES IN BASELINE MICROSTRUCTURE

A wide variety of factors are known to influence TMR's success (Hu et al., 2020). Here we aimed to determine if inter-individual variability in brain (micro)structure could confer susceptibility to the manipulation. To this end, we were not interested in the TMR effect at any particular session, but rather in the common variance of the cueing benefit shared across the post-stimulation sessions (Fig.2b-c). Thus, we performed a PCA on the cueing benefit at S2, S3 and S4 in order to obtain a single measure which we will call 'TMR susceptibility'. Our VBM analysis of the T1w scans collected at S1 showed no relationship between TMR susceptibility and baseline GM volume ($p > 0.05$).

Next, we carried out analysis of baseline microstructure and TMR susceptibility using our multimodal measure. We used baseline (S1) maps of MD and Fr as inputs, with TMR susceptibility entered as the main regressor. This showed a relationship between baseline microstructure in right precentral and postcentral gyrus (58, -6, 20) and TMR susceptibility ($p = 0.041$; Fig.6a-c, Table S4; Fig.S4), such that individuals with greater response to TMR had less MD and more Fr at baseline. This finding suggests that the individual variation in sensorimotor microstructure could predict susceptibility to TMR of procedural memory. Importantly, this finding is independent of participants' demographics (sex, age), general sleep patterns (as measured by the PSQI score), time spent in N2, baseline reaction time and learning capabilities on the SRTT, all of which were controlled for in the analysis.

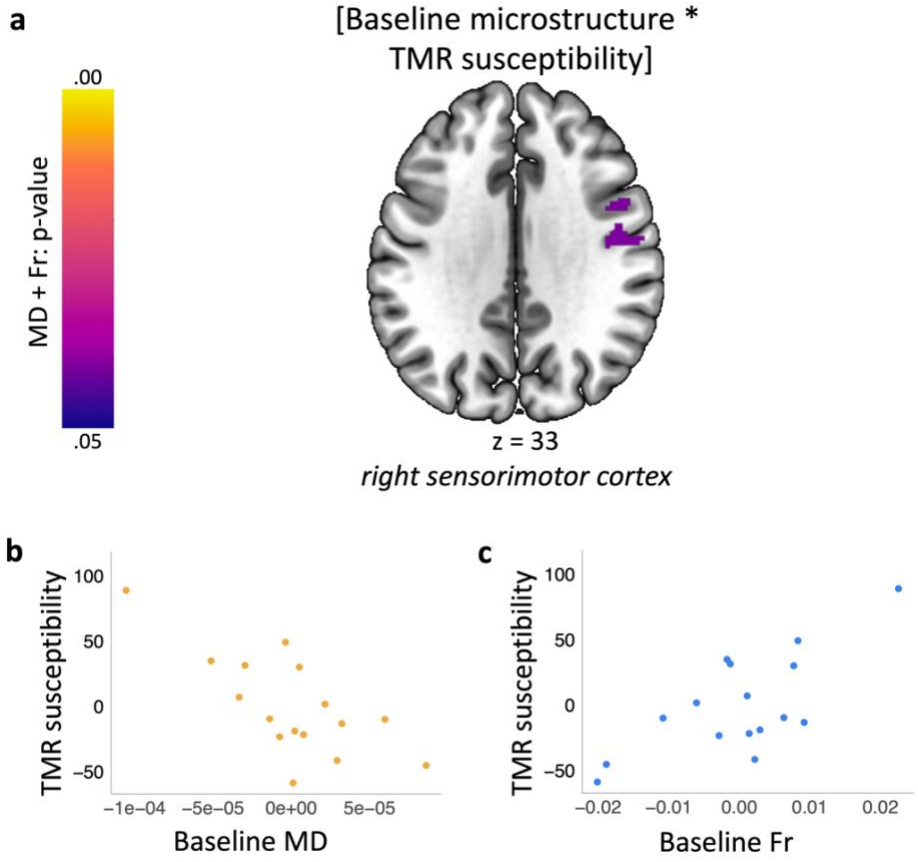

Fig. 6. TMR susceptibility is associated with baseline sensorimotor microstructure. (a) *Results of the multimodal analysis testing the relationship between TMR susceptibility and baseline microstructure. Colour bars indicate p-values for the results thresholded at a significance level of $p_{FWE} < 0.05$ (red), corrected for multiple voxel-wise comparisons within pre-defined ROI for bilateral sensorimotor cortex. Results are overlaid on a Montreal Neurological Institute (MNI) brain.* ***(b-c)*** *Mean baseline MD (b) and Fr (c) extracted from the clusters significant at $p_{FWE} < 0.05$ shown in (a). Scatterplots are presented for visualisation purposes only and should not be used for statistical inference. Each data point represents a single participant, axes represent residual values after correcting*

for age, sex, PSQI score, percentage of time spent in N2, baseline reaction time and baseline learning capabilities on the SRTT. MD: Mean Diffusivity; Fr: Restricted Water Fraction; S1-4: Session 1-4; n = 16.

4 DISCUSSION

We set out to investigate the relationship between plasticity in tissue microstructure and beneficial effects of memory reactivation during sleep. To this end, we combined TMR with DW-MRI and structural data to test whether baseline micro-architecture of the brain can be used to determine one's susceptibility to TMR, and whether TMR can impact on brain microstructure, thus giving rise to the behavioural effects observed. First, we find that long-term cueing benefit is associated with gradual microstructural plasticity within memory and task-related regions. Specifically, our data suggests that precuneus undergoes microstructural plasticity throughout the consolidation process, supporting TMR-related benefits 10 and 20 days after the manipulation, respectively. In addition to precuneus, early microstructural changes in striatum and late microstructural changes in sensorimotor cortex also relate to the beneficial effects of cueing 20 days post-TMR. Second, we show that the time spent in N2 sleep is related to overnight change in grey matter (micro)structure but does not impact on the TMR-related plasticity. Finally, we demonstrate that individual differences in baseline sensorimotor microstructure predict behavioural TMR susceptibility, i.e., the variance shared between cueing benefit at the post-TMR sessions.

4.1 TMR-INDUCED PLASTICITY IN PRECUNEUS

We show a relationship between both early (0 – 24 h post-TMR) and late (24 h – 10 days post-TMR) precuneus plasticity and cueing benefit 10 days and 20 days post-TMR, respectively. These results suggest that repeated reactivation of a memory trace could engender gradual microstructural changes within precuneus that are associated with the gradual emergence of behavioural benefits from the manipulation. In Chapter 3 we have shown that TMR of a procedural memory also engages precuneus functionally, but this occurs relatively early in the consolidation process. Given the well-described role of precuneus in memory retrieval (Wagner et al., 2005; Treder et al., 2021), our previous results could reflect the difference in recall strength of cued and uncued sequences during their execution. Indeed, TMR and memory reactivation per se share a lot of parallels with memory retrieval. However, the long-term time scale of our current results as well as the microstructural changes that we report suggest that the role of precuneus may extend beyond retrieval only. We believe that precuneus could act as an 'episodic buffer' (Vilberg et

al., 2008), building up representations of the retrieved information before they are transferred to a more permanent store. Indeed, precuneus has already been shown to undergo rapid, learning-dependent microstructural plasticity, indicative of memory engram development within this region (Brodt et al., 2018). The structure is known to harbour behaviourally relevant memory representations (Brodt et al., 2016; Jeong & Xu, 2016) and its function is traditionally associated with motor learning (Cohen & Anderson, 2002; Shadmehr & Holcomb, 1997). Our current results expand the existing literature by demonstrating that memory reactivation during sleep mediates microstructural plasticity which continues days after a single night of cueing within precuneus, perhaps facilitating the development of a stable and long-lasting memory trace in this structure. This, in turn, gives rise to the emergence of behavioural benefits of reactivation, reflected in the difference between the cued and uncued sequence that we observe 20 days post-TMR. Thus, we argue that (targeted) memory reactivation during sleep has a powerful impact on both memory processing and brain plasticity, and that its effects extend beyond the initial night of sleep.

4.2 NEUROPLASTICITY AND MICROSTRUCTURE OF THE MOTOR SYSTEM

Our findings support the suggestion that the long-term cueing benefit of TMR is mediated by early plasticity in putamen and late plasticity in precentral and postcentral gyri. We show that changes within these structures are specifically related to the behavioural effects 20 days post-TMR, suggesting that such microstructural plasticity in the motor system may give rise to the emergence of behavioural TMR effects. Both striatum and sensorimotor structures are thought to be critical for long-term storage of motor sequences (Doyon et al., 2003). We build on this literature by arguing that memory reactivation during sleep may engender microplasticity within these regions, and thus stabilise memory traces harboured by the cortico-striatal system, shaping the sleep-dependent procedural benefits. Memory reactivation has been observed in ventral striatum immediately after learning (Pennartz et al., 2014) and this could drive the early microstructural plasticity in the adjacent regions, including putamen. In turn, the late microstructural plasticity that we observe in primary motor and somatosensory cortices likely reflects their slowly evolving reorganisation (Kami et al., 1995; Kleim et al., 2004; Matsuzaka et al., 2007; Gao et al., 2018; Ganguly & Carmena, 2009). This late plasticity could also underpin the TMR-related functional engagement and grey matter volume increase of the sensorimotor cortex which we observed in Chapter 3. Interestingly, a recent rodent study found that cortico-striatal functional coupling increases during offline periods of rest and is required for long-term skill learning (Lemke et al., 2021).

Furthermore, this coupling seems to be mediated by NREM sleep spindles (Lemke et al., 2021), which are known to be involved in motor learning (Boutin & Doyon, 2020). One intriguing possibility is that neuronal ensembles within sensorimotor cortex and striatum undergo simultaneous replay during post-learning sleep and this leads to their functional coupling. Simultaneous activity in primary motor cortex and dorsal striatum has already been recorded during motor learning (Costa et al., 2004). Our results raise the hypothesis that memory reactivation could also co-occur in these regions during sleep and thereby drive the synaptic plasticity within the underlying substrate. If this is correct, it might suggest that such co-replay could underpin the microstructural changes and the subsequent behavioural benefits observed in our dataset.

We further show that individual differences in the microstructural architecture of sensorimotor cortex measured at baseline are associated with TMR susceptibility. Thus, our results combine to suggest that the microstructure of the sensorimotor cortex can both change in response to cueing motor memory reactivation and confer susceptibility to the stimulation. The success of TMR may therefore depend on the inter-individual variation in the microstructure of precentral and postcentral gyri. That is, the intrinsic micro-architecture of these task-related regions may either control memory encoding capacity, impact on the response to the manipulation or determine the effectiveness of the reactivation process itself. This finding adds to the existing literature on the factors modulating TMR's success (Hu et al., 2020; Creery et al., 2015; Schechtman et al., 2021; Cairney et al., 2016), perhaps explaining some of the discrepancies in the TMR literature.

4.3 BIOLOGICAL INTERPRETATION OF THE DW-MRI FINDINGS

The results of the current study demonstrate that DW-MRI can provide a valuable tool to investigate behaviourally relevant changes in brain microstructure. Furthermore, the multimodal approach that we adopted here revealed a common pattern across two diffusion markers: MD and Fr. This not only makes our findings more robust but also provides insights into the biological changes that could underpin sleep-dependent memory consolidation. Biological interpretation of diffusion measures is not straightforward (Zatorre et al., 2012), but combining multiple modalities increases the chances of picking up features that are shared by the two markers. In case of MD and Fr, water diffusion within the restricted (intracellular) volume fraction seems to be a common feature that both markers are sensitive to. Thus, the microstructural changes associated with memory reactivation could involve

remodelling of the cylindrical tissue compartments, such as neural and glial processes (Tavor et al., 2013). Indeed, rapid structural modifications after learning have been reported in astrocytic processes (Theodosis et al., 2008; Blumenfeld-Katzir et al., 2011) and dendritic spines (Xu et al 2009). In fact, both NREM (Yang et al., 2014) and REM sleep (Li et al., 2017) have been implicated in dendritic spine plasticity within hours after learning, while disrupting memory reactivation during sleep impaired post-training spine formation (Yang et al., 2014). By the same token, repeated reactivation through TMR during sleep could have boosted similar forms of plasticity in the cylindrical compartments of precuneus, striatum and sensorimotor cortex in our dataset, thus giving rise to the observed changes in the DW-MRI metrics. However, swelling of cells (particularly astrocytes, Macvicar et al., 2002), and thus a shift in the ratio of extra- to intra-cellular space (Le Bihan, 2012; Theodosis et al., 2008; Johansen-Berg et al., 2012) could also alter the diffusion properties of the tissue and, consequently, the MD and Fr values. Indeed, synaptogenesis (Kleim et al., 2004) and astrocytic hypertrophy (Kleim et al., 2007) are detectable only after 7-10 days of training, thus matching the time scale of our late microstructural plasticity. Nevertheless, the cellular processes driving MD and Fr changes are generally difficult to identify and histological approaches would be needed to confirm the biological interpretation of our results.

In a broader context, DW-MRI allowed us to study the dynamic and distributed nature of the TMR-related changes. Our results demonstrate that cued memory reactivation can modify tissue microstructure. Notably, we show the resulting plasticity encompasses several cortical areas, continues days after the stimulation nights and supports long-term consolidation of memories that are reactivated during sleep. Thus, we extend the existing literature by providing direct evidence for reactivation-mediated redistribution of memory traces across the brain (Born et al., 2006; Diekelmann & Born, 2010b). Given the long-term character of the detected changes, we speculate that cueing memory reactivation must have either primed the relevant synapses for later processing (Diekelmann & Born, 2010b) or biased plasticity-related protein capture towards the targeted memory traces (Seibt & Frank, 2019). The consequential bias in synaptic plasticity would explain why a single night of cueing was capable of modifying tissue microstructure up to 10 days later. We further identify precuneus and motor structures as important neocortical memory hubs for long-term retention of procedural memories. The microstructural changes in precuneus, striatum and sensorimotor cortex were specifically related to the behavioural effects 20 days post-TMR, which was the only time point where we find group level evidence for the difference between the cued and uncued sequence (Chapter 3). This suggests that the microstructural plasticity continuously

parallels the gradual development of behavioural cueing benefit, eventually contributing to the emergence of behavioural effects of TMR.

4.4 SLEEP RELATED CHANGES

We show a negative relationship between the percentage of time spent in N2 and the overnight change in both parahippocampal grey matter volume, and hippocampal and parahippocampal MD. The VBM finding supports the idea that hippocampal contribution to memory processing diminishes as a sleep-mediated hippocampal-neocortical reorganisation of memory representations takes place (Born & Wilhelm, 2012; Buzsáki, 1996; Born et al., 2006; Rasch & Born, 2012; Takashima et al., 2009). Although the literature emphasises the role of N3 in systems consolidation, N2 is known to play a key role in motor sequence memory (Laventure et al., 2016; Nishida & Walker, 2007) but the relationship between N2 and learning-related plasticity has so far been neglected. It is important to point out, however, that the volumetric change that we observe in the hippocampus was not directly related to the behavioural effects of TMR, and N2 did not affect the TMR-related changes.

Nevertheless, our VBM result is hard to reconcile with the negative relationship between N2 and MD, given that a reduction in MD is generally thought to reflect an *increase* in tissue barriers that restrict water motion (Sagi et al., 2012) and thus tissue growth. However, alterations in DW-MRI parameters could also reflect changes in body hydration (Elvsåshagen et al., 2015) which was not controlled for in this study. Our current data further hint at microstructural changes that are *uniquely* captured by MD, but not Fr or the multimodal measure of MD and Fr combined. MD measures the average mobility of water molecules (Maffei et al., 2015), whereas Fr reflects water diffusion from the intra-axonal space only (Assaf et al., 2004). This leads us to speculate that N2 could particularly affect diffusivity of the extra-cellular/axonal space of the hippocampus (i.e., astrocytes, glia, and extracellular matrix) (Assaf et al., 2004). Diffusion MRI signal, including MD, is sensitive to microglia and astrocytes activation (Garcia-Hernandez et al., 2021; Weber et al., 2015), but histological studies would be necessary to directly probe the relationship between glial cells and N2. MD reduction could also reflect exchange of water between the extra- and intra-cellular compartments that occurs during glymphatic clearance (Jessen et al., 2015). Interestingly, the negative relationship between MD and NREM sleep has been already linked to the glymphatic hypothesis (Tuura et al., 2021), suggesting that MD could act as a glymphatic marker.

Although challenging to interpret, these results add to the existing literature linking sleep with brain plasticity, by demonstrating that N2 may be involved in shaping grey-matter (micro)structure of the brain. While REM sleep has been implicated in myelination, corticalization and reorganisation of memory traces (Li et al., 2017; Bellesi et al., 2013; de Vivo & Bellesi, 2019; Almeida-Filho et al., 2018; Landmann et al., 2015; Bridi et al., 2015), our current data hint at a particular role of N2 in the (micro)structural plasticity.

5 CONCLUSION

We show that gradual microstructural changes, distributed across several cortical areas, track the emergence of behavioural benefits stemming from memory reactivation. Specifically, we find that microstructural plasticity in precuneus and motor system over different periods of time is associated with long-term benefits of procedural memory TMR. These findings support the long-lived belief that stable memory traces develop gradually and reorganise the underlying tissue (Frankland & Bontempi, 2005). Our results were specific to the cueing benefit 20 days post-manipulation, suggesting that the microstructural changes observed are specifically linked to the behavioural gain from memory reactivation. They also demonstrate that DW-MRI can be used to detect behaviourally relevant processes that underpin sleep-dependent memory consolidation. Finally, we shed new light on the factors that influence TMR's effectiveness by demonstrating that individual variation in the microstructure of the task-related regions can be used to predict one's susceptibility to the manipulation.

6 SUPPLEMENTARY MATERIAL

SUPPLEMENTARY TABLES:

Table S1. Microstructural plasticity associated with cueing benefit at different sessions.

Cluster statistics for precuneus, putamen and sensorimotor cortex which showed a positive relationship microstructural plasticity (MD and Fr) and cueing benefit at different sessions. MD and Fr were either analysed together in a multimodal framework (i) or separately using unimodal analyses (ii, iii).

Analysis	ROI	Region	MNI x, y, z (mm)	Number of voxels	T peak	P_{FWE} peak
A. [Early microstructural plasticity * cueing benefit at S3]						
i) Multimodal	Precuneus	Left precuneus	-6, -60, 18	1328	-	**0.041***
ii) Unimodal: MD		-	-10, -58, 30	62	2.65	0.619
iii) Unimodal: Fr		Left precuneus	-2, -56, 8	1378	8.02	0.077
B. [Late microstructural plasticity * cueing benefit at S4]						
i) Multimodal	Precuneus	Right precuneus	4, -58, 16	1943	-	**0.027***
ii) Unimodal: MD		Right precuneus	-6, -54, 30	1992	10.08	**0.033***
iii) Unimodal: Fr		-	8, -52, 6	867	8.93	0.116
C. [Early microstructural plasticity * cueing benefit at S4]						
i) Multimodal	Dorsal Striatum	Right putamen	34, -6, -8	633	-	**0.016***
ii) Unimodal: MD		Right putamen	32, 2, -10	563	5.20	0.054^
iii) Unimodal: Fr		-	20, 8, -4	79	3.34	0.563
D. [Late microstructural plasticity * cueing benefit at S4]						
i) Multimodal	Sensorimotor Cortex	Left precentral and postcentral gyri	-60, -18, 14	2159	-	**0.018***
ii) Unimodal: MD		Left precentral and postcentral gyri	-60, -20, 14	3987	13.15	**0.010***
iii) Unimodal: Fr		-	48, -8, 56	54	7.71	0.783

*Regions listed were significant at peak voxel threshold of $p_{FWE} < 0.05$, after correction for multiple voxel-wise comparisons within pre-defined bilateral ROI (as listed in the first column) and the number of modalities (two modalities, MD and Fr). Peak voxel MNI coordinates and peak T values are given. Covariates of no interest included in the analysis: age, sex, PSQI score, baseline reaction time, baseline learning capabilities on the SRTT, cueing benefit at S2, cueing benefit at S4 (for A only), cueing benefit at S3 (for B-D). S3-4: Session 3-4; * p < 0.05, ^ p < 0.06. n = 16 for (A, C), n = 15 for (B, D).*

Table S2. Sleep-related brain changes.

Clusters showing increased (inc) or decreased (dec) changes in GM volume and microstructure overnight, and when considering covariates of the percentage of time spent in N2 and N3. No significant clusters were found when considering REM sleep. MD and Fr were either analysed together in a multimodal framework (C i) or separately using unimodal analyses (C ii, C iii).

Analysis	Region	MNI x, y, z (mm)	Number of voxels	T peak	P_{FWE} peak
A. [Δ GM volume from S1 to S2 * N2]					
VBM	Left Parahippocampus $_{(dec)}$	-16, -33, -14	14	5.70	**0.018***

B. [Δ GM volume from S1 to S2 * N3]					
VBM	Right Fusiform $_{(dec)}$	34, -34, -15	1	4.71	**0.042***
C. [Δ microstructure from S1 to S2 * N2]					
i) Multimodal	-	28, -28, 18	332	-	0.098
ii) Unimodal: MD	Right Hippocampus and Parahippocampus $_{(dec)}$	36, -8, -26	654	5.28	**0.045***
iii) Unimodal: Fr	-	-16, -4, -36	74	4.14	0.544

For (A-B): regions listed were significant at peak voxel threshold of $p_{FWE} < 0.05$, after correction for multiple voxel-wise comparisons within pre-defined ROI for bilateral hippocampus and parahippocampus. For (C): regions listed were significant at peak voxel threshold of $p_{FWE} < 0.05$, after correction for multiple voxel-wise comparisons and the number of modalities (two modalities, MD and Fr), within the pre-defined bilateral ROI as in (A-B). Since fusiform gyrus was not our ROI, the result in (B) has likely arisen due to the imperfection of the method and is thus not discussed any further. Peak voxel MNI coordinates, and peak T values are given. Covariates of no interest included in the analysis: age, sex, percentage of time spent in REM, percentage of time spent in N3 (for A and C only), percentage of time spent in N2 (for B only). n = 29 for (A, B), n = 16 for (C).

Table S3. Microstructural plasticity associated with cueing benefit at different sessions with N2 covaried out.
Cluster statistics for precuneus, putamen and sensorimotor cortex which showed a positive relationship microstructural plasticity (MD and Fr) and cueing benefit at different sessions, as in Table S1. MD and Fr were either analysed together in a multimodal framework (i) or separately using unimodal analyses (ii, iii).

Analysis	ROI	Region	MNI x, y, z (mm)	Number of voxels	T peak	P_{FWE} peak
A. [Early microstructural plasticity * cueing benefit at S3]						
i) Multimodal	Precuneus	Left precuneus	-8, -58, 18	1264	-	**0.030***
ii) Unimodal: MD		-	-8, -60, 32	45	2.66	0.674
iii) Unimodal: Fr		Left precuneus	-10, -46, 8	1286	7.44	0.082
B. [Late microstructural plasticity * cueing benefit at S4]						
i) Multimodal	Precuneus	Right precuneus	6, -54, 14	1886	-	**0.034***
ii) Unimodal: MD		Right precuneus	-6, -54, 30	2010	24.95	**0.031***
iii) Unimodal: Fr		-	6, -54, 14	744	16.06	0.138
C. [Early microstructural plasticity * cueing benefit at S4]						
i) Multimodal	Dorsal Striatum	Right putamen	34, -8, -6	593	-	**0.021***
ii) Unimodal: MD		Right putamen	32, 2, -10	547	4.88	0.075
iii) Unimodal: Fr		-	16, 8, -6	76	3.42	0.586
D. [Late microstructural plasticity * cueing benefit at S4]						
i) Multimodal	Sensorimotor Cortex	Left precentral and postcentral gyri	-62, -16, 14	2252	-	**0.026***
ii) Unimodal: MD		Left precentral and postcentral gyri	-60, -20, 14	4001	17.30	**0.014***
iii) Unimodal: Fr		-	48, -8, 56	48	7.37	0.735

Regions listed were significant at peak voxel threshold of $p_{FWE} < 0.05$, after correction for multiple voxel-wise comparisons within pre-defined bilateral ROI (as listed in the first column) and the number of modalities (two modalities, MD and Fr). Peak voxel MNI coordinates and peak T values are given. Covariates of no interest included in the analysis: age, sex, PSQI score, baseline

*reaction time, baseline learning capabilities on the SRTT, cueing benefit at S2, cueing benefit at S4 (for A only), cueing benefit at S3 (for B-D), percentage of time spent in N2. S3-4: Session 3-4; * p < 0.05, ^ p < 0.06. n = 16 for (A, C), n = 15 for (B, D).*

Table S4. Baseline microstructure and TMR susceptibility.

Cluster statistics for sensorimotor cortex which showed a positive relationship between baseline microstructure and TMR susceptibility (i.e., PCA-transformed cueing benefit at session 2, 3 and 4).

Analysis	ROI	Region	MNI x, y, z (mm)	Number of voxels	T peak	P_{FWE} peak
i) Multimodal	Sensorimotor Cortex	Left precentral and postcentral gyri	58, -6, 20	1691	-	**0.041***
ii) Unimodal: MD		-	54, 0, 18	1396	9.42	0.052^
iii) Unimodal: Fr		-	-34, -28, 40	233	5.00	0.219

*Regions listed were significant at peak voxel threshold of $p_{FWE} < 0.05$, after correction for multiple voxel-wise comparisons within pre-defined bilateral ROI (as listed in the first column) and the number of modalities (two modalities, MD and Fr). Peak voxel MNI coordinates and peak T values are given. Covariates of no interest included in the analysis: age, sex, PSQI score, baseline reaction time and baseline learning capabilities on the SRTT, percentage of time spent in N2. * p < 0.05, ^ p < 0.06. n = 16.*

SUPPLEMENTARY FIGURES:

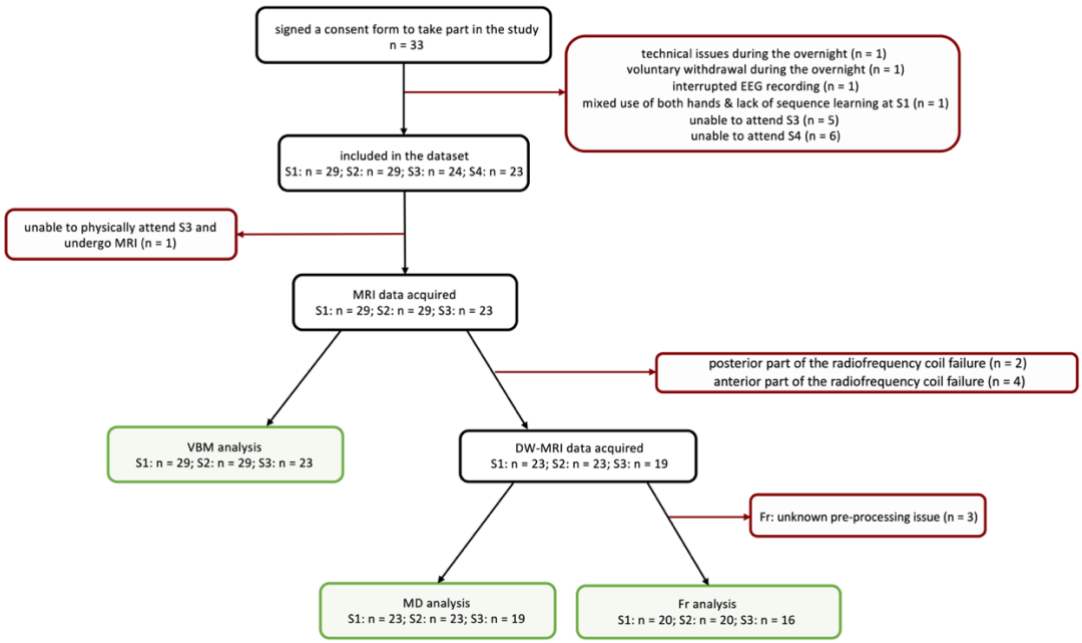

Fig. S1. A flowchart showing participants included and excluded from the analysis. *In black and white, the number of participants included in the study at different time points, with the final sample size shown in green. In red, the number of participants excluded from different analyses, together with a reason for the exclusion. S1-S4: Session 1 – Session 4; Fr: Restricted water fraction; MD: Mean Diffusivity; VBM: Voxel-Based Morphometry.*

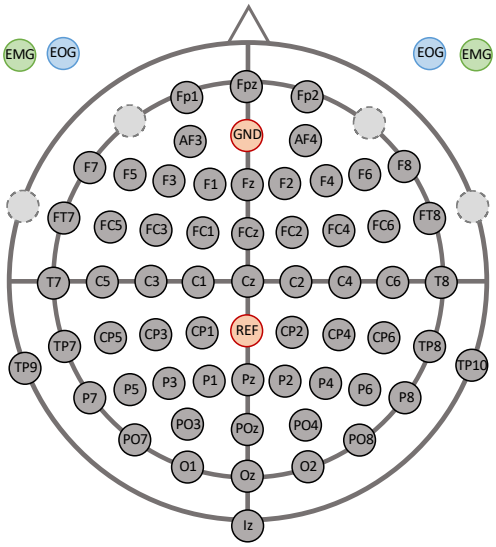

***Fig. S2. EEG electrodes layout**. Orange: ground (GND) and reference (REF) electrodes; light grey (dashed circles): original position of the electrodes used to record EMG and EOG; green: EMG electrodes; blue: EOG electrodes.*

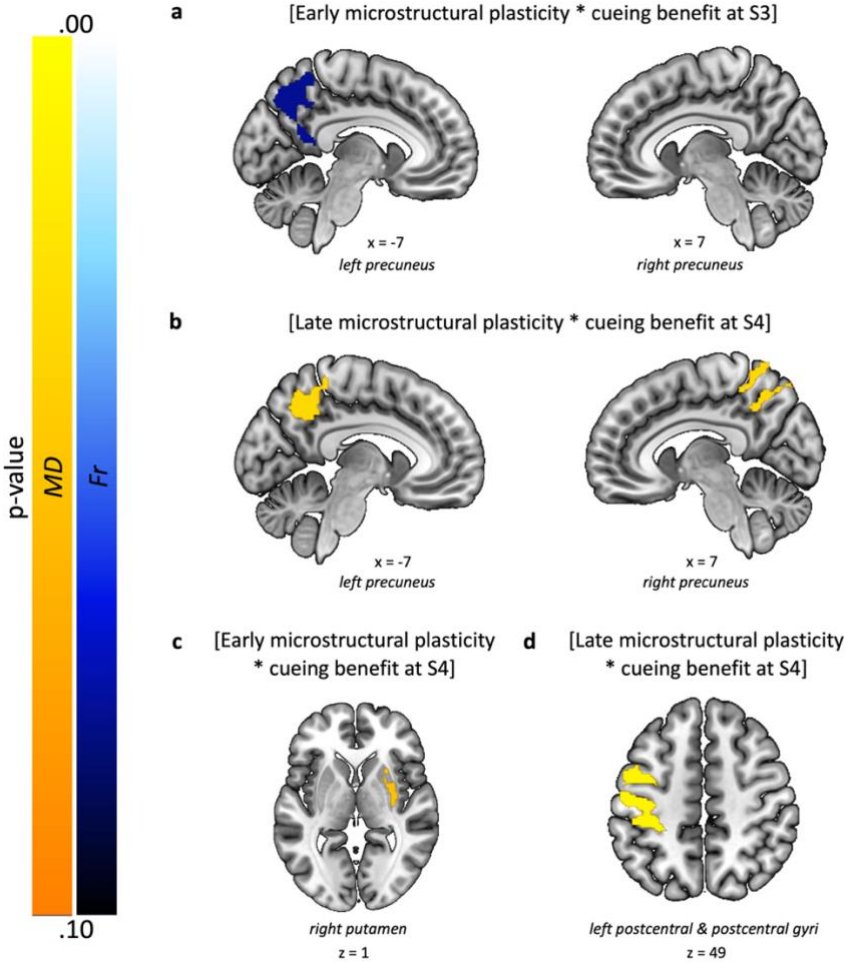

***Fig. S3. Results of unimodal analyses conducted for MD and Fr separately, testing the same relationships as in Fig.3-4**. (**a, b**) Unimodal results for the same contrasts as in Fig.3a and Fig.3d, respectively. (**c, d**) Unimodal results for the same contrasts as in Fig.4a and Fig.4d, respectively. Colour bars indicate p-values at $p_{FWE} < 0.1$, corrected for multiple modalities and the number of voxels within the chosen ROI. In orange, MD clusters; in blue, Fr clusters.*

Results are overlaid on a Montreal Neurological Institute (MNI) brain. Colour bars indicate 1 - p-value, derived from 5000 permutations. S1-4: Session 1-4. n = 16 for (a, c), n = 15 for (b, d).

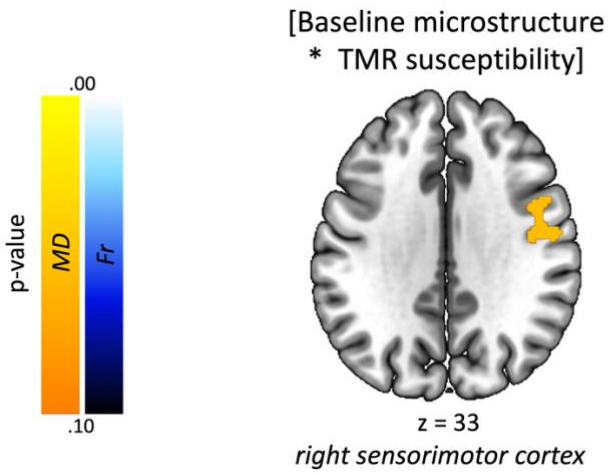

Fig. S4. Results of unimodal analyses conducted for MD and Fr separately, testing the same contrast as in Fig.6*. Colour bars indicate p-values at $p_{FWE} < 0.1$, corrected for multiple modalities and the number of voxels within the chosen ROI. In orange, MD clusters; in blue, Fr clusters. No Fr clusters above the $p_{FWE} < 0.1$ threshold were revealed. Results are overlaid on a Montreal Neurological Institute (MNI) brain. Colour bars indicate 1 - p-value, derived from 5000 permutations. S1-4: Session 1-4. n = 16.*

CHAPTER 5

General Discussion

1 THESIS OVERVIEW

The overarching aim of this thesis was to explore the long-term effects of TMR and thereby add to the current understanding of the mechanisms that underpin sleep dependent memory consolidation over time. Nowadays, there is no doubt that sleep benefits consolidation and that memory reactivation plays a central role in this process. There is also no denying that some memories last a lifetime. However, to date, sleep and memory research focused mostly on the relatively short-term benefits of this intriguing state. Thus, there is still much to learn about sleep's contribution to the retention of what has been learned years or decades ago. What are the mechanisms that drive long-term consolidation and is memory reactivation one of them? How do the effects of memory reactivation evolve over time?

These questions inspired me to conduct the experiments described in this thesis. To tackle them, I used TMR to manipulate motor memory reactivation during sleep and examine the effects at different points in time and using different imaging modalities. In **Chapter 2**, I investigated the behavioural dynamics over six weeks following TMR of a SRTT. I was further interested in the electrophysiological correlates of the long-term benefits observed. In **Chapter 3**, I tracked the functional and structural evolution of a motor memory trace to determine whether memory reactivation can foster learning-dependent changes in its underlying substrate. Lastly, in **Chapter 4**, I delved deeper into the neuroplasticity underpinning memory reactivation during sleep, this time focusing on the microstructural changes that support TMR effects.

This final chapter will integrate the results that emerge from this thesis and discuss their wider implications for sleep and memory research. I will further reflect on memory engrams and paint a broader picture of how continuous processing, redistribution, and reorganisation of memory traces allow us to remember the past. Finally, I will discuss some important questions that remain in the field and suggest potential ways to tackle them.

2 BACK TO SLEEP AND MEMORY MODELS

In the introduction to this thesis, I discussed some of the most prominent models of sleep and memory. I also reviewed a vast body of research that strongly indicates memory reactivation as the key mechanism underlying consolidation. Now, I would like to consider these models and the existing literature again, in light of the findings arising from the experimental chapters of this thesis.

2.1 DUAL PROCESS AND SEQUENTIAL HYPOTHESES

The Dual Process Hypothesis posits that SWS-rich sleep benefits declarative memories while REM-rich sleep is important for non-declarative memories (Yaroush et al., 1971; Fowler, 1973; Plihal & Born, 1997; Plihal & Born, 1999; Wagner et al., 2002; Smith, 1995). This hypothesis does not seem to fit with our findings. In all the experimental chapters we show that procedural memory strongly benefits from TMR during NREM sleep, contrary to what the model predicts. Chapter 2 also points to the relationship between cueing benefit and the time spent in N2, but not REM. Thus, the Dual Process Hypothesis does not account for our findings, as well as those reported by others (Huber et al., 2004; Huber et al., 2006; Aeschbach et al., 2008; Gais et al., 2000; Fogel et al., 2007; Rauchs et al., 2004). That is, unless our manipulation targeted the declarative aspect of the SRTT. Sequence learning is known to be hippocampal-dependent (Albouy et al., 2008; Albouy et al., 2013a; Albouy et al., 2013b; Albouy et al., 2015), especially if the participants become aware of the learned material. Indeed, our participants showed above-chance explicit memory of both sequences at the last experimental session (six weeks for Chapter 2 and twenty days for Chapter 3) which, in case of Chapter 3, also happened to be the session for which TMR showed the greatest benefits. Thus, our NREM TMR could have benefited skill learning only once the explicit knowledge of the task had been gained. However, because we only ever tested the explicit knowledge at the end of each study, we cannot rule out that it had been gained earlier than what we report. It would also be hard to believe that a single night of cueing did not affect *any* aspect of memory processing until weeks later, when the targeted memory became declarative. That is especially true given previous studies from our lab that report TMR benefits on the SRTT the morning after NREM stimulation (Koopman et al., 2020; Cousins et al., 2014; Cousins et al., 2016), as well as no effect of REM TMR on the same task (Koopman et al., 2020). These findings are contrary to what the Dual Process Hypothesis predicts, and we believe that the model cannot fully account for our results either.

In turn, the Sequential Hypothesis highlights the importance of orderly succession of NREM and REM sleep, focusing on their interaction and complementary roles in memory processing (Giuditta et al., 1995; Ambrosini & Giuditta, 2001). It is difficult to say whether our findings support this model. Although we do not report any findings related to REM sleep, the contribution of REM sleep and its electrophysiological characteristics to procedural memory consolidation was not directly tested in this thesis. Furthermore, our electrophysiological data was collected only during the first experimental night. Given the Sequential Hypothesis and the recent suggestion that the delayed benefits of sleep may be taking place in REM (Pereira & Lewis, 2020), it seems plausible that REM sleep would come into play later during the consolidation process. In that sense, the post-TMR REM sleep could have contributed to the long-term benefits of TMR that we report in our experimental chapters. Hence, the Sequential Hypothesis is neither contradicted by our data, nor necessarily supported by it, while the role of REM sleep in long-term procedural memory consolidation remains to be established.

2.2 ACTIVE SYSTEM CONSOLIDATION HYPOTHESIS

Moving on to the Active System Consolidation Hypothesis (ASC), the experimental findings of this thesis provide evidence in favour of its assumptions. Firstly, the ASC argues that memory reactivation during SWS plays both an active and crucial role in memory consolidation (Born et al., 2006; Diekelmann & Born, 2010b). This fits well with the benefits of NREM sleep TMR that we repeatedly observe in our data. Under the ASC framework, we can argue that TMR had successfully biased reactivation of the cued memories, thereby leading to their stronger consolidation over time.

Secondly, the ASC stems from the standard two-stage model of consolidation and thus posits that memory reactivation mediates the transfer of memories from their temporary store to a long-term store. Hippocampus is often portrayed as the temporal store and its contribution to memory processing is known to diminish as the sleep-mediated reorganisation of memory traces takes place (Buzsáki, 1986; Born & Wilhelm, 2012; Born et al., 2006; Rasch & Born, 2013; Takashima et al., 2009). Consistent with this, our results from Chapter 4 show that parahippocampal grey matter volume decreases with an increase in the amount of time spent in N2. Furthermore, Chapters 3 and 4 point to the relationship between repeated reactivation of memory traces during sleep and slowly evolving reorganisation of sensorimotor regions that are often regarded as the long-term storage sites for procedural

memories (Kami et al., 1995; Kleim et al., 2004; Matsuzaka et al., 2007; Gao et al., 2018; Ganguly & Carmena, 2009). Thus, our findings fit well with the ASC assumptions, demonstrating that memory reactivation engenders physical changes in memory representations and mediates their re-distribution for long-term storage. Importantly, we also extend the ASC framework by arguing that memory reactivation during sleep could support the development and evolution of memory engrams (Chapters 3 and 4, see section *3.4. Memory reactivation during sleep fosters engram development*).

Finally, the ASC places the emphasis on the coordinated interplay between sharp-wave ripples, thalamocortical sleep spindles and neocortical slow waves, and their role in consolidation. Some evidence in favour of this notion comes from Chapters 2 and 3, where we report an increase in spindle density and SO-spindle coupling strength immediately upon cue onset. This could be indicative of early processing of memory traces that is triggered by the cues, consistent with what other TMR studies report (Antony et al., 2018; Cairney et al., 2018). Truth be told, however, the relationship between these oscillatory characteristics of NREM sleep and the behavioural advantage of cueing is not entirely clear from our data. In Chapter 2 we report no relationship between cueing benefit and spindle density, and the correlation with spindle laterality did not survive FDR correction. Instead, we find a negative association between cueing benefit and SO-spindle coupling strength during the no-cue period of N2 which is hard to reconcile with the existing literature. Then, in Chapter 3, the correlational analysis did not reveal any significant findings. Furthermore, a previous SRTT-TMR study in our lab (Koopman et al., 2020b) showed no difference in the fast spindle-band response to the auditory cues between the adaptation night (when the sounds were not yet associated with the SRTT) and the experimental night (when the same sounds became meaningful post-learning), suggesting that the increase in spindle density observed in this thesis could simply reflect the brain's response to any sound, regardless of its salience or meaning (Sato et al., 2007). However, that was not the case in Cairney et al. (2018), where an increase in spindle activity following TMR was observed only for the memory-related cues and not for the new stimuli. Similar results were obtained by Oyarzún et al. (2017). Furthermore, a great wealth of studies has shown the importance of sleep spindles in memory consolidation (Peyrache et al., 2009; Staresina et al., 2015; Jegou et al., 2019; Wang et al., 2019; Cairney et al., 2018; Lustenberger et al., 2016; Ngo et al., 2013; Antony et al., 2018). Thus, despite the lack of control condition in our studies and a clear relationship between sleep oscillatory patterns and cueing benefit, we believe that the surge in spindle

density and SO-spindle strength following TMR cues hints to more than just a simple response to *a* sound.

2.3 SYNAPTIC HOMEOSTASIS HYPOTHESIS

Lastly, the Synaptic Homeostasis Hypothesis (SHY) holds that the fundamental function of SWS is to globally down-scale synapses, which restores the brain's ability to learn, improves signal-to-noise ratio and thereby promotes consolidation of the selected memories (Tononi & Cirelli, 2003; Tononi & Cirelli, 2006). Since the original conceptualisation of the model largely disregards the role of memory reactivation in sleep-dependent consolidation, it is difficult to say how the SHY assumptions could account for the TMR effects observed in this thesis. However, the latest reincarnation of SHY acknowledges the importance of reactivation during sleep, postulating that it could protect synapses from downscaling (Tononi & Cirelli, 2014). Under this framework, TMR would also protect the cued memory representations from synaptic weakening, maintaining them above the 'consolidation' threshold. This would not be the case for the uncued memories, thus resulting in the post-TMR difference between the cued and uncued memory performance (Chapter 2 and Chapter 3). Indeed, a recent study demonstrated that sleep results in a net decrease in the expression of SEP-GluA1 – a marker of synaptic strength – but the dendritic spines that had been involved in pre-sleep skill learning appeared to show resistance to this kind of global downscaling (Miyamoto et al., 2021). However, the relationship between synaptic downscaling and memory reactivation remains an open question. Likewise, it is unclear whether synaptic downscaling underpins the results in this thesis, especially since the microstructural plasticity that we report in Chapter 4 are unlikely to reflect very small and localised changes in, e.g., dendritic spines (Johansen-Berg et al., 2012). Nevertheless, we believe that synaptic and systems consolidation operate in concert to support long-term sleep-dependent consolidation (see section *3 Memory reactivation supports long-term consolidation and storage of motor memories*).

To conclude, this thesis provides compelling evidence in support of the key assumptions made by the ASC, as well as some aspects of the other sleep and memory models that exist in the field. While the Dual Process Hypothesis is unlikely to account for our results, we believe that the cyclical progression of NREM and REM sleep plays an important role in memory consolidation, even though our results provide no direct evidence of such. The latest refinements of the SHY render the model plausible in light of our findings, but the spatial

resolution of our data did not allow us to determine whether synaptic downscaling could indeed explain our results. All in all, the discussed models only provide a vague idea on the possible mechanisms driving the results of this thesis. What they lack are the time course of the sleep-dependent changes and the specific brain regions involved in reactivation-mediated consolidation, which brings us to the next section of this discussion.

3 MEMORY REACTIVATION SUPPORTS LONG-TERM CONSOLIDATION AND STORAGE OF MOTOR MEMORIES

The title of this thesis is 'Evolving plasticity in brain and behaviour after targeted memory reactivation during sleep'. The data collected throughout allowed us to characterise the long-term behavioural effects of memory reactivation as well as the neuro-plastic evolution of the reactivated memory representations, which had never been done before. But precisely how did memory reactivation contribute to our findings? Although it is truly remarkable that playing sounds during sleep can change our brain structure, how exactly is that possible? These questions will guide the current section in an attempt to integrate our results and uncover the potential mechanisms that foster long-term consolidation and could have given rise to the results reported in this thesis.

3.1 BEHAVIOURAL EFFECTS OF TMR OVER TIME

In Chapters 2 and 3 we show, for the first time, that a single night of TMR can benefit procedural memories in the long run. In that sense, the behavioural results from Chapters 2 and 3 are consistent with each other. However, the exact duration of the TMR effects differed between the two studies. In Chapter 2 we find that the biggest difference between the cued and uncued sequence occurred 10 days post-stimulation, but this was not the case in Chapter 3. Instead, Chapter 3 suggests that the benefits of cueing may emerge even later, with a significant difference between the two sequences 20 days post-stimulation. An immediate question that comes to mind when interpreting these findings is – given the results of Chapter 2, why was the TMR effect absent 10 days post-stimulation in Chapter 3? The simplest explanation is of course that the environment in which the participants performed the task differed between the two studies. In Chapter 2, the SRTT was performed in front of a computer screen, using a computer keyboard and with no background sounds present. Instead, in Chapter 3, participants were lying down in the MRI scanner and used

somewhat clunky MR-safe button boxes. This rather challenging environment could have impacted on the behavioural effect of TMR, allowing it to emerge only once the conditions were comfortable (i.e., 20 days post-TMR, during which the SRTT was performed online and in participants' own homes). However, our data suggest that the MRI environment did not limit how fast the participants could perform the task, and there is no reason to expect that it would impact differentially on the two sequences and thus affect the difference between them (i.e., cueing benefit). Alternatively, the loud noises from the MRI machine could have made it harder to learn the associations between the task and the auditory cues, thus delaying the effects of TMR until 20 days later. Another, perhaps more intriguing possibility is that the TMR effect is strongly dependent on individual variations. This idea would fit with the growing literature on the factors modulating the effectiveness of TMR or conferring susceptibility to the manipulation (reviewed in the General Introduction, section *4.2.4 Factors modulating the effectiveness of TMR*). It is also consistent with our own finding from Chapter 4 which suggests that the individual variation in the microarchitecture of task-specific regions determines one's sensitivity to TMR. Thus, it is possible that the difference between the cued and uncued sequence 10 days post-TMR in Chapter 3 did not reach the significance threshold due to inherent characteristics of the dataset analysed.

The absence of a behavioural effect 24 h post-TMR in both Chapters 2 and 3 remains another, perhaps more pressing issue. Given the TMR literature, as well as numerous other studies using TMR of a SRTT (Cousins et al., 2014a; Cousins et al., 2016; Koopman et al., 2020b), we had no doubt prior to the experiments that the TMR effect would emerge immediately post-sleep. We introduced the first re-test session 24 h post-TMR as a form of sanity check, but our real interest lay in what would happen afterwards. Contrary to our expectations, we provide no evidence of cueing benefit 24 h post-TMR and we suspect there could be two reasons for that. Firstly, such an unexpected finding could have occurred because our second session was scheduled in the evening, rather than in the morning as in previous studies using the same task (Cousins et al., 2014a; Cousins et al., 2016; Koopman et al., 2020b). This would suggest that TMR impacts on the targeted memories immediately after sleep, but the effects of stimulation decrease throughout the day until they are no longer evident the following evening. However, it seems unlikely that the effects would then re-emerge in the long-term, making this explanation rather implausible. Alternatively, we believe that a more compelling reason for the absence of TMR effect 24 h post-manipulation could be the jittering of TMR cues during sleep (as mentioned in the discussions of Chapters 2 and 3). In both Chapter 2 and Chapter 3, we introduced jittering instead of constant intervals between sounds to study

the temporal dynamics of memory reactivation. However, randomising the inter-trial interval also decreased predictability of sequence elements. This perhaps made it harder to consolidate the transitions that make up the sequence and could have delayed the behavioural effects of stimulation. Indeed, prior TMR studies used fixed inter-trial intervals and confirmed that cueing memory reactivation during sleep specifically acts to consolidate the sequence (Cousins et al., 2014a; Cousins et al., 2016; Koopman et al., 2020b). Furthermore, characterisation of the reactivation events from Chapter 2 revealed several interesting findings indicative of altered cue processing with jittered protocol (Abdellahi et al., 2021a). Specifically, a classifier analysis showed that reactivation did not happen immediately after a jittered cue, as shown following equally spaced sounds (Abdellahi et al., 2021b). Instead, the reactivation events were delayed and more spread-out in time (Abdellahi et al., 2021a). Although beyond the scope of this thesis, these results suggest that jittering interfered with the natural pace of the reactivation events, perhaps slowing down the consolidation process and, as a result, delayed the behavioural effects of stimulation until several weeks post-cueing (10 days in Chapter 2, 20 days in Chapter 3).

That said, this thesis demonstrates that a single night of cueing can affect memories up to 20 days post-TMR. Even if the behavioural impacts were delayed due to our jittered TMR protocol, it seems remarkable that cueing exerted its effects so long after the initial night of sleep. Our results suggest that memory reactivation is a powerful mechanism that underpins sleep-dependent consolidation in the long-term, but what exactly allows TMR impacts to emerge after so long? What is the underlying basis of the behavioural effects observed in Chapter 2 and 3?

3.2 SYNAPTIC TAGGING AND CAPTURE ALLOWS MEMORIES TO LAST

As already noted in the General Introduction to this thesis, memory literature distinguishes between synaptic (short-term) and systems (long-term) consolidation (Dudai, 2004; Frankland & Bontempi, 2005). The neuroplasticity that underpins these two types of consolidation manifests itself in many forms and at different time points following learning (Zatorre et al., 2012; Almeida & Lyons, 2017). We believe that the long-term effects of TMR observed in our studies stem from both synaptic and systems consolidation, and that they are governed by various underlying processes. Let us start by considering synaptic consolidation.

The broad timeline of activity-dependent changes, as proposed by Almeida and Lyons (2017), begins with synaptic potentiation/depression (LTP/LTD) and structural adaptations, already happening minutes after learning. According to the synaptic tagging and capture hypothesis, this stage involves molecular 'tagging' of the potentiated synapses, allowing them to capture the plasticity-related proteins (PRPs) and undergo further structural changes over time (Frey, & Morris, 1997; Redondo & Morris, 2011). Seibt and Frank (2019) propose that the tag is set during wake but the reactivation of primed neurons during NREM sleep promotes synaptic capture of the PRPs. By the same token, cueing memory reactivation during NREM sleep could have biased the PRPs capture towards the targeted memory traces in our studies by means of biasing their reactivation (Bendor & Wilson, 2012). PRP capture is followed by PRPs translation into proteins and structural plasticity. This step is thought to occur during REM sleep (Ribeiro et al., 2002) and ultimately leads to stabilisation of the tagged synapses (Seibt & Frank, 2019). In other words, the tagged and reactivated synapses persist over time which, under this framework, would explain why biasing memory reactivation using TMR also biased long-term consolidation of the targeted memories (Chapters 2 and 3). The aforementioned processes would also account for the TMR-related neuroplasticity observed in Chapter 3 and Chapter 4.

Alternatively, and in accordance with the ASC, memory reactivation during NREM sleep could itself trigger LTP at the learning-related synapses, tagging the relevant memories for later processing in subsequent REM sleep (Diekelmann & Born, 2010b). This idea seems to be supported by electrophysiological studies which suggest a particular role of sleep spindles in this process (Rosanova & Ulrich, 2005; Sejnowski & Destexhe, 2000; Werk et al., 2005; Cairney et al., 2018), in line with our own findings (Chapter 2, Chapter 3). The ASC could, however, work in concert with the SHY. That is, reactivation of memory traces during sleep may not only tag the relevant synapses for plastic changes but also protect them from global downscaling that happens during the night regardless of previous learning experience (Tononi & Cirelli, 2014). Reactivation may achieve this by either strengthening the learning-related synapses and thus putting them in a better position to survive downscaling, or by making them resistant to depression by setting a 'protective tag' at the relevant sites (see section *2.3 Synaptic Homeostasis Hypothesis)*. In this framework, one could also speculate that as long as the learning-related synapses (or even whole circuits) are (re)activated they will survive global downscaling and continue to undergo plasticity. However, the moment these connections stop being used, they will grow weaker or perhaps lose the tag, and eventually surrender to the global downscaling. This would be consistent with the Hebbian

'use it or lose it' rule (Hebb, 1955) and may explain why the behavioural effects of cueing do not survive until 6 weeks post-encoding (Chapter 2).

Regardless of when exactly the tag is set or lost, if reactivation during NREM sleep is indeed the main driver for synaptic plasticity that occurs during REM sleep, our results imply two important things. (1) Memory reactivation during NREM sleep initiates a cascade of molecular events that leads up to long-term changes at the level of behaviour; (2) The (micro)structural changes that we observe are likely to have occurred during post-learning REM sleep, even though we are unable to provide direct evidence for that. Indeed, rodent experiments implicate REM sleep in dendritic spines remodelling in motor regions following motor skill acquisition (Li et al., 2017), although NREM sleep is also thought to play a role (Yang et al., 2014). Notably though, Pereira and Lewis (2020) extend the Seibt and Frank (2019) model by suggesting further steps in the sleep-dependent consolidation process: myelination, corticalization, and reorganisation of memory traces, all mediated by REM sleep (Pereira & Lewis, 2020). This brings us to the long-term plasticity and the dynamics of systems consolidation in sleep-dependent memory processing.

3.3 SYSTEMS CONSOLIDATION DISTRIBUTES MEMORY TRACES

So far, we have seen how synaptic consolidation could account for the reactivation-mediated long-term consolidation of memories observed in this thesis (Chapter 2 and Chapter 3). However, the model does not clarify why we observed plasticity in different brain regions and at different points in time following learning (Chapter 3 and Chapter 4). These results could be explained by the two-stage model of memory consolidation which postulates that memories are re-coded from a fast-learning short-term store (e.g., hippocampus) to a slow-learning long-term store (e.g., neocortex), wherein they are stabilised, reprocessed, and integrated into the pre-existing schemas (Marr, 1970; Squire & Alvarez, 1995) (see *General Introduction*, section *3.1.3 Memory Consolidation*). The model sets the origin of the ASC which posits that memory reactivation during NREM sleep is essential for this process (Born et al., 2006; Diekelmann & Born, 2010b).

Although there is an ongoing debate as to when system consolidation kicks in, it could perhaps be indexed by hippocampal disengagement. Our own results suggest that hippocampus decreases in grey matter volume overnight, and that this reduction correlates with the amount of time spent in N2 (Chapter 4). Although the diminishing contribution of

hippocampus with NREM sleep fits well with the ASC, it is important to stress that we do not report a direct link between sleep and *TMR-related* structural alteration in this region. In other words, we cannot argue that memory reactivation alters hippocampal function or structure, despite the ASC assumptions. Some of the potential reasons could be that our MRI metrics were not sensitive enough to detect hippocampal plasticity or that the hippocampus is not involved in consolidation of our task. However, neither of these possibilities agrees with the existing literature. Firstly, Sagi et al. (2012) were able to detect microstructural changes in hippocampus 2 h after learning using the same DW-MRI metric (mean diffusivity) as we used in Chapter 4. Secondly, hippocampus has been implicated in SRTT consolidation (Albouy et al., 2008; Albouy et al., 2013a; Albouy et al., 2013b; Albouy et al., 2015), whereas a previous study from our lab showed that SWS is associated with a TMR-related functional engagement of hippocampus the morning after learning (Cousins et al., 2016). Thus, alternatively, hippocampus could have undergone plasticity only within the first few hours post-learning (Brodt et al., 2018), during which we did not collect any MRI data. Indeed, hippocampus could have engaged immediately after encoding and then disengaged during the first night of sleep, resulting in no net change between the pre- and post-sleep sessions. Although this would be consistent with the ASC, and perhaps also SHY, the literature reports mixed evidence regarding hippocampal involvement in memory consolidation over time. On the one hand, a decrease in hippocampal responses has been observed both after learning followed by a single night of sleep and over longer periods of time (Durrant et al., 2013; Takashima et al., 2006). In fact, both sleep spindles and slow wave sleep duration have been shown to predict hippocampal disengagement after post-learning sleep (Hennies et al., 2016; Takashima et al., 2006). On the other hand, proponents of the Multiple Trace Theory (MTT) argue that episodic memories rely on the medial temporal lobe across their entire lifespan (Nadel & Moscovitch, 1997). Evidence also exists for an increase, rather than a decrease, in hippocampal response after learning followed by 12 h of sleep compared to wake (Lewis et al., 2011a; Lewis et al., 2011b), with enhanced hippocampal responses up to 48 h after learning (Gais et al., 2007). Nevertheless, the complete lack of MRI findings within the hippocampus in this thesis was unexpected and could perhaps be explained by the lack of sufficient temporal resolution of our experiments. It also provides an exciting avenue for further research into the reactivation-mediated hippocampal plasticity after motor sequence learning.

While we find no evidence for hippocampal contribution to sleep-dependent consolidation of motor memory traces, we report reactivation-mediated functional and microstructural

changes in a subregion of posterior parietal cortex (i.e., precuneus) as early as within 24 h post-encoding (Chapter 3 and Chapter 4). These results challenge the traditional model of systems consolidation which is generally thought to require several days or weeks to complete (Frankland & Bontempi, 2005; Dudai, 2004). Although the precise onset of cortical consolidation is difficult to pinpoint, several studies have now shown that neocortex is capable of accelerated consolidation, e.g., in the presence of a pre-existing schema (Tse et al., 2007; Tse et al., 2011) or during a high cognitive demand (Quillfeldt, 2019). In fact, recent reports suggest that memories can be encoded in precuneus within hours (Brodt et al., 2018; Brodt et al., 2016). Our findings extend the existing literature by arguing that memory reactivation plays a key role in this rapid consolidation process. Indeed, the structural and microstructural changes that we show in Chapters 3 and 4 constitute the first demonstration of TMR-mediated physical changes in the underlying neural substrate that support long-term memory storage. But precisely which neural processes could underpin offline skill learning?

In Chapter 4 we propose several biological processes that could have given rise to the (micro)structural plasticity observed not only in precuneus, but also in striatum and sensorimotor cortex. Although histological studies would need to confirm our speculations, the potential candidates for the reactivation-mediated changes in our diffusion metrics include: remodelling of the cylindrical tissue compartments (e.g., neuronal and glial processes) (Theodosis et al., 2008; Blumenfeld-Katzir et al., 2011; Xu et al., 2009); increase in brain-derived neurotrophic factor (BDNF) expression, number of synaptic vesicles and astrocytes activation (Sagi et al., 2012); swelling of cells (particularly astrocytes) (Macvicar et al., 2002; Kleim et al., 2007), and synaptogenesis (Kleim et al., 2004). Although in this thesis we did not examine post-TMR changes in myelin-sensitive markers, we cannot exclude the possibility that memory reactivation also leads to alterations in myelin content, as well as axonal morphology and density. This is especially true given that myelin is known to correlate with mean diffusivity (Peters et al., 2019), one of the metrics used in Chapter 4. New oligodendrocytes can differentiate within hours, providing metabolic support to the nearby axons in the order of days, while myelin formation and axon remodelling are thought to underlie long-term neuroplasticity that emerges over days and weeks (Almeida & Lyons, 2017). REM sleep has been shown to promote oligodendrocyte activity (Bellesi et al., 2013) and myelin production (de Vivo & Bellesi, 2019), consistent with the notion that the observed (micro)structural changes could have occurred during the post-learning REM sleep.

Apart from re-coding of memories from their short- to long-term store, this later stage of (sleep-dependent) consolidation also involves reorganisation of memory traces and their integration into the pre-existing networks (Marr, 1970; Squire & Alvarez, 1995; Pereira & Lewis, 2020). Indeed, in Chapters 3 and 4 we demonstrate that TMR can engender structural and microstructural changes at several cortical sites, perhaps indicating that memory reactivation plays a key role in redistribution and reorganisation of memory representations across the cortex. This takes us from the memory-processing function of sleep to the sleep-dependent development and evolution of memory engrams.

3.4 MEMORY REACTIVATION DURING SLEEP FOSTERS ENGRAM FORMATION

We demonstrate a dynamic contribution of striatum, precuneus, and sensorimotor cortex to the behavioural emergence of TMR effects (Chapter 3, Chapter 4). Due to the widely distributed nature of the observed plasticity, we argue that reactivating memories during sleep is instrumental for the development and evolution of memory engrams. The term 'engram' was originally used to refer to an "enduring though primarily latent modification in the irritable substance produced by a stimulus" (Semon, 1921). Put simply, a memory engram refers to the physical trace of a memory, a learning-induced change in the neural substrate that is causal for storing and recalling past events (Tonegawa et al., 2018; Josselyn & Tonegawa, 2020). The current understanding is that memories are stored in the synaptic connections between populations of neurons (i.e., neuronal ensembles) that are widely distributed throughout the brain (Josselyn & Tonegawa, 2020; Dudai, 2004; Josselyn et al., 2015; Semon, 1921). Thus, memory engrams often encompass several brain regions, while the ongoing process of systems consolidation makes them a moving target over time (Josselyn et al., 2015). This distributed and dynamic nature presents a particular challenge to capture and characterise memory engrams. In an attempt to evaluate recent experimental evidence for uncovering the engram, Josselyn et al. (2015) proposed four defining criteria of an engram. First, a memory engram must emerge as a result of a specific experience and reflect its consent (criterion 1: content). Second, it has to engender a persistent change in the brain (criterion 2: persistence). Third, reactivation of an engram enables memory retrieval and can thereby impact on behaviour (criterion 3: ecphory). Fourth, a memory engram must endure over time, existing in a dormant state between encoding and retrieval episodes (criterion 4: dormancy). Any change within a neural substrate that conforms to these criteria can be regarded as a memory engram.

Several different brain regions have been identified as memory engrams for various tasks and at different stages of their consolidation (Miry et al., 2021; Brodt et al., 2018; Josselyn & Tonegawa, 2020; Josselyn et al., 2015; Brodt & Gais, 2021). In the procedural domain, neuroplasticity following motor skill acquisition has been particularly well characterised (King et al., 2017; Seidler, 2010; Lage et al., 2015; Hardwick et al., 2013; Janacsek et al., 2020; Doyon et al., 2009; Wang, et al., 2014; Albouy et al., 2008). The contribution of different brain regions varies considerably between the different stages of procedural learning (Dayan & Cohen, 2011; Costa et al., 2004), with further evidence suggesting a dynamic shift in neuronal representations of the internal model over time (Shadmehr & Holcomb, 1997; Monfils et al., 2005). The role of sleep and memory reactivation during sleep in (motor) engram development has been speculated (King et al., 2017; Tonegawa et al., 2018; Josselyn et al., 2015; Josselyn & Tonegawa, 2020), but direct evidence had so far been lacking. Our results from Chapters 3 and 4 provide considerable insight into the sleep-dependent formation and evolution of a motor engram over time. If our findings are considered collectively, we argue that precuneus and sensorimotor cortex fulfil all four criteria for an engram, and thus add to the current understanding of the role of reactivation during sleep in memory consolidation.

3.4.1 MEMORY ENGRAM IN PRECUNEUS

Let us consider precuneus first. In Chapter 3 we demonstrate that TMR leads to increased precuneus activation for the cued vs uncued sequence the next day, the extent of which predicts behavioural benefits of stimulation at the same time point. These results suggest that memory representations stored in precuneus not only reflect the encoded information (criterion 1: content) but can also impact on behaviour (criterion 3: ecphory). Our results from Chapter 4 further suggest that memory reactivation engenders physical, microstructural plasticity within precuneus (criterion 2: persistence), that continues days after the initial encoding and can be measured in between retest sessions (criterion 4: dormancy). Thus, our findings satisfy all defining criteria for an engram (Josselyn et al., 2015), suggesting that (targeted) memory reactivation supports engram formation in precuneus. But why would a motor memory engram develop in this particular region? And why did precuneus respond to cueing motor memory reactivation in the first place?

Precuneus constitutes a subregion of the posterior parietal cortex (PPC) which has received increasing attention in the context of memory storage and retrieval (Wagner et al., 2005; Myskiw & Izquierdo, 2012; Gilmore et al., 2015). PPC is traditionally associated with motor

function (Shadmehr & Holcomb, 1997) and is known to be involved in movement planning (Cohen, & Andersen, 2002) and motor execution (Zhang & Chiang-shan, 2012). This could indicate that the representations harboured within precuneus facilitate the initial phase of a movement. Thus, an increase in precuneus activation for the cued vs uncued sequence (Chapter 3) could simply reflect a difference in execution time between the two sequences. However, PPC's engagement in motor imagery (Zhang & Chiang-shan, 2012) suggests that it may be well suited for offline rehearsal, perhaps even participating in reactivation of motor memories during sleep (Himmer et al., 2021). Indeed, the central function of the PPC, including precuneus itself, is undeniably memory retrieval (Wagner et al., 2005; Cabeza et al., 2008). The functional involvement of precuneus during memory recall (including our own observations in Chapter 3) could arise from the region being able to either hold memory representation (Vilberg & Rugg, 2008) or bind its distributed traces (Shimamura, 2011). The latter is especially notable given that precuneus is considered a critical node for memory processing (Hebscher et al., 2019) that is tightly interconnected with multiple brain areas (Buckner et al., 2008; Zhang & Chiang-shan, 2012). This puts it in an excellent position to act as a convergence zone for distributed memory traces and functions, alongside other regions of the parietal memory network (Gilmore et al., 2015). In light of our fMRI findings (Chapter 3), it would be reasonable to conclude that TMR triggered reactivation of the targeted sequence either in precuneus itself, as recently suggested (Himmer et al., 2021), or in its upstream regions, which led to increased activation and thus preferential processing of the cued sequence within precuneus. This, in turn, could give rise to the behavioural effects observed in Chapters 2 and 3. However, given the microstructural plasticity observed in precuneus in this thesis (Chapter 4), as well as in the literature (Brodt et al., 2018), we believe that the role of precuneus goes beyond just memory retrieval and processing. Instead, we argue that precuneus could act as a transient storage site, building up physical representations of the retrieved memories before they are transferred to a more permanent location.

PPC has already been identified as a hippocampus-independent cortical memory store (Brodt et al., 2016) that can harbour behaviourally relevant memory representations (Brodt et al., 2016; Jeong & Xu, 2016). Crucially though, precuneus fulfils all criteria for an engram which developed rapidly (i.e., within 2 h post-learning) and in response to repeated encoding-retrieval epochs during wake (Brodt et al., 2018). Such an intensive rehearsal of the learned material closely resembles memory reactivation during sleep (Himmer et al., 2019), which inspired our own search for an engram in this region. Consequently, we show that repeated

reactivation of a motor memory trace during sleep also engenders a memory engram in precuneus (Chapter 3, Chapter 4). However, we hypothesise that its contribution to long-term consolidation changes over time, in keeping with the dynamic and distributed nature of memory engrams (Josselyn et al., 2015). In Chapter 4, we report continuous microstructural plasticity (i.e., over the whole course of the study) spanning the entire region of interest that was associated with the emergence of cueing benefit in the long run. However, in Chapter 3, we show that the long-term cueing benefit is also facilitated by a functional *disengagement* of ventral precuneus from 24 h to 10 days post-encoding. This suggests that as the ventral precuneus disengages, it perhaps allows other regions to take over its role. It also suggests that the microstructural plasticity that we report in Chapter 4 could reflect strengthening of the underlying memory representations as much as their weakening. Thus, our results suggest that precuneus may be particularly involved in early consolidation of memories that are reactivated during sleep. As the time passes, we believe that the information housed within precuneus is either transferred to a more permanent storage site, or that the engram becomes distributed over several task-related regions that specialise in different functions (Josselyn & Tonegawa, 2020; Zelikowsky et al., 2014). Our results from Chapters 3 and 4 suggest that sensorimotor cortex is the candidate region for long-term retention of motor engram ensembles.

3.4.2 MEMORY ENGRAM IN SENSORIMOTOR CORTEX

In Chapter 3 we find that an increased activation of the postcentral gyrus during cued vs uncued sequence performance 10 days post-encoding is associated with long-term cueing benefit. This result provides evidence that addresses both the content (criterion 1) and the ecphory (criterion 3) criteria for defining a memory engram (Josselyn et al., 2015). We further show that the long-term-cueing benefit also correlates with an increase in grey matter volume of precentral gyrus (Chapter 3) and microstructural plasticity in pre- and post-central gyri (Chapter 4), thus satisfying the persistence criterion (criterion 2). Since both the volumetric change and the microstructural plasticity were measured in between retest sessions, we believe that sensorimotor cortex fulfils the dormancy criterion as well (criterion 4). Taken together, our results suggest that repeated reactivation of a motor memory trace fosters gradual development of memory engram in sensorimotor cortex, thereby supporting long-term retention of motor skills.

The contribution of sensorimotor cortex to memory consolidation was somehow expected, given the procedural nature of our task. Precentral gyrus (i.e., the primary motor cortex, or M1) is a strong candidate for a motor engram hub (Ganguly & Carmena, 2009; Gao et al., 2018; Hwang et al., 2021) and its slow reorganisation after learning has already been linked to the long-term retention of motor skills (Kami et al., 1995; Matsuzaka et al., 2007; Kleim et al., 2004). In light of the results that emerge from this thesis, we think that memory reactivation during sleep plays a key role in the gradual development of a long-lasting motor engram in M1. Furthermore, if memory reactivation or processing of the targeted memories continues during subsequent nights of sleep it could further impact on the engram, perhaps refining its neuronal activity patterns (Peters et al., 2014) or fostering selective synaptic plasticity as in wake (Hwang et al., 2021). In fact, motor skill acquisition occurs through dynamic reorganisation of motor memory representations in M1 (Monfils et al., 2005), particularly in the late stage of motor learning (Kleim et al., 2004). Thus, the late microstructural plasticity that we report in Chapter 4 could reflect the ongoing reorganisation of the cued sequence motor map that parallels the gradual development of behavioural cueing benefit (Chapter 3). As the topography of the map becomes more spatially complex and defined, so does the capacity for skilled movements (Monfils et al., 2005). This, in turn, could drive the emergence of a group level effect in our behavioural data in the long term (Chapter 3).

Although speculative, this scenario is consistent with the role of sleep in reorganisation of memory traces (Landmann et al., 2015; Landmann et al., 2014; Lewis & Durrant, 2011; Lewis et al., 2018). Sleep literature also highlights the role of memory reactivation during NREM sleep in schema formation and integration (Landmann et al., 2014; Lewis & Durrant, 2011). In the motor domain, sleep is known to facilitate development of a goal-based component (Robertson, 2009; Cohen et al., 2005; Albouy et al., 2013c) that is thought to reflect the abstracted 'gist' of the task, or the procedural schema (Landmann et al., 2014). Integration of new motor information into the pre-existing schemas also occurs overnight (e.g., for motor sequences see King et al., 2019). The role of NREM sleep in gist abstraction is further supported by the observation that TMR of an implicitly learned SRTT during NREM sleep promotes explicit knowledge of the targeted sequence the next day (Cousins et al., 2014a). Contrary to that finding, we show no difference between the explicit memory for the cued and uncued sequence (Chapter 2, Chapter 3). This could be an unintended consequence of including the imagery task during our training session, thereby facilitating the explicit knowledge gain for both sequences before sleep (Koopman et al., 2020a). However, the

absence of a TMR effect to explicit knowledge could also be explained by the fact that our explicit memory task was delivered relatively late post-TMR (six weeks for Chapter 2 and twenty days for Chapter 3 vs 24 h for Cousins et al., 2014a). It is possible that the explicit knowledge for the cued sequence was gained initially (as in Cousins et al., 2014a), but further reorganisation of the SRTT schema over time facilitated the emergence of explicit knowledge for the other sequence as well. Both of these scenarios would explain the above-chance explicit memory of the two sequences at the end of each study (Chapter 2, Chapter 3). Nevertheless, it remains unclear whether (micro)structural plasticity of M1 (Chapter 3, Chapter 4) could have supported gist abstraction in this case, or whether other brain regions were involved.

Together, the results presented throughout this thesis indicate that memory reactivation has a powerful impact on memories. Its effects extend beyond simply processing the learned information to include redistribution and restructuring of memory traces across the cortex. We further argue that repeated reactivation of a memory trace engenders engram development, and that precuneus and sensorimotor cortex constitute important neocortical memory hubs that support long-term retention of procedural memories.

4 LIMITATIONS OF THE EXPERIMENTS

As a final discussion point of this thesis, I would like to bring attention to some important limitations of this thesis and thereby provide a more balanced view of the reported results. First, given a relatively small sample size of the experiments, which differed between 14 and 30 depending on the experimental chapter and analysis (Chapter 2: 14-18 participants; Chapter 3: 21-30 participants; Chapter 4: 15-29 participants), the issue of statistical power must be brought up. Statistical power is the probability of correctly rejecting the null hypothesis given the sample size at hand (Dorey, 2011). A lack of sufficient power contributes to the reproducibility crisis which remains a persistent issue in science (Vankov et al., 2014). The importance of large samples seems to be especially relevant in neuroimaging, where inflated effect sizes are particularly common (Turner et al., 2018; Marek et al., 2022). Most sleep studies are underpowered as well, which cast doubt not only on the findings arising from this thesis but also the sleep field in general.

Second, the work conducted in this thesis lacks sufficient number of control conditions which makes the interpretation of some results challenging. For example, an adaptation night with

control sounds that had not yet been associated with the task (as in Koopman et al., 2020) would help disentangle neural processing of the cues from the brain response to any sound, regardless its salience or meaning (see section *2.2 Active Systems Consolidation Hypothesis*). Likewise, a control group with no TMR during the night would allow for a between-participants study design and thus a direct comparison between brain (micro)structure of the TMR and no-TMR group. Instead, the analyses on the MRI data collected from the TMR group only limited the experimental questions to a *correlational relationship* between TMR and brain characteristics.

Lastly, the experiment forming Chapters 3 and 4 would benefit from an fMRI scan encompassing the whole SRTT session, as well as additional scans at more frequent time points. Functional assessment throughout the behavioural sessions would eliminate the need for splitting the SRTT in half, and thus reduce experimental noise. An additional scan at day 20 would let us determine the impact of (micro)structural plasticity directly preceding the emergence of behavioural benefit, as well as functional activity during the SRTT performance. Furthermore, continuous assessment of brain function during the stimulation night would not only provide sufficient temporal resolution to determine if early hippocampal engagement contributed to long-term behavioural effects observed, but also allow to examine BOLD activity during sleep – something that was not possible with the current design.

5 OPEN QUESTIONS AND FUTURE DIRECTIONS

Throughout this discussion I have suggested some directions for future research. Although the experiments conducted in this thesis taught us a whole lot about how memory reactivation during sleep impacts on brain plasticity and function in the long term, they also uncovered several open questions that remain in the field. Is sensorimotor cortex the ultimate memory hub of procedural learning? What happens to these memory traces over even longer periods of time? And does TMR of other types of memories impact on other brain networks in a similar manner? These are only a few of the unknowns that arise from our findings, and which will require a great deal of research to solve. In this section, I will highlight some potential avenues for exploration in the future.

An exciting research challenge that emerges from the work presented in this thesis is to explore more detailed synaptic, cellular and circuit level changes that underpin the

microstructural findings of Chapter 4. Although we propose several biological processes that could have given rise to observed plasticity, histological studies are required to make direct links between DW-MRI measures and the underlying tissue modification. This also ties in with the SHY postulates (Tononi & Cirelli, 2014), which could not be tested using the imaging methods employed in this thesis. Two-photon imaging, for instance, constitutes a promising tool to track the evolution of reactivated ensembles at a single spine resolution (Miyamoto et al., 2021). When combined with genetic and pharmacological approaches, it could also allow us to determine if synaptic tagging and capture contributes to the remarkable benefits of memory reactivation during sleep (Seibt & Frank, 2019).

The role of sleep, particularly REM sleep, during post-stimulation night and its electrophysiological characteristics in the long-term effects of TMR remains another open question. A similar study to the one conducted in Chapter 3 and 4 but with continuous sleep recordings throughout its duration could be undertaken to determine when the delayed effects of sleep are taking place (Pereira & Lewis, 2020). REM sleep has been repeatedly implicated in myelination, corticalization, and reorganisation of memory traces (Li et al., 2017; Bellesi et al., 2013; de Vivo & Bellesi, 2019; Almeida-Filho et al., 2018; Landmann et al., 2015; Bridi et al., 2015) and therefore could have contributed to the long-term effects of TMR reported in this thesis. Yet, our results from Chapter 4 suggest that stage 2 of NREM sleep may be important in shaping grey matter microstructure early in the consolidation process. This, however, requires further investigation. Likewise, we cannot rule out that some of the (micro)structural changes that we observe in Chapters 3 and 4 occurred in wake (Bellesi & de Vivo, 2020). In fact, there still is an ongoing controversy regarding whether synapses undergo potentiation during wake (Tononi & Cirelli, 2014) or sleep (Rasch & Born, 2013). Further research into the longitudinal changes following memory reactivation will be necessary to clarify these issues.

In relation to the null behavioural findings 24 h post-TMR in Chapters 2 and 3, we discussed the impact of cue jittering on the delayed effects of TMR (section *3.1 Behavioural effects of TMR over time*). Currently, there is little work on how the cueing procedure itself could affect TMR's success. Neither the number of items (Schechtman et al., 2021) nor the number cues per item (Schechtman et al., 2020) seem to affect the behavioural benefits of cueing. The impact of temporal parameters of TMR has not been yet investigated, but our work suggests that it may affect cue processing (Abdellahi et al., 2021a), perhaps interfering with the natural pace of the reactivation events. This raises an important question: is TMR really

biasing reactivation, or could it interfere with it? And are the mechanisms underlying TMR and endogenous memory reactivation truly the same? To date, several studies demonstrated that TMR can not only boost memories but also intentionally promote forgetting (Simon et al., 2018; Oudiette et al., 2014), and unintentionally decrease retention of the overlapping memories (Joensen et al., 2022). This indicates that TMR could indeed interfere with the consolidation process. Alternatively, it could also override the selective mechanism of sleep-dependent memory processing (Stickgold & Walker, 2013). The latter is especially notable given that cueing memory reactivation during sleep was shown to rescue low-value memories from forgetting (Oudiette et al., 2013), which suggests that TMR can interact with the mechanism that tags memories for forgetting (Stickgold & Walker, 2013; Saletin et al., 2011). In sum, understanding the relationship between the cueing procedure and memory consolidation, as well as the parallels between spontaneous and targeted memory reactivation have still a long way to go.

6 CONCLUSION

This thesis investigated the long-term consolidation and neuro-plastic evolution of memories that are reactivated during sleep. By combining TMR with multimodal neuroimaging techniques we provide converging evidence for memory reactivation in NREM sleep as a powerful mechanism to shape memory representations over time and throughout the cortex. Our findings demonstrate that just one night of procedural TMR can impact on the (micro)structure and function of memory and motor systems, facilitating the development of a stable trace over subsequent nights of un-manipulated sleep. We believe that these long-lasting effects of TMR stem from both synaptic and systems consolidation, and that reactivation during sleep could be instrumental for the formation and evolution of memory engrams. Together, this thesis provides a critical piece in the long-standing puzzle of sleep-dependent consolidation in the long run, though further research is needed to establish the exact mechanisms of how sleep selects and retains memories for a lifetime

REFERENCES

Abdellahi, E., A., M. (2021a). Chapter 4: The effect of temporal jittering of cues on TMR reactivation in SWS sleep. In *Detecting neural replay in sleep with EEG classifiers.* [Unpublished doctoral thesis]. Cardiff University, United Kingdom.

Abdellahi, M. E., Koopman, A. C., Treder, M. S., & Lewis, P. A. (2021b). Targeting targeted memory reactivation: characteristics of cued reactivation in sleep. *bioRxiv*.

Abraham, W. C., Logan, B., Greenwood, J. M., & Dragunow, M. (2002). Induction and experience-dependent consolidation of stable long-term potentiation lasting months in the hippocampus. *Journal of Neuroscience*, *22*(21), 9626-9634.

Aeschbach, D., Cutler, A. J., & Ronda, J. M. (2008). A role for non-rapid-eye-movement sleep homeostasis in perceptual learning. *Journal of Neuroscience*, *28*(11), 2766-2772.

Afzali, M., Pieciak, T., Newman, S., Garyfallidis, E., Özarslan, E., Cheng, H., & Jones, D. K. (2021). The sensitivity of diffusion MRI to microstructural properties and experimental factors. *Journal of Neuroscience Methods*, *347*, 108951.

Ai, S., Yin, Y., Chen, Y., Wang, C., Sun, Y., Tang, X., ... & Shi, J. (2018). Promoting subjective preferences in simple economic choices during nap. e*life*, *7*, e40583

Alberini, C. M., & LeDoux, J. E. (2013). Memory reconsolidation. *Current Biology*, *23*(17), R746-R750.

Albouy, G., Fogel, S., King, B. R., Laventure, S., Benali, H., Karni, A., ... & Doyon, J. (2015). Maintaining vs. enhancing motor sequence memories: respective roles of striatal and hippocampal systems. *Neuroimage*, *108*, 423-434.

Albouy, G., Fogel, S., Pottiez, H., Nguyen, V. A., Ray, L., Lungu, O., ... & Doyon, J. (2013c). Daytime sleep enhances consolidation of the spatial but not motoric representation of motor sequence memory. *PloS one*, *8*(1), e52805.

Albouy, G., King, B. R., Maquet, P., & Doyon, J. (2013a). Hippocampus and striatum: Dynamics and interaction during acquisition and sleep-related motor sequence memory consolidation. *Hippocampus*, *23*(11), 985-1004.

Albouy, G., Ruby, P., Phillips, C., Luxen, A., Peigneux, P., & Maquet, P. (2006). Implicit oculomotor sequence learning in humans: Time course of offline processing. *Brain research*, *1090*(1), 163-171.

Albouy, G., Sterpenich, V., Balteau, E., Vandewalle, G., Desseilles, M., Dang-Vu, T., ... & Peigneux, P. (2008). Both the hippocampus and striatum are involved in consolidation of motor sequence memory. *Neuron*, *58*(2), 261-272.

Albouy, G., Sterpenich, V., Vandewalle, G., Darsaud, A., Gais, S., Rauchs, G., ... & Maquet, P. (2013b). Interaction between hippocampal and striatal systems predicts subsequent consolidation of motor sequence memory. *PloS one*, *8*(3), e59490.

Almeida-Filho, D. G., Queiroz, C. M., & Ribeiro, S. (2018). Memory corticalization triggered by REM sleep: mechanisms of cellular and systems consolidation. *Cellular and Molecular Life Sciences*, *75*(20), 3715-3740.

Almeida, R. G., & Lyons, D. A. (2017). On myelinated axon plasticity and neuronal circuit formation and function. *Journal of Neuroscience*, *37*(42), 10023-10034.

Ambrosini, M. V., & Giuditta, A. (2001). Learning and sleep: the sequential hypothesis. *Sleep medicine reviews*, *5*(6), 477-490.

Ambrosini, M. V., Langella, M., Carnevale, U. G., & Giuditta, A. (1992). The sequential hypothesis of sleep function. III. The structure of postacquisition sleep in learning and nonlearning rats. *Physiology & behavior*, *51*(2), 217-226.

Ambrosini, M. V., Mariucci, G., Bruschelli, G., Colarieti, L., & Giuditta, A. (1995). Sequential hypothesis of sleep function. V. Lengthening of post-trial SS episodes in reminiscent rats. *Physiology & behavior*, *58*(5), 1043-1049.

Ambrosini, M. V., Sadile, A. G., Carnevale, U. G., Mattiaccio, A., & Giuditta, A. (1988b). The sequential hypothesis on sleep function. II. A correlative study between sleep variables and newly synthesized brain DNA. *Physiology & behavior*, *43*(3), 339-350.

Ambrosini, M. V., Sadile, A. G., Carnevale, U. G., Mattiaccio, M., & Giuditta, A. (1988a). The sequential hypothesis on sleep function. I. Evidence that the structure of sleep depends on the nature of the previous waking experience. *Physiology & behavior*, *43*(3), 325-337.

Amzica, F., & Steriade, M. (1996). Progressive cortical synchronization of ponto-geniculo-occipital potentials during rapid eye movement sleep. *Neuroscience*, *72*(2), 309-314

Amzica, F., & Steriade, M. (1997). The K-complex: its slow (< 1-Hz) rhythmicity and relation to delta waves. *Neurology*, *49*(4), 952-959.

Amzica, F., & Steriade, M. (1998). Electrophysiological correlates of sleep delta waves. *Electroencephalography and clinical neurophysiology*, *107*(2), 69-83.

Anaya, E. M., Pisoni, D. B., & Kronenberger, W. G. (2017). Visual-spatial sequence learning and memory in trained musicians. *Psychology of music*, *45*(1), 5-21.

Andrillon, T., Pressnitzer, D., Léger, D., & Kouider, S. (2017). Formation and suppression of acoustic memories during human sleep. *Nature communications*, *8*(1), 1-15.

Antonenko, D., Diekelmann, S., Olsen, C., Born, J., & Mölle, M. (2013). Napping to renew learning capacity: enhanced encoding after stimulation of sleep slow oscillations. *European Journal of Neuroscience*, *37*(7), 1142-1151.

Antony, J. W., Ferreira, C. S., Norman, K. A., & Wimber, M. (2017). Retrieval as a Fast Route to Memory Consolidation. *Trends in Cognitive Sciences*, *21*(8), 573–576.

Antony, J. W., Gobel, E. W., O'hare, J. K., Reber, P. J., & Paller, K. A. (2012). Cued memory reactivation during sleep influences skill learning. *Nature neuroscience*, *15*(8), 1114-1116.

Antony, J. W., Piloto, L., Wang, M., Pacheco, P., Norman, K. A., & Paller, K. A. (2018). Sleep spindle refractoriness segregates periods of memory reactivation. *Current Biology*, *28*(11), 1736-1743.

Arzi, A., Shedlesky, L., Ben-Shaul, M., Nasser, K., Oksenberg, A., Hairston, I. S., & Sobel, N. (2012). Humans can learn new information during sleep. *Nature neuroscience*, *15*(10), 1460-1465.

Ashburner, J. (2007). A fast diffeomorphic image registration algorithm. *Neuroimage*, *38*(1), 95-113.

Ashburner, J. (2007). A fast diffeomorphic image registration algorithm. *Neuroimage*, *38*(1), 95-113.

Ashburner, J. (2010). *VBM Tutorial*. *Wellcome Trust Centre for Neuroimaging, London, UK*. Retrieved from http://www.fil.ion.ucl.ac.uk/~john/misc/VBMclass10.pdf

Ashburner, J., & Friston, K. J. (2000). Voxel-based morphometry—the methods. *Neuroimage*, *11*(6), 805-821.

Ashburner, J., & Friston, K. J. (2005). Unified segmentation. *Neuroimage*, *26*(3), 839-851.

Assaf, Y., Freidlin, R. Z., Rohde, G. K., & Basser, P. J. (2004). New modeling and experimental framework to characterize hindered and restricted water diffusion in brain white matter. *Magnetic Resonance in Medicine: An Official Journal of the International Society for Magnetic Resonance in Medicine*, *52*(5), 965-978.

Assefa, S. Z., Diaz-Abad, M., Wickwire, E. M., & Scharf, S. M. (2015). The functions of sleep. *AIMS Neuroscience*, *2*(3), 155-171.

Barakat, M., Carrier, J., Debas, K., Lungu, O., Fogel, S., Vandewalle, G., ... & Doyon, J. (2013). Sleep spindles predict neural and behavioral changes in motor sequence consolidation. *Human brain mapping*, *34*(11), 2918-2928.

Barakat, M., Doyon, J., Debas, K., Vandewalle, G., Morin, A., Poirier, G., ... & Carrier, J. (2011). Fast and slow spindle involvement in the consolidation of a new motor sequence. *Behavioural brain research*, *217*(1), 117-121.

Barco, A., Bailey, C. H., & Kandel, E. R. (2006). Common molecular mechanisms in explicit and implicit memory. *Journal of neurochemistry*, *97*(6), 1520-1533.

Barnes, D. C., & Wilson, D. A. (2014). Slow-wave sleep-imposed replay modulates both strength and precision of memory. *Journal of Neuroscience*, *34*(15), 5134-5142.

Baron, R. M., & Kenny, D. A. (1986). The moderator–mediator variable distinction in social psychological research: Conceptual, strategic, and statistical considerations. *Journal of Personality and Social Psychology*, *51*(6), 1173–1182.

Barrett, T. R., & Ekstrand, B. R. (1972). Effect of sleep on memory: III. Controlling for time-of-day effects. *Journal of experimental psychology*, *96*(2), 321.

Bates, D., Mächler, M., Bolker, B., Walker, S. (2015). Fitting Linear Mixed-Effects Models Using lme4. J. *Stat. Softw*. 67, 1–48.

Battaglia, F. P., Sutherland, G. R., Cowen, S. L., Mc Naughton, B. L., & Harris, K. D. (2005). Firing rate modulation: a simple statistical view of memory trace reactivation. *Neural networks*, *18*(9), 1280-1291.

Batterink, L. J., Creery, J. D., & Paller, K. A. (2016). Phase of spontaneous slow oscillations during sleep influences memory-related processing of auditory cues. *Journal of Neuroscience*, *36*(4), 1401-1409.

Belal, S., Cousins, J., El-Deredy, W., Parkes, L., Schneider, J., Tsujimura, H., ... & Lewis, P. (2018). Identification of memory reactivation during sleep by EEG classification. *Neuroimage*, *176*, 203-214.

Bellesi, M., & de Vivo, L. (2020). Structural synaptic plasticity across sleep and wake. *Current Opinion in Physiology*, *15*, 74-81.

Bellesi, M., Pfister-Genskow, M., Maret, S., Keles, S., Tononi, G., & Cirelli, C. (2013). Effects of sleep and wake on oligodendrocytes and their precursors. *Journal of Neuroscience*, *33*(36), 14288-14300.

Benchenane, K., Peyrache, A., Khamassi, M., Tierney, P. L., Gioanni, Y., Battaglia, F. P., & Wiener, S. I. (2010). Coherent theta oscillations and reorganization of spike timing in the hippocampal-prefrontal network upon learning. *Neuron*, *66*(6), 921-936.

Bendor, D., & Wilson, M. A. (2012). Biasing the content of hippocampal replay during sleep. *Nature neuroscience*, *15*(10), 1439-1444.

Benjamini, Y., & Hochberg, Y. (1995). Controlling the False Discovery Rate: A Practical and Powerful Approach to Multiple Testing. *Journal of the Royal Statistical Society: Series B (Methodological)*, *57*(1), 289–300.

Berens, P. (2009). CircStat: a MATLAB toolbox for circular statistics. *Journal of statistical software*, *31*(1), 1-21.

Berger, H. (1929). Über das elektroenkephalogramm des menschen. *Archiv für psychiatrie und nervenkrankheiten*, *87*(1), 527-570.

Bergmann, T. O., Mölle, M., Diedrichs, J., Born, J., & Siebner, H. R. (2012). Sleep spindle-related reactivation of category-specific cortical regions after learning face-scene associations. *Neuroimage*, *59*(3), 2733-2742.

Berry, R. B., Gamaldo, C. E., Harding, S. M., Brooks, R., Lloyd, R. M., Vaughn, B. V., & Marcus, C. L. (2015). AASM Scoring Manual Version 2.2 Updates: New Chapters for Scoring Infant Sleep Staging and Home Sleep Apnea Testing. *Journal of Clinical Sleep Medicine*, *11*(11), 1253–1254.

Blumenfeld-Katzir, T., Pasternak, O., Dagan, M., & Assaf, Y. (2011). Diffusion MRI of structural brain plasticity induced by a learning and memory task. *PloS one*, *6*(6), e20678.

Bönstrup, M., Iturrate, I., Hebart, M. N., Censor, N., & Cohen, L. G. (2020). Mechanisms of offline motor learning at a microscale of seconds in large-scale crowdsourced data. *NPJ science of learning*, *5*(1), 1-10.

Borich, M. R., Brodie, S. M., Gray, W. A., Ionta, S., & Boyd, L. A. (2015). Understanding the role of the primary somatosensory cortex: Opportunities for rehabilitation. *Neuropsychologia*, *79*, 246–255.

Born, J. (2010). Slow-wave sleep and the consolidation of long-term memory. *The World Journal of Biological Psychiatry*, *11*(sup1), 16-21.

Born, J., & Fehm, H. L. (1998). Hypothalamus-pituitary-adrenal activity during human sleep: a coordinating role for the limbic hippocampal system. *Experimental and clinical endocrinology & diabetes*, *106*(03), 153-163.

Born, J., & Wilhelm, I. (2012). System consolidation of memory during sleep. *Psychological research*, *76*(2), 192-203.

Born, J., Rasch, B., & Gais, S. (2006). Sleep to remember. *The Neuroscientist*, *12*(5), 410-424.

Boutin, A., & Doyon, J. (2020). A sleep spindle framework for motor memory consolidation. *Philosophical Transactions of the Royal Society B*, *375*(1799), 20190232.

Brainard, D. H. (1997). The psychophysics toolbox. *Spatial vision*, *10*(4), 433-436.

Bridi, M. C. D., Aton, S. J., Seibt, J., Renouard, L., Coleman, T., & Frank, M. G. (2015). Rapid eye movement sleep promotes cortical plasticity in the developing brain. *Science Advances*, *1*(6), e1500105.

Brodt, S., & Gais, S. (2021). Memory engrams in the neocortex. *The Neuroscientist*, *27*(4), 427-444.

Brodt, S., Gais, S., Beck, J., Erb, M., Scheffler, K., & Schönauer, M. (2018). Fast track to the neocortex: A memory engram in the posterior parietal cortex. *Science*, *362*(6418), 1045-1048.

Brodt, S., Pöhlchen, D., Flanagin, V. L., Glasauer, S., Gais, S., & Schönauer, M. (2016). Rapid and independent memory formation in the parietal cortex. *Proceedings of the National Academy of Sciences*, *113*(46), 13251-13256.

Buckner, R. L., Andrews-Hanna, J. R., & Schacter, D. L. (2008). The brain's default network: anatomy, function, and relevance to disease. *Annals of the new York Academy of Sciences*, *1124*(1), 1-38.

Bushey, D., Tononi, G., & Cirelli, C. (2011). Sleep and synaptic homeostasis: structural evidence in Drosophila. *Science*, *332*(6037), 1576-1581.

Buysse, D. J., Reynolds III, C. F., Monk, T. H., Berman, S. R., & Kupfer, D. J. (1989). The Pittsburgh Sleep Quality Index: a new instrument for psychiatric practice and research. *Psychiatry research*, *28*(2), 193-213.

Buzsáki, G. (1986). Hippocampal sharp waves: their origin and significance. *Brain research*, *398*(2), 242-252.

Buzsáki, G. (1996). The hippocampo-neocortical dialogue. *Cerebral cortex*, *6*(2), 81-92.

Buzsáki, G. (2015). Hippocampal sharp wave-ripple: A cognitive biomarker for episodic memory and planning. *Hippocampus*, *25*(10), 1073-1188.

Cabeza, R., Ciaramelli, E., Olson, I. R., & Moscovitch, M. (2008). The parietal cortex and episodic memory: an attentional account. *Nature reviews neuroscience*, *9*(8), 613-625.

Cairney, S. A., Durrant, S. J., Hulleman, J., & Lewis, P. A. (2014). Targeted memory reactivation during slow wave sleep facilitates emotional memory consolidation. *Sleep*, *37*(4), 701-707.

Cairney, S. A., El Marj, N., & Staresina, B. P. (2018). Memory consolidation is linked to spindle-mediated information processing during sleep. *Current Biology*, *28*(6), 948-954.

Cairney, S. A., Lindsay, S., Sobczak, J. M., Paller, K. A., & Gaskell, M. G. (2016). The benefits of targeted memory reactivation for consolidation in sleep are contingent on memory accuracy and direct cue-memory associations. *Sleep*, 39(5), 1139-1150.

Cairney, S. A., Sobczak, J. M., Lindsay, S., & Gaskell, M. G. (2017). Mechanisms of memory retrieval in slow-wave sleep. *Sleep*, *40*(9).

Campbell, S. S., & Tobler, I. (1984). Animal sleep: a review of sleep duration across phylogeny. *Neuroscience & Biobehavioral Reviews*, *8*(3), 269-300.

Canolty, R. T., Edwards, E., Dalal, S. S., Soltani, M., Nagarajan, S. S., Kirsch, H. E., ... & Knight, R. T. (2006). High gamma power is phase-locked to theta oscillations in human neocortex. *Science*, *313*(5793), 1626-1628.

Canto, C. B., Onuki, Y., Bruinsma, B., van der Werf, Y. D., & De Zeeuw, C. I. (2017). The sleeping cerebellum. *Trends in Neurosciences*, *40*(5), 309-323.

Carr, M. F., Jadhav, S. P., & Frank, L. M. (2011). Hippocampal replay in the awake state: a potential substrate for memory consolidation and retrieval. *Nature neuroscience*, *14*(2), 147-153.

Carskadon, M. A., & Dement, W. C. (2005). Normal human sleep: an overview. *Principles and practice of sleep medicine*, *4*(1), 13-23.

Carskadon, M. A., & Herz, R. S. (2004). Minimal olfactory perception during sleep: why odor alarms will not work for humans. *Sleep*, *27*(3), 402-405.

Cash, S. S., Halgren, E., Dehghani, N., Rossetti, A. O., Thesen, T., Wang, C., ... & Ulbert, I. (2009). The human K-complex represents an isolated cortical down-state. *Science*, *324*(5930), 1084-1087.

Ceccarelli, A., Jackson, J. S., Tauhid, S., Arora, A., Gorky, J., Dell'Oglio, E., … Neema, M. (2012). The Impact of Lesion In-Painting and Registration Methods on Voxel-Based Morphometry in Detecting Regional Cerebral Gray Matter Atrophy in Multiple Sclerosis. *American Journal of Neuroradiology*, *33*(8), 1579–1585.

Cellini, N., & Capuozzo, A. (2018). Shaping memory consolidation via targeted memory reactivation during sleep. *Annals of the New York Academy of Sciences*, *1426*(1), 52-71.

Chauvette, S., Seigneur, J., & Timofeev, I. (2012). Sleep oscillations in the thalamocortical system induce long-term neuronal plasticity. *Neuron*, *75*(6), 1105-1113.

Clemens, Z., Mölle, M., Erőss, L., Barsi, P., Halász, P., & Born, J. (2007). Temporal coupling of parahippocampal ripples, sleep spindles and slow oscillations in humans. *Brain*, *130*(11), 2868-2878.

Clopath, C. (2012). Synaptic consolidation: an approach to long-term learning. *Cognitive neurodynamics*, *6*(3), 251-257.

Cohen, D. A., Pascual-Leone, A., Press, D. Z., & Robertson, E. M. (2005). Off-line learning of motor skill memory: a double dissociation of goal and movement. *Proceedings of the National Academy of Sciences*, *102*(50), 18237-18241.

Cohen, N. J., & Squire, L. R. (1980). Preserved learning and retention of pattern-analyzing skill in amnesia: Dissociation of knowing how and knowing that. *Science*, *210*(4466), 207-210.

Cohen, Y. E., & Andersen, R. A. (2002). A common reference frame for movement plans in the posterior parietal cortex. *Nature Reviews Neuroscience*, *3*(7), 553-562.

Collignon, A., Maes, F., Delaere, D., Vandermeulen, D., Suetens, P., & Marchal, G. (1995). Automated multi-modality image registration based on information theory. In *Information processing in medical imaging* (Vol. 3, No. 6, pp. 263-274).

Cordi, M. J., Diekelmann, S., Born, J., & Rasch, B. (2014). No effect of odor-induced memory reactivation during REM sleep on declarative memory stability. *Frontiers in systems neuroscience*, *8*, 157.

Corkin, S. (2002). What's new with the amnesic patient HM?. *Nature reviews neuroscience*, *3*(2), 153-160.

Costa, R. M., Cohen, D., & Nicolelis, M. A. (2004). Differential corticostriatal plasticity during fast and slow motor skill learning in mice. *Current Biology*, *14*(13), 1124-1134.

Cousins, J. (2014b). *The role of post-learning reactivation in memory consolidation* [Doctoral dissertation]. University of Manchester, United Kingdom.

Cousins, J. N., El-Deredy, W., Parkes, L. M., Hennies, N., & Lewis, P. A. (2014a). Cued memory reactivation during slow-wave sleep promotes explicit knowledge of a motor sequence. *Journal of Neuroscience*, *34*(48), 15870-15876.

Cousins, J. N., El-Deredy, W., Parkes, L. M., Hennies, N., & Lewis, P. A. (2016). Cued reactivation of motor learning during sleep leads to overnight changes in functional brain activity and connectivity. *PLoS biology*, *14*(5), e1002451.

Cousins, J. N., Sasmita, K., & Chee, M. W. (2018). Memory encoding is impaired after multiple nights of partial sleep restriction. *Journal of sleep research*, *27*(1), 138-145.

Cox, R., Hofman, W. F., & Talamini, L. M. (2012). Involvement of spindles in memory consolidation is slow wave sleep-specific. *Learning & Memory*, *19*(7), 264-267.

Cox, R., Hofman, W. F., de Boer, M., & Talamini, L. M. (2014). Local sleep spindle modulations in relation to specific memory cues. *Neuroimage*, *99*, 103-110.

Cox, R., Schapiro, A. C., Manoach, D. S., & Stickgold, R. (2017). Individual differences in frequency and topography of slow and fast sleep spindles. *Frontiers in human neuroscience*, *11*, 433.

Creery, J. D., Oudiette, D., Antony, J. W., & Paller, K. A. (2015). Targeted memory reactivation during sleep depends on prior learning. *Sleep*, *38*(5), 755-763.

Crick, F., & Mitchison, G. (1983). The function of dream sleep. *Nature*, *304*(5922), 111-114.

Dag, U., Lei, Z., Le, J. Q., Wong, A., Bushey, D., & Keleman, K. (2019). Neuronal reactivation during post-learning sleep consolidates long-term memory in Drosophila. *elife*, *8*, e42786.

Dang-Vu, T. T., McKinney, S. M., Buxton, O. M., Solet, J. M., & Ellenbogen, J. M. (2010). Spontaneous brain rhythms predict sleep stability in the face of noise. *Current biology*, *20*(15), R626-R627

Datta, S. (1997). Cellular basis of pontine ponto-geniculo-occipital wave generation and modulation. *Cellular and molecular neurobiology*, *17*(3), 341-365.

Datta, S., & Hobson, J. A. (2000). The rat as an experimental model for sleep neurophysiology. *Behavioral neuroscience*, *114*(6), 1239.

Davidson, T. J., Kloosterman, F., & Wilson, M. A. (2009). Hippocampal replay of extended experience. *Neuron*, *63*(4), 497-507.

Dayan, E., & Cohen, L. G. (2011). Neuroplasticity subserving motor skill learning. *Neuron*, *72*(3), 443-454.

De Lavilléon, G., Lacroix, M. M., Rondi-Reig, L., & Benchenane, K. (2015). Explicit memory creation during sleep demonstrates a causal role of place cells in navigation. *Nature neuroscience*, *18*(4), 493-495.

De Santis, S., Drakesmith, M., Bells, S., Assaf, Y., & Jones, D. K. (2014). Why diffusion tensor MRI does well only some of the time: variance and covariance of white matter tissue microstructure attributes in the living human brain. *Neuroimage*, *89*, 35-44.

de Vivo, L., & Bellesi, M. (2019). The role of sleep and wakefulness in myelin plasticity. *Glia*, *67*(11), 2142-2152.

Debas, K., Carrier, J., Orban, P., Barakat, M., Lungu, O., Vandewalle, G., ... & Benali, H. (2010). Brain plasticity related to the consolidation of motor sequence learning and motor adaptation. *Proceedings of the National Academy of Sciences*, *107*(41), 17839-17844.

Dehnavi, F., Moghimi, S., Sadrabadi Haghighi, S., Safaie, M., & Ghorbani, M. (2019). Opposite effect of motivated forgetting on sleep spindles during stage 2 and slow wave sleep. *Sleep*, *42*(7), zsz085.

Deliens, G., Leproult, R., Neu, D., & Peigneux, P. (2013). Rapid eye movement and non-rapid eye movement sleep contributions in memory consolidation and resistance to retroactive interference for verbal material. *Sleep*, *36*(12), 1875-1883.

Dement, W. C. (2005). History of sleep medicine. *Neurologic clinics*, *23*(4), 945-965.

Denis, D., Mylonas, D., Poskanzer, C., Bursal, V., Payne, J. D., & Stickgold, R. (2020). Sleep spindles facilitate selective memory consolidation. *BioRxiv*.

Deuker, L., Olligs, J., Fell, J., Kranz, T. A., Mormann, F., Montag, C., ... & Axmacher, N. (2013). Memory consolidation by replay of stimulus-specific neural activity. *Journal of Neuroscience*, *33*(49), 19373-19383.

Diba, K., & Buzsáki, G. (2007). Forward and reverse hippocampal place-cell sequences during ripples. *Nature neuroscience*, *10*(10), 1241-1242.

Diekelmann, S., & Born, J. (2010a). Slow-wave sleep takes the leading role in memory reorganization. *Nature Reviews Neuroscience*, *11*(3), 218-218.

Diekelmann, S., & Born, J. (2010b). The memory function of sleep. *Nature Reviews Neuroscience*, *11*(2), 114-126.

Diekelmann, S., Biggel, S., Rasch, B., & Born, J. (2012). Offline consolidation of memory varies with time in slow wave sleep and can be accelerated by cuing memory reactivations. *Neurobiology of learning and memory*, *98*(2), 103-111

Diekelmann, S., Born, J., & Rasch, B. (2016). Increasing explicit sequence knowledge by odor cueing during sleep in men but not women. *Frontiers in behavioral neuroscience*, *10*, 74.

Diekelmann, S., Büchel, C., Born, J., & Rasch, B. (2011). Labile or stable: opposing consequences for memory when reactivated during waking and sleep. *Nature neuroscience*, *14*(3), 381-386.

Donchin, O., Sawaki, L., Madupu, G., Cohen, L. G., & Shadmehr, R. (2002). Mechanisms influencing acquisition and recall of motor memories. *Journal of neurophysiology*, *88*(4), 2114-2123.

Donohue, K. C., & Spencer, R. M. (2011). Continuous re-exposure to environmental sound cues during sleep does not improve memory for semantically unrelated word pairs. *Journal of Cognitive Education and Psychology*, *10*(2), 167-177.

Doran, S. M., Wessel, T., Kilduff, T. S., Turek, F., & Renger, J. J. (2008). Translational models of sleep and sleep disorders. In *Animal and Translational Models for CNS Drug Discovery* (pp. 395-456). Academic Press.

Dorey, F. J. (2011). In brief: Statistics in brief: Statistical power: What is it and when should it be used?.

Doyon, J., Bellec, P., Amsel, R., Penhune, V., Monchi, O., Carrier, J., ... & Benali, H. (2009). Contributions of the basal ganglia and functionally related brain structures to motor learning. *Behavioural brain research*, *199*(1), 61-75.

Doyon, J., Owen, A. M., Petrides, M., Sziklas, V., & Evans, A. C. (1996). Functional anatomy of visuomotor skill learning in human subjects examined with positron emission tomography. *European Journal of Neuroscience*, *8*(4), 637-648.

Doyon, J., Penhune, V., & Ungerleider, L. G. (2003). Distinct contribution of the cortico-striatal and cortico-cerebellar systems to motor skill learning. *Neuropsychologia*, *41*(3), 252-262.

Doyon, J., Song, A. W., Karni, A., Lalonde, F., Adams, M. M., & Ungerleider, L. G. (2002). Experience-dependent changes in cerebellar contributions to motor sequence learning. *Proceedings of the National Academy of Sciences*, *99*(2), 1017-1022.

Dragoi, G., & Tonegawa, S. (2011). Preplay of future place cell sequences by hippocampal cellular assemblies. *Nature*, *469*(7330), 397-401.

Dragoi, G., & Tonegawa, S. (2013). Distinct preplay of multiple novel spatial experiences in the rat. *Proceedings of the National Academy of Sciences*, *110*(22), 9100-9105.

Drosopoulos, S., Schulze, C., Fischer, S., & Born, J. (2007). Sleep's function in the spontaneous recovery and consolidation of memories. *Journal of Experimental Psychology: General*, *136*(2), 169.

Dudai, Y. (2004). The neurobiology of consolidations, or, how stable is the engram?. *Annual Review of Psychology*, *55*, 51-86.

Dudai, Y. (2012). The restless engram: consolidations never end. *Annual review of neuroscience*, *35*, 227-247.

Dupret, D., O'neill, J., Pleydell-Bouverie, B., & Csicsvari, J. (2010). The reorganization and reactivation of hippocampal maps predict spatial memory performance. *Nature neuroscience*, *13*(8), 995-1002.

Durrant, S. J., Cairney, S. A., & Lewis, P. A. (2013). Overnight consolidation aids the transfer of statistical knowledge from the medial temporal lobe to the striatum. *Cerebral Cortex*, *23*(10), 2467-2478.

Duss, S. B., Reber, T. P., Hänggi, J., Schwab, S., Wiest, R., Müri, R. M., ... & Henke, K. (2014). Unconscious relational encoding depends on hippocampus. *Brain*, *137*(12), 3355-3370.

Dworak, M., McCarley, R. W., Kim, T., Kalinchuk, A. V., & Basheer, R. (2010). Sleep and brain energy levels: ATP changes during sleep. *Journal of Neuroscience*, *30*(26), 9007-9016.

Ebbinghaus, H. (1885). *Über das gedächtnis: untersuchungen zur experimentellen psychologie*. Duncker & Humblot.

Eckert, M. J., McNaughton, B. L., & Tatsuno, M. (2020). Neural ensemble reactivation in rapid eye movement and slow-wave sleep coordinate with muscle activity to promote rapid motor skill learning. *Philosophical Transactions of the Royal Society B*, *375*(1799), 20190655.

Ego-Stengel, V., & Wilson, M. A. (2010). Disruption of ripple-associated hippocampal activity during rest impairs spatial learning in the rat. *Hippocampus*, *20*(1), 1-10.

Eichenbaum, H. (2015). Does the hippocampus preplay memories?. *Nature neuroscience*, *18*(12), 1701-1702.

Ekstrand, B. R. (1967). Effect of sleep on memory. *Journal of experimental psychology*, *75*(1), 64.

Elvsåshagen, T., Norbom, L. B., Pedersen, P. Ø., Quraishi, S. H., Bjørnerud, A., Malt, U. F., ... & Westlye, L. T. (2015). Widespread changes in white matter microstructure after a day of waking and sleep deprivation. *PloS one*, *10*(5), e0127351.

Emmons, W. H., & Simon, C. W. (1956). The non-recall of material presented during sleep. *The American journal of psychology*, *69*(1), 76-81.

Euston, D. R., Tatsuno, M., & McNaughton, B. L. (2007). Fast-forward playback of recent memory sequences in prefrontal cortex during sleep. *Science*, *318*(5853), 1147-1150.

Faraguna, U., Vyazovskiy, V. V., Nelson, A. B., Tononi, G., & Cirelli, C. (2008). A causal role for brain-derived neurotrophic factor in the homeostatic regulation of sleep. *Journal of Neuroscience*, *28*(15), 4088-4095.

Farthouat, J., Gilson, M., & Peigneux, P. (2017). New evidence for the necessity of a silent plastic period during sleep for a memory benefit of targeted memory reactivation. *Sleep Spindles & Cortical Up States*, *1*(1), 14-26.

Feld, G. B., Weis, P. P., & Born, J. (2016). The limited capacity of sleep-dependent memory consolidation. *Frontiers in psychology*, *7*, 1368.

Fernández-Mendoza, J., Lozano, B., Seijo, F., Santamarta-Liébana, E., José Ramos-Platón, M., Vela-Bueno, A., & Fernández-González, F. (2009). Evidence of subthalamic PGO-like waves during REM sleep in humans: a deep brain polysomnographic study. *Sleep*, *32*(9), 1117-1126.

Fernandez, L. M., & Lüthi, A. (2020). Sleep spindles: mechanisms and functions. *Physiological reviews*, *100*(2), 805-868.

Ficca, G., Lombardo, P., Rossi, L., & Salzarulo, P. (2000). Morning recall of verbal material depends on prior sleep organization. *Behavioural brain research*, *112*(1-2), 159-163.

Fischer, S., Drosopoulos, S., Tsen, J., & Born, J. (2006). Implicit learning–explicit knowing: a role for sleep in memory system interaction. *Journal of cognitive neuroscience*, *18*(3), 311-319.

Fischer, S., Hallschmid, M., Elsner, A. L., & Born, J. (2002). Sleep forms memory for finger skills. *Proceedings of the National Academy of Sciences*, *99*(18), 11987-11991.

Fischer, S., Nitschke, M. F., Melchert, U. H., Erdmann, C., & Born, J. (2005). Motor memory consolidation in sleep shapes more effective neuronal representations. *Journal of Neuroscience*, *25*(49), 11248-11255.

Fogel, S. M., & Smith, C. T. (2006). Learning-dependent changes in sleep spindles and Stage 2 sleep. *Journal of sleep research*, *15*(3), 250-255.

Fogel, S. M., & Smith, C. T. (2011). The function of the sleep spindle: a physiological index of intelligence and a mechanism for sleep-dependent memory consolidation. *Neuroscience & Biobehavioral Reviews*, *35*(5), 1154-1165.

Fogel, S. M., Smith, C. T., & Cote, K. A. (2007). Dissociable learning-dependent changes in REM and non-REM sleep in declarative and procedural memory systems. *Behavioural brain research*, *180*(1), 48-61.

Fogel, S., Albouy, G., King, B. R., Lungu, O., Vien, C., Bore, A., ... & Doyon, J. (2017a). Reactivation or transformation? Motor memory consolidation associated with cerebral activation time-locked to sleep spindles. *PloS one*, *12*(4), e0174755.

Fogel, S., Vien, C., Karni, A., Benali, H., Carrier, J., & Doyon, J. (2017b). Sleep spindles: a physiological marker of age-related changes in gray matter in brain regions supporting motor skill memory consolidation. *Neurobiology of aging*, *49*, 154-164.

Forget, D., Morin, C. M., & Bastien, C. H. (2011). The role of the spontaneous and evoked k-complex in good-sleeper controls and in individuals with insomnia. *Sleep*, *34*(9), 1251-1260.

Foster, D. J., & Wilson, M. A. (2006). Reverse replay of behavioural sequences in hippocampal place cells during the awake state. *Nature*, *440*(7084), 680-683.

Fowler, M. J., Sullivan, M. J., & Ekstrand, B. R. (1973). Sleep and memory. *Science*, *179*(4070), 302-304.

Frankland, P. W., & Bontempi, B. (2005). The organization of recent and remote memories. *Nature reviews neuroscience*, *6*(2), 119-130.

Frey, U., & Morris, R. G. (1997). Synaptic tagging and long-term potentiation. *Nature*, *385*(6616), 533-536.

Friston, K. J., Frith, C. D., Frackowiak, R. S. J., & Turner, R. (1995). Characterizing Dynamic Brain Responses with fMRI: A Multivariate Approach. *NeuroImage*, *2*(2), 166–172.

Friston, K. J., Holmes, A. P., Worsley, K. J., Poline, J.-P., Frith, C. D., & Frackowiak, R. S. J. (1994). Statistical parametric maps in functional imaging: A general linear approach. *Human Brain Mapping*, *2*(4), 189–210.

Fuentemilla, L., Miró, J., Ripollés, P., Vilà-Balló, A., Juncadella, M., Castañer, S., ... & Rodríguez-Fornells, A. (2013). Hippocampus-dependent strengthening of targeted memories via reactivation during sleep in humans. *Current Biology*, *23*(18), 1769-1775.

Fushimi, M., Niiyama, Y., Fujiwara, R., Satoh, N., & Hishikawa, Y. (1998). Some sensory stimuli generate spontaneous K-complexes. *Psychiatry and clinical neurosciences*, *52*(2), 150-152.

Gais, S., & Born, J. (2004). Declarative memory consolidation: mechanisms acting during human sleep. *Learning & Memory*, *11*(6), 679-685.

Gais, S., Albouy, G., Boly, M., Dang-Vu, T. T., Darsaud, A., Desseilles, M., ... & Peigneux, P. (2007). Sleep transforms the cerebral trace of declarative memories. *Proceedings of the National Academy of Sciences*, *104*(47), 18778-18783.

Gais, S., Plihal, W., Wagner, U., & Born, J. (2000). Early sleep triggers memory for early visual discrimination skills. *Nature neuroscience*, *3*(12), 1335-1339.

Ganguly, K., & Carmena, J. M. (2009). Emergence of a stable cortical map for neuroprosthetic control. *PLoS biology*, *7*(7), e1000153.

Gao, C., Fillmore, P., & Scullin, M. K. (2020). Classical music, educational learning, and slow wave sleep: A targeted memory reactivation experiment. *Neurobiology of learning and memory*, *171*, 107206.

Gao, P. P., Goodman, J. H., Sacktor, T. C., & Francis, J. T. (2018). Persistent increases of PKMζ in sensorimotor cortex maintain procedural long-term memory storage. *Iscience*, *5*, 90-98.

Garcia-Hernandez, R., Cerda, A. C., Carpena, A. T., Drakesmith, M., Koller, K., Jones, D. K., ... & De Santis, S. (2021). Mapping microglia and astrocytes activation in vivo using diffusion MRI. *bioRxiv*, 2020-02.

Genc, S., Tax, C. M., Raven, E. P., Chamberland, M., Parker, G. D., & Jones, D. K. (2020). Impact of b-value on estimates of apparent fibre density. *Human brain mapping*, *41*(10), 2583-2595.

Genzel, L., Dragoi, G., Frank, L., Ganguly, K., De La Prida, L., Pfeiffer, B., & Robertson, E. (2020). A consensus statement: defining terms for reactivation analysis. *Philosophical Transactions of the Royal Society B*, *375*(1799), 20200001.

Genzel, L., Kroes, M. C., Dresler, M., & Battaglia, F. P. (2014). Light sleep versus slow wave sleep in memory consolidation: a question of global versus local processes?. *Trends in neurosciences*, *37*(1), 10-19.

Gerrard, J. L., Burke, S. N., McNaughton, B. L., & Barnes, C. A. (2008). Sequence reactivation in the hippocampus is impaired in aged rats. *Journal of Neuroscience*, *28*(31), 7883-7890.

Gilmore, A. W., Nelson, S. M., & McDermott, K. B. (2015). A parietal memory network revealed by multiple MRI methods. *Trends in cognitive sciences*, *19*(9), 534-543.

Girardeau, G., Benchenane, K., Wiener, S. I., Buzsáki, G., & Zugaro, M. B. (2009). Selective suppression of hippocampal ripples impairs spatial memory. *Nature neuroscience*, *12*(10), 1222-1223.

Girardeau, G., Cei, A., & Zugaro, M. (2014). Learning-induced plasticity regulates hippocampal sharp wave-ripple drive. *Journal of Neuroscience*, *34*(15), 5176-5183.

Giuditta, A., Ambrosini, M. V., Montagnese, P., Mandile, P., Cotugno, M., Zucconi, G. G., & Vescia, S. (1995). The sequential hypothesis of the function of sleep. *Behavioural brain research*, *69*(1-2), 157-166.

Göldi, M., & Rasch, B. (2019). Effects of targeted memory reactivation during sleep at home depend on sleep disturbances and habituation. *NPJ science of learning*, *4*(1), 1-7.

Göldi, M., van Poppel, E. A. M., Rasch, B., & Schreiner, T. (2019). Increased neuronal signatures of targeted memory reactivation during slow-wave up states. *Scientific reports*, *9*(1), 1-10.

Groch, S., McMakin, D., Guggenbühl, P., Rasch, B., Huber, R., & Wilhelm, I. (2016). Memory cueing during sleep modifies the interpretation of ambiguous scenes in adolescents and adults. *Developmental cognitive neuroscience*, *17*, 10-18.

Groch, S., Preiss, A., McMakin, D. L., Rasch, B., Walitza, S., Huber, R., & Wilhelm, I. (2017a). Targeted reactivation during sleep differentially affects negative memories in socially anxious and healthy children and adolescents. *Journal of Neuroscience*, *37*(9), 2425–2434.

Groch, S., Schreiner, T., Rasch, B., Huber, R., & Wilhelm, I. (2017b). Prior knowledge is essential for the beneficial effect of targeted memory reactivation during sleep. *Scientific reports*, *7*(1), 1-7.

Grosmark, A. D., Sparks, F. T., Davis, M. J., & Losonczy, A. (2021). Reactivation predicts the consolidation of unbiased long-term cognitive maps. *Nature Neuroscience*, 1-12.

Guerrien, A., Dujardin, K., Mandal, O., Sockeel, P., & Leconte, P. (1989). Enhancement of memory by auditory stimulation during postlearning REM sleep in humans. *Physiology & behavior*, *45*(5), 947-950.

Hahn, M. A., Heib, D., Schabus, M., Hoedlmoser, K., & Helfrich, R. F. (2020). Slow oscillation-spindle coupling predicts enhanced memory formation from childhood to adolescence. *elife*, *9*, e53730.

Halász, P. (2016). The K-complex as a special reactive sleep slow wave–a theoretical update. *Sleep medicine reviews*, *29*, 34-40.

Hardwick, R. M., Rottschy, C., Miall, R. C., & Eickhoff, S. B. (2013). A quantitative meta-analysis and review of motor learning in the human brain. *Neuroimage*, *67*, 283-297.

Hars, B., & Hennevin, E. (1987). Impairment of learning by cueing during postlearning slow-wave sleep in rats. *Neuroscience letters*, *79*(3), 290-294.

Hars, B., & Hennevin, E. (1990). Reactivation of an old memory during sleep and wakefulness. *Animal Learning & Behavior*, *18*(4), 365-376.

Hars, B., Hennevin, E., & Pasques, P. (1985). Improvement of learning by cueing during postlearning paradoxical sleep. *Behavioural brain research*, *18*(3), 241-250.

Hauner, K. K., Howard, J. D., Zelano, C., & Gottfried, J. A. (2013). Stimulus-specific enhancement of fear extinction during slow-wave sleep. *Nature neuroscience*, *16*(11), 1553-1555.

Hayashi, M. L., Choi, S. Y., Rao, B. S., Jung, H. Y., Lee, H. K., Zhang, D., ... & Tonegawa, S. (2004). Altered cortical synaptic morphology and impaired memory consolidation in forebrain-specific dominant-negative PAK transgenic mice. *Neuron*, *42*(5), 773-787.

Hayes, A. F. (2014). Introduction to Mediation, Moderation, and Conditional Process Analysis: A Regression-Based Approach. New York, NY: The Guilford Press. *Journal of Educational Measurement*, *51*(3), 335–337.

He, J., Sun, H. Q., Li, S. X., Zhang, W. H., Shi, J., Ai, S. Z., ... & Lu, L. (2015). Effect of conditioned stimulus exposure during slow wave sleep on fear memory extinction in humans. *Sleep*, *38*(3), 423-431.

Hebb, D. O. (1955). The mammal and his environment. *American Journal of Psychiatry*, *111*(11), 826-831.

Hebscher, M., Meltzer, J. A., & Gilboa, A. (2019). A causal role for the precuneus in network-wide theta and gamma oscillatory activity during complex memory retrieval. *elife*, *8*, e43114.

Heine, R. (1914). *über Wiedererkennen und rückwirkende Hemmung*. Johann Ambrosius Barth.

Henke, K. (2010). A model for memory systems based on processing modes rather than consciousness. *Nature Reviews Neuroscience*, *11*(7), 523-532.

Henke, K., Mondadori, C. R., Treyer, V., Nitsch, R. M., Buck, A., & Hock, C. (2003). Nonconscious formation and reactivation of semantic associations by way of the medial temporal lobe. *Neuropsychologia*, *41*(8), 863-876.

Hennevin, E., Hars, B., Maho, C., & Bloch, V. (1995). Processing of learned information in paradoxical sleep: relevance for memory. *Behavioural brain research*, *69*(1-2), 125-135.

Hennies, N., Ralph, M. A. L., Kempkes, M., Cousins, J. N., & Lewis, P. A. (2016). Sleep spindle density predicts the effect of prior knowledge on memory consolidation. *Journal of Neuroscience*, *36*(13), 3799-3810.

Herz, R. S. (2016). The role of odor-evoked memory in psychological and physiological health. *Brain sciences*, *6*(3), 22.

Himmer, L., Bürger, Z., Fresz, L., Maschke, J., Wagner, L., Brodt, S., ... & Gais, S. (2021). Localizing spontaneous memory reprocessing during human sleep. *bioRxiv*.

Himmer, L., Schönauer, M., Heib, D. P. J., Schabus, M., & Gais, S. (2019). Rehearsal initiates systems memory consolidation, sleep makes it last. *Science advances*, *5*(4), eaav1695.

Hirase, H., Leinekugel, X., Czurkó, A., Csicsvari, J., & Buzsáki, G. (2001). Firing rates of hippocampal neurons are preserved during subsequent sleep episodes and modified by novel awake experience. *Proceedings of the National Academy of Sciences*, *98*(16), 9386-9390.

Hoddes, E., Zarcone, V., Smythe, H., Phillips, R., & Dement, W. C. (1973). Quantification of sleepiness: a new approach. *Psychophysiology*, *10*(4), 431-436.

Hoffman, K. L., & Mcnaughton, B. L. (2002). Coordinated reactivation of distributed memory traces in primate neocortex. *Science*, *297*(5589), 2070-2073.

Hofstetter, S., Tavor, I., Moryosef, S. T., & Assaf, Y. (2013). Short-term learning induces white matter plasticity in the fornix. *Journal of Neuroscience*, *33*(31), 12844-12850.

Howe, T., Wilson, M. A., Ji, D., & Jones, M. W. (2019). Extending evidence for REM-associated replay in hippocampal CA1 place cells. In *Program No. 333.10. 2019 Neuroscience Meeting Planner*.

Hu, X., Antony, J. W., Creery, J. D., Bodenhausen, G. V., Paller, K. A., & Vargas, I. M. (2015). Unlearning implicit social biases during sleep. *Science*, *348*(6238), 1013–1015.

Hu, X., Cheng, L. Y., Chiu, M. H., & Paller, K. A. (2020). Promoting memory consolidation during sleep: A meta-analysis of targeted memory reactivation. *Psychological bulletin*, *146*(3), 218.

Huber, R., Felice Ghilardi, M., Massimini, M., & Tononi, G. (2004). Local sleep and learning. *Nature*, *430*(6995), 78-81.

Huber, R., Ghilardi, M. F., Massimini, M., Ferrarelli, F., Riedner, B. A., Peterson, M. J., & Tononi, G. (2006). Arm immobilization causes cortical plastic changes and locally decreases sleep slow wave activity. *Nature neuroscience*, *9*(9), 1169-1176.

Huber, R., Tononi, G., & Cirelli, C. (2007). Exploratory behavior, cortical BDNF expression, and sleep homeostasis. *Sleep*, *30*(2), 129-139.

Humiston, G. B., & Wamsley, E. J. (2019). Unlearning implicit social biases during sleep: A failure to replicate. *PloS one*, *14*(1), e0211416.

Hutchison, I. C., & Rathore, S. (2015). The role of REM sleep theta activity in emotional memory. *Frontiers in psychology*, *6*, 1439.

Hutchison, I. C., Pezzoli, S., Tsimpanouli, M. E., Abdellahi, M. E., Pobric, G., Hulleman, J., & Lewis, P. A. (2021). Targeted memory reactivation in REM but not SWS selectively reduces arousal responses. *Communications biology*, *4*(1), 1-6.

Hwang, F. J., Roth, R. H., Wu, Y. W., Sun, Y., Liu, Y., & Ding, J. B. (2021). Motor learning selectively strengthens cortical and striatal synapses of motor engram neurons. *Available at SSRN 3951494*.

Iber, C., Ancoli-Israel, S., Chesson, A. L., & Quan, S. F. (2007). *The AASM manual for the scoring of sleep and associated events: rules, terminology and technical specifications* (Vol. 1). Westchester, IL: American academy of sleep medicine.

Iglewicz, B., & Hoaglin, D. (1993). How to detect and handle outliers. 16. *The ASQC basic references in quality control: statistical techniques.*

Inostroza, M., & Born, J. (2013). Sleep for preserving and transforming episodic memory. *Annual review of neuroscience*, *36*, 79-102.

Ioannides, A. A., Liu, L., & Kostopoulos, G. K. (2019). The Emergence of Spindles and K-complexes and the role of the dorsal caudal part of the anterior cingulate as the generator of K-complexes. *Frontiers in neuroscience*, *13*, 814.

Janacsek, K., Shattuck, K. F., Tagarelli, K. M., Lum, J. A., Turkeltaub, P. E., & Ullman, M. T. (2020). Sequence learning in the human brain: a functional neuroanatomical meta-analysis of serial reaction time studies. *Neuroimage*, *207*, 116387.

Jegou, A., Schabus, M., Gosseries, O., Dahmen, B., Albouy, G., Desseilles, M., ... & Dang-Vu, T. T. (2019). Cortical reactivations during sleep spindles following declarative learning. *Neuroimage*, *195*, 104-112.

Jenkins, I. H., Brooks, D. J., Nixon, P. D., Frackowiak, R. S., & Passingham, R. E. (1994). Motor sequence learning: a study with positron emission tomography. *Journal of Neuroscience*, *14*(6), 3775-3790.

Jenkins, J. G., & Dallenbach, K. M. (1924). Obliviscence during sleep and waking. *The American Journal of Psychology*, *35*(4), 605-612.

Jeong, S. K., & Xu, Y. (2016). Behaviorally relevant abstract object identity representation in the human parietal cortex. *Journal of Neuroscience*, *36*(5), 1607-1619.

Jessen, N. A., Munk, A. S. F., Lundgaard, I., & Nedergaard, M. (2015). The glymphatic system: a beginner's guide. *Neurochemical research*, *40*(12), 2583-2599.

Jezzard, P., & Balaban, R. S. (1995). Correction for geometric distortion in echo planar images from B0 field variations. *Magnetic Resonance in Medicine*, *34*(1), 65–73.

Ji, D., & Wilson, M. A. (2007). Coordinated memory replay in the visual cortex and hippocampus during sleep. *Nature neuroscience*, *10*(1), 100-107.

Joensen, B. H., Harrington, M., Berens, S., Cairney, S., Gaskell, M. G., & Horner, A. J. (2022). Targeted memory reactivation during sleep can induce forgetting of overlapping memories.

Johansen-Berg, H., Baptista, C. S., & Thomas, A. G. (2012). Human structural plasticity at record speed. *Neuron*, *73*(6), 1058-1060.

Johnson, B. P., Scharf, S. M., & Westlake, K. P. (2018). Targeted memory reactivation during sleep, but not wake, enhances sensorimotor skill performance: A pilot study. *Journal of motor behavior*, *50*(2), 202-209.

Johnson, B. P., Scharf, S. M., Verceles, A. C., & Westlake, K. P. (2021). Enhancing motor learning in people with stroke via memory reactivation during sleep. *Rehabilitation Psychology*.

Johnson, B. P., Scharf, S. M., Verceles, A. C., & Westlake, K. P. (2019). Use of targeted memory reactivation enhances skill performance during a nap and enhances declarative memory during wake in healthy young adults. *Journal of sleep research*, *28*(5), e12832.

Johnson, L. A., Euston, D. R., Tatsuno, M., & McNaughton, B. L. (2010). Stored-trace reactivation in rat prefrontal cortex is correlated with down-to-up state fluctuation density. *Journal of Neuroscience*, *30*(7), 2650-2661.

Josselyn, S. A., & Tonegawa, S. (2020). Memory engrams: Recalling the past and imagining the future. *Science*, *367*(6473).

Josselyn, S. A., Köhler, S., & Frankland, P. W. (2015). Finding the engram. *Nature Reviews Neuroscience*, *16*(9), 521-534.

Kami, A., Meyer, G., Jezzard, P., Adams, M. M., Turner, R., & Ungerleider, L. G. (1995). Functional MRI evidence for adult motor cortex plasticity during motor skill learning. *Nature*, *377*(6545), 155-158.

Karashima, A., Nakamura, K., Watanabe, M., Sato, N., Nakao, M., Katayama, N., & Yamamoto, M. (2001). Synchronization between hippocampal theta waves and PGO waves during REM sleep. *Psychiatry and Clinical Neurosciences*, *55*(3), 189-190.

Karlsson, M. P., & Frank, L. M. (2009). Awake replay of remote experiences in the hippocampus. *Nature neuroscience*, *12*(7), 913-918.

Kellner, E., Dhital, B., Kiselev, V. G., & Reisert, M. (2016). Gibbs-ringing artifact removal based on local subvoxel-shifts. *Magnetic resonance in medicine*, *76*(5), 1574-1581.

Kim, A., Latchoumane, C., Lee, S., Kim, G. B., Cheong, E., Augustine, G. J., & Shin, H. S. (2012). Optogenetically induced sleep spindle rhythms alter sleep architectures in mice. *Proceedings of the National Academy of Sciences*, *109*(50), 20673-20678.

King, B. R., Dolfen, N., Gann, M. A., Renard, Z., Swinnen, S. P., & Albouy, G. (2019). Schema and motor-memory consolidation. *Psychological Science*, *30*(7), 963-978.

King, B. R., Hoedlmoser, K., Hirschauer, F., Dolfen, N., & Albouy, G. (2017). Sleeping on the motor engram: The multifaceted nature of sleep-related motor memory consolidation. *Neuroscience & Biobehavioral Reviews*, *80*, 1-22.

Kleim, J. A., Hogg, T. M., VandenBerg, P. M., Cooper, N. R., Bruneau, R., & Remple, M. (2004). Cortical synaptogenesis and motor map reorganization occur during late, but not early, phase of motor skill learning. *Journal of Neuroscience*, *24*(3), 628-633.

Kleim, J. A., Markham, J. A., Vij, K., Freese, J. L., Ballard, D. H., & Greenough, W. T. (2007). Motor learning induces astrocytic hypertrophy in the cerebellar cortex. *Behavioural brain research*, *178*(2), 244-249.

Klinzing, J. G., Niethard, N., & Born, J. (2019). Mechanisms of systems memory consolidation during sleep. *Nature neuroscience*, *22*(10), 1598-1610.

Klinzing, J. G., Tashiro, L., Ruf, S., Wolff, M., Born, J., & Ngo, H. V. V. (2021). Auditory stimulation during sleep suppresses spike activity in benign epilepsy with centrotemporal spikes. *Cell Reports Medicine*, *2*(11), 100432.

Kodama, M., Ono, T., Yamashita, F., Ebata, H., Liu, M., Kasuga, S., & Ushiba, J. (2018). Structural Gray Matter Changes in the Hippocampus and the Primary Motor Cortex on An-Hour-to-

One- Day Scale Can Predict Arm-Reaching Performance Improvement. *Frontiers in Human Neuroscience*, *12*(June), 1–11.

Koopman, A. (2020a). *Sleep's role in the reprocessing and restructuring of memory* (Doctoral dissertation, Cardiff University).

Koopman, A. C., Abdellahi, M. E., Belal, S., Rakowska, M., Metcalf, A., Sledziowska, M., Hunter, T., & Lewis, P. (2020b). Targeted memory reactivation of a serial reaction time task in SWS, but not REM, preferentially benefits the non-dominant hand. *bioRxiv*.

Korman, M., Doyon, J., Doljansky, J., Carrier, J., Dagan, Y., & Karni, A. (2007). Daytime sleep condenses the time course of motor memory consolidation. *Nature neuroscience*, *10*(9), 1206-1213.

Kudrimoti, H. S., Barnes, C. A., & McNaughton, B. L. (1999). Reactivation of hippocampal cell assemblies: effects of behavioral state, experience, and EEG dynamics. *Journal of Neuroscience*, *19*(10), 4090-4101.

Kuriyama, K., Stickgold, R., & Walker, M. P. (2004). Sleep-dependent learning and motor-skill complexity. *Learning & memory*, *11*(6), 705-713.

Lacroix, M. M., de Lavilléon, G., Lefort, J., El Kanbi, K., Bagur, S., Laventure, S., ... & Benchenane, K. (2018). Improved sleep scoring in mice reveals human-like stages. *bioRxiv*, 489005.

Lage, G. M., Ugrinowitsch, H., Apolinário-Souza, T., Vieira, M. M., Albuquerque, M. R., & Benda, R. N. (2015). Repetition and variation in motor practice: a review of neural correlates. *Neuroscience & Biobehavioral Reviews*, *57*, 132-141.

Landmann, N., Kuhn, M., Maier, J. G., Spiegelhalder, K., Baglioni, C., Frase, L., ... & Nissen, C. (2015). REM sleep and memory reorganization: potential relevance for psychiatry and psychotherapy. *Neurobiology of learning and memory*, *122*, 28-40.

Landmann, N., Kuhn, M., Piosczyk, H., Feige, B., Baglioni, C., Spiegelhalder, K., ... & Nissen, C. (2014). The reorganisation of memory during sleep. *Sleep medicine reviews*, *18*(6), 531-541.

Lange, T., Dimitrov, S., & Born, J. (2010). Effects of sleep and circadian rhythm on the human immune system. *Annals of the New York Academy of Sciences*, *1193*(1), 48-59.

Lansink, C. S., Goltstein, P. M., Lankelma, J. V., Joosten, R. N., McNaughton, B. L., & Pennartz, C. M. (2008). Preferential reactivation of motivationally relevant information in the ventral striatum. *Journal of Neuroscience*, *28*(25), 6372-6382.

Lansink, C. S., Goltstein, P. M., Lankelma, J. V., McNaughton, B. L., & Pennartz, C. M. (2009). Hippocampus leads ventral striatum in replay of place-reward information. *PLoS biology*, *7*(8), e1000173.

Latchoumane, C. F. V., Ngo, H. V. V., Born, J., & Shin, H. S. (2017). Thalamic spindles promote memory formation during sleep through triple phase-locking of cortical, thalamic, and hippocampal rhythms. *Neuron*, *95*(2), 424-435.

Laureys, S., Peigneux, P., Phillips, C., Fuchs, S., Degueldre, C., Aerts, J., ... & Maquet, P. (2001). Experience-dependent changes in cerebral functional connectivity during human rapid eye movement sleep. *Neuroscience*, *105*(3), 521-525.

Laventure, S., Fogel, S., Lungu, O., Albouy, G., Sévigny-Dupont, P., Vien, C., ... & Doyon, J. (2016). NREM2 and sleep spindles are instrumental to the consolidation of motor sequence memories. *PLoS Biology*, *14*(3), e1002429.

Laventure, S., Pinsard, B., Lungu, O., Carrier, J., Fogel, S., Benali, H., ... & Doyon, J. (2018). Beyond spindles: interactions between sleep spindles and boundary frequencies during cued reactivation of motor memory representations. *Sleep*, *41*(9), zsy142.

Lazari, A., Salvan, P., Cottaar, M., Papp, D., van der Werf, O. J., Johnstone, A., ... & Johansen-Berg, H. (2021). Reassessing associations between white matter and behaviour with multimodal microstructural imaging. *Cortex*, *145*, 187-200.

Le Bihan, D. (2012). Diffusion, confusion and functional MRI. *Neuroimage*, *62*(2), 1131-1136.

Lee, A. K., & Wilson, M. A. (2002). Memory of sequential experience in the hippocampus during slow wave sleep. *Neuron*, *36*(6), 1183-1194.

Léger, D., Debellemaniere, E., Rabat, A., Bayon, V., Benchenane, K., & Chennaoui, M. (2018). Slow-wave sleep: From the cell to the clinic. *Sleep medicine reviews*, *41*, 113-132.

Lehmann, M., Schreiner, T., Seifritz, E., & Rasch, B. (2016). Emotional arousal modulates oscillatory correlates of targeted memory reactivation during NREM, but not REM sleep. *Scientific reports*, *6*(1), 1-13.

Lemke, S. M., Ramanathan, D. S., Darevksy, D., Egert, D., Berke, J. D., & Ganguly, K. (2021). Coupling between motor cortex and striatum increases during sleep over long-term skill learning. *elife*, *10*, e64303.

Lenth, R., Singmann, H., Love, J., Buerkner, P., & Herve, M. (2019). *emmeans: Estimated marginal means, aka least-squares means (Version 1.3. 4)*. Available at: https://cran.r-project.org/package=emmeans

Lewis, P. A., & Durrant, S. J. (2011). Overlapping memory replay during sleep builds cognitive schemata. *Trends in cognitive sciences*, *15*(8), 343-351.

Lewis, P. A., Cairney, S., Manning, L., & Critchley, H. D. (2011a). The impact of overnight consolidation upon memory for emotional and neutral encoding contexts. *Neuropsychologia*, *49*(9), 2619-2629.

Lewis, P. A., Couch, T. J., & Walker, M. P. (2011b). Keeping time in your sleep: overnight consolidation of temporal rhythm. *Neuropsychologia*, *49*(1), 115-123.

Lewis, P. A., Knoblich, G., & Poe, G. (2018). How memory replay in sleep boosts creative problem-solving. *Trends in cognitive sciences*, *22*(6), 491-503.

Li, W., Ma, L., Yang, G., & Gan, W. B. (2017). REM sleep selectively prunes and maintains new synapses in development and learning. *Nature neuroscience*, *20*(3), 427-437.

Likova, L. T., Mineff, K. N., & Nicholas, S. C. (2021). Mental Visualization in the Cerebellum: Rapid Non-motor Learning at Sub-Lobular and Causal Network Levels. *Frontiers in Systems Neuroscience*, 81.

Lim, A. S., Lozano, A. M., Moro, E., Hamani, C., Hutchison, W. D., Dostrovsky, J. O., ... & Murray, B. J. (2007). Characterization of REM-sleep associated ponto-geniculo-occipital waves in the human pons. *Sleep*, *30*(7), 823-827.

Loganathan, R. (2014). The Role of Sleep in Motor Learning. *PostDoc Journal*, 2(4), 18-29.

Loomis, A. L., Harvey, E. N., & Hobart III, G. A. (1938). Distribution of disturbance-patterns in the human electroencephalogram, with special reference to sleep. *Journal of Neurophysiology*, *1*(5), 413-430.

Louie, K., & Wilson, M. A. (2001). Temporally structured replay of awake hippocampal ensemble activity during rapid eye movement sleep. *Neuron*, *29*(1), 145-156.

Lustenberger, C., Boyle, M. R., Alagapan, S., Mellin, J. M., Vaughn, B. V., & Fröhlich, F. (2016). Feedback-controlled transcranial alternating current stimulation reveals a functional role of sleep spindles in motor memory consolidation. *Current Biology*, *26*(16), 2127-2136.

Lutz, N. D., Admard, M., Genzoni, E., Born, J., & Rauss, K. (2021). Occipital sleep spindles predict sequence learning in a visuo-motor task. *Sleep*, *44*(8), zsab056.

Macvicar, B. A., Feighan, D., Brown, A., & Ransom, B. (2002). Intrinsic optical signals in the rat optic nerve: role for K+ uptake via NKCC1 and swelling of astrocytes. *Glia*, *37*(2), 114-123.

Maffei, C., Soria, G., Prats-Galino, A., & Catani, M. (2015). Imaging white-matter pathways of the auditory system with diffusion imaging tractography. *Handbook of clinical neurology*, *129*, 277-288.

Maldjian, J. A., Laurienti, P. J., Kraft, R. A., & Burdette, J. H. (2003). An automated method for neuroanatomic and cytoarchitectonic atlas-based interrogation of fMRI data sets. *Neuroimage*, *19*(3), 1233-1239.

Mander, B. A., Santhanam, S., Saletin, J. M., & Walker, M. P. (2011). Wake deterioration and sleep restoration of human learning. *Current biology*, *21*(5), R183-R184.

Maquet, P., Laureys, S., Peigneux, P., Fuchs, S., Petiau, C., Phillips, C., ... & Cleeremans, A. (2000). Experience-dependent changes in cerebral activation during human REM sleep. *Nature neuroscience*, *3*(8), 831-836.

Maquet, P., Peigneux, P., Laureys, S., Boly, M., Dang-Vu, T., Desseilles, M., & Cleermans, A. (2003b). Memory processing during human sleep as assessed by functional neuroimaging. *Revue neurologique*, *159*(11; SUPP), 6S27-6S29.

Maquet, P., Schwartz, S., Passingham, R., & Frith, C. (2003a). Sleep-related consolidation of a visuomotor skill: brain mechanisms as assessed by functional magnetic resonance imaging. *Journal of Neuroscience*, *23*(4), 1432-1440.

Marek, S., Tervo-Clemmens, B., Calabro, F. J., Montez, D. F., Kay, B. P., Hatoum, A. S., ... & Dosenbach, N. U. (2022). Reproducible brain-wide association studies require thousands of individuals. *Nature*, *603*(7902), 654-660.

Marr, D. (1970). A theory for cerebral neocortex. *Proceedings of the Royal Society of London. Series B. Biological Sciences*, *176*(1043), 161-234.

Marr, D., Willshaw, D., & McNaughton, B. (1991). Simple memory: a theory for archicortex. In *From the Retina to the Neocortex* (pp. 59-128). Birkhäuser Boston.

Mateos-Aparicio, P., & Rodríguez-Moreno, A. (2019). The impact of studying brain plasticity. *Frontiers in cellular neuroscience*, *13*, 66.

Matsuzaka, Y., Picard, N., & Strick, P. L. (2007). Skill representation in the primary motor cortex after long-term practice. *Journal of neurophysiology*, *97*(2), 1819-1832.

McClelland, J. L., McNaughton, B. L., & O'Reilly, R. C. (1995). Why there are complementary learning systems in the hippocampus and neocortex: insights from the successes and failures of connectionist models of learning and memory. *Psychological review*, *102*(3), 419.

Mednick, S., Nakayama, K., & Stickgold, R. (2003). Sleep-dependent learning: a nap is as good as a night. *Nature neuroscience*, *6*(7), 697-698.

Mikutta, C., Feige, B., Maier, J. G., Hertenstein, E., Holz, J., Riemann, D., & Nissen, C. (2019). Phase-amplitude coupling of sleep slow oscillatory and spindle activity correlates with overnight memory consolidation. *Journal of sleep research*, *28*(6), e12835.

Miller, M. A., Wright, H., Hough, J., & Cappuccio, F. P. (2014). Sleep and cognition. In *Sleep and its disorders affect society*. IntechOpen.

Miry, O., Li, J., & Chen, L. (2021). The quest for the hippocampal memory engram: From theories to experimental evidence. *Frontiers in Behavioral Neuroscience*, 270.

Miyamoto, D., Marshall, W., Tononi, G., & Cirelli, C. (2021). Net decrease in spine-surface GluA1-containing AMPA receptors after post-learning sleep in the adult mouse cortex. *Nature communications*, *12*(1), 1-13.

Mölle, M., Bergmann, T. O., Marshall, L., & Born, J. (2011). Fast and slow spindles during the sleep slow oscillation: disparate coalescence and engagement in memory processing. *Sleep*, *34*(10), 1411-1421.

Monfils, M. H., Plautz, E. J., & Kleim, J. A. (2005). In search of the motor engram: motor map plasticity as a mechanism for encoding motor experience. *The Neuroscientist*, *11*(5), 471-483.

Mori, S., & Zhang, J. (2006). Principles of diffusion tensor imaging and its applications to basic neuroscience research. *Neuron*, *51*(5), 527-539.

Morin, A., Doyon, J., Dostie, V., Barakat, M., Tahar, A. H., Korman, M., ... & Carrier, J. (2008). Motor sequence learning increases sleep spindles and fast frequencies in post-training sleep. *Sleep*, *31*(8), 1149-1156.

Morris, R. G. M. (2006). Elements of a neurobiological theory of hippocampal function: the role of synaptic plasticity, synaptic tagging and schemas. *European Journal of Neuroscience*, *23*(11), 2829-2846.

Muehlroth, B. E., Sander, M. C., Fandakova, Y., Grandy, T. H., Rasch, B., Shing, Y. L., & Werkle-Bergner, M. (2019). Precise slow oscillation–spindle coupling promotes memory consolidation in younger and older adults. *Scientific reports*, *9*(1), 1-15.

Myskiw, J. C., & Izquierdo, I. (2012). Posterior parietal cortex and long-term memory: some data from laboratory animals. *Frontiers in integrative neuroscience*, *6*, 8.

Nádasdy, Z., Hirase, H., Czurkó, A., Csicsvari, J., & Buzsáki, G. (1999). Replay and time compression of recurring spike sequences in the hippocampus. *Journal of Neuroscience*, *19*(21), 9497-9507

Nadel, L., & Moscovitch, M. (1997). Memory consolidation, retrograde amnesia and the hippocampal complex. *Current opinion in neurobiology*, *7*(2), 217-227.

Nakanishi, H., Sun, Y., Nakamura, R. K., Mori, K., Ito, M., Suda, S., ... & Sokoloff, L. (1997). Positive correlations between cerebral protein synthesis rates and deep sleep in Macaca mulatta. *European Journal of Neuroscience*, *9*(2), 271-279.

Nakashiba, T., Buhl, D. L., McHugh, T. J., & Tonegawa, S. (2009). Hippocampal CA3 output is crucial for ripple-associated reactivation and consolidation of memory. *Neuron*, *62*(6), 781-787.

Navarrete, M., Schneider, J., Ngo, H. V. V., Valderrama, M., Casson, A. J., & Lewis, P. A. (2020). Examining the optimal timing for closed-loop auditory stimulation of slow-wave sleep in young and older adults. *Sleep*, *43*(6), zsz315.

Neumann, F., Oberhauser, V., & Kornmeier, J. (2020). How odor cues help to optimize learning during sleep in a real life-setting. *Scientific reports*, *10*(1), 1-8.

Ngo, H. V. V., Martinetz, T., Born, J., & Mölle, M. (2013). Auditory closed-loop stimulation of the sleep slow oscillation enhances memory. *Neuron*, *78*(3), 545-553.

Ni, K. M., Hou, X. J., Yang, C. H., Dong, P., Li, Y., Zhang, Y., ... & Li, X. M. (2016). Selectively driving cholinergic fibers optically in the thalamic reticular nucleus promotes sleep. *elife*, *5*, e10382.

Niknazar, M., Krishnan, G. P., Bazhenov, M., & Mednick, S. C. (2015). Coupling of thalamocortical sleep oscillations are important for memory consolidation in humans. *PloS one*, *10*(12), e0144720.

Nishida, M., & Walker, M. P. (2007). Daytime naps, motor memory consolidation and regionally specific sleep spindles. *PloS one*, *2*(4), e341.

Nissen, M. J., & Bullemer, P. (1987). Attentional requirements of learning: Evidence from performance measures. *Cognitive psychology*, *19*(1), 1-32.

Nobre, A. C., Correa, A., & Coull, J. T. (2007). The hazards of time. *Current opinion in neurobiology*, *17*(4), 465-470.

O'Keefe, J., & Dostrovsky, J. (1971). The hippocampus as a spatial map: preliminary evidence from unit activity in the freely-moving rat. *Brain research*.

O'Neill, J., Pleydell-Bouverie, B., Dupret, D., & Csicsvari, J. (2010). Play it again: reactivation of waking experience and memory. *Trends in neurosciences*, *33*(5), 220-229.

Ohayon, M. M., Carskadon, M. A., Guilleminault, C., & Vitiello, M. V. (2004). Meta-analysis of quantitative sleep parameters from childhood to old age in healthy individuals: developing normative sleep values across the human lifespan. *Sleep*, *27*(7), 1255-1273.

Ólafsdóttir, H. F., Barry, C., Saleem, A. B., Hassabis, D., & Spiers, H. J. (2015). Hippocampal place cells construct reward related sequences through unexplored space. *elife*, *4*, e06063.

Oostenveld, R., Fries, P., Maris, E., & Schoffelen, J. M. (2011). FieldTrip: open source software for advanced analysis of MEG, EEG, and invasive electrophysiological data. *Computational intelligence and neuroscience*, *2011*.

Oudiette, D., & Paller, K. A. (2013). Upgrading the sleeping brain with targeted memory reactivation. *Trends in cognitive sciences*, *17*(3), 142-149.

Oudiette, D., Antony, J. W., & Paller, K. A. (2014). Fear not: manipulating sleep might help you forget. *Trends in cognitive sciences*, *18*(1), 3-4.

Oudiette, D., Antony, J. W., Creery, J. D., & Paller, K. A. (2013). The role of memory reactivation during wakefulness and sleep in determining which memories endure. *Journal of Neuroscience*, *33*(15), 6672-6678.

Oyarzún, J. P., Morís, J., Luque, D., de Diego-Balaguer, R., & Fuentemilla, L. (2017). Targeted memory reactivation during sleep adaptively promotes the strengthening or weakening of overlapping memories. *Journal of Neuroscience*, *37*(32), 7748-7758.

Paller, K. A. (2017). Sleeping in a brave new world: Opportunities for improving learning and clinical outcomes through targeted memory reactivation. *Current directions in psychological science*, *26*(6), 532-537.

Patel, A. K., Reddy, V., & Araujo, J. F. (2020). Physiology, sleep stages. *StatPearls [Internet]*.

Pavlides, C., & Winson, J. (1989). Influences of hippocampal place cell firing in the awake state on the activity of these cells during subsequent sleep episodes. *Journal of neuroscience*, *9*(8), 2907-2918.

Peigneux, P., Laureys, S., Fuchs, S., Collette, F., Perrin, F., Reggers, J., ... & Maquet, P. (2004). Are spatial memories strengthened in the human hippocampus during slow wave sleep?. *Neuron*, *44*(3), 535-545.

Peigneux, P., Laureys, S., Fuchs, S., Destrebecqz, A., Collette, F., Delbeuck, X., … Maquet, P. (2003). Learned material content and acquisition level modulate cerebral reactivation during posttraining rapid-eye-movements sleep. *NeuroImage*, *20*(1), 125–134.

Peirce, J., Gray, J. R., Simpson, S., MacAskill, M., Höchenberger, R., Sogo, H., ... & Lindeløv, J. K. (2019). PsychoPy2: Experiments in behavior made easy. *Behavior research methods*, *51*(1), 195-203.

Penfield, W., & Milner, B. (1958). Memory deficit produced by bilateral lesions in the hippocampal zone. *AMA archives of Neurology & Psychiatry*, *79*(5), 475-497.

Pennartz, C. M. A., Lee, E., Verheul, J., Lipa, P., Barnes, C. A., & McNaughton, B. L. (2004). The ventral striatum in off-line processing: ensemble reactivation during sleep and modulation by hippocampal ripples. *Journal of Neuroscience*, *24*(29), 6446-6456.

Pereira, S. I. R., & Lewis, P. A. (2020). The differing roles of NREM and REM sleep in the slow enhancement of skills and schemas. *Current Opinion in Physiology*, *15*, 82-88.

Pereira, S. I. R., Beijamini, F., Weber, F. D., Vincenzi, R. A., da Silva, F. A. C., & Louzada, F. M. (2017). Tactile stimulation during sleep alters slow oscillation and spindle densities but not motor skill. *Physiology & behavior*, *169*, 59-68.

Peters, A. J., Chen, S. X., & Komiyama, T. (2014). Emergence of reproducible spatiotemporal activity during motor learning. *Nature*, *510*(7504), 263-267.

Peters, J. M., Struyven, R. R., Prohl, A. K., Vasung, L., Stajduhar, A., Taquet, M., ... & Warfield, S. K. (2019). White matter mean diffusivity correlates with myelination in tuberous sclerosis complex. *Annals of clinical and translational neurology*, *6*(7), 1178-1190.

Peyrache, A., & Seibt, J. (2020). A mechanism for learning with sleep spindles. *Philosophical Transactions of the Royal Society B*, *375*(1799), 20190230.

Peyrache, A., Khamassi, M., Benchenane, K., Wiener, S. I., & Battaglia, F. P. (2009). Replay of rule-learning related neural patterns in the prefrontal cortex during sleep. *Nature neuroscience*, *12*(7), 919-926.

Pfeiffer, B. E., & Foster, D. J. (2013). Hippocampal place-cell sequences depict future paths to remembered goals. *Nature*, *497*(7447), 74-79.

Piantoni, G., Poil, S. S., Linkenkaer-Hansen, K., Verweij, I. M., Ramautar, J. R., Van Someren, E. J., & Van Der Werf, Y. D. (2013). Individual differences in white matter diffusion affect sleep oscillations. *Journal of Neuroscience*, *33*(1), 227-233.

Plihal, W., & Born, J. (1997). Effects of early and late nocturnal sleep on declarative and procedural memory. *Journal of cognitive neuroscience*, *9*(4), 534-547.

Plihal, W., & Born, J. (1999). Effects of early and late nocturnal sleep on priming and spatial memory. *Psychophysiology*, *36*(5), 571-582.

Poe, G. R., Nitz, D. A., McNaughton, B. L., & Barnes, C. A. (2000). Experience-dependent phase-reversal of hippocampal neuron firing during REM sleep. *Brain research*, *855*(1), 176-180.

Preacher, K. J., & Kelley, K. (2011). Effect size measures for mediation models: Quantitative strategies for communicating indirect effects. *Psychological Methods*, *16*(2), 93–115.

Preacher, K. J., & Leonardelli, G. J. (2001). Calculation for the Sobel test: An interactive calculation tool for mediation tests. Retrieved January 20, 2011, from http://quantpsy.org/sobel/sobel.htm

Purcell, S. M., Manoach, D. S., Demanuele, C., Cade, B. E., Mariani, S., Cox, R., ... & Stickgold, R. (2017). Characterizing sleep spindles in 11,630 individuals from the National Sleep Research Resource. *Nature communications*, *8*(1), 1-16.

Qin, Y. L., McNaughton, B. L., Skaggs, W. E., & Barnes, C. A. (1997). Memory reprocessing in corticocortical and hippocampocortical neuronal ensembles. *Philosophical Transactions of the Royal Society of London. Series B: Biological Sciences*, *352*(1360), 1525-1533.

Qualtrics. (2005). Qualtrics. Retrieved from https://www.qualtrics.com

Quillfeldt, J. A. (2019). Temporal flexibility of systems consolidation and the Synaptic Occupancy/Reset theory (SORT): Cues about the nature of the engram. *Frontiers in Synaptic Neuroscience*, 1.

R Core Team. (2012). R: a language and environment for statistical computing. R Foundation for Statistical Computing. R Foundation for Statistical Computing, Vienna, Au, Vienna, Austria.

Ramírez-Salado, I., & Cruz-Aguilar, M. A. (2014). The origin and functions of dreams based on the PGO activity. *Salud mental*, *37*(1), 49-58.

Rasch, B. & Born, J. (2013). About sleep's role in memory. *Physiological Reviews,* 93, 681–766.

Rasch, B. Buchel, C., Gais, S., & Born, J. (2007). Odor cues during slow-wave sleep prompt declarative memory consolidation. *Science*, *315*, 5817.

Rauchs, G., Bertran, F., Guillery-Girard, B., Desgranges, B., Kerrouche, N., Denise, P., ... & Eustache, F. (2004). Consolidation of strictly episodic memories mainly requires rapid eye movement sleep. *Sleep*, *27*(3), 395-401.

Rauchs, G., Desgranges, B., Foret, J., & Eustache, F. (2005). The relationships between memory systems and sleep stages. *Journal of sleep research*, *14*(2), 123-140.

Redondo, R. L., & Morris, R. G. (2011). Making memories last: the synaptic tagging and capture hypothesis. *Nature Reviews Neuroscience*, *12*(1), 17-30.

Ribeiro, S., Mello, C. V., Velho, T., Gardner, T. J., Jarvis, E. D., & Pavlides, C. (2002). Induction of hippocampal long-term potentiation during waking leads to increased extrahippocampal zif-268 expression during ensuing rapid-eye-movement sleep. *Journal of neuroscience*, *22*(24), 10914-10923.

Riedner, B. A., Vyazovskiy, V. V., Huber, R., Massimini, M., Esser, S., Murphy, M., & Tononi, G. (2007). Sleep homeostasis and cortical synchronization: III. A high-density EEG study of sleep slow waves in humans. *Sleep*, *30*(12), 1643-1657.

Rihm, J. S., & Rasch, B. (2015). Replay of conditioned stimuli during late REM and stage N2 sleep influences affective tone rather than emotional memory strength. *Neurobiology of learning and memory*, *122*, 142-151.

Rihm, J. S., Diekelmann, S., Born, J., & Rasch, B. (2014). Reactivating memories during sleep by odors: odor specificity and associated changes in sleep oscillations. *Journal of cognitive neuroscience*, *26*(8), 1806-1818.

Ritter, S. M., Strick, M., Bos, M. W., Van Baaren, R. B., & Dijksterhuis, A. P. (2012). Good morning creativity: task reactivation during sleep enhances beneficial effect of sleep on creative performance. *Journal of sleep research*, *21*(6), 643-647.

Robertson, E. M. (2007). The serial reaction time task: implicit motor skill learning?. *Journal of Neuroscience*, *27*(38), 10073-10075.

Robertson, E. M. (2009). From creation to consolidation: a novel framework for memory processing. *PLoS biology*, *7*(1), e1000019.

Robertson, E. M., Pascual-Leone, A., & Press, D. Z. (2004). Awareness modifies the skill-learning benefits of sleep. *Current biology*, *14*(3), 208-212.

Rolls, A., Makam, M., Kroeger, D., Colas, D., De Lecea, L., & Heller, H. C. (2013). Sleep to forget: interference of fear memories during sleep. *Molecular psychiatry*, *18*(11), 1166-1170.

Romano Bergstrom, J. C., Howard, J. H., & Howard, D. V. (2012). Enhanced Implicit Sequence Learning in College-age Video Game Players and Musicians. *Applied Cognitive Psychology*, *26*(1), 91–96.

Romano, J. C., Howard Jr, J. H., & Howard, D. V. (2010). One-year retention of general and sequence-specific skills in a probabilistic, serial reaction time task. *Memory*, *18*(4), 427-441.

Rosanova, M., & Ulrich, D. (2005). Pattern-specific associative long-term potentiation induced by a sleep spindle-related spike train. *Journal of Neuroscience*, *25*(41), 9398-9405.

Roth, M., Shaw, J., & Green, J. (1956). The form, voltage distribution and physiological significance of the K-complex. *Electroencephalography and clinical neurophysiology*, *8*(3), 385-402.

Rudoy, J. D., Voss, J. L., Westerberg, C. E., & Paller, K. A. (2009). Strengthening individual memories by reactivating them during sleep. *Science*, *326*(5956), 1079-1079.

Rudrapatna, S. U., Parker, G. D., Roberts, J., & Jones, D. K. (2018). Can we correct for interactions between subject motion and gradient-nonlinearity in diffusion MRI. In *Proc. Int. Soc. Mag. Reson. Med* (Vol. 1206).

Sagi, Y., Tavor, I., Hofstetter, S., Tzur-Moryosef, S., Blumenfeld-Katzir, T., & Assaf, Y. (2012). Learning in the fast lane: new insights into neuroplasticity. *Neuron*, *73*(6), 1195-1203.

Sairanen, V., Leemans, A., & Tax, C. M. (2018). Fast and accurate Slicewise OutLIer Detection (SOLID) with informed model estimation for diffusion MRI data. *Neuroimage*, *181*, 331-346.

Saletin, J. M., Goldstein, A. N., & Walker, M. P. (2011). The role of sleep in directed forgetting and remembering of human memories. *Cerebral cortex*, *21*(11), 2534-2541.

Sampaio-Baptista, C., Vallès, A., Khrapitchev, A. A., Akkermans, G., Winkler, A. M., Foxley, S., ... & Johansen-Berg, H. (2020). White matter structure and myelin-related gene expression alterations with experience in adult rats. *Progress in neurobiology*, *187*, 101770.

Sassin, J. F., Parker, D. C., Mace, J. W., Gotlin, R. W., Johnson, L. C., & Rossman, L. G. (1969). Human growth hormone release: relation to slow-wave sleep and sleep-waking cycles. *Science*, *165*(3892), 513-515.

Sato, Y., Fukuoka, Y., Minamitani, H., & Honda, K. (2007). Sensory stimulation triggers spindles during sleep stage 2. *Sleep*, *30*(4), 511-518.

Schabus, M., Dang-Vu, T. T., Albouy, G., Balteau, E., Boly, M., Carrier, J., ... & Maquet, P. (2007). Hemodynamic cerebral correlates of sleep spindles during human non-rapid eye movement sleep. *Proceedings of the National Academy of Sciences*, *104*(32), 13164-13169.

Schapiro, A. C., McDevitt, E. A., Rogers, T. T., Mednick, S. C., & Norman, K. A. (2018). Human hippocampal replay during rest prioritizes weakly learned information and predicts memory performance. *Nature communications*, *9*(1), 1-11.

Schechtman, E., Antony, J. W., Lampe, A., Wilson, B. J., Norman, K. A., & Paller, K. A. (2021). Multiple memories can be simultaneously reactivated during sleep as effectively as a single memory. *Communications biology*, *4*(1), 1-13.

Schechtman, E., Witkowski, S., Lampe, A., Wilson, B. J., & Paller, K. A. (2020). Targeted memory reactivation during sleep boosts intentional forgetting of spatial locations. *Scientific reports*, *10*(1), 1-9.

Schneider, E., Züst, M. A., Wuethrich, S., Schmidig, F., Klöppel, S., Wiest, R., ... & Henke, K. (2021). Larger capacity for unconscious versus conscious episodic memory. *Current Biology*, *31*(16), 3551-3563.

Schoen, L. S., & Badia, P. (1984). Facilitated recall following RFM and NREM naps. *Psychophysiology*, *21*(3), 299-306.

Schönauer, M., Alizadeh, S., Jamalabadi, H., Abraham, A., Pawlizki, A., & Gais, S. (2017). Decoding material-specific memory reprocessing during sleep in humans. *Nature communications*, *8*(1), 1-9.

Schönauer, M., Geisler, T., & Gais, S. (2014). Strengthening procedural memories by reactivation in sleep. *Journal of cognitive neuroscience*, *26*(1), 143-153.

Schouten, D. I., Pereira, S. I., Tops, M., & Louzada, F. M. (2017). State of the art on targeted memory reactivation: Sleep your way to enhanced cognition. *Sleep Medicine Reviews*, *32*, 123-131.

Schreiner, T., & Rasch, B. (2015). Boosting vocabulary learning by verbal cueing during sleep. *Cerebral Cortex*, *25*(11), 4169-4179.

Schreiner, T., Doeller, C. F., Jensen, O., Rasch, B., & Staudigl, T. (2018). Theta phase-coordinated memory reactivation reoccurs in a slow-oscillatory rhythm during NREM sleep. *Cell reports*, *25*(2), 296-301.

Schreiner, T., Lehmann, M., & Rasch, B. (2015). Auditory feedback blocks memory benefits of cueing during sleep. *Nature communications*, *6*(1), 1-11.

Schreiner, T., Petzka, M., Staudigl, T., & Staresina, B. P. (2021). Endogenous memory reactivation during sleep in humans is clocked by slow oscillation-spindle complexes. *Nature communications* 12 (1), 1-10.

Scoville, W. B., & Milner, B. (1957). Loss of recent memory after bilateral hippocampal lesions. *Journal of neurology, neurosurgery, and psychiatry*, *20*(1), 11.

Seibt, J., & Frank, M. G. (2019). Primed to sleep: the dynamics of synaptic plasticity across brain states. *Frontiers in Systems Neuroscience*, *13*, 2.

Seidler, R. D. (2010). Neural correlates of motor learning, transfer of learning, and learning to learn. *Exercise and sport sciences reviews*, *38*(1), 3.

Sejnowski, T. J., & Destexhe, A. (2000). Why do we sleep?. *Brain research*, *886*(1-2), 208-223.

Semon R. (1921). The mneme. London: G. Allen & Unwin

Shadmehr, R., & Holcomb, H. H. (1997). Neural correlates of motor memory consolidation. *Science*, *277*(5327), 821-825.

Shanahan, L. K., Gjorgieva, E., Paller, K. A., Kahnt, T., & Gottfried, J. A. (2018). Odor-evoked category reactivation in human ventromedial prefrontal cortex during sleep promotes memory consolidation. *elife*, *7*, e39681.

Shen, J., Kudrimoti, H., McNaughton, B., & Barnes, C. (1998). Reactivation of neuronal ensembles in hippocampal dentate gyrus during sleep after spatial experience. *Journal of Sleep Research*, *7*(S1), 6-16.

Shimamura, A. P. (2011). Episodic retrieval and the cortical binding of relational activity. *Cognitive, Affective, & Behavioral Neuroscience*, *11*(3), 277-291.

Shimizu, R. E., Connolly, P. M., Cellini, N., Armstrong, D. M., Hernandez, L. T., Estrada, R., ... & Simons, S. B. (2018). Closed-loop targeted memory reactivation during sleep improves spatial navigation. *Frontiers in human neuroscience*, *12*, 28.

Shrivastava, D., Jung, S., Saadat, M., Sirohi, R., & Crewson, K. (2014). How to interpret the results of a sleep study. *Journal of community hospital internal medicine perspectives*, *4*(5), 24983.

Siegel, J. M. (2008). Do all animals sleep?. *Trends in neurosciences*, *31*(4), 208-213.

Silber, M. H., Ancoli-Israel, S., Bonnet, M. H., Chokroverty, S., Grigg-Damberger, M. M., Hirshkowitz, M., ... & Iber, C. (2007). The visual scoring of sleep in adults. *Journal of clinical sleep medicine*, *3*(02), 121-131.

Silva, D., Feng, T., & Foster, D. J. (2015). Trajectory events across hippocampal place cells require previous experience. *Nature neuroscience*, *18*(12), 1772-1779.

Simon, K. C., Gómez, R. L., & Nadel, L. (2018). Losing memories during sleep after targeted memory reactivation. *Neurobiology of learning and memory*, *151*, 10-17.

Skaggs, W. E., & McNaughton, B. L. (1996). Replay of neuronal firing sequences in rat hippocampus during sleep following spatial experience. *Science*, *271*(5257), 1870-1873.

Skaggs, W. E., McNaughton, B. L., Wilson, M. A., & Barnes, C. A. (1996). Theta phase precession in hippocampal neuronal populations and the compression of temporal sequences. *Hippocampus*, *6*(2), 149-172.

Smith, C. (1995). Sleep states and memory processes. *Behavioural brain research*, *69*(1-2), 137-145.

Smith, C. (2001). Sleep states and memory processes in humans: procedural versus declarative memory systems. *Sleep medicine reviews*, *5*(6), 491-506.

Smith, C. T., Aubrey, J. B., & Peters, K. R. (2004a). Different roles for REM and stage 2 sleep in motor learning: A proposed model. *Psychologica Belgica*, *44*, 81-104.

Smith, C., & MacNeill, C. (1994). Impaired motor memory for a pursuit rotor task following Stage 2 sleep loss in college students. *Journal of sleep research*, *3*(4), 206-213.

Smith, C., & Weeden, K. (1990). Post training REMs coincident auditory stimulation enhances memory in humans. *Psychiatric Journal of the University of Ottawa*.

Smith, S. M., Jenkinson, M., Woolrich, M. W., Beckmann, C. F., Behrens, T. E., Johansen-Berg, H., ... & Matthews, P. M. (2004b). Advances in functional and structural MR image analysis and implementation as FSL. *Neuroimage*, *23*, S208-S219.

Sobel, M. E. (1982). Asymptotic Confidence Intervals for Indirect Effects in Structural Equation Models. *Sociological Methodology*, *13*, 290.

Spencer, R. M., Sunm, M., & Ivry, R. B. (2006). Sleep-dependent consolidation of contextual learning. *Current Biology*, *16*(10), 1001-1005.

Squire, L. R. (2004). Memory systems of the brain: a brief history and current perspective. *Neurobiology of learning and memory*, *82*(3), 171-177.

Squire, L. R., & Alvarez, P. (1995). Retrograde amnesia and memory consolidation: a neurobiological perspective. *Current opinion in neurobiology*, *5*(2), 169-177.

Squire, L. R., & Dede, A. J. (2015). Conscious and unconscious memory systems. *Cold Spring Harbor perspectives in biology*, *7*(3), a021667.

Squire, L. R., & Zola, S. M. (1996). Structure and function of declarative and nondeclarative memory systems. *Proceedings of the National Academy of Sciences*, *93*(24), 13515-13522.

Staresina, B. P., Bergmann, T. O., Bonnefond, M., Van Der Meij, R., Jensen, O., Deuker, L., ... & Fell, J. (2015). Hierarchical nesting of slow oscillations, spindles and ripples in the human hippocampus during sleep. *Nature neuroscience*, *18*(11), 1679-1686.

Stee, W., & Peigneux, P. (2021). Post-learning micro-and macro-structural neuroplasticity changes with time and sleep. *Biochemical pharmacology*, *191*, 114369.

Steriade, M. (2006). Grouping of brain rhythms in corticothalamic systems. *Neuroscience*, *137*(4), 1087-1106

Sterpenich, V., Schmidt, C., Albouy, G., Matarazzo, L., Vanhaudenhuyse, A., Boveroux, P., ... & Maquet, P. (2014). Memory reactivation during rapid eye movement sleep promotes its generalization and integration in cortical stores. *Sleep*, *37*(6), 1061-1075.

Sterpenich, V., van Schie, M. K., Catsiyannis, M., Ramyead, A., Perrig, S., Yang, H. D., ... & Schwartz, S. (2021). Reward biases spontaneous neural reactivation during sleep. *Nature Communications*, *12*(1), 1-11.

Stickgold, R. (2005). Sleep-dependent memory consolidation. *Nature*, *437*(7063), 1272-1278.

Stickgold, R., & Walker, M. P. (2013). Sleep-dependent memory triage: evolving generalization through selective processing. *Nature neuroscience*, *16*(2), 139-145.

Stickgold, R., Whidbee, D., Schirmer, B., Patel, V., & Hobson, J. A. (2000). Visual discrimination task improvement: A multi-step process occurring during sleep. *Journal of cognitive neuroscience*, *12*(2), 246-254.

Sutherland, G. R., & McNaughton, B. (2000). Memory trace reactivation in hippocampal and neocortical neuronal ensembles. *Current opinion in neurobiology*, *10*(2), 180-186.

Takashima, A., Nieuwenhuis, I. L., Jensen, O., Talamini, L. M., Rijpkema, M., & Fernández, G. (2009). Shift from hippocampal to neocortical centered retrieval network with consolidation. *Journal of Neuroscience*, *29*(32), 10087-10093.

Takashima, A., Petersson, K. M., Rutters, F., Tendolkar, I., Jensen, O., Zwarts, M. J., ... & Fernández, G. (2006). Declarative memory consolidation in humans: a prospective functional magnetic resonance imaging study. *Proceedings of the National Academy of Sciences*, *103*(3), 756-761.

Tambini, A., & Davachi, L. (2019). Awake reactivation of prior experiences consolidates memories and biases cognition. *Trends in cognitive sciences*, *23*(10), 876-890.

Tambini, A., Berners-Lee, A., & Davachi, L. (2017). Brief targeted memory reactivation during the awake state enhances memory stability and benefits the weakest memories. *Scientific reports*, *7*(1), 1-17.

Tavor, I., Botvinik-Nezer, R., Bernstein-Eliav, M., Tsarfaty, G., & Assaf, Y. (2020). Short-term plasticity following motor sequence learning revealed by diffusion magnetic resonance imaging. *Human brain mapping*, *41*(2), 442-452.

Tavor, I., Hofstetter, S., & Assaf, Y. (2013). Micro-structural assessment of short term plasticity dynamics. *Neuroimage*, *81*, 1-7.

Tax, C., M., W., Kleban, E., Chamberland, M., Baraković, M., Rudrapatna, U, Jones, D., K. (2021). Measuring compartmental T2-orientational dependence in human brain white matter using a tiltable RF coil and diffusion-T2 correlation MRI. *Neuroimage, 236*.

Theodosis, D. T., Poulain, D. A., & Oliet, S. H. (2008). Activity-dependent structural and functional plasticity of astrocyte-neuron interactions. *Physiological reviews*, *88*(3), 983-1008.

Thompson, R. F., & Kim, J. J. (1996). Memory systems in the brain and localization of a memory. *Proceedings of the national academy of sciences*, *93*(24), 13438-13444.

Tibshirani, R. J., & Efron, B. (1993). An introduction to the bootstrap. *Monographs on Statistics and Applied Probability*, *57*, 1–436.

Tilley, A. J. (1979). Sleep learning during stage 2 and REM sleep. *Biological Psychology*, *9*(3), 155-161.

Tobler, I., Franken, P., Trachsel, L., & Borbély, A. A. (1992). Models of sleep regulation in mammals. *Journal of sleep research*, *1*(2), 125-127.

Tonegawa, S., Morrissey, M. D., & Kitamura, T. (2018). The role of engram cells in the systems consolidation of memory. *Nature Reviews Neuroscience*, *19*(8), 485-498.

Tononi, G., & Cirelli, C. (2003). Sleep and synaptic homeostasis: a hypothesis. *Brain research bulletin*, *62*(2), 143-150.

Tononi, G., & Cirelli, C. (2006). Sleep function and synaptic homeostasis. *Sleep medicine reviews*, *10*(1), 49-62.

Tononi, G., & Cirelli, C. (2014). Sleep and the price of plasticity: from synaptic and cellular homeostasis to memory consolidation and integration. *Neuron*, *81*(1), 12-34.

Tournier, J. D., Calamante, F., & Connelly, A. (2012). MRtrix: diffusion tractography in crossing fiber regions. *International journal of imaging systems and technology*, *22*(1), 53-66.

Treder, M., Charest, I., Michelmann, S., Martín-Buro, M. C., Roux, F., Carceller-Benito, F., ... & Staresina, B. P. (2021). The hippocampus as the switchboard between perception and memory. *bioRxiv*, 2020-05.

Tse, D., Langston, R. F., Kakeyama, M., Bethus, I., Spooner, P. A., & Wood, E. R. Morris RGM (2007). *Schemas and memory consolidation. Science*, *316*, 76-82.

Tse, D., Takeuchi, T., Kakeyama, M., Kajii, Y., Okuno, H., Tohyama, C., ... & Morris, R. G. (2011). Schema-dependent gene activation and memory encoding in neocortex. *Science*, *333*(6044), 891-895.

Tulving, E. (1983). Elements of episodic memory.

Turner, B. O., Paul, E. J., Miller, M. B., & Barbey, A. K. (2018). Small sample sizes reduce the replicability of task-based fMRI studies. *Communications Biology*, *1*(1), 1-10.

Tuura, R. O. G., Volk, C., Callaghan, F., Jaramillo, V., & Huber, R. (2021). Sleep-related and diurnal effects on brain diffusivity and cerebrospinal fluid flow. *Neuroimage*, *241*, 118420.

Ullman, M. T. (2001). The neural basis of lexicon and grammar in first and second language: The declarative/procedural model. *Bilingualism: Language and cognition*, *4*(2), 105-122.

Ullman, M. T. (2004). Contributions of memory circuits to language: The declarative/procedural model. *Cognition*, *92*(1-2), 231-270.

Ulrich, D. (2016). Sleep spindles as facilitators of memory formation and learning. *Neural plasticity*, *2016*.

Van Der Werf, Y. D., Altena, E., Schoonheim, M. M., Sanz-Arigita, E. J., Vis, J. C., De Rijke, W., & Van Someren, E. J. (2009). Sleep benefits subsequent hippocampal functioning. *Nature neuroscience*, *12*(2), 122-123.

Van Dongen, E. V., Takashima, A., Barth, M., Zapp, J., Schad, L. R., Paller, K. A., & Fernández, G. (2012). Memory stabilization with targeted reactivation during human slow-wave sleep. *Proceedings of the National Academy of Sciences*, *109*(26), 10575-10580.

Van Ormer, E. B. (1933). Sleep and retention. *Psychological bulletin*, *30*(6), 415.

Vankov, I., Bowers, J., & Munafò, M. R. (2014). Article commentary: on the persistence of low power in psychological science. *Quarterly journal of experimental psychology*, *67*(5), 1037-1040.

Veale, J. F. (2014). Edinburgh Handedness Inventory - Short Form: A revised version based on confirmatory factor analysis. *Laterality: Asymmetries of Body, Brain and Cognition*, *19*(2), 164–177.

Verstynen, T., Phillips, J., Braun, E., Workman, B., Schunn, C., & Schneider, W. (2012). Dynamic sensorimotor planning during long-term sequence learning: the role of variability, response chunking and planning errors. *PLoS One*, *7*(10).

Vilberg, K. L., & Rugg, M. D. (2008). Memory retrieval and the parietal cortex: a review of evidence from a dual-process perspective. Neuropsychologia, 46(7), 1787-1799.

Voss, P., Thomas, M. E., Cisneros-Franco, J. M., & de Villers-Sidani, É. (2017). Dynamic brains and the changing rules of neuroplasticity: implications for learning and recovery. *Frontiers in psychology*, *8*, 1657.

Vyazovskiy, V. V., Cirelli, C., Pfister-Genskow, M., Faraguna, U., & Tononi, G. (2008). Molecular and electrophysiological evidence for net synaptic potentiation in wake and depression in sleep. *Nature neuroscience*, *11*(2), 200-208.

Vyazovskiy, V. V., Riedner, B. A., Cirelli, C., & Tononi, G. (2007). Sleep homeostasis and cortical synchronization: II. A local field potential study of sleep slow waves in the rat. *Sleep*, *30*(12), 1631-1642.

Wagner, A. D., Shannon, B. J., Kahn, I., & Buckner, R. L. (2005). Parietal lobe contributions to episodic memory retrieval. *Trends in cognitive sciences*, *9*(9), 445-453.

Wagner, U., Fischer, S., & Born, J. (2002). Changes in emotional responses to aversive pictures across periods rich in slow-wave sleep versus rapid eye movement sleep. *Psychosomatic medicine*, *64*(4), 627-634.

Walker, M. P. (2009). The role of slow wave sleep in memory processing. *Journal of Clinical Sleep Medicine*, *5*(2 suppl), S20-S26.

Walker, M. P., & van Der Helm, E. (2009). Overnight therapy? The role of sleep in emotional brain processing. *Psychological bulletin*, *135*(5), 731.

Walker, M. P., Brakefield, T., Morgan, A., Hobson, J. A., & Stickgold, R. (2002). Practice with sleep makes perfect: sleep-dependent motor skill learning. *Neuron*, *35*(1), 205-211.

Walker, M. P., Stickgold, R., Alsop, D., Gaab, N., & Schlaug, G. (2005). Sleep-dependent motor memory plasticity in the human brain. *Neuroscience*, *133*(4), 911-917.

Walker, M., P, Brakefield, T., Hobson, J. A., & Stickgold, R. (2003). Dissociable stages of human memory consolidation and reconsolidation. *Nature*, *425*(6958), 616–620.

Walker, M., P. (2005). A refined model of sleep and the time course of memory formation. *Behavioral and Brain Sciences*, *28*(1), 51–64.

Wang, B., Antony, J. W., Lurie, S., Brooks, P. P., Paller, K. A., & Norman, K. A. (2019). Targeted memory reactivation during sleep elicits neural signals related to learning content. *Journal of Neuroscience*, *39*(34), 6728-6736.

Wang, W., Nakadate, K., Masugi-Tokita, M., Shutoh, F., Aziz, W., Tarusawa, E., ... & Shigemoto, R. (2014). Distinct cerebellar engrams in short-term and long-term motor learning. *Proceedings of the National Academy of Sciences*, *111*(1), E188-E193.

Weber, R. A., Hui, E. S., Jensen, J. H., Nie, X., Falangola, M. F., Helpern, J. A., & Adkins, D. L. (2015). Diffusional kurtosis and diffusion tensor imaging reveal different time-sensitive stroke-induced microstructural changes. *Stroke*, *46*(2), 545-550.

Werk, C. M., Harbour, V. L., & Chapman, C. A. (2005). Induction of long-term potentiation leads to increased reliability of evoked neocortical spindles in vivo. *Neuroscience*, *131*(4), 793-800.

White, E. L., & DeAmicis, R. A. (1977). Afferent and efferent projections of the region in mouse sml cortex which contains the posteromedial barrel subfield. *The Journal of Comparative Neurology*, *175*(4), 455–481.

Wickham, H. (2009). *ggplot2: Elegant Graphics for Data Analysis*. New York, NY: Springer New York.

Wilhelm, I., Diekelmann, S., Molzow, I., Ayoub, A., Mölle, M., & Born, J. (2011). Sleep selectively enhances memory expected to be of future relevance. *Journal of Neuroscience*, *31*(5), 1563-1569.

Wilson, M. A., & McNaughton, B. L. (1994). Reactivation of hippocampal ensemble memories during sleep. *Science*, *265*(5172), 676-679.

Wimmer, R. D., Astori, S., Bond, C. T., Rovó, Z., Chatton, J. Y., Adelman, J. P., ... & Lüthi, A. (2012). Sustaining sleep spindles through enhanced SK2-channel activity consolidates sleep and elevates arousal threshold. *Journal of Neuroscience*, *32*(40), 13917-13928.

Winkler, A. M., Ridgway, G. R., Webster, M. A., Smith, S. M., & Nichols, T. E. (2014). Permutation inference for the general linear model. *Neuroimage*, *92*, 381-397.

Winkler, A. M., Webster, M. A., Brooks, J. C., Tracey, I., Smith, S. M., & Nichols, T. E. (2016). Non-parametric combination and related permutation tests for neuroimaging. *Human brain mapping*, *37*(4), 1486-1511.

Wixted, J. T. (2004). The psychology and neuroscience of forgetting. *Annual Review in Psychology*, *55*, 235-269.

Wuethrich, S., Hannula, D. E., Mast, F. W., & Henke, K. (2018). Subliminal encoding and flexible retrieval of objects in scenes. *Hippocampus*, *28*(9), 633-643.

Xie, L., Kang, H., Xu, Q., Chen, M. J., Liao, Y., Thiyagarajan, M., ... & Nedergaard, M. (2013). Sleep drives metabolite clearance from the adult brain. *`science*, *342*(6156), 373-377.

Xu, T., Yu, X., Perlik, A. J., Tobin, W. F., Zweig, J. A., Tennant, K., ... & Zuo, Y. (2009). Rapid formation and selective stabilization of synapses for enduring motor memories. *Nature*, *462*(7275), 915-919.

Yang, G., Lai, C. S. W., Cichon, J., Ma, L., Li, W., & Gan, W. B. (2014). Sleep promotes branch-specific formation of dendritic spines after learning. *Science*, *344*(6188), 1173-1178.

Yaroush, R., Sullivan, M. J., & Ekstrand, B. R. (1971). Effect of sleep on memory: II. Differential effect of the first and second half of the night. *Journal of experimental psychology*, *88*(3), 361.

Ylinen, A., Soltész, I., Bragin, A., Penttonen, M., Sik, A., & Buzsáki, G. (1995). Intracellular correlates of hippocampal theta rhythm in identified pyramidal cells, granule cells, and basket cells. *Hippocampus*, *5*(1), 78-90.

Yotsumoto, Y., Sasaki, Y., Chan, P., Vasios, C. E., Bonmassar, G., Ito, N., ... & Watanabe, T. (2009). Location-specific cortical activation changes during sleep after training for perceptual learning. *Current Biology*, *19*(15), 1278-1282.

Zatorre, R. J., Fields, R. D., & Johansen-Berg, H. (2012). Plasticity in gray and white: neuroimaging changes in brain structure during learning. *Nature neuroscience*, *15*(4), 528-536.

Zelano, C., & Sobel, N. (2005). Humans as an animal model for systems-level organization of olfaction. *Neuron*, *48*(3), 431-454.

Zelikowsky, M., Hersman, S., Chawla, M. K., Barnes, C. A., & Fanselow, M. S. (2014). Neuronal ensembles in amygdala, hippocampus, and prefrontal cortex track differential components of contextual fear. *Journal of neuroscience*, *34*(25), 8462-8466.

Zhang, H., Fell, J., & Axmacher, N. (2018). Electrophysiological mechanisms of human memory consolidation. *Nature communications*, *9*(1), 1-11.

Zhang, S., & Chiang-shan, R. L. (2012). Functional connectivity mapping of the human precuneus by resting state fMRI. *Neuroimage*, *59*(4), 3548-3562.

Zhao, X., Lynch, J. G., & Chen, Q. (2010). Reconsidering Baron and Kenny: Myths and Truths about Mediation Analysis. *Journal of Consumer Research*, *37*(2), 197–206.

Zielinski, M. R., McKenna, J. T., & McCarley, R. W. (2016). Functions and mechanisms of sleep. *AIMS neuroscience*, *3*(1), 67.

Zittrell F. (2019). CircHist: Circular histogram in MATLAB. 10.5281/zenodo.3445083. Accessed 26 July 2021.

Züst, M. A., Ruch, S., Wiest, R., & Henke, K. (2019). Implicit vocabulary learning during sleep is bound to slow-wave peaks. *Current biology*, *29*(4), 541-553.